Investigating neuronal mitochondrial DNA loss in Drosophila melanogaster

Cagin, Umut

Awarding institution:
King's College London

Investigating neuronal mitochondrial DNA loss in *Drosophila melanogaster*

Thesis submitted to King's College London for the degree of Doctor of Philosophy

in Molecular Neuroscience

By

Umut Cagin, BSc

Wolfson Centre for Age-Related Diseases

School of Biomedical and Health Sciences

King's College London

2008-2012

Declaration

I hereby certify that the research presented in this thesis is my own, except where stated in the text.

Umut Cagin

September 2012

Acknowledgement

First of all, I would like to thank to my supervisor Dr. Joe Bateman for his continuous support and understanding throughout my PhD. It was such a great experience working with him in the last four years. He was more like a friend to me rather than just a supervisor. So, thanks a lot Joe.

And next are the most important people for me in life, Mentes, Filiz and Buse, my family, which supported me at every single moment and in every single situation. I feel so lucky to have such great parents and a gorgeous sister. Although they were living miles away back home in Cyprus, their support was extraordinary. I could not come to this point without you, thanks a lot to all three of you for being by my side and supporting me whatever it takes.

I would like to thank to past and present members of the lab, Aamna, Amelie, Christina, Ilaria, Nancy, Ariana and Emma, for all the help and friendship. I would also like to thank my friends at the Wolfson CARD, Andrea, Lousie, Rie, Anna, Melina, Sangeetha, Martina, Rachel, Fiona and Praveen (the brother) for the amazing atmosphere in the department. Furthermore, I am glad to have very close friends outside Wolfson which I shared lots of things with, Suleyman, Acelya, Mustafa, Burak and Kazim. Thanks a lot for everything guys.

Abstract

Mitochondria supply the majority of cellular ATP and have additional important roles in calcium signalling, apoptosis and lipid metabolism. Mutations in or loss of mitochondrial DNA (mtDNA) can cause neurodegeneration and has been linked to Parkinson's disease. However, the pathological consequences of mtDNA loss in neurons are very poorly understood.

We have used the fruitfly, *Drosophila melanogaster*, to study how loss of mtDNA affects neuronal function. We find that both ubiquitous RNAi and overexpression of the mtDNA binding protein TFAM causes reduced mtDNA content and lethality. TFAM RNAi or overexpression specifically in motor neurons causes locomotion defects during development and age-related behavioural defects in adult flies. This demonstrates that maintenance of mtDNA is required for normal motor neuron function.

In further behavioural assays we show reductions in evoked jump response, demonstrating that mtDNA loss inhibits motor neuron activity. Also, using confocal imaging we find that mtDNA loss does not cause neuronal loss or changes in synaptic bouton number during development. However, we observe a significant decrease in the number of mitochondria and the number of pre-synaptic active zones (the sites of neurotransmitter release) in motor neurons with reduced mtDNA content. Taken together these data show that neuronal mtDNA loss results in defects in synaptic development and reduced motor neuron function. We further show that these phenotypes can also result from other methods of mtDNA depletion, such as mitochondrial specific expression of the restriction enzyme XhoI. Furthermore,

possible roles of TOR pathway and autophagy on motoneuron synapses were investigated. The phenotypes observed may represent the initial pathological consequences of mtDNA loss in neurodegenerative disease.

Table of Contents

List of Figures

List of Tables

List of abbreviations

5’ dRP:	5’-deoxyribose phosphate
AD:	Alzhmeimer’s disease
ALS:	amyotropic lateral scelerosis
APP:	amyloid precurson protein
Aβ:	β-amyloid
CMT:	Charcot-Marie-Tooth disease
CMT2A:	Charcot-Marie-Tooth type 2A
cPEO:	chronic progressive external opthalmoplegia
dGK:	deoxyguanosine kinase
DNK:	deoxyribonucleoside kinase
DOA:	dominant optic atrophy
Drp1:	dynamin-related protein 1
DSB:	double-strand break
EtBr:	ethidium bromide
ETC:	electron transport chain
HD:	Huntington’s disease
HIG1:	hypoxia inducible group 1
HMG:	high mobility group
HSP:	hereditary spastic paraplegia
HTT:	Huntingtin

IMM: inner mitochondrial membrane

IMS: intermembrane space

KIFs: kinesin superfamily proteins

KSS: Kearns-Sayre syndrome

LHON: Leber's hereditary neuropathy

lopo: low power

MB: Mushroom Body

MDS: mtDNA depletion syndrome

Mfn: mitofusin

MIRO: mitochondrial rho

MNGIE: mitochondrial neurogastrointestinal encephalomyopathy

MnSOD: manganese superoxide dismutase

MtDNA: mitochondrial DNA

mTERF: mitochondrial transcription termination factor

mtTFB1: mitochondrial transcription factor B1

mtTFB2: mitochondrial transcription factor B2

NMJ: neuromuscular junction

OA: optic atrophy

O_H: origin of replication for the heavy strand

O_L: origin of replication for the light strand

OMM: outer mitochondrial membrane

Opa1: optic atrophy 1

OXPHOS: oxidative phosphorylation

PD: Parkinson’s disease

PGC1-α: peroxisome proliferator-activated receptor-γ-coactivator 1-α

PI3K: phosphatidylinositol 3-kinase

POLRMT: mitochondrial RNA polymerase

RE: restriction enzyme

RIs: replication intermediates

ROS: reactive oxygen species

SCA: spinocerebellar ataxia

SDH: succinate dehydrogenase

SIM: structured illumination microscopy

SSBP: single strand binding protein

STED: stimulated emission depletion

T7 gp4: T7 gene 4 protein

TBP: TATA-box binding protein

TCA: tricarboxylic acid

TFAM: mitochondrial transcription factor A

TFB2M: mitochondrial transcription factor B2

TK2: thymidine kinase

TOPO: topoisomerase

TOR: target of rapamycin

TP: thymidine phosphorylase

Chapter 1. General introduction

1.1 Mitochondrial basics

1.1.1 The discovery of mitochondria

In 1897 Carl Benda first used the term “mitochondria” to describe granules, rods or filaments found in the cytoplasm of nearly all cells. These tiny structures were previously refered to as chondriosomes, chromidia, microsomes. The word mitochondria derives from the Greek words “mitos” meaning thread and “chondrin” meaning small grain. Mitochondria are organelles found in eukaryotic cells that are believed to be the result of a symbiotic event where an aerobic bacterium colonized a primordial eukaryotic cell that lacked the ability to use oxygen metabolically. This symbiotic relationship became permanent and these bacteria evolved into mitochondria, which allowed the cells to perform aerobic respiration to produce energy, together with anaerobic glycolysis (DIMAURO and SCHON 2003). The widely accepted hypothesis (although it has been questioned by some researchers) for the origin of mitochondria is endosymbiosis (MARGULIS 1970). It has been suggested that mitochondria evolved from eubacteria like precursors via endosymbiosis (LANG *et al.* 1997). More specifically members of the rickettsial subdivision of α-proteobacteria, a group of obligate intracellular parasites such as *Rickettsia*, *Anaplasma* and *Ehrlichia*, are considered to be the closest relatives of mitochondria (GRAY *et al.* 1999). The mechanism of this symbiotic event is not known, but could be linked to the increase in atmospheric oxygen (LANE 2005). One strong selective pressure for the evolution of mitochondria may have been the increase in oxygen in

the atmosphere and the oceans, which selected for new biochemical pathways needed to survive in the oxygen-rich environment. The advantage of having mitochondria lay in the fact that cells were able to use the newly available atmospheric oxygen to generate energy. In the original endosymbiotic hypothesis it was proposed that an early eukaryotic cell engulfed an aerobic eubacterium. There are several classes of single celled eukaryotes (all classified under the group archezoa, including *V.necatrix*, *Nosema*, *Entamoeba histolytica*, *Giardia lamblia*) that lack mitochondria, that would seem to support this hypothesis. However, studies over the last 15 years have shown that all extant eukaryotes that lack mitochondria that have been analysed did at one time contain mitochondria, which have subsequently been lost (discussed in (LANE 2005)). Therefore the evolution of mitochondria may have occurred simultaneously with the occurrence of eukaryotic cells and so may have been the defining event that allowed eukaryotic cells to proliferate and populate the planet (as proposed by Nick Lane, (LANE 2005)). Also there is now evidence the symbiotic event may have occurred between a methanogen (a bacteria that uses sulphur as a carbon source) and a eubacterium, which existed in an oxygen deficient environment. Whatever the origin of mitochondria there is a strong argument to suggest that they have been a major driving force in the shaping the evolution of multi-cellular life.

So why is this small organelle crucial for eukaryotic cells? The primary answer is summarized by one word: energy. It was first hypothesized in 1912 by B.F. Kingsbury that mitochondria were the respiratory centres of the cells (ERNSTER and SCHATZ 1981). This was proved to be the case in 1949 by Eugene Kennedy and Albert Lehninger, when they showed that respiratory enzymes are located in mitochondria (KENNEDY and LEHNINGER 1949). The primary function of mitochondria is to supply energy for the cell in the form of ATP and so they are often

referred to as the ‘power house’ of the cell. Most processes in cells depend in some way on the energy supplied by mitochondria. Mitochondria also have roles in biochemical pathways such as the citric acid cycle, β-oxidation of fatty acids, biosynthesis of haem and they are also key organelles regulating calcium signalling and apoptosis.

1.1.2 The structure and function of mitochondria

The double membrane structure of mitochondria reflects their function in ATP production and their architecture was revealed nearly half a century ago by electron microscopy (PALADE 1953). Mitochondria are formed of four compartments, the outer mitochondrial membrane (OMM), the inner mitochondrial membrane (IMM), the intermembrane space (IMS) and the matrix. The IMM is folded inside the matrix forming structures known as cristae (Figure 1.1). Electron microscopic images taken from cross sections of cells revealed the kidney-shaped or bean-shaped structure of mitochondria. However advances in confocal microscopy have shown that mitochondria are found in dynamic and interconnected networks (Figure 1.1) (BEREITER-HAHN 1990).

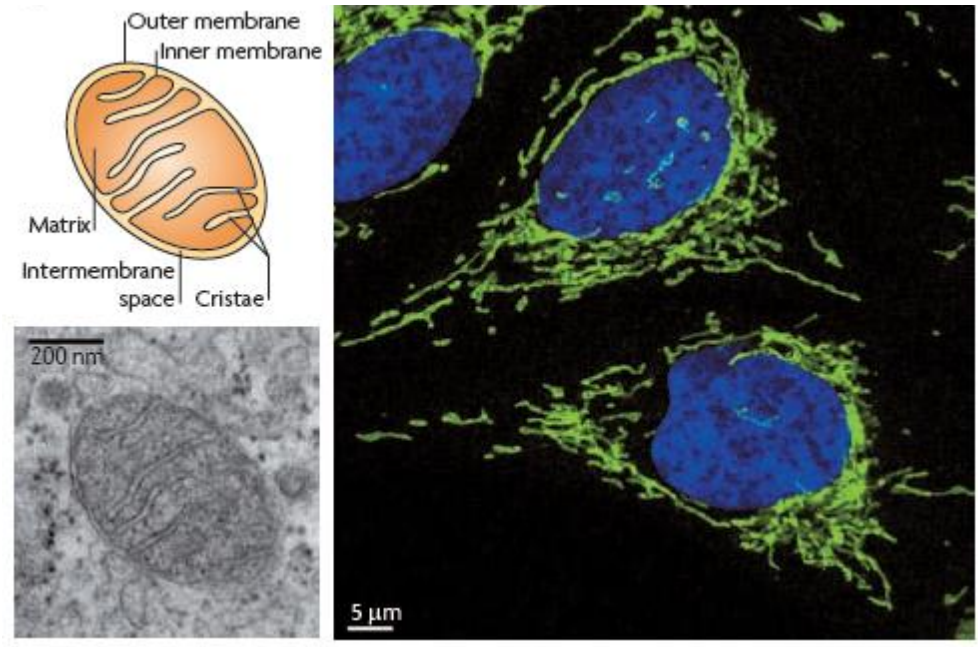

Figure 1.1 Structure of mitochondria.

Kidney shaped cartoon illustration shows the double membrane morphology and electron microscopy shows similar structures (on left). Immunofluorescence reveals the tubular and interconnected network (green). Adapted from Westermann 2010 (WESTERMANN 2010).

Oxidative phosphorylation (OXPHOS), is the process responsible for synthesizing ATP by the passage of electrons through the electron transport chain (ETC) (Figure 1.2). The ETC consists of five multiprotein complexes (complex I to complex V) and two electron carriers (coenzyme Q and cytochrome c) (Figure 1.2) (HATEFI 1985; SARASTE 1999). These complexes are located in the IMM and so the efficiency of the ETC is increased by the folded structure of the cristae, which increases the surface area of the IMM (PERIER and VILA 2012). The passage of electrons (derived from the oxidation of NADH and $FADH_2$ in intermediary metabolism) through the first four ETC complexes results in a proton gradient across mitochondrial membrane. More specifically, pumping of H^+ across the IMM by complex I (NADH hydrogenase),

complex III (cytochrome c reductase) and complex IV (cytochrome c oxidase) generates the proton gradient which allows complex V (ATP synthase) to use this proton gradient to convert ADP to ATP. ATP is transported to the cytosol by adenosine nucleotide translocators in the IMM and OMM (PERIER and VILA 2012). ATP synthesis via OXPHOS from the primary energy source glucose is advantageous for the cell compared to glycolysis. Glycolysis occurs in the cytosol and converts glucose to pyruvate resulting in production of 2 ATP molecules. However, once pyruvate is transported into mitochondria, it is converted into 8 NADH, 2 $FADH_2$ and 2 ATP molecules by the TCA (tricarboxylic acid) cycle. Energy stored in 8 NADH and 2 $FADH_2$ are converted into 32 ATP molecules by OXPHOS under optimal conditions (LIEMBURG-APERS *et al.* 2011). This shows that ATP production via OXPHOS is highly advantageous to eukaryotic cells compared to glycolysis. It is interesting to note that prokaryotes use the cellular membrane to generate a proton gradient that drives an ATP synthase and so this represents a universal mechanism for energy generation (Figure 1.2).

The action of the ETC also generates reactive oxygen species (ROS) via complex I and complex III. Under normal conditions antioxidant mechanisms such as the ROS-scavenging enzyme SOD2 (superoxide dismutase) functions to reduce ROS levels (ANDREYEV *et al.* 2005). ROS can damage various macromolecules including lipids, proteins and nucleic acids (MURPHY 2009). Complex I and complex III both have nuclear and mitochondrial encoded subunits and therefore mutations in both genomes can increase ROS production (FUKUI and MORAES 2009). Increased ROS production has also been linked to neurodegenerative diseases (see below).

The ETC complexes are multimeric complexes each formed of different number of subunits. Complex I is formed of 46 subunits, complex II (succinate dehydrogenase-

ubiquinone oxireductase) is much smaller and formed of 4 subunits, whereas complex III, IV and V are formed of 11, 14 and 16 subunits respectively. Most of the components of the OXPHOS system are encoded by the nuclear genome. However 13 of these components (in complex I, III, IV and V, but none of complex II) are encoded by the mitochondrial genome (Figure 1.2). Mitochondria are the only organelle in most animal cells to have their own genome, known as mitochondrial DNA (mtDNA). Correct assembly of the OXPHOS complexes is crucial for the function of the ETC and mutations in either of the nuclear or mitochondrial genome can result in mitochondrial respiratory chain diseases (reviewed in (DiMAURO and SCHON 2003; FERNANDEZ-VIZARRA *et al.* 2009)). OXPHOS deficiency can result in a wide range of phenotypes. Cells that cannot produce ATP using the OXPHOS system shunt pyruvate to lactate to produce ATP instead and this results in lactic acidosis (BREUER *et al.* 2012). Therefore aerobic respiration using the OXPHOS system is highly advantageous both for maintaining healthy cells and supplying enough energy.

The OXPHOS system, shown in figure 1.2, is formed of five separate complexes, however recent studies have demonstrated the existence of higher-order structures, so called "supercomplexes" (SHOUBRIDGE 2012). These respiratory supercomplexes are made up of two or more individual respratory chain complexes and can help to increase the efficiency of electron transport, control ROS levels, or increase individual complex stability (BOEKEMA and BRAUN 2007). Three independent studies characterized the Rcf1 protein as a supercomplex assembly factor (using baker's yeast) (CHEN *et al.* 2012; STROGOLOVA *et al.* 2012; VUKOTIC *et al.* 2012). This protein is a member of the hypoxia inducible group 1 (HIG1) family and has two human homologs, HIGD1A and HIGD2A. Rcf1 has roles in the assembly of the

complex III/complex IV supercomplex by incorporating peripheral complex IV subunits (cox13, the human coxVIa homologue) (CHEN *et al.* 2012; STROGOLOVA *et al.* 2012; VUKOTIC *et al.* 2012).

There are approximately 1500 proteins in the mitochondrial proteome (CALVO and MOOTHA 2010). The vast majority of these proteins are encoded by the nuclear genome and transported to mitochondria. However, 13 of these proteins are encoded by mtDNA. All of these 13 polypeptides encoded by mtDNA have roles in the OXPHOS system. The remaining OXPHOS proteins, which number around 100, are encoded by the nuclear genome. The remaining >1000 proteins in mitochondria are also encoded by the nuclear genome and function in processes such as maintenance and expression of mtDNA, mitochondrial protein synthesis, mitochondrial proteolysis, mitochondrial protein import, mitochondrial morphology, iron-sulfur cluster synthesis, citric acid cycle metabolism and fatty acid oxidation (LARSSON 2010). Therefore, the interplay between the nuclear and mitochondrial genome is vital to coordinate mitochondrial function (SMEITINK *et al.* 2001).

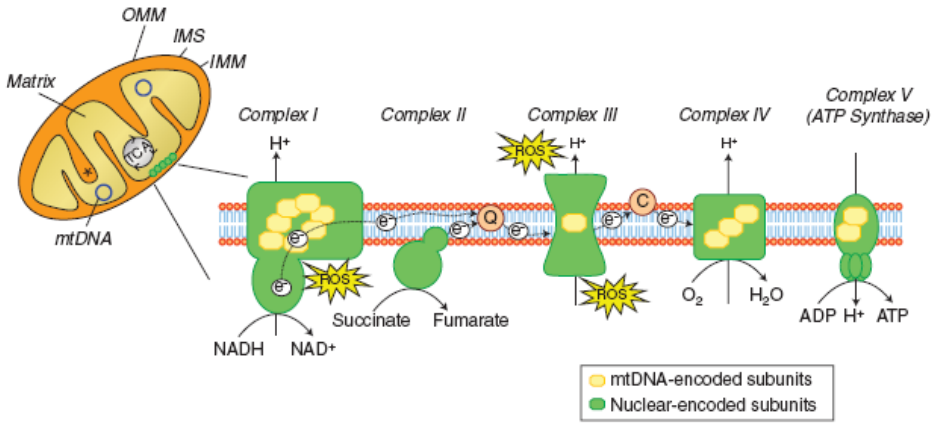

Figure 1.2 Schematic representation of mitochondrial ETC complexes.

The respiratory chain is localized in the inner mitochondrial membrane (IMM). The OXPHOS system is formed of approximately 100 proteins and 13 of them are encoded by mtDNA (shown in yellow). H^+ ions are pumped through the IMM and electrons are transported through the ETC complexes resulting in ATP synthesis. Adapted from Perier 2012(PERIER and VILA 2012).

1.2 The Mitochondrial Genome

1.2.1 General Properties of mtDNA

It is nearly 50 years since the discovery of mtDNA in chicken tissue sections by electron microscopy, where it was described as 'intramitochondrial fibrous material with DNA characteristics' (NASS and NASS 1963a; NASS and NASS 1963b). After the discovery of the mitochondrial genome, further studies showed the existence of DNA

in mitochondria in various different cell types and organisms. mtDNA has fundamentally the same evolutionarily conserved role in all eukaryotes, to encode a limited number of RNAs and proteins to maintain mitochondrial function (TZAGOLOFF and MYERS 1986).

Many of the nuclear encoded mtDNA related proteins are evolutionarily conserved. For example, sequence alignment of the mtDNA polymerase (Polγ) from multiple organisms (*S. cerevisiae*, *S. Pombe*, *P. pastoris*, *D. melonagaster*, *X. laevis* and *M. musculus*) showed that they exhibit sequence similarity and belong to the same family of polymerases (LECRENIER *et al.* 1997).

The size and structure of mtDNA was first reported over 40 years ago using mtDNA from human leukaemic leucocytes (CLAYTON and VINOGRAD 1967). Another keystone in mitochondrial research was the sequencing of the mtDNA, which was considered as the initiation of the Human Genome Project (ANDERSON *et al.* 1981; ANDREWS *et al.* 1999). Although the function of mtDNA is conserved, it has variations in conformation, size, as well as gene content and expression between species (CUMMINGS 1992). For example, genome size varies between <6kb in the human malaria parasite to >200 kb in land plants, due mostly to variation in the size of the noncoding D-loop region (GRAY *et al.* 1999). The human mitochondrial genome is a circular, double-stranded 16,569bp molecule (Figure 1.3) (ANDERSON *et al.* 1981). Human mtDNA is compact and very gene-dense containing 37 genes of which 13 encode components of the OXPHOS system, 22 are tRNAs and 2 are rRNAs required for translation of the 13 polypeptides (FALKENBERG *et al.* 2007). There are no introns in mtDNA genes and non-coding bases between genes are very few. The only non-coding region is the D-loop, which contains control elements for mtDNA replication and transcription and is 1.1kb in human mtDNA (SHADEL and

CLAYTON 1997). The two strands of the mtDNA are known as the heavy (H) and the light (L) strand and each has a different pyrimidine versus purine content (ANDREWS *et al.* 1999).

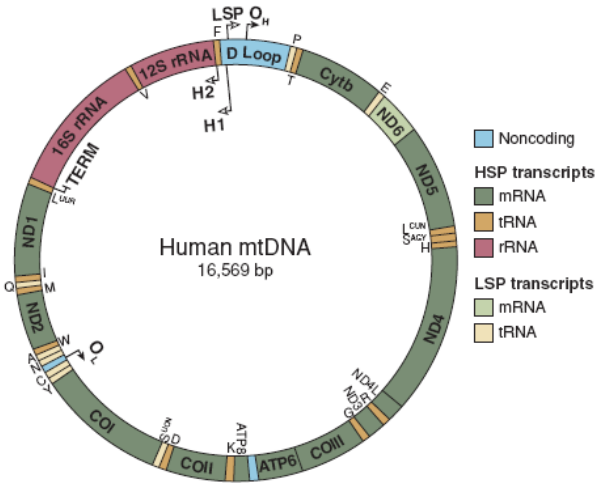

Figure 1.3 Map of human mtDNA.

The D-Loop is the non-coding region (shown in blue). The genes encoded by mtDNA are shown in different colours depending on whether they are encoded on the heavy strand or the light strand Adapted from Falkenberg 2007(FALKENBERG *et al.* 2007).

1.2.2 Mitochondrial transcription and translation

Mitochondrial transcription and translation (Figure 1.4) are dependent on the nuclear genome since the proteins needed for these processes are encoded by nuclear DNA and imported into mitochondria (FALKENBERG *et al.* 2007). Mitochondria have their own ribosomes, which are structurally similar to bacterial ribosomes (RORBACH *et al.* 2007). Transcription of mtDNA is also important for mtDNA replication as it produces RNA primers required for the initiation of mtDNA replication at the O_H

replication origin (FALKENBERG *et al.* 2007). The core proteins required for mitochondrial transcription are mitochondrial RNA polymerase (POLRMT), mitochondrial transcription factor B2 (TFB2M) and mitochondrial transcription factor A (TFAM) (FALKENBERG *et al.* 2002). These three proteins are necessary for transcription of mtDNA encoded genes, while other factors modulate the activity of this process, such as mitochondrial transcription termination factors (MTERF1-4) (LINDER *et al.* 2005). TFAM is of particular importance as POLRMT and TFB2M will not even initiate transcription in the absence of TFAM (GASPARI *et al.* 2004). Moreover, recombinant TFAM together with partially purified POLRMT is sufficient for transcription activation in vitro (DAIRAGHI *et al.* 1995; FALKENBERG *et al.* 2002).

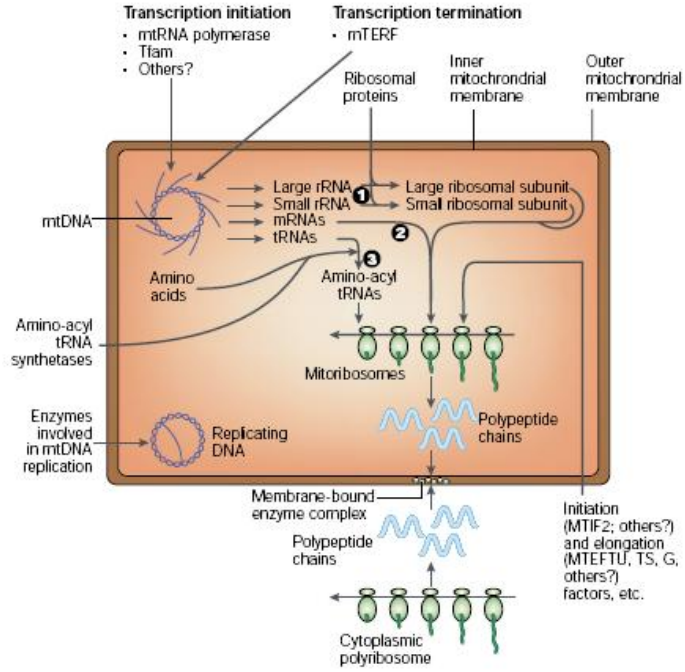

Figure 1.4 mtDNA transcription and translation

Nuclear encoded factors are needed for mtDNA replication and transcription. There are 13 mRNAs, 22tRNAs and 2 rRNAs (12S and 16S rRNA) transcribed from mtDNA. 2 rRNAs and other nuclear encoded ribosomal proteins make mitoribosomes. Various other nuclear encoded factors are transported into mitochondria to synthesize the 13 polypeptides. This process is composed of three steps: posttranscriptional modification (1), polyadenylation (2) and tRNA processing (3). Adapted from Smeitink 2001(SMEITINK *et al.* 2001).

1.2.3 MtDNA replication

MtDNA is maternally inherited and the copy number in each cell varies between tissues depending on the energy demand (TAYLOR and TURNBULL 2005). In order to have an adequate mtDNA copy number it has to be replicated at a rate required to meet the energetic needs of the cell. The mitochondrial DNA polymerase, Polγ, is the

sole DNA polymerase in mitochondria and is found in a heterotrimeric form, consisting of the catalytic subunit Polγ-α and the dimeric accessory subunit Polγ-β (KAGUNI 2004). The catalytic subunit is 140 kDa in size and has 3'-5' exonuclease and 5' dRP (5'-deoxyribose phosphate) lyase activity. Together with this activity, Polγ catalyzes the release of the 5' terminal sugar from apurinic/apyrimidinic sites and fills the single nucleotide gap by generating a substrate for DNA ligase (LONGLEY *et al.* 1998). The accessory subunit is 55 kDa in size and is needed for tight DNA binding and processive DNA synthesis (GRAZIEWICZ *et al.* 2006; LIM *et al.* 1999). A DNA helicase, Twinkle, that unwinds mtDNA in the 5' to 3' direction is also required for mtDNA replication (KORHONEN *et al.* 2003). The mtDNA single stranded binding protein (SSBP) stabilizes the single strand once it is unwound by Twinkle (VAN TUYLE and PAVCO 1985). The core factors needed for the mtDNA replication are Polγ-α, Polγ-β, Twinkle and SSBP (Figure 1.5). The mtDNA replisome consists of these proteins and has been shown to be sufficient to synthesize mtDNA in vitro (KORHONEN *et al.* 2004).

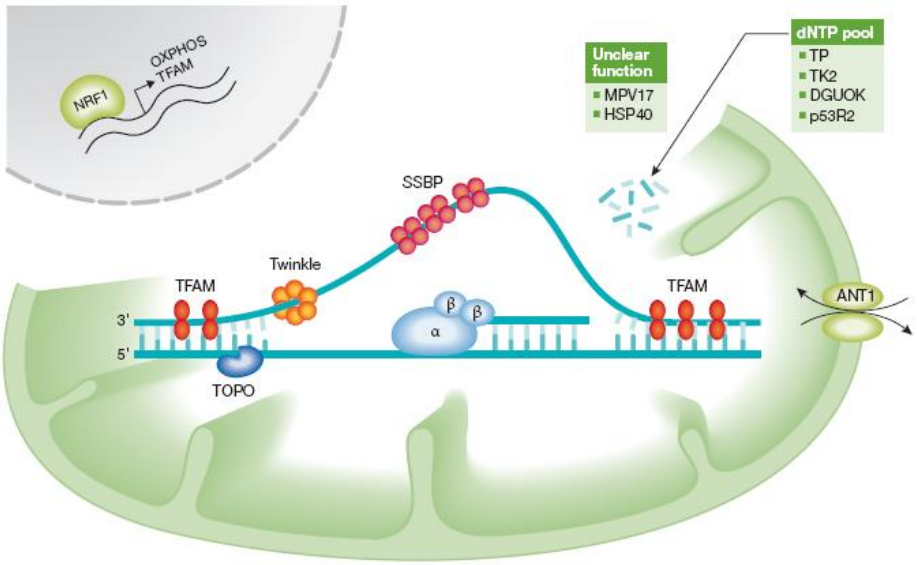

Figure 1.5 The mtDNA replication fork.

Diagram shows the factors needed for replication and maintenance of mtDNA, which all are encoded by the nuclear genome and are transcriptionally regulated by NRF1. The replication fork consists of mtDNA (in blue) and factors that have a direct role in mtDNA replication: Polγ (α and β subunits), Twinkle (helicase), SSBP (single strand binding protein), TOPO (topoisomerase) and TFAM (mitochondrial transcription factor A). The mitochondrial dNTP pool is supplied by TP (thymidine phosphorylase), TK2 (thymidine kinase 2), DGUOK (deoxyguanosine kinase) and p53R2 (ribonucleotide reductase subunit). There are other factors such as MPV17 (a mitochondrial membrane protein) and HSP40 (a mitochondrial chaperone) which when inactivated can inhibit mtDNA replication. Adapted from Tynissima 2009 (TYYNISMAA and SUOMALAINEN 2009).

The mechanism of mammalian mtDNA replication is under debate. There are two possible models, the strand-displacement model and the strand coupled model (Figure 1.6) (BOGENHAGEN and CLAYTON 2003b). The strand-displacement model, based on data from electron microscopy and end-mapping of mtDNA (CLAYTON 1982), states that replication begins with the leading-strand (known as the heavy

strand because it is guanine rich) synthesis from O_H (origin of replication for the heavy strand) proceeding for a significant distance before the initiation of lagging strand synthesis. Lagging strand (also known as the light strand) synthesis starts from O_L (origin of replication for the light strand), which is exposed when two thirds of the genome has been replicated by leading strand synthesis. This mode of replication does not result in Okazaki fragments and is therefore classified as unidirectional, continuous and asymmetric (BOGENHAGEN and CLAYTON 2003a; BOGENHAGEN and CLAYTON 2003b; LARSSON 2010). The bidirectional model was developed through studies using 2DAGE (2D-gel electrophoresis) (HOLT *et al.* 2000; REYES *et al.* 2005; YANG *et al.* 2002). This technique is based on application of restriction-enzyme digested DNA to a native gel, firstly in the absence of ethidium bromide (EtBr; the first dimension) and then in the presence of EtBr (the second dimension) (BREWER and FANGMAN 1987). Three types of patterns were observed when 2DAGE was used to analyse mtDNA replication: (i) spots, which represent fragments that are not involved in replication, (ii) Y-arcs, which represents fragments involved in replication and do not contain an origin and (iii) bubble-arcs, which represent fragments containing replication origins (O_H and O_L). This showed that one class of replication intermediates (RIs) was resistant to single strand nuclease digestion and mobility of these RIs represents coupled leading and lagging strand synthesis (HOLT *et al.* 2000). Both the models have both supporting and contradictory data and more work needs to be done in order to understand if the differences observed are real or experimental artefacts (STUMPF and COPELAND 2011). It is possible that both modes of replication could exist depending on the organism, tissue/cell type or energy requirements.

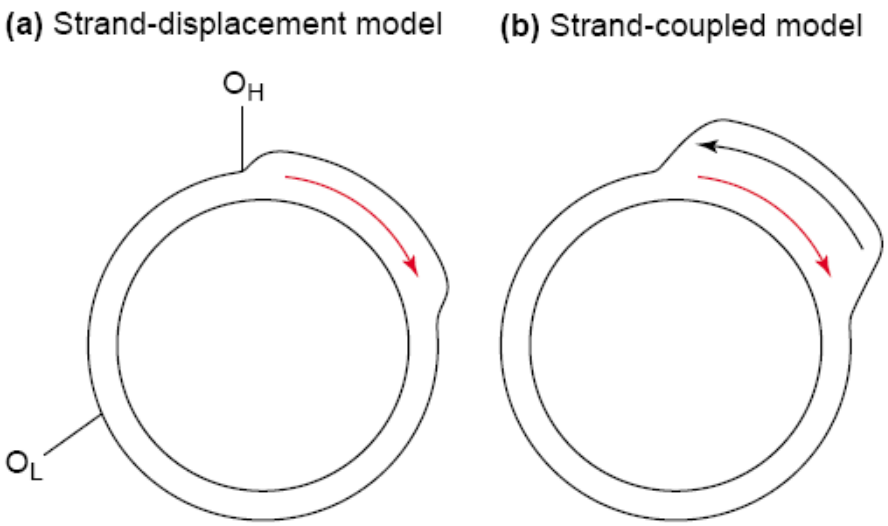

Figure 1.6 Two models of mtDNA replication.

(a) mtDNA replication starts unidirectionally from O_H and as the leading strand (red) reaches the O_L, lagging strand synthesis starts. (b) Lagging strand synthesis can be initiated at multiple sites and can result in discontinuous synthesis of Okazaki fragments. Adapted from Bogenhagen 2003 (BOGENHAGEN and CLAYTON 2003b).

1.2.4 The mtDNA nucleoid

Understanding the morphological features of mtDNA was one of the milestones in mtDNA research. mtDNA is not naked but is found in nucleoprotein complexes called nucleoids (GARRIDO *et al.* 2003). The precise number of proteins interacting with and maintaining mtDNA is not known, but may be around 30 (CHEN and BUTOW 2005). Cross-linking studies have been used to identify nucleoid proteins in yeast, *xenopus* and HeLa cells (BOGENHAGEN *et al.* 2003; KAUFMAN *et al.* 2000; WANG and BOGENHAGEN 2006). These studies identified known DNA binding proteins and replication factors, but also several metabolic proteins not previously

thought to interact with mtDNA. However, several of these 'bifunctional proteins' have been shown to be required for mtDNA maintenance and to directly bind mtDNA (BATEMAN *et al.* 2002a; BATEMAN *et al.* 2002b; CHEN and BUTOW 2005). These studies identified and classified nucleoid proteins based on their co-purification with mtDNA after formaldehyde cross-linking. In contrast, Larsson suggested much stricter criteria for the characteristics of nucleoid proteins : (i) the protein should interact with mtDNA (by copurification or cross-linking); (ii) the protein should have intrinsic biophysical properties consistent with packaging DNA; (iii) the protein should be sufficiently abundant to coat mtDNA; (iv) the protein should colocalize with mtDNA by high-resolution microscopy; (v) the protein should be essential for maintenance of mtDNA in vivo (PARK and LARSSON 2011). To date TFAM is the only protein that fulfils all of these criteria (ALAM *et al.* 2003; PARK and LARSSON 2011). Apart from its roles in mitochondrial transcription TFAM packages mtDNA (ALAM *et al.* 2003). Human TFAM is a 25.6kDa high mobility group (HMG) protein, since it has two HMG boxes (Figure 1.7A) (KANKI *et al.* 2004; PARISI and CLAYTON 1991; RUBIO-COSIALS *et al.* 2011). The yeast homologue of TFAM, ABF2, can bend, unwind and package DNA (FISHER *et al.* 1992; KAUFMAN *et al.* 2007). Studies in mice have shown that there is one TFAM molecule per 10-20 bp of mammalian mtDNA (EKSTRAND *et al.* 2004; PELLEGRINI *et al.* 2009). More precise visualization and calculations showed that there is one TFAM molecule per 16.6 bp of mtDNA (KUKAT *et al.* 2011). The mechanism of packaging of mtDNA by TFAM has been investigated using X ray crystallography. These studies showed that TFAM shapes mtDNA, forcing a U-turn in the DNA by reversing the direction of DNA helix (NGO *et al.* 2011; RUBIO-COSIALS *et al.* 2011). To achieve this, the two HMG boxes in TFAM bend DNA 90^0 each and the linker

region interacts with the bent DNA resulting a reversal in direction. It is also believed that this bending of mtDNA by TFAM can result in organizing the transcription initiation complex, similar to the role of the TATA-box binding protein (TBP) in nuclear transcription. More specifically, this results in placing the C-terminus of TFAM (which is important for transcription activation) close to the transcription start site, which is occupied by the POLRMT-TFB2M complex (DAIRAGHI *et al.* 1995; HALLBERG and LARSSON 2011; SOLOGUB *et al.* 2009). Future studies will further elucidate the dual-role of TFAM in mtDNA nucleoid structure and mtDNA transcription, but the current model is shown in figure 1.7B.

In order to understand mtDNA organization and dynamics various tools have been used to visualize mtDNA nucleoids. A GFP tagged form of the Twinkle helicase was found to colocalise with mitotracker, which is a mitochondrial specific dye (SPELBRINK *et al.* 2001). TFAM and mtSSB have also been shown in imaging studies to colocalise with nucleoids (GARRIDO *et al.* 2003). Other studies reported that mtDNA nucleoids are punctate structures which are enriched in TFAM, as shown in figure 1.7C (LEGROS *et al.* 2004). Antibody staining against DNA showed an overlapping staining pattern with TFAM puncta (LEGROS *et al.* 2004). These studies all used confocal microscopy to visualise nucleoids and nucleoid proteins. Confocal microscopy is limited by the diffraction limit of light and so cannot accurately resolve structures below approximately 0.5 μm, which is the upper range of the size of mtDNA nucleoids. Super-resolution microscopy has therefore been used to more accurately determine the characteristics of nucleoids. Two studies have used this approach, one using stimulated emission depletion (STED) microscopy (KUKAT *et al.* 2011) and another using structure illumination microscopy (SIM) (KOPEK *et al.* 2012). In the study carried out by Kukat and co-workers, it was shown that nucleoids

have a uniform size of around 100 nm, in cultured mammalian cells, compared with 300 nm measured by confocal microscopy and that there is usually one copy of mtDNA (average 1.4 molecules) per nucleoid (KUKAT *et al.* 2011). This was surprising as it had been reported previously that each nucleoid contains multiple copies of the mitochondrial genome, such as 6 to 10 copies (IBORRA *et al.* 2004), 2 to 8 copies (LEGROS *et al.* 2004) or 5 copies (GILKERSON *et al.* 2008). The finding of a single copy per nucleoid is consistent with the so-called "faithful" model of mtDNA inheritance, which posits that nucleoids do not exchange DNA with each other (GILKERSON *et al.* 2008; KUKAT *et al.* 2011). Furthermore, studies performed by Kopek and Brown have shown that nucleoids can vary in size resulting from differences in sample preparation and labelling techniques (e.g. antibody labelling versus protein fusions) (BROWN *et al.* 2011; KOPEK *et al.* 2012). Future studies will be required to directly compare results obtained using different super-resolution techniques, and importantly, to study the properties of nucleoids in vivo, rather than in cultured cells.

A

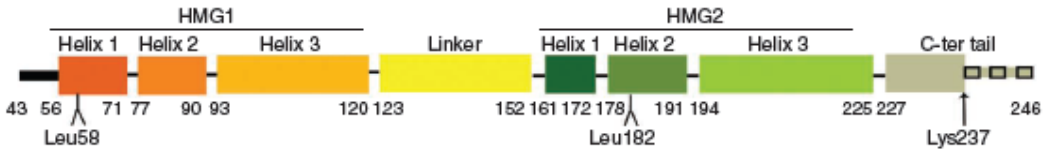
HMG1
HMG2
Helix 1
Helix 2
Helix 3
Linker
Helix 1
Helix 2
Helix 3
C-ter tail
43 56 71 77 90 93 120 123 152 161 172 178 191 194 225 227 246
Leu58
Leu182
Lys237

B

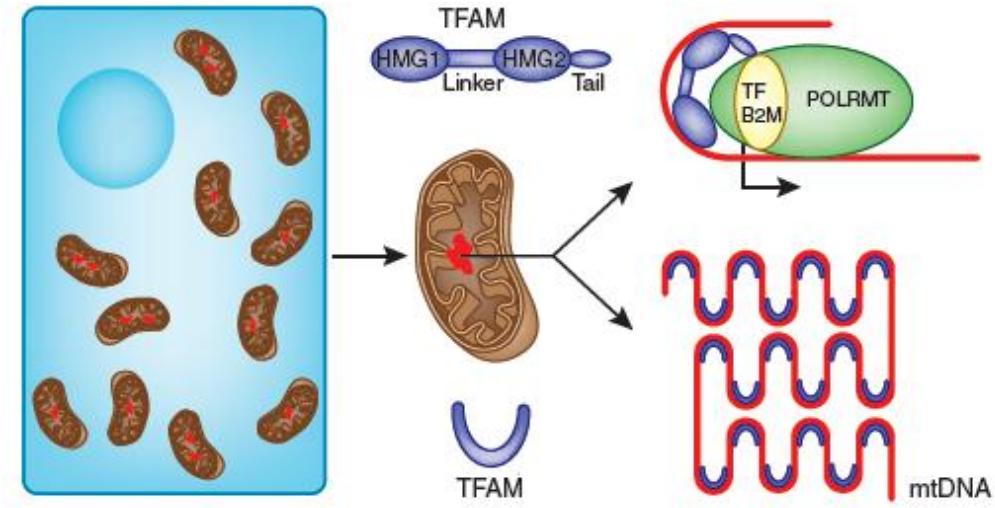
TFAM
HMG1
HMG2
Linker
Tail
TF
B2M
POLRMT
TFAM
mtDNA

C

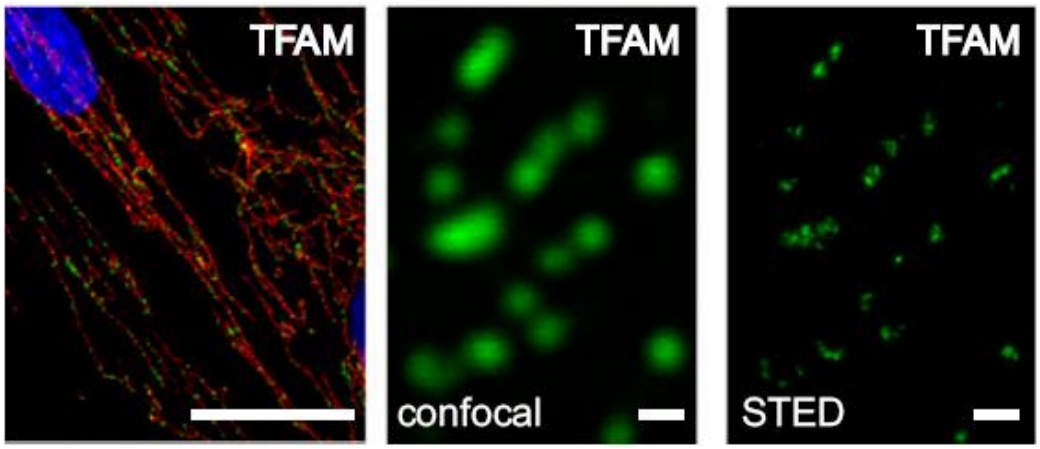
TFAM
TFAM
confocal
TFAM
STED

Figure 1.7 The structure and localization of TFAM.

(A) The structure of TFAM protein (adapted from Rubio-Cosials 2011). **(B)** TFAM packages mtDNA by introducing U-turns (adapted from Hallberg 2011). **(C)** TFAM is associated with nucleoids. Green is TFAM staining, red is TOM20 staining showing the mitochondrial network and blue is nuclear staining using DAPI. Differences in the resolution using confocal and STED microscopy are compared. Adapted from Kukat 2011(KUKAT *et al.* 2011).

1.3 Mitochondrial dynamics and mitochondrial diseases

1.3.1 Mitochondrial diseases

Mitochondrial dysfunction can lead to human disease and mitochondrial disorders are one of the most common inherited disorders of metabolism (SCHAEFER *et al.* 2008). Recent studies have described the prevalence of mitochondrial disease to be around at least 1 in 5,000 (YLIKALLIO and SUOMALAINEN 2011). The first disease described as a mitochondrial disorder was a case of hypermetabolism with defects in the maintenance of mitochondrial respiratory control (LUFT *et al.* 1962). The symptoms of mitochondrial diseases are very diverse, reflecting the broad function of mitochondria in different tissues. Transmission of mitochondrial diseases can be maternal, autosomal or X-linked due to the dual control of the organelle by nuclear and mitochondrial genomes. Since most of the mitochondrial proteins are encoded by the nuclear genome, most of the mitochondrial diseases are caused by defects in

nuclear encoded proteins. I will firstly summarize the mechanisms causing mitochondrial diseases and then focus specifically on mtDNA related disorders.

In addition to its roles in the biosynthesis of amino acids and steroids, oxidation of fatty acids and apoptosis, the main function of the mitochondrion is to produce ATP through the combined efforts of the TCA and OXPHOS systems. Most of the syndromes characterized as mitochondrial diseases result from OXPHOS defects and clinical symptoms include neuronal seizures, myoclonus ataxia, progressive muscle weakness, stroke-like episodes and cognitive impairment (DiMAURO and SCHON 2003). Mitochondrial dysfunction has been implicated in various neurodegenerative diseases including Alzheimer's disease (AD), amyotrophic lateral sclerosis (ALS), Charcot-Marie-Tooth disease (CMT), Huntington's disease (HD), hereditary spastic paraplegia (HSP), optic atrophy (OA), Parkinson's disease (PD) and spinocerebellar ataxia (SCA) (SCHON and PRZEDBORSKI 2011).

The dynamic nature of mitochondria is very important for the regulation of cellular redox status, mtDNA integrity, organellar function and cell death (LIESA *et al.* 2009). Defects in the proteins involved in mitochondrial dynamics can result in developmental abnormalities, neuromuscular degeneration and metabolic disorders (CHEN and CHAN 2009). Mitochondrial transport, fusion and fission of mitochondria and mitochondrial turnover are the main processes important for the dynamic nature of the mitochondrial network (Figure 1.8).

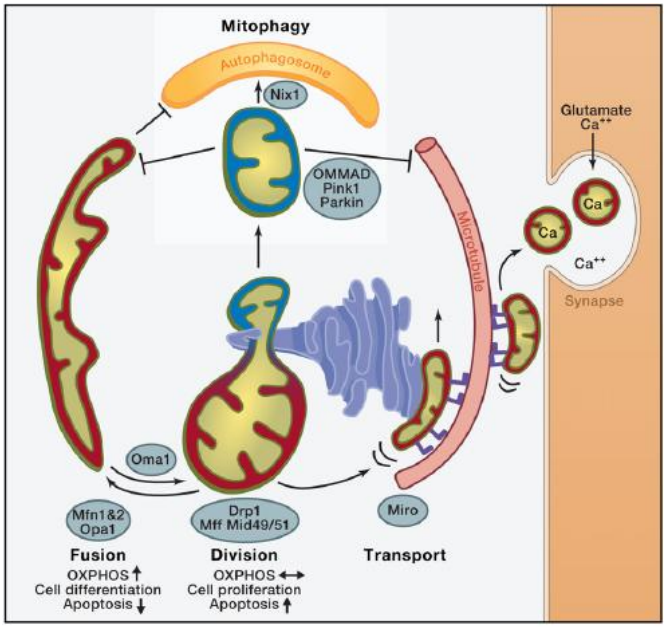

Figure 1.8 Roles of mitochondrial dynamics.

The processes that regulate the dynamic nature of mitochondria are fusion, fission (division), transport and mitophagy. Mitochondria with high membrane potential are shown in red and the ones with low membrane potential are in blue. Factors/proteins having roles in these processes are shown in blue circles. Adapted from Nunnari 2012(NUNNARI and SUOMALAINEN 2012).

1.3.2 Mitochondrial transport

One of the key advances in the understanding of mitochondrial dynamics was the investigation of mitochondria using live imaging microscopy. These studies showed that mitochondria are motile organelles which move along the cytoskeleton (HOLLENBECK and SAXTON 2005). Mitochondrial dynamics in neurons is of particular importance since neurons have a highly polarised morphology and each compartment has different energy requirements. The main compartments of the

neuron are the cell body (soma), the axon, the dendrites and the synapse. The areas with particularly high energy demands are the presynaptic and postsynaptic terminals, active growth cones or axonal branches and the nodes of Ranvier, which contain more mitochondria than other parts of the cell (SHENG and CAI 2012).

Axonal anterograde and retrograde transport of mitochondria occur along microtubules using multiple kinesin family members and cytoplasmic dynein molecules. Apart from this bidirectional movement, mitochondria frequently change direction, pause or switch to persistent docking (SHENG and CAI 2012). This allows the cell to transport healthy mitochondria generated in the soma to the parts of the neuron with high energy demands and metabolic requirements. Mitochondrial transport is an essential process for neuronal development and defects can contribute to neurodegenerative diseases such as AD (RUTHEL and HOLLENBECK 2003; STOKIN and GOLDSTEIN 2006). Two classes of proteins with important roles in mitochondrial transport are the kinesin superfamily proteins (KIFs) and the cytoplasmic dyneins. KIF5 (also known as kinesin1) has roles in anterograde transport (CAI *et al.* 2005). In *Drosophila* Milton is a well characterized motor adaptor protein that interacts with KIF5 and mitochondrial rho (MIRO) (a RHO family GTPase on the mitochondrial outer membrane) and takes part in anterograde mitochondrial transport. Mutations in *MIRO* cause depletion of mitochondria in distal synaptic terminals (GORSKA-ANDRZEJAK *et al.* 2003; GUO *et al.* 2005; STOWERS *et al.* 2002).

1.3.3 Mitochondrial fusion and fission

The main processes regulating mitochondrial shape and size are fission and fusion. Continuous cycles of fission and fusion are controlled by conserved fission and fusion promoting factors. The fusion promoting factors in humans are the mitofusins (Mfn1 and Mfn2) and optic atrophy1 (Opa1), whereas fission is mainly regulated by dynamin-related protein 1 (Drp1). Drp1 is a cytosolic protein, while Opa1 and Mfn localise to the inner and outer mitochondrial membrane respectively (DETMER and CHAN 2007). The balance between these proteins determines the morphology of mitochondria throughout the cell. Mutations in fusion-related proteins have been linked with several diseases, such as mutations in Mfn2, which result in Charcot-Marie-Tooth type 2A (CMT2A) that affects sensory and motor neurons (ZUCHNER *et al.* 2004). Additionally, autosomal dominant optic atrophy (DOA), which results in degeneration of retinal ganglia cells, can be caused by mutations in *OPA1* (ALEXANDER *et al.* 2000; DELETTRE *et al.* 2000). Mutations in the Mfns and Opa1 in mice cause embryonic lethality and mitochondrial dysfunction (ALAVI *et al.* 2007; CHEN *et al.* 2003; DAVIES *et al.* 2007). In yeast decreased fission result in longitudinal and interconnected tubular mitochondria, whereas decreased fusion results in fragmented mitochondria (SESAKI and JENSEN 1999).

The correct functioning of mitochondrial dynamics is crucial for the segregation and transmission of mtDNA. Early studies carried out in yeast showed that mutations in Fzo1p and Mgm1p (Mfns and Opa1 orthologs) caused loss of mtDNA (HERMANN *et al.* 1998; RAPAPORT *et al.* 1998). Studies in mammals showed similar results in that the fusion proteins Mfns and Opa1 are required for mtDNA maintenance (CHEN *et*

al. 2007). It has also been reported that depletion of Drp1 results in mitochondrial dysfunction through mtDNA loss (PARONE *et al.* 2008). One explanation for the loss of mtDNA in these mutants is that mitochondrial fusion increases the tolerance of cells to mutant mtDNA and protects the integrity of mtDNA through intermolecular exchange (SEO *et al.* 2010). Fission and fusion may also have general protective effects on the mitochondrial network by buffering of the matrix contents (including mtDNA) (CHEN *et al.* 2007; CHEN *et al.* 2010).

1.3.4 Mitochondrial turnover

Mitochondrial turnover is controlled by two processes: mitochondrial biogenesis and mitochondrial specific autophagy (mitophagy). It is generally believed that mitochondrial biogenesis is inefficient in aged individuals (FANNIN *et al.* 1999; SUGIYAMA *et al.* 1993). Mitochondrial biogenesis can be adjusted by physiological stimuli such as exercise and calorie restriction. The major regulatory pathway for mitochondrial biogenesis is through the peroxisome proliferator-activated receptor-γ-coactivator 1α (PGC1-α) (SCARPULLA 2008; WU *et al.* 1999), and downstream of this includes the estrogen-related receptor-α (ERR-α), NRF-1, NRF-2 and Mfn2 (CARTONI *et al.* 2005; SORIANO *et al.* 2006). Figure 1.9 shows the relationship between fusion/fission, mitochondrial biogenesis and mitophagy and highlights the interplay between these events (SEO *et al.* 2010).

Degradation of dysfunctional mitochondria is a key process in maintaining a robust mitochondrial network. Cells eliminate dysfunctional and damaged mitochondria

through the autophagic process, which involves lysosomal degradation of cellular components by hydrolytic enzymes (HE and KLIONSKY 2009). One of the main functions of autophagy is to supply recycled molecules to the cell under nutrient deprivation. Autophagy also functions as a quality control mechanism by degrading dysfunctional organelles and protein aggregates. In mitophagy, defective mitochondria are labelled by other proteins that are recognised by the autophagy machinery. It has been shown in yeast that this process is independently regulated from bulk autophagy (KANKI and KLIONSKY 2008). Dysfunctional mitochondria have low membrane potential and presumably high ROS levels due to a dysfunctional OXPHOS system, which results in their elimination by the autophagic machinery (TWIG and SHIRIHAI 2011). The mitochondrial fusion/fission machinery is closely linked to mitophagy, such that loss of fusion or increased fission correlates with increased mitophagy; overexpression of Drp1 results in mitophagy under pro-apoptotic stimuli (ARNOULT *et al.* 2005). Although fission is an important process for the clearance of mitochondria, it is hypothesized that it is permissive for mitophagy rather than directly activating it, since only a small percentage of fragmented mitochondria are cleared by mitophagy (TWIG *et al.* 2008b). Several studies have shown that increased fission, via Opa1 knockdown, can result in reduced mitochondrial size and increased autophagy (CHEN and CHAN 2005; CIPOLAT *et al.* 2004). Mitochondrial fusion is also implicated in quality control as it can blunt or eliminate the deleterious effects of misfolded proteins or mutant mtDNA by mixing rare dysfunctional mitochondria with a functional network (GILKERSON *et al.* 2008; TWIG and SHIRIHAI 2011). Defects in proteins responsible for mitochondrial quality control can result in neurodegenerative disease and will be explored in detail in the next section.

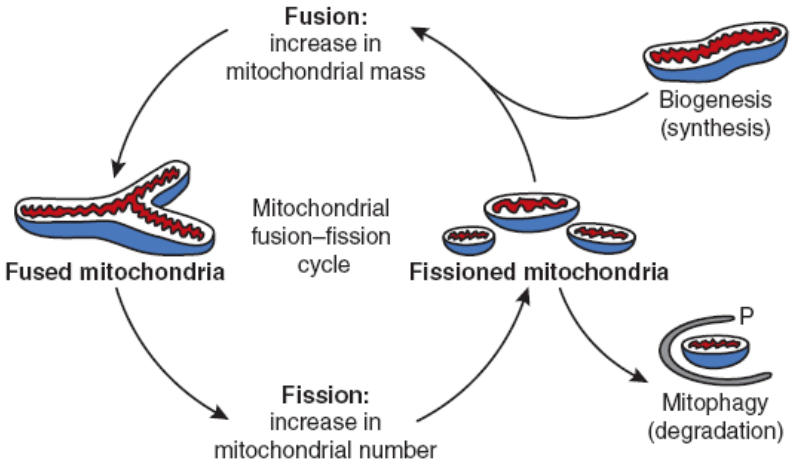

Figure 1.9 Mitochondrial turnover.

The relationship between the continuous fission/fusion cycle with biogenesis and degradation of mitochondria are represented by arrows. Adapted from Seo 2010 (SEO *et al.* 2010).

1.3.5 Mitochondrial dysfunction in neurodegenerative diseases

The brain is particularly dependent on mitochondrial generated energy since it represents 2% of body weight but consumes 20% of the available oxygen (COSKUN *et al.* 2012). Mitochondrial morphology and localisation in neurons is highly regulated and reflects the energetic requirements of specific compartments. As in other cell types, fusion/fission, transport and mitophagy regulate mitochondrial morphology and localisation in neurons (Figure 1.9). Mitochondrial defects in neurons will deplete energy levels and eventually result in neuronal dysfunction and apoptosis.

Mitochondrial dysfunction and abnormalities in the dynamics of mitochondria have been reported in neurodegenerative diseases such as AD, HD, ALS and PD (reviewed in (SHENG and CAI 2012)). Figure 1.10 is a schematic representation showing neurodegenerative diseases caused by defects in mitochondrial dynamics. One of the hallmarks of AD is the accumulation of β-amyloid (Aβ) containing plaques derived from APP (amyloid precursor protein). It has been reported that overexpression of APP in neurons results in mitochondrial fragmentation as a result of alterations in fusion/fission proteins (WANG *et al.* 2008). Furthermore, defects in mitochondrial axonal transport have been implicated in AD (STOKIN and GOLDSTEIN 2006; WANG *et al.* 2009). HD is caused by mutations in the *Huntingtin* gene (*HTT*) and results in impaired energy metabolism, abnormal Ca^{2+} signalling and changes in mitochondrial membrane potential and mitochondrial structure (SEO *et al.* 2010). It was also reported that mutations in *HTT* can affect fusion/fission by altering Drp1 localization (BOSSY-WETZEL *et al.* 2008). The HTT protein has been proposed to act as a molecular switch for organellar transport in neurons as a positive regulator of vesicular transport. Anteriograde transport is promoted when HTT is phosphorylated by Akt at serine 421 causing recruitment of kinesin-1, whereas un-phosphorylated HTT results in promotion of retrograde transport (COLIN *et al.* 2008). In support of this, mutations in HTT result in impaired axonal transport of mitochondria in neurons (CHANG *et al.* 2006; ORR *et al.* 2008; SONG *et al.* 2011; TRUSHINA *et al.* 2004).

Another widely studied neurodegenerative disease is PD, which in the inherited form can be caused by defects in Parkin (PARK) and PINK1 (DODSON and GUO 2007). PD is the second most common neurodegenerative disease and is characterized by degeneration of dopaminergic neurons in the substantia nigra (EXNER *et al.* 2007). The *PINK1* gene encodes a mitochondrially targeted Ser/Thr kinase and *parkin*

encodes an E3 ubiquitin-protein ligase. Some fraction of PINK1 protein is localized to mitochondria, while Parkin is mainly cytoplasmic (WHITWORTH and PALLANCK 2009; ZHOU *et al.* 2008). More specifically, mutations in *Park2* (which encodes Parkin) can cause the most common form of autosomal recessive juvenile parkinsonism (KITADA *et al.* 1998). In a *Drosophila* model of PD, *parkin* mutants were shown to cause dopaminergic cell loss (WHITWORTH *et al.* 2005). Furthermore, knockout of *pink* and *parkin* in *Drosophila* cause muscle degeneration and enlarged mitochondria (CLARK *et al.* 2006; GREENE *et al.* 2003) by promoting mitochondrial fission (DENG *et al.* 2008; POOLE *et al.* 2008). *PINK1* knockdown in mouse dopaminergic neurons also results in swollen mitochondria (WOOD-KACZMAR *et al.* 2008). However, in human PD patient *PINK1* mutant fibroblasts fragmented mitochondria were reported, suggesting increased fission. Furthermore the same study showed that reduction of *PINK1* in HeLa cells affected mitochondrial morphology and membrane potential and that this could be rescued by expression of *parkin* (EXNER *et al.* 2007). PINK1 and Parkin are also involved in mitochondrial quality control mechanisms (DAGDA and CHU 2009; NARENDRA *et al.* 2008; POGSON *et al.* 2011; WHITWORTH and PALLANCK 2009). It has been shown that Parkin can be selectively recruited to damaged mitochondria with decreased membrane potential and this leads to mitophagy (NARENDRA *et al.* 2008). This suggests that mutations in *Parkin* in PD patients may cause dysregulation of mitochondrial quality control. Furthermore PINK1 forms a complex with MIRO-Milton, which in turn can affect transport of mitochondria (WEIHOFEN *et al.* 2009). MIRO, which is a component of motor/adaptor complex on the mitochondrial surface can be phosphorylated by PINK1, which subsequently activates proteasomal degradation of MIRO in a Parkin-dependent manner. Removal of MIRO also prevents mitochondrial movement and

results in quarantine of mitochondria prior to their clearance (KANE and YOULE 2011; WANG *et al.* 2011). This shows the importance of PINK1 to label damaged mitochondria and prevent more global damage to other parts of the cell by blocking their transport. However, mitochondrial abnormalities in a mouse *TFAM* knockout were not dependent on Parkin activity; this will be discussed further in section 1.5.3. Therefore the importance of PINK1/Parkin still needs to be confirmed in other disease models.

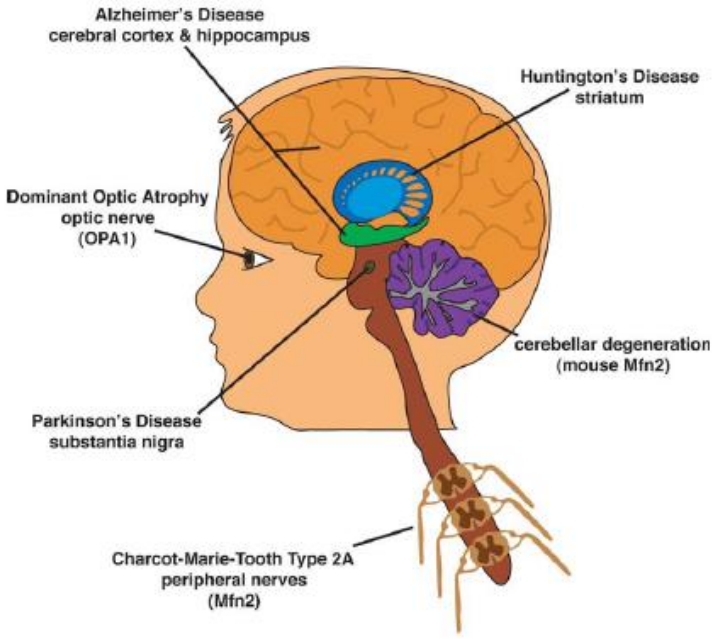

Figure 1.10 Neurodegenerative diseases caused by dysfunctional mitochondrial dynamics.

Primary affected neuronal systems are shown. Adapted from Chen 2009(CHEN and CHAN 2009).

1.4 mtDNA and disease

1.4.1 Mitochondrial diseases caused by mutations in the mitochondrial genome.

In order to study mtDNA diseases a multidisciplinary approach is essential linking clinical, histochemical and biochemical data obtained from relevant tissues (GREAVES *et al.* 2012; MCFARLAND *et al.* 2010). All mtDNA disorders result in defects in oxidative phosphorylation, regardless of the mutation (BETTS *et al.* 2004). COX (cytochrome c oxidase) deficiency is the most common and penetrant phenotype and was first reported in chronic progressive external ophthalmoplegia (cPEO) patients (JOHNSON *et al.* 1983). COX/SDH (succinate dehydrogenase) immunohistochemical staining is commonly used to classify normal and deficient neurons in mitochondrial diseases

Diseases caused by mutations in mtDNA were first reported in the late 1980's (HOLT *et al.* 1988; WALLACE *et al.* 1988). One of the mutations characterized was in an American Leber's hereditary neuropathy (LHON) pedigree, which is an ocular disease characterized by rapid onset blindness, caused by a mutation in mtDNA nt11778, encoding subunit 4 of the NADH dehydrogenase (complex I) (WALLACE *et al.* 1988). After the characterization of the first patients with mtDNA disorders, many other studies followed confirming the link between mtDNA mutations and disease (reviewed in (GREAVES *et al.* 2012; TAYLOR and TURNBULL 2005)).

The tissues affected in mtDNA disorders are highly variable. However tissues with a high metabolic demand such as the cerebellum, the extra-ocular muscles, heart, liver, smooth muscle of the colon, kidney and skeletal muscles are commonly affected. The true impact of mtDNA disease is hard to determine because of the tissue heterogeneity, the occurrence of multiple mutations and complex diagnostic criteria. In a study carried out in the north east of England it was reported that 9.2 in 100,000 adults have mtDNA disease, while 16.5 in 100,000 children and young adults were at the risk of developing mtDNA disease (SCHAEFER *et al.* 2008). This makes mtDNA disorders one of the most common neuromuscular disorders.

Mutant forms of mtDNA are usually found in a heteroplasmic state, i.e. the coexistence wild-type and mutant mtDNA in the same cell (LARSSON and CLAYTON 1995). The proportion of mutant mtDNA versus wild-type is a critical factor in determining the severity of the disease. In mammalian cells there can be 1000-10000 copies of mtDNA per cell. This ensures that mutations in a single copy do not affect overall mitochondrial function (TRIFUNOVIC and LARSSON 2008). However, clonal expansion of mtDNA copies can still result in mitochondrial dysfunction. Furthermore, stochastic inheritance of mtDNA molecules during cell division can result in daughter cells with high amounts of mutant mtDNA. It is widely believed that there is a "critical threshold" of mutant mtDNA copies above which disease symptoms will manifest. This threshold ranges from 90% mutant mtDNA copies for some tRNA mutations to 60% for mtDNA deletions (LARSSON and CLAYTON 1995; WALLACE and FAN 2009) (Figure 1.11). MtDNA nucleoid segregation during cell division is poorly understood, but could be critical in regulating heteroplasmy and thus the severity of mtDNA diseases.

Primary mtDNA disorders (disorders caused by mutations in the mitochondrial genome) are mostly caused by single large-scale deletions and there are more than 120 different characterized deletions published in mitochondrial databases (www.mitomap.org, MITOMAP, 2009). These deletions mostly occur at tandem repeat sequences and are formed by aberrant repair of damaged mtDNA in somatic tissues and are sporadic and not transmitted to offspring (CHINNERY *et al.* 2004; KRISHNAN *et al.* 2008; SCHON *et al.* 1989). The most common diseases observed caused by mtDNA deletions are Pearson's syndrome, Kearns-Sayre syndrome (KSS) and cPEO, which usually result from a single large scale deletion affecting more than one gene (MORAES *et al.* 1989; ROTIG *et al.* 1990; ZEVIANI *et al.* 1988). Point mutations in protein encoding and mitochondrial rRNA and tRNA genes also cause primary mtDNA disorders. Mutations in rRNA and tRNA genes cause defects in overall mitochondrial protein synthesis, while mutations in protein encoding genes result in abnormalities in individual respiratory chain complexes (MARIOTTI *et al.* 1994). One of the most common mitochondrial disorders caused by point mutations is LHON, which is caused by three mutations (3460 G>A, 11778G>A and 14484T>C) affecting *ND1*, *ND4* and *ND6* respectively (HOWELL *et al.* 1991; JOHNS *et al.* 1992; WALLACE *et al.* 1988). Another common mtDNA disease is Leigh syndrome, which results from a mutation (8993T>C) in the *ATP6* gene (SHOFFNER *et al.* 1992). MELAS (mitochondrial encephalomyopathy with lactic acidosis and stroke-like episodes) is another common disease resulting from individual mutations in *TRNL1* (3243A>G and 3271T>C), and *ND1* and *ND5* genes (GOTO *et al.* 1990; KIRBY *et al.* 2004; SANTORELLI *et al.* 1997).

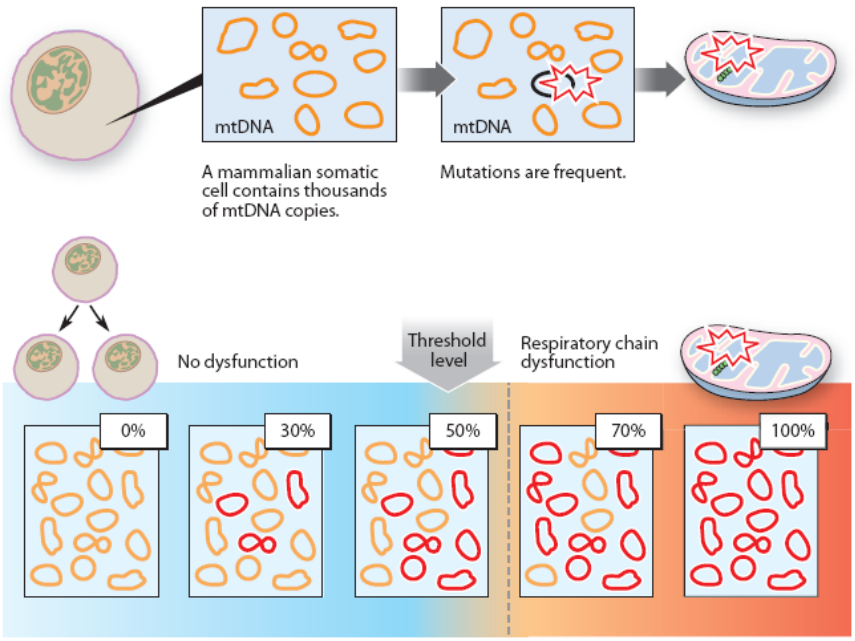

Figure 1.11 Clonal expansion of mutated mtDNA molecules.

MtDNA mutations occur frequently and low levels of mutated mtDNA do not result in dysfunction. mtDNA is replicated independent from the cell cycle and postmitotic cells can have mtDNA replication. Mitotic segregation of mtDNA can result in cells with high amounts of mutated mtDNA. Adapted from Larsson 2010 (LARSSON 2010).

1.4.2 Mitochondrial diseases caused by mutations in nuclear genes

There are two genetic mechanisms that can result in defects in mitochondrial function. The first is from maternally inherited mutations in the mtDNA. The second is via mutations in nuclear encoded mitochondrial genes. Proteins encoded by the nuclear genome that function in mtDNA replication have been frequently found to cause mtDNA-related disorders. mtDNA related nuclear genes that cause disease fall into two categories: those that directly affect the mtDNA replication fork (such as the

mtDNA polymerase *Polγ* and the helicase *Twinkle*) and genes that affect the supply of nucleotides for mtDNA replication (such as the mitochondrial thymidine kinase *TK2*, the deoxguanosine kinase *dGK* and the adenine nucleotide transporter *ANT1*) (COPELAND 2008).

Polγ is one of the most widely studied nuclear genes implicated in mtDNA-related disorders. In vitro studies have shown that Polγ has an error rate of 1 in 50,000 bp (LONGLEY *et al.* 2001). More than 150 mutations in *Polγ* have been identified in patients with mitochondrial diseases (Human DNA Polymerase Gamma Mutation Database (http://tools.niehs.nih.gov/polg/). These mutations can be found in all domains of Polγ and cause PEO, Alpers syndrome (NAVIAUX and NGUYEN 2004), Ataxia-neuropathy (VAN GOETHEM *et al.* 2004) and male infertility (ROVIO *et al.* 2001) (Figure 1.12). mtDNA mutations have been identified in the affected tissues in all of these syndromes (STUMPF and COPELAND 2011). Most of the mutations in *Polγ* (reported as shown in Figure 1.12) are recessive and commonly found in combination with other mutations in *Polγ* or other mtDNA replication related genes such as *Twinkle* and *ANT1* (KUJOTH *et al.* 2007). It has also been reported that mutations in *Twinkle* and *ANT1* cause sporadic PEO (AGOSTINO *et al.* 2003).

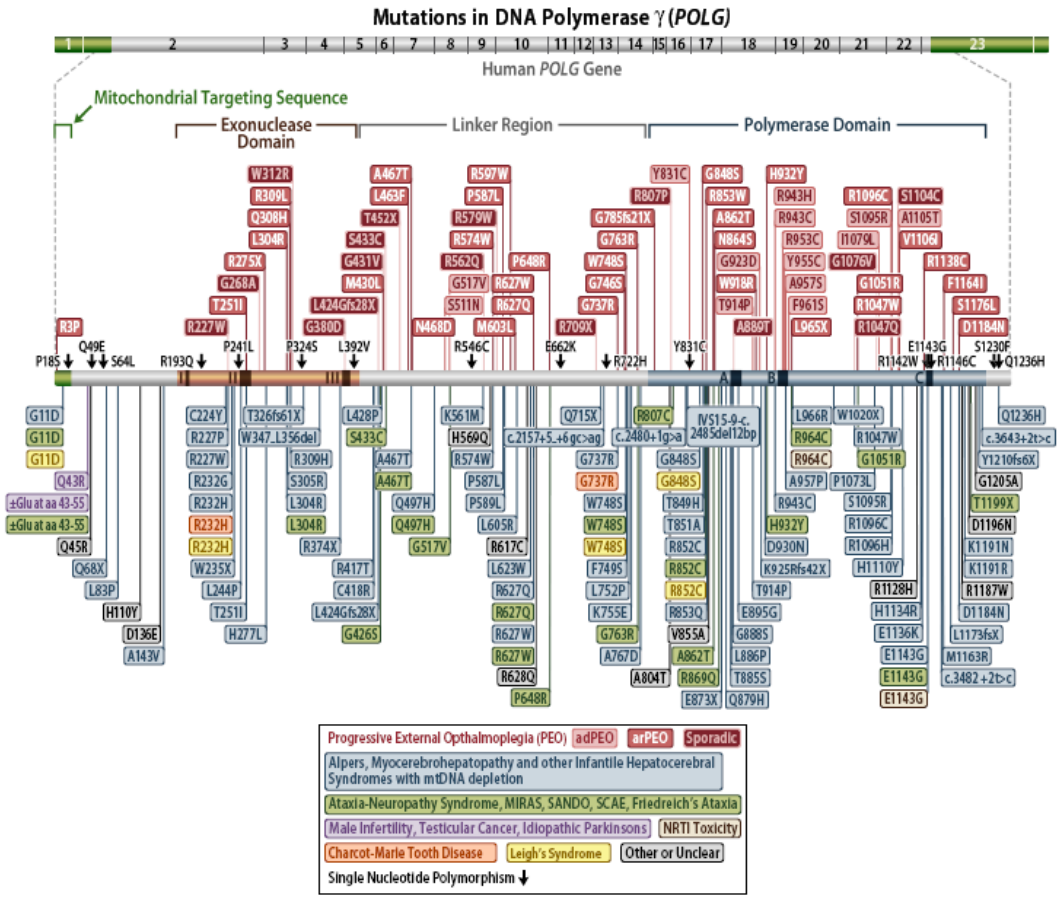

Figure 1.12 Mutations in *Polγ* and diseases caused by these mutations.

The box below shows groups of diseases in different colours, such as PEO causing mutations which are in red (Human DNA Polymerase Gamma Mutation Database (http://tools.niehs.nih.gov/polg/)).

1.4.3 mtDNA depletion syndrome

MDS (mtDNA depletion syndrome) is a group of diseases characterized by a reduction in mtDNA copy number and is caused by defects in nuclear encoded genes. MDS was first characterized as an autosomal recessive disorder (MORAES *et al.* 1991). This disease is widely reported in childhood respiratory deficiency

conditions (SARZI *et al.* 2007). One of the distinct properties of MDS is that it mainly affects the liver, skeletal muscles, kidney and brain, however other tissues can also exhibit symptoms (Figure 1.13) (SUOMALAINEN and ISOHANNI 2010).

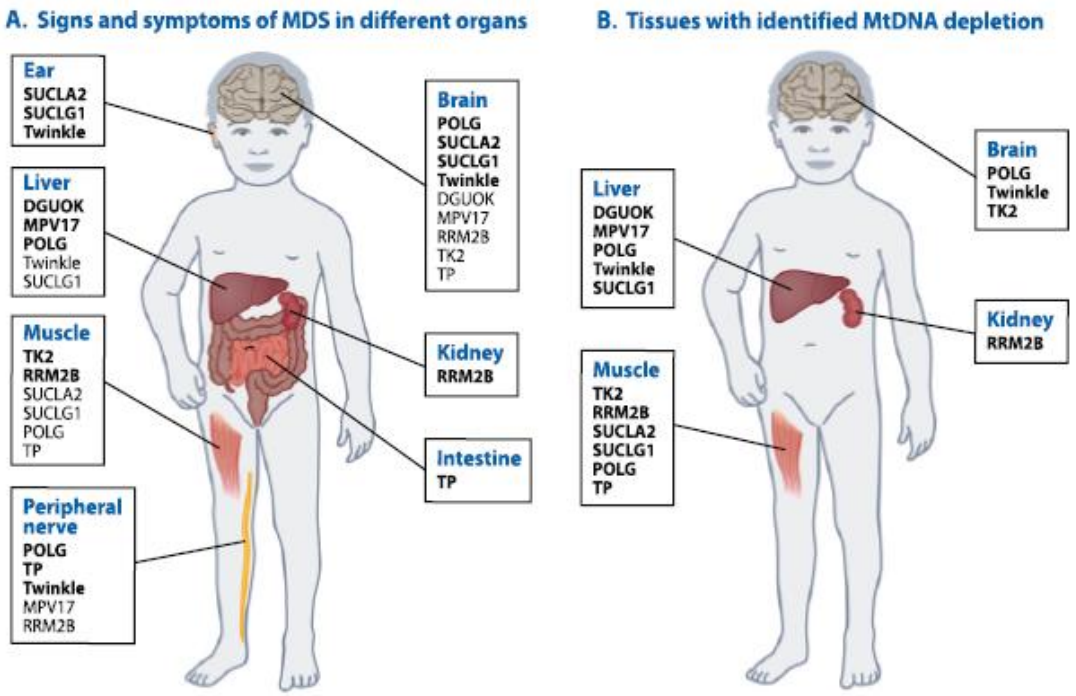

Figure 1.13 Genes causing mtDNA depletion syndrome (MDS).
Tissues affected by MDS and the genes in which mutations have been identified are shown in boxes. Adapted from Suomalainen 2010 (SUOMALAINEN and ISOHANNI 2010).

Mitochondrial dNTPs are supplied either through active transport of cytosolic dNTPs or through a salvage pathway that requires TK2 (Figure 1.14). Mutations in *TK2* have been reported as the most common cause of MDS (SAADA *et al.* 2001). Deoxyguanosine kinase (dGK) is an essential kinase for the purine nucleoside salvage pathway and mutations in *dGK* cause MDS (FREISINGER *et al.* 2006; MANDEL *et al.* 2001). Ribonucleotide reductase is another important enzyme for supplying the dNTP pool and defects in this gene have also been reported to cause

MDS (BORNSTEIN *et al.* 2008; BOURDON *et al.* 2007; KOLLBERG *et al.* 2009). Another widely studied enzyme in dNTP pool regulation is thymidine phosphorylase (TP). Mutations in TP have been found in most common forms of mitochondrial neurogastrointestinal encephalomyopathy (MNGIE) (NISHINO *et al.* 1999; NISHINO *et al.* 2001).

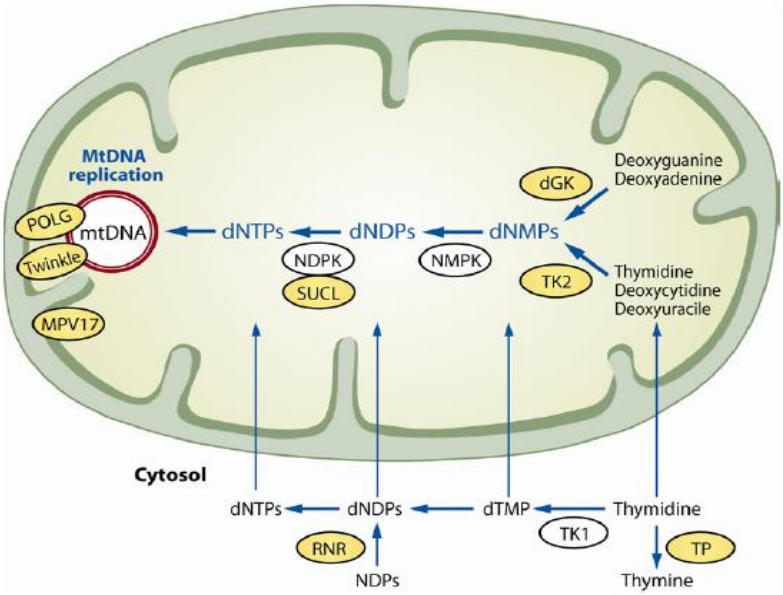

Figure 1.14 Proteins implicated in mtDNA depletion syndrome (MDS). Mitochondrial dNTP metabolism and proteins that have been found to be mutated in MDS are shown in yellow. Adapted from Suomalainen 2010 (SUOMALAINEN and ISOHANNI 2010).

Mutations in nuclear genes encoding components of the mtDNA replication apparatus can, in addition to mtDNA mutations, cause mtDNA depletion and thus MDS. MtDNA depletion caused by mutations in *Polγ* can cause early childhood diseases such as Alpers syndrome (NAVIAUX *et al.* 1999). Defects in Polγ account for 25% of the mitochondriopathies in Britain and Italy (CHINNERY and ZEVIANI 2008). mtDNA depletion has also been detected in PEO and mitochondrial myopathy

resulting from mutations in *Twinkle* (SPELBRINK *et al.* 2001), where mtDNA depletion was found in the brain and liver but not in skeletal muscles (HAKONEN *et al.* 2007; NIKALI *et al.* 2005; SARZI *et al.* 2007).

Additional mechanisms that can cause mtDNA depletion are defects in metabolic enzymes, such as the alpha and beta subunit of succinyl-CoA ligase (ELPELEG *et al.* 2005) (OSTERGAARD *et al.* 2007). Recently a protein of unknown function, MPV17, was linked with MDS (SPINAZZOLA *et al.* 2006). Although its function is not clear, MPV17 is known to be an integral mitochondrial inner membrane protein. Functional studies on its yeast homologue showed that it has roles in regulating the flux of TCA cycle intermediates into the cytoplasm, maintenance of cristae structure and nucleoid structure (DALLABONA *et al.* 2010).

1.4.4 mtDNA in neurodegenerative diseases and ageing

Neuronal dysfunction is a common symptom of mitochondrial disease (MCFARLAND *et al.* 2010). Complex I deficiency has been widely observed in primary mtDNA disorders resulting in neurodegeneration. Pathological features in the CNS are usually progressive and clinical features include optic atrophy, seizures, dementia, ataxia, extrapyrimidal features, stroke like episodes and progressive weakness (BETTS *et al.* 2004). Widely studied neurological disorders caused by mtDNA abnormalities include MELAS, MERRF, multiple mtDNA deletions causing PEO, ataxia and neuropathy and Leigh's Syndrome (BETTS *et al.* 2004). Neuropathological

features include nonspecific histological lesions, neuronal loss, necrosis, gliosis, demyelination and spongiform degeneration (TANJI and BONILLA 2001).

As mentioned before mitochondrial dysfunction via, for example, defects in mitochondrial dynamics, has been linked to neurodegenerative diseases such as AD, PD and ALS. Although in the majority of cases these diseases are sporadic and caused by a combination of genetic and environmental factors, mutations in either nuclear encoded mitochondrial genes or mtDNA encoded genes may be a contributory factor. Accordingly, for example complex I deficiency has been implicated in Parkinson's disease (SCHAPIRA *et al.* 1990; SCHAPIRA *et al.* 1989). Furthermore mtDNA deletions accumulate in the substantia nigra of aged individuals, but are more frequent in patients with PD (BENDER *et al.* 2006; KRAYTSBERG *et al.* 2006). AD has also been linked to mtDNA abnormalities and respiratory chain dysfunction (CAMPBELL *et al.* 2012b; COTTRELL *et al.* 2001a; COTTRELL *et al.* 2001b; KRISHNAN *et al.* 2012; ONYANGO *et al.* 2006).

Mitochondrial dysfunction in neurodegenerative and age-related diseases has been widely studied. In 1972, Harman hypothesized that ROS leak from the mitochondrial ETC causes damage to macromolecules and also to mtDNA. mtDNA mutations then lead to further respiratory dysfunction and this vicious cycle contributes to ageing (HARMAN 1972). This hypothesis has become known as the "mitochondrial theory of ageing" (MIQUEL *et al.* 1980). Although this theory has not been proven, studies have linked mitochondrial dysfunction with ageing. The rate of OXPHOS deficiency has been shown to correlate with age in skeletal muscles (TROUNCE *et al.* 1989) and the rate of COX-deficiency has been correlated with age in cardiomyocytes (MULLER-HOCKER 1989). Moreover, aged human muscle biopsies have an association between COX-deficiency and clonally expanded mtDNA mutations

(FAYET *et al.* 2002). A number of studies have also demonstrated a link between COX-deficiency and ageing in other tissues (reviewed in (GREAVES *et al.* 2012)).

Mutations in mtDNA have also been identified in ageing pathologies. Early studies linked mtDNA damage with ageing in rats: increased levels of mtDNA deletions were observed in aged animals (PIKO *et al.* 1988). Increased levels of mtDNA deletions have also been found in aged human brains (CORRAL-DEBRINSKI *et al.* 1992a; CORRAL-DEBRINSKI *et al.* 1992b). An increased accumulation of mtDNA mutations in aged tissues can potentially lead to an increase in ROS levels (LINNANE *et al.* 1989). Furthermore, enhancing the antioxidant defence mechanism, therefore decreasing the net ROS production, can increase lifespan. For example, overexpressing manganese superoxide dismutase (MnSOD) and methionine sulphoxide reductase can extend lifespan in short-lived strains of *Drosophila* (RUAN *et al.* 2002; SUN *et al.* 2002). Overexpressing mitochondrially-targeted catalase can increase lifespan in already long-lived mouse strains (SCHRINER *et al.* 2005). MtDNA dysfunction has been linked with ROS accumulation (KUJOTH *et al.* 2005). However, contradictory results were also reported where mtDNA mutations were not accompanied by ROS-induced damage in a mouse model expressing an error-prone version of the catalytic subunit of Polγ (TRIFUNOVIC *et al.* 2005). These mice had normal levels of ROS production and no increased sensitivity to oxidative stress-induced cell death. The results of this study were therefore contradictory to the mitochondrial theory of ageing. More studies should be carried out to better understand the effect of ROS in ageing.

Since the proportion of mutant mtDNA in tissues is usually low, recent studies have focused on single-cell analysis of mtDNA mutations. Using this method, respiratory chain deficiency was observed in a subset of cardiomyocytes associated with cellular

ageing (MULLER-HOCKER 1989). Neurons in the substantia nigra are particularly affected in PD and COX deficiency was observed in these neurons under normal ageing conditions (ITOH *et al.* 1996). Micro-dissection of COX deficient neurons also showed increased levels of mtDNA deletions in aged individuals and higher levels in PD patients than aged controls (BENDER *et al.* 2006; KRAYTSBERG *et al.* 2006).

The generation of 'cybrid' cell lines is a widely used technique to study mtDNA abnormalities in AD and PD. The cybrid technique was developed during the 1970s in order to investigate the functional consequences of mutant mtDNA species and was subsequently used to study human neurodegenerative diseases (BUNN *et al.* 1974). Cybrid cells are generated by fusing nucleated, mtDNA depleted cells with cytoplasts, which are enucleated mtDNA containing cells, to generate cybrid cells containing the donor (cytoplast) mtDNA. Many studies have used platelets (which lack nuclei, but contain mitochondria and mtDNA) from AD patients to generate cybrid cell lines that contain AD patient mtDNA. These AD patient cybrid cell lines have been consistently shown to have reduced membrane potential, reduced OXPHOS activity, increased free radical production and oxidative stress markers, altered calcium homeostasis and activated stress signalling and apoptosis pathways (SWERDLOW 2007; SWERDLOW *et al.* 1997). These studies have demonstrated that AD patient mitochondria, or mtDNA, are dysfunctional and has in part led to the "mitochondrial cascade hypothesis" of sporadic AD (SWERDLOW and KHAN 2004). This hypothesis proposes that both nuclear and mtDNA encoded genes determine a person's basal ETC efficiency and ROS production. Mitochondrial function declines with age until a critical threshold is reached that is determined by the starting mitochondrial population and the rate of mitochondrial decline. Dysfunctional mitochondria ultimately initiate AD histopathology via increases in Aβ production,

tau phosphorylation, synaptic loss, cell cycle re-entry and neurodegeneration (SWERDLOW *et al.* 2010).

Cybrid studies have also been used to model means of preventing mtDNA loss. Human NT2 teratocarcinoma cells carrying the mtDNA mutation 3243A>G (which causes MELAS) result in mtDNA loss (TURNER *et al.* 2005), but this mtDNA loss phenotype can be rescued by overexpression of *TIM17A*, a conserved mitochondrial IMM translocase (IACOVINO *et al.* 2009). The mechanism of how *TIM17A* prevents mtDNA loss is not known, however this was the first study to identify a gene that can restore mtDNA levels in human cells.

1.5 Animal models mtDNA of diseases

1.5.1 The importance of modelling mtDNA diseases

There are a number of important questions about the biology of mitochondrial diseases that can be addressed using animal models. Firstly, although mtDNA diseases all cause OXPHOS defects and insufficient ATP synthesis, the phenotypes are hugely variable and cannot be explained by energy deficits alone, so why are mtDNA diseases are phenotypically variable? Secondly, mutant mtDNA is found in a heteroplasmic state and the relationship between heteroplasmy and disease outcome is poorly understood. Thirdly, the mechanisms of controlling mtDNA segregation are not known. Fourthly, what are the physiological consequences of

mtDNA disorders? Finally, how does the mtDNA nucleoid regulate mtDNA replication, gene expression and segregation? (TYYNISMAA and SUOMALAINEN 2010). The organisation of the mtDNA genome varies between animal species, but the proteins needed for mtDNA transactions are conserved (BOORE 1999). Therefore, animal modelling of mtDNA diseases through genetic manipulation of conserved proteins can provide novel insight into these diseases.

1.5.2 Modelling mtDNA mutations

The so called 'Mito-mouse' was generated by isolating mtDNA containing natural deletions from aged mice in synaptosome preparations and fusing these with a cell line lacking mtDNA. Cybrid lines were screened for mtDNA deletions and one such line (containing a 4696bp deletion of 6 tRNA genes and 7 ETC genes) was enucleated, fused to donor embryos by electrofusion and implanted into pseudopregnant female mice. The offspring were then screened for heteroplasmic animals containing mutant and wild-type mtDNA and used for breeding to obtain germline transmission (INOUE *et al.* 2000).These mice had heteroplasmic single mtDNA deletions in high amounts, which resulted in respiratory chain deficiency in tissues such as heart, skeletal muscles and kidneys. The Mito-mice developed abnormalities characteristic of mitochondrial diseases such as anaemia, myopathy, cardiomyopathy, deafness, renal failure and shortened lifespan (INOUE *et al.* 2000; NAKADA *et al.* 2004). The inheritance of the mutant mtDNA was a key advantage for this model for studying the mitochondrial disease pathogenesis. Furthermore the

symptoms observed overlap with early-onset Pearson syndrome, which is caused by a single heteroplasmic mtDNA deletion (TYYNISMAA and SUOMALAINEN 2009).

Another direct method of manipulation of mtDNA was developed using transgenic mice expressing mitochondrial-targeted bacterial endonucleases. The aim of this model was to study the effects of double-stand breaks (DSB) in mtDNA. Large deletions in mtDNA can occur via defects in mtDNA replication, or by a DSB followed by aberrant DNA repair (KRISHNAN *et al.* 2008). MtDNA DSBs have been modelled in *Drosophila* Schneider cells via bleomycin treatment. DNA Repair mechanisms were shown to repair deleted parts in a time course manner, demonstrating the importance of DSBs and the DNA repair system in maintenance of mtDNA (MOREL *et al.* 2008). Moraes and co-workers expressed a mitochondrially-targetted version of the PstI endonuclease in skeletal muscles and this induced DSB breaks. Mitochondrial myopathy was seen in these mice and mtDNA isolated from skeletal muscle contained 7kb deletions and mtDNA depletion also occurred (SRIVASTAVA and MORAES 2001; SRIVASTAVA and MORAES 2005). Mitochondrially-targetted PstI was also expressed in neurons (in subset of CNS neurons in a doxycycline-regulated manner) and age related neurological phenotypes were observed in these mice (FUKUI and MORAES 2009). One of the advantages of this model is the ability to control the mito-PstI expression spatially and temporally, since constitutive expression can result in severe mtDNA depletion and loss of cell. Furthermore, this model is potentially useful to understand the mechanisms behind the clonal expansion of mutant mtDNA, which can either result from random genetic drift or replicative advantage of deleted mtDNA (DIAZ *et al.* 2002; ELSON *et al.* 2001).

Similar studies have been carried out in flies by expressing a mitochondrially-targetted form of XhoI (mitoXhoI), which is a single cutter of *Drosophila* mtDNA at position 2369 in the *mtCoI* gene. Ubiquitous expression of *mitoXhoI* resulted in embryonic lethality, with a few escapers reaching the third instar larval stage, and eye specific expression severely affected eye development (XU *et al.* 2008).The main focus of this study was to generate suppressor lines where the DSB had been incorrectly repaired to introduce a point mutation. They expressed the RE in the germ line and most of the flies were sterile, but there were rare escapers. These rare escaper flies had a mtDNA point mutation in the XhoI site in the *mtCoI* gene and had mitochondrial phenotypes and defects such as growth retardation, neurodegeneration, muscular atrophy and reduced lifespan. The authors suggested the same technique could be used in mice to generate heritable point mutations in specific mtDNA genes. This method has the advantage that many different restriction enzymes singly cut mtDNA and so could potentially be used to isolate point mutants in a number of different mtDNA genes.

1.5.3 Modelling nuclear DNA mutations in mtDNA replication genes

Engineering mutations in nuclear genes that regulate mtDNA is another method to model mtDNA diseases. As previously mentioned, mutations in *Polγ* are one of the major causes of mitochondrial diseases, since 2% of the population carries pathogenic variants (HAKONEN *et al.* 2005; HUDSON and CHINNERY 2006). *Polγ* deficient models have been extensively studied in mice. *Polγ* knockout mouse are

embryonic lethal with no COX activity and loss of mtDNA (HANCE *et al.* 2005). This study showed that heterozygous *Polγ* mice develop into adulthood with no apparent phenotype and no effect on mtDNA level, although *Polγ* transcript level is halved. This suggests that a 50% reduction in *Polγ* expression is not limiting for mtDNA replication. The *Polγ* mouse model POLG Y955C was developed to specifically target to cardiac tissue (LEWIS *et al.* 2007). These mice express a version of *Polγ* with a mutation at position 955 (Y955C), which is the most common disease causing mutation in *Polγ* and is accociated with PEO and Parkinsonism (LUOMA *et al.* 2004). The tyrosine 955 in Polγ maintains the high fidelity of DNA synthesis by interacting with incoming dNTPs in the active site within the polymerase domain (PONAMAREV *et al.* 2002). Mutation of this residue results in stalling of mtDNA synthesis due to minimal catalytic activity and severely reduced processivity. POLG Y955C mice had a shorter median lifespan and cardiac tissues showed mtDNA depletion, oxidative stress and dysmorphic mitochondria (LEWIS *et al.* 2007). Although this model provided important information about *Polγ* dysfunction, transgenic overexpression may not be as informative as loss-of-function and gene replacement models (STUMPF and COPELAND 2011).

Mouse models have been created that increase the rate of mtDNA mutations by substituting the catalytic aspartates for alanines (at position 181 in exon 1 proofreading domain) in the exonuclease domain of Polγ, which results in proofreading deficiency. Expression of this mutant *Polγ* in cardiac tissues resulted in an over 23-fold increase in mtDNA point mutations, large mtDNA deletions and increased in pro-apoptotic gene expression, but had no effect on respiratory function or oxidative stress (MOTT *et al.* 2004; MOTT *et al.* 2001; ZHANG *et al.* 2000). In addition to the observation of increased apoptosis in cardiac tissue, targeting the

proofreading mutant *Polγ* to pancreatic islet cells also resulted in increased apoptosis (BENSCH *et al.* 2009; MOTT *et al.* 2001). Although the mechanism linking mtDNA mutations to apoptosis is not clear, it has been suggested that signalling from the mitochondria to the nucleus could result in failure of the anti-apoptotic response or enhanced expression of pro-apoptotic and stress response genes (MOTT *et al.* 2001; SOMEYA *et al.* 2008). Furthermore, release of cytochrome c from mitochondria may directly enhance apoptosis as a result of mtDNA mutation (DUBEC *et al.* 2008).

An important mouse model in this field is known as the 'mutator mouse'. These mice contain a knocked-in version of *Polγ* containing a mutation in the second exonuclease domain (D257A) (this mutation is at a different position to the previous model and is in exon 2) in the catalytic subunit that decreases the proofreading activity of the enzyme, but has no effect on the DNA polymerase activity (KUJOTH *et al.* 2005; TRIFUNOVIC *et al.* 2004). Mutation frequency was significantly increased in heart, liver and duodenum, but only a slight increase was observed in sperm (KUJOTH *et al.* 2005). These mice showed premature-ageing like phenotypes such as weight loss, reduced subcutaneous fat content, hair loss, osteoporosis and reduced fertility. Histological analysis showed abnormalities in tissues such as spleen, liver, heart and testis. Similar to the cardiac-specific expression model, there was no effect on oxidative stress or ROS production. Furthermore, there was no defect in cell proliferation, but mutator mice showed early onset activation of a caspase-3 mediated apoptotic pathway (KUJOTH *et al.* 2005). This model was initially seen as particularly valuable since it linked mtDNA mutations with ageing pathologies.

This mutator mouse model has been controversial as it was originally claimed it showed that mtDNA mutations cause ageing. However, subsequent studies showed that the mtDNA mutations in these mice occurred throughout development, which is

different to what happens in ageing, when mtDNA mutations occur later in life. The mutator mouse was further investigated for its relationship with ageing by using more sensitive assays. Although mutator mice have an 11-fold increase in mtDNA point mutations with age, they can sustain a 500-fold mtDNA mutation burden compared to control mice, which suggests that mtDNA mutations do not limit the lifespan of wild-type mice (VERMULST *et al.* 2007). Similar *Polγ* mutations to those in the mutator mice, causing a high rate of mtDNA mutations, have not been identified in humans, further questioning the direct relevance of this model.

Manipulation of *Polγ* levels has also been analysed in tissue culture cells. Knockdown of *Polγ-β* in human 143B osteosarcoma cells resulted in mtDNA depletion and an increased number of nucleoids. Conversely overexpression of *Polγ-β* in HEK and U2OS cells resulted in fewer but larger nucleoids, without affecting mtDNA copy number. These data suggest that Polγ can affect mtDNA nucleoid structure, but the affects may depend on cell type (DI RE *et al.* 2009).

Drosophila has been used as a model to study mtDNA related diseases, with particular emphasis on *Polγ*. Flies with mutations in the catalytic subunit of *Polγ* (*tamas*; identified from an EMS screen) were pupal-lethal and showed defects in the larval response to light (IYENGAR *et al.* 1999). Flies with a null mutation in the accessory subunit of *Polγ* (*Polγ-β*) showed loss of mtDNA, disruption of mitochondrial morphology, impairment in cell proliferation in larval CNS and lethality at the pupal stage (IYENGAR *et al.* 2002). Mutations in *Polγ-β* cause PEO and this was the first *Polγ-β* animal model (COPELAND 2008; VAN GOETHEM *et al.* 2001). *tamas* and *Polγ- β* mutations also caused mtDNA depletion, an increase in mitochondrial density in proximal nerves and an increase in bidirectional mitochondria flux. Velocity of anteriograde mitochondrial transport was also slightly

reduced, but retrograde transport velocity was not changed (BAQRI *et al.* 2009). These mitochondrial transport phenotypes could result from a compensatory mechanism where neurons attempt to supply the nerve terminals with mitochondria produced in the cell body. However, increased transport of dysfunctional mitochondria may have deleterious effects.

In a more recent study, *tamas* expression was silenced by RNAi in *Drosophila* in order to model neurodegeneration. Ubiquitous knockdown of *tamas* resulted in lowered respiratory chain activity and developmental lethality. *tamas* RNAi in dopaminergic neurons caused cell loss, but had no effect in cholinergic neurons. The lethality caused by ubiqitous knockdown of *tamas* was partially rescued by overexpression of components of the mitochondrial quality control system, *parkin* and *Drp1*, but was fully rescued (as was the dopaminergic neuron cell loss) by overexpression of the alternative oxidase *AOX*, which bypasses complex III/IV deficiency (HUMPHREY *et al.* 2012). This study provided further evidence of the sensitivity of dopaminergic neurons to mitochondrial dysfunction.

Another *Drosophila* study used overexpression of *tamas* either ubiquitously, or specifically in the nervous system. Constitutive overexpression of *tamas* caused pupal lethality and mtDNA loss. It was proposed that this was due to replication stalling either via reduced catalytic activity, or interaction of excess Polγ-α with other components of the replication apparatus (LEFAI *et al.* 2000). Flies overexpressing *tamas* specifically in the nervous system only had a mild reduction in adult eclosion, but adult fly lifespan was decreased more than 50%. Furthermore, OXPHOS activity was significantly reduced in these flies and they had reduced resistance to the ROS-generating agent paraquat. Both mtDNA replication rate and mtDNA copy number were reduced in these flies (in the whole organism) and there

was increased cell death in larval CNS (MARTINEZ-AZORIN *et al.* 2008). It is possible that increasing the amount of Polγ might result in un-favourable interactions with other components of the mtDNA replication apparatus, such as mtSSB and Twinkle, which results in dysfunction or inhibition in mtDNA replication. The phenotypes observed are analogous to MDS diseases and correlate with the reduction in mtDNA level.

Mutations in the *Twinkle* helicase have been reported in dominant adult onset PEO and this has been modelled in mice that express murine Twinkle with mutations homologous to those found in the patients. Twinkle^{dup} mice expressed a version of Twinkle containing a duplication of amino acids 353-365, the same as found in patients with PEO (TYYNISMAA *et al.* 2005). These 'deletor mice' had respiratory chain deficiency in skeletal muscles and some neuronal populations, with accumulation of multiple mtDNA deletions in muscle and brain tissues (TYYNISMAA *et al.* 2005). Analysis of mtDNA levels showed that mtDNA copy number was reduced 40% in the brain, but was not changed in the heart and muscles. Detailed investigation of replication intermediates (RIs) suggested replication stalling in the heart, muscle, kidney and brain, but not in the liver. The differences observed may be due to tissue specific differences in Twinkle expression (GOFFART *et al.* 2009). Mitochondrial myopathy was first observed in Twinkle^{dup} mice around 12 months and was progressive, mimicking the relative age of onset in human PEO patients. In human patients the amount of mtDNA deletions can be between 40-60% of total mtDNA, however the percentage was very low in young deletor mice and increased with age (SUOMALAINEN *et al.* 1992; ZEVIANI *et al.* 1989). The dynamics of mtDNA depletion with age are hard to compare between the mouse model and human disease since human mtDNA deletions have only been detected from 20 years of age.

Although Polγ and Twinkle act together in mtDNA replication, the main difference between "mutator mice" and "deletor mice" is the fact that mutator mice show premature aging phenotypes and deletor mice do not. This suggests that dysfunction of Twinkle may not be sufficient to cause extensive mtDNA mutagenesis, or alternatively dysfunction in Polγ could result in premature ageing via other mechanisms. Overexpression of wild-type Twinkle resulted in increased mtDNA copy number but did not cause any pathological phenotypes (TYYNISMAA *et al.* 2004).

Kaguni and co-workers modelled PEO in *Drosophila* tissue culture cells by expressing mutated versions of *Drosophila* Twinkle (CG5924). Two forms of CG5924 with mutations at positions analogous to lysine^{318} (*Drosophila*, K388A) and aspartate^{424} (*Drosophila*, D483A) in the active site of human Twinkle, which are essential for helicase activity but not for hexamer formation, were expressed in *Drosophila* Schneider cells. This resulted in cell death in 4-6 weeks and caused severe reduction in mtDNA copy number (4-20% of the control cells), demonstrating that this system could be used for assaying CG5924 function. Overexpression of CG5924 variants with mutations in the linker and helicase domains, homologous to those affected in PEO patients, in *Drosophila* cells resulted in a 7-11 fold reduction in mtDNA copy number (MATSUSHIMA and KAGUNI 2007). The N-terminal domain of the *Drosophila* mtDNA helicase was also studied by the same group since mutations in this region are also linked to PEO. The mtDNA helicase shows sequence similarity to the bacteriophage primase-helicase T7 gene 4 protein (T7 gp4). The T7 gp4 N-terminal region contains the primase domain, but the function of the N-terminal domain in the mtDNA helicase has not been described in detail. *Drosophila* Schneider cells expressing versions of CG5924 with mutations in the N-

terminal region, analogous to those found in PEO patients, had reduced mtDNA copy number. However, the mutated residues are not thought to be important for primase activity, suggesting that the N-terminal region plays a role in the helicase function of the enzyme in flies (MATSUSHIMA and KAGUNI 2009).

The C-terminal domain of Twinkle was also studied using deletions and alanine substitution mutations which revealed that K574, R576, Y577, F588 and Y595 are the important residues for mtDNA maintenance, since mutation of these residues resulted in reduced mtDNA copy number and cell death. Furthermore, the C-terminus is important for nucleotide hydrolysis, since amino acid substitution mutants in this region cause defects in this process (MATSUSHIMA *et al.* 2008). These studies have provided important insight into the structure and function of Twinkle and its role in mtDNA maintenance.

Another protein that is essential for mtDNA replication is the mtSSB (mitochondrial single stranded binding protein). It is one of the three components of the minimal mtDNA replisome, together with Polγ and Twinkle and can stimulate the unwinding activity of the Twinkle helicase (KORHONEN *et al.* 2003; KORHONEN *et al.* 2004). The *Drosophila* homologue of *mtSSB* is *lopo (low power)* and mutations in *lopo* result in lethality at the third instar larval stage. *lopo* mutant larvae have reduced cell proliferation in CNS, loss of mtDNA and reduced respiratory capacity (MAIER *et al.* 2001). These findings are supported by knockdown experiments in *Drosophila* Schneider cells, which results in mtDNA depletion and proliferation defects. These phenotypes in Schneider cells were rescued by overexpression of wild-type mtSSB, but not with overexpression of double mutants in ssDNA-binding and Polγ stimulating domains (FARR *et al.* 2004). Although there are no reports linking mutations in mtSSB to MDS in humans, these studies showed the importance of lopo

in mtDNA maintenance and survival. Overexpression of wild-type mtSSB could potentially be used as a therapeutic strategy to rescue mtDNA loss.

The mtDNA transcription machinery consists of an RNA polymerase, TFAM, transcription factors B1 and B2 (mtTFB1 and mtTFB2) and termination factors (mTERFs). TFAM is the best studied component and has a dual role in transcription and maintenance of mtDNA (FISHER *et al.* 1989; KANKI *et al.* 2004; KAUFMAN *et al.* 2007). *TFAM* knockout models have been generated as a way to deplete mtDNA and model MDS. Homozygous *TFAM*-/- mice are embryonic lethal with severely reduced TFAM protein levels and loss of mtDNA copy number (LARSSON *et al.* 1998). These mice had reduced COX expression and abnormalities in mitochondrial structure. Heterozygous *TFAM*+/- mice were viable, but had a 50% reduction in *TFAM* expression levels, which resulted in a 34% reduction in mtDNA level and a 22% reduction in mitochondrial transcript level (LARSSON *et al.* 1998). Human *TFAM* expression did not rescue the lethality observed in *TFAM* homozygous knockout mice, owing to the fact that expression of *hTFAM* did not alter mitochondrial transcript level, respiratory chain function and mitochondrial mass, although it did increase mtDNA copy number (EKSTRAND *et al.* 2004). These experiments suggested that differences between human and mouse TFAM in the C-terminal region, which is required for transcriptional activity (DAIRAGHI *et al.* 1995), prevented expression of *hTFAM* from rescuing the mouse *TFAM* mutant.

The importance of TFAM in maintaining mtDNA copy number has also been demonstrated in *Drosophila* Kc167 cells. RNAi of *TFAM* in these cells resulted in a 40% reduction in mtDNA copy number. Surprisingly, this did not result in any change in membrane potential, cell proliferation, or in mitochondrial mRNA transcript levels (GOTO *et al.* 2001). Although not much is known about the role of

TFAM in transcription of mtDNA in insects, these data suggested that TFAM is dispensable for transcription of mitochondrial mRNAs in Kc167 cells. Studies in HeLa cells showed that of *TFAM* knockdown resulted in mtDNA depletion and caused defects in mtDNA nucleoid segregation (KASASHIMA *et al.* 2011). These cell culture studies confirm the role of TFAM in maintaining mtDNA levels and nucleoid organisation.

Tissue specific manipulation of *TFAM* levels in mouse models has been very informative. Mice with heart and muscle-specific inactivation of *TFAM* are viable, but they die at around postnatal day 20. MtDNA depletion was observed both in heart and skeletal muscles together with a reduction in respiratory complexes I and IV levels, but not in complex II levels and increased apoptosis in cardiomyocytes (WANG *et al.* 1999). Homozygous *TFAM* knockout mice also show massive apoptosis at E (embryonic day) 9.5 (WANG *et al.* 2001).

Skeletal muscle-specific inactivation of *TFAM* was studied as a model for human mitochondrial myopathy. Inactivation of *TFAM* in skeletal muscles of mice resulted in progressive myopathy characterized by enlarged mitochondria and abnormal cristae (WREDENBERG *et al.* 2002). Loss of *TFAM* resulted in reduced mtDNA and mitochondrial transcript levels, dysfunction of the respiratory chain and reduced ATP production. Immunohistochemistry, electron microscopy and analysis of citrate synthase activity showed increased mitochondrial mass, which was suggested as a way to compensate for the respiratory chain deficiency and insufficient ATP production (WREDENBERG *et al.* 2002). TFAM was also knocked out specifically in pancreatic β-cells and resulted in a reduction in COX activity, with no effect on SDH activity and dysmorphic enlarged mitochondria. These mice subsequently developed diabetes (SILVA *et al.* 2000).

Neuronal specific manipulation of *TFAM* is a useful model to understand the importance of mtDNA in neurons and the role of mtDNA loss in neurodegenerative diseases. PD and also normal ageing results in a decline in respiratory chain function and accumulation of mtDNA mutations (KRISHNAN *et al.* 2007; LARSSON 2010). PD patients have respiratory chain deficient dopaminergic neurons and an increased rate of mtDNA deletions in these neurons (BENDER *et al.* 2006; BENDER *et al.* 2008). PD has been modelled in mice by inactivation of *TFAM* in dopaminergic (DA)-neurons (EKSTRAND *et al.* 2007). These 'MitoPark mice' start to show decreased mitochondrial *COI* expression from 6 weeks of age in the substantia nigra and ventral tengmental area and by 14 weeks of age have behavioural symptoms, starting with decreased locomotion and reduced exploratory behaviour and progressively affecting tremor, twitching and limb rigidity. These phenotypes were associated with progressive loss of DA neurons and nerve terminals. L-DOPA treatment was found to improve the motor function in these mice. Intraneuronal inclusions (Lewy bodies) were observed from 6 weeks of age and these structures were associated with mitochondrial membrane structures, suggesting a possible role for mitochondrial dysfunction in the development of inclusions (EKSTRAND *et al.* 2007). MitoPark mice also have altered synaptic ion channel properties and impaired DA release, which may explain the locomotor phenotypes (GOOD *et al.* 2011). Mitochondrial morphology was studied in MitoPark mice and mitochondrial fragmentation and enlarged mitochondrial aggregates were observed in DA neurons. Moreover, distal pools of mitochondria were reduced in number but had normal mitochondrial morphology. The mechanism suggested to cause depletion of mitochondria in axon terminals was impaired retrograde axonal transport of mitochondria (STERKY *et al.* 2011). These phenotypes suggest that defects in mitochondrial quality control

mechanisms may be responsible for DA neuron degeneration in this mouse model. The ubiquitin ligase Parkin is an important factor in mitochondrial quality control. However, there was no evidence of Parkin recruitment to defective mitochondria and knockout of Parkin did not modify the mitochondrial phenotypes observed (STERKY *et al.* 2011). Mitopark mice have been a useful model demonstrating the requirements for TFAM in DA neuron function and the importance of mitochondrial function in these neurons. However, recent data showing Parkin-independent mechanisms raises the question of whether these mice can be a used as a PD model.

AIMS OF PROJECT

In order to understand how mtDNA contributes to neurodegenerative diseases, I aimed to understand the consequences of mtDNA loss in neurons. The aims of the project were:

-To model mtDNA depletion in neurons in *Drosophila melanogaster*.

-To investigate the consequences of mtDNA loss in motoneurons.

-To investigate possible mechanisms causing motoneuron dysfunction related to mtDNA depletion.

Chapter 2. MATERIALS AND METHODS

2.1 Materials

Kits:

Wizard Genomic DNA Purification Kit (Promega)

LightCycler FastStart DNA Master^{PLUS} SYBER Green I (Roche)

First strand cDNA synthesis kit (Fermentas)

ATP Bioluminescence Assay Kit HSII (Roche)

Bradford protein assay (Bio-Rad)

Antibodies and dyes:

Miranda (mouse, 1 in 10, Dr. Richard Tuxworth)

Wingless (mouse, 1 in 200, DSHB)

Elav (mouse, 1 in 100, DSHB)

TFAM (rabbit, 1 in 1000, Abcam)

HRP-Cy3 (goat, 1 in 500, Dr. Richard Tuxworth)

Nc82/bruchpilot (mouse, 1 in 30, DSHB)

DAPI (already added in Vectashield mounting media, Vector Laboratories)

Secondary antibodies (1 in 500 dilution): Alexa Flour 488, Alexa Flour 594, Alexa Flour 633 (Invitrogen)

Rhodamine1,2,3 (13 μm, Sigma-Aldrich)

2.2 Methods

2.2.1 Fly breeding

All flies were maintained on cornmeal, glucose, yeast extract, agar media in temperature-controlled incubators at 25^0C. Incubators had a 12 hour light/dark cycle and virgin flies used to set up crosses were collected in the morning and afternoon.

Fly food used for crosses (R2 recipe):

For 10L of dH_2O:

Agar---80g (Fisher)

Ground yellow corn---200g

Glucose---800g (Sigma)

Brewer's yeast---1000g (MP Biomed Europe)

These ingredients were mixed and cooked in a Systec MediaPrep media preparator/steriliserand the rest (listed below) were mixed and put in after the temperature had cooled to below 60^0C:

methyl 4-hydroxybenzoate (Sigma)---22.5 g;

propionic acid (Fisher Scientific) ---37.5 ml;

ethanol ---200 ml.

After 10 minutes or more of mixing, the media were dispensed into vials and bottles (Regina Industries Ltd.) as required.

Fly food for lifespan experiment (German food recipe):

For 1 L of dH_2O:

Agar---8g (Fisher)

Brewer's Yeast---80g (MP Biomed Europe)

Yeast extract---20g (Sigma)

Peptone---20g (Oxoid Ltd.)

Sucrose---30g (Sigma)

Glucose---60g (Fisher)

$MgSO_4$---0.5g (VWR)

$CaCl_2$---0.5g (VWR)

The ingredients were mixed and the microwaved until they reached boiling point and then boiled for several minutes, then allowed to cool to 60^0C in a water bath. 6ml of propionic acid and 1g of methyl 4-hydroxybenzoate in 10ml of EtOH were then added. The solution was mixed well and 7ml poured into each vial and allowed to cool.

2.2.2 Fly stocks

In *Drosophila*, one of the widely used tools for targeted gene expression is the *UAS-Gal4* system. Using this method, the expression of a gene of interest can be directed to different tissues or cell types by using *Gal4* driver lines (BRAND and PERRIMON 1993). The *Gal4* driver lines used in this study were as follows:

Driver	Tissue Expressed	Source	Stock Number
Actin-Gal4 (II)	Ubiquitous	Bloomington	4414
Actin-Gal4 (III)	Ubiquitous	Bloomington	3954
MZ1407-Gal4	Neurons and Neuroblasts	Sousa-Nunes et al. 2009	
Elav-Gal4	Nervous system beginning embryonic stage 12	Bloomington	458
OK107-Gal4	Mushroom Body	DGRC	106098
OK371-Gal4	Glutamatergic neurons	Bloomington	26160

Table 2.1 List of *Gal4* driver lines used in this study.

Other stocks:

Wild type/control flies: *Oregon R* (Bloomington, 5), w^{1118} (Bloomington, 6326), w^{DAH} (Linda Partridge's lab), *PRSP2* (RFP expressing stock, Kaul and Bateman, 2009)

UAS stocks:

UAS-TFAM (this study), *UAS-TFAMGFP* (this study), *UAS-mitoXhoI* (O'Farell lab), *UAS-mitoGFP* (Bloomington, 8442), *UAS-TOR*^{DN} (Bloomington, 7013), *UAS-DP110*^{active} (Bloomington, 8294), *UAS-Atg1* (Shen 2009), *UAS-CD8GFP* (Tear lab), *UAS-Dcr2* (Bloomington, 24648).

For details of the RNAi lines used see table 3.1.

2.2.3 Lifespan Assays

Ethidium bromide (EtBr) experiment: Isogenised w^{1118} flies were used to carry out the EtBr lifespan experiments. In order to synchronize the age of the flies and minimize environmental effects, grape-juice plate cages were set up. Adult flies were crossed in these cages and embryos collected twice per day. Approximately similar numbers of embryos (500) were developed in bottles containing German food, maintained at 25^0C. Eclosed adult flies were grown in vials of control and EtBr containing food. Two different concentrations of EtBr (Fisher Scientific) were used: 0.2mM and 2mM. 20 flies were placed in each tube and 100 flies were aged in five tubes per condition. Flies were flipped into new tubes every two days and the number of dead flies recorded. This was continued until all of the flies in their corresponding vials were dead. This experiment was repeated three times on different dates.

Genetic manipulation: motoneuron driver (*OK371-Gal4, UAS-Dcr2, UAS-CD8GFP*) virgin flies and various (*w*, *UAS-TFAMIR-3* and *UAS-TFAMGFP*) male flies were crossed in grape-juice plate cages. Approximately similar numbers of embryos (500) were developed in bottles containing German food, maintained at 25^0C. Eclosed flies were placed in five vials containing German food, with 20 flies in each vial. The rest of the experiment was carried out as previously explained for the EtBr treatment experiment.

2.2.4 Measuring mtDNA Levels

EtBr treatment

The effect of EtBr on mtDNA was investigated both at the larval and adult stage. Approximately 100 w^{1118} embryos were collected using grape juice plates and these were then placed on control and 1mM EtBr containing food. 5 third instar L3 larvae per sample were used to extract genomic DNA and three samples were prepared per condition. For adult flies, w^{1118} flies (collected on grape juice plates) were aged on 0.2mM and 2mM containing food or normal food. 5 adult flies were used to extract genomic DNA from flies grown on normal food at day 2 and day 40 together, or from flies grown on 0.2mM and 2mM EtBr containing food at day 40. A total of three samples were prepared per condition.

DNA extraction and quantitative real time PCR

Genomic DNA was purified either from larvae or adult flies, depending on the experiment. Samples were homogenized by using a glass 0.1ml mortar and pestle (Fisher Scientific) on ice. Genomic DNA isolation was carried out using the Wizard® Genomic DNA Purification Kit (Promega) according to the manufacturer's protocol. Real time qPCR, which uses fluorescent reporters to measure absolute or relative amounts of DNA, was performed by using a Corbett Rotor-Gene RG-3000 machine, LightCycler® FastStart DNA Master^{PLUS} SYBR Green I (Roche) reaction mixture and gene specific primers. PCR reactions were carried out for 40 cycles: denaturation at 95^0C for 10 s, annealing at 60^0C for 15 s and extension at 72^0C for 20

s. Finally, by dissociation (increasing temperature from 72^0C to 95^0C) uniqueness of amplicons was analyzed. C_T (threshold cycle) values for the mitochondrial gene *cytochrome c oxidase subunit I* (*mt:CoI*) and the nuclear gene glyceraldehyde 3-phosphate dehydrogenase (*Gapdh1)* were then used to calculate the ΔC_T between these two genes for each sample. This value was used as the relative mtDNA level. Standard curves for *mt:CoI* and *Gapdh1*, using a series of 8 (3-fold) dilutions of genomic DNA, were run in all experiments to determine the efficiency of the reaction and were only used when the efficiency was >95%. Primer sequences for *mtCoI* and *Gapdh1* are shown in Table 2.2.

Gene	Primers	Sequence
mtCoI	Forward primer	5`-GAGCTGGAACAGGATGAACTG-3`
	Reverse primer	5`-TTGAAGAAATCCCTGCTAAATGT-3`
Gapdh1	Forward primer	5`-GACGAAATCAAGGCTAAGGTCG-3`
	Reverse primer	5`-AATGGGTGTCGCTGAAGAAGTC-3`

Table 2.2 Primer sequences for measuring mtDNA level by qPCR.

2.2.5 Measuring *TFAM* transcript level

20 third instar larvae were homogenized in TRIzol® reagent (Invitrogen) and stored at -80^0C. The next day, the homogenate was incubated at room temperature for 5 minutes and 0.2ml of chloroform/1ml of TRIzol was added. After centrifuging at 4^0C at 12000g, the aqueous layer (containing the RNA) was transferred into a new tube

and RNA was precipitated by adding 0.5 ml of isopropanol and centrifugation at 4^0C at 12000g. The precipitated RNA was washed with 75% EtOH and centrifuged at a lower speed (at 7,500g) for 5 minutes. After air drying the pellet, the RNA was re-suspended in 30 µl of dH_2O. 2µg of RNA was incubated with oligonucleotide hexamers (Fermentas) for 10 minutes at 65^0C in order to prime cDNA synthesis. MuLV RT (reverse transcriptase), dNTPs, RNase inhibitor and reaction buffer (First strand cDNA synthesis kit, Fermentas) were added to the RNA-hexamer mix. This mixture was incubated at 25^0C for 5 minutes and then 37^0C for 1 hour. The reaction was terminated by heating to 70^0C for 5 minutes and the synthesized cDNA was stored at -20^0C.

Quantitative PCR (qPCR), was carried out to measure *TFAM* transcript levels by using the same Real-Time PCR machine and enzyme mixture as used for the mtDNA levels measurement protocol. C_T values for *TFAM* and the housekeeping gene *RpL1* were used to calculate the ΔC_T between these two genes for each sample and thus the relative level of *TFAM* transcript. Standard curves for *TFAM* and *RpL1*, using a series of 8 (3-fold) dilutions of cDNA, were run in all experiments to determine the efficiency of the reaction and were only used when the efficiency was >95%. Primers used for *TFAM* and *RpL1* are shown in Table 2.3.

Gene	Primers	Sequence
TFAM	Forward Primer	5'-GAGTCGCGCAAGGAGATG-3'
	Reverse Primer	5'-GGATCGATAAGATTTCCGTGAC-3'
RpL1	Forward Primer	5'-TCCACCTTGAAGAAGGGCTA-3'
	Reverse Primer	5'-TTGCGGATCTCCTCAGACTT-3'

Table 2.3 Primer sequences used to measure *TFAM* transcript level by qPCR.

2.2.6 Measuring ATP Levels

The effect of neuronal knockdown of various genes on ATP levels was analysed by dissecting 20 adult brains. The ATP Bioluminescence Assay Kit HSII (Roche) was used to measure ATP levels. Brains were dissected in PBS and the cell lysis reagent (in the kit) was used to homogenise dissected brains in glass homogeniser (mortar and pestle). Samples were diluted in 1 in 10 using the dilution buffer supplied. ATP level standards were also prepared in the working range of 10^{-6} to 10^{-12} moles. 50 µl of experimental samples and 8 serial dilution standard samples were used together with 50 µl of luciferase reagent. 96-well plates (Thermo Scientific, nunc) were used to measure the level of ATP by measuring the level of luminescence using a luminometer (9100-001, VERITAS^{TM} Microplate Luminometer, TURNER Biosytems, Currently Promega).

Samples homogenized using the cell lysis reagent were used to measure the amount of total protein for normalization using a Bradford micro-assay (Bio-Rad) kit and a

MRX microplate reader (DYNEX Techynologies Inc., MAGELLAN BIOSCIENCES). A BSA (bovine serum albumin) serial dilution standard was used in the range of 8-80µg/ml. This standard was then used to determine the amount of protein in each experimental sample. Then, the ATP level was divided by the total protein level in order to determine the normalised level of ATP in each sample.

2.2.7 Generation of transgenic flies

The *UAS-TFAM* construct was generated by PCR amplification of the full length *TFAM* coding sequence from the cDNA clone LD40493 (DGRC) using primers Tfam.EcoRI.Fw and Tfam.XbaI.Rv (Table 2.4) containing *EcoRI* and *XbaI* sites (restriction enzyme sites are underlined in Table 2.4). The PCR product was then cloned into *EcoRI* and *XbaI* sites in pUAST.

The *UAS-TFAMGFP* construct was generated by PCR amplification of the full length *TFAM* coding sequence from the cDNA clone LD40493 (DGRC) using primers TFAM 5 and TFAM pENT R (Table 2.4). The PCR product was directionally cloned into the topoisomerase charged pENTR Gateway® system vector (Invitrogen). Gateway® recombination cloning was then used to clone the *TFAM* cDNA into the pTWG vector (http://www.ciwemb.edu/labs/murphy/Gateway%20vectors.html), which contains the UASt promoter and a C-terminal eGFP tag.

Construct	Primers	Sequence
UAS-TFAM	Tfam.EcoRI.Fw	5’GAGAGAGAATTCATGATCTACACCACAACA-3’
	Tfam.XbaI.Rv	5’GAGATCTAGACTATATATCTTTGGAGGCC-3’
UAS-TFAMGFP	TFAM5	5’CACCATGATCTACACCACAACACTG-3’
	TFAM pENTR R	5’TATATCTTTGGAGGCCAGCGTCTTG-3’

Table 2.4 Primer sequences used for cloning *TFAM* and *TFAMGFP*.
Restriction enzyme cutting sites are underlined for EcoRI and XbaI.

UAS-TFAM and *UAS-TFAMGFP* constructs were generated by Ilaria Nissoli and Christina Christoforou. Transgenic flies were generated by either BestGene or Fly Facility.

2.2.8 Immunohistochemistry

Larval and adult CNS, wing disc dissections

For adult CNS dissection flies were anesthesized with CO_2 prior to dissections. L3 larvae or adult fly heads were dissected with fine forceps (Agar Scientific) in ice cold

phosphate buffered saline (PBS: sodium chloride 8.0 g/l, potassium chloride 0.2 g/l, di-sodium hydrogen phosphate 1.15 g/l, potassium dihydrogen phosphate 0.2 g/l, pH7.4, OXOID) under a dissection microscope. Dissected brains and imaginal discs were placed in a 1.5ml tube containing 4% formaldehyde (Thermo Scientific)/PBS on ice. Once all samples were dissected, the tube was moved to a platform rocker (Rotarod) for 30-45 minutes to fix the tissues. They were then washed three times in PBST (PBS, 0.1% triton X100) for 10 minutes each. Tissues were then blocked in 10% normal goat serum (NGS, SIGMA-ALDRICH)/PBS for 20-30 minutes prior to primary antibody incubation. Blocked tissues were incubated with primary antibodies at relevant dilutions in 10% NGS/PBST at 4^0C overnight. Tissues were then washed three times with PBST for 10 minutes at room temperature (RT) on platform rocker. Corresponding secondary antibodies were prepared at appropriate dilutions and tissues were incubated in this solution in dark (by wrapping tubes in aluminium foil) for 1.5 hrs in RT. Tissues were then washed 3 times with PBST for 10 minutes each. Finally these samples were dissected (by removing unwanted tissue) on microscope slides. Vectashield mounting media with DAPI (Vector Laboratories) was added to the slides and cover slips were placed carefully on top. Slides were kept at 4^0C in dark until imaging.

Larval flat preps

Late third instar larvae were placed on a dish containing ice cold PBS, to reduce the muscle contractions, for 2-3 minutes. Then the larvae were transferred to a Sylgard dish containing a drop of cold PBS. Dissections were carried out using fine forceps, micro-pins (Entomoravia) and iridectomy scissors (Fine Science Tools). Larvae were

pinned dorsal side up by placing pins between the mouth hooks and the spiracles. Then using iridectomy scissors, the body wall was cut from anterior to posterior and the intestines, fat bodies and the tracheal system were removed using forceps. Larvae were then pinned out flat using micro-pins. Flat preps were fixed with 4% formaldehyde/PBS for 30 minutes. Fixed larvae were then transferred to 1.5ml tubes and washed 3 times with PBST for 10 minutes each. Subsequent staining and washes were carried out as for CNS dissections. The neuromuscular junction synapse on muscle group 4 and proximal and distal compartments of motoneuron axons were imaged using a Zeiss LSM710 confocal microscope.

2.2.9 Axonal mitochondrial membrane potential analysis

Larval tissue was prepared according to a method described by Brink and colleagues in order to maintain the properties of live, intact larvae (Brink 2009). Firstly larvae were placed in cold Schneider's media (Invitrogen), which contains 12.33mM L-glutamate and so inhibits spontaneous muscle contraction. Larvae were then transferred to a Sylgard dish containing 1ml of Schneider's media. The posterior segments were then dissected using iridectomy scissors and using a micro-pin, the mouth parts were pushed backwards through the body cavity to turn the larva inside out. Next, the fat body and intestines were removed and the Scheinder's media was replaced twice.Rhodamine-1,2,3 (Invitrogen) was the added in Schneider's media to a final concentration of 13 μM and the samples were incubated for 10 minutes. The dye was washed by replacing twice with fresh Scheinder's media. The larval

preparation was mounted on a double-bridged slide. This slide was prepared by glueing two square 18mm (#1.5) coverslips (VWR) onto a slide, leaving a 2mm gap. The larval preparation was then placed in this gap containing Schneider's media and a clean coverslip was placed on top.

2.2.10 Microscopy and image Processing

Images were obtained using a Zeiss LSM710 confocal microscope with ZEN software. The resolution of all of the images was 1024 X 1024 pixels, taken with 4 times averaging. The magnification and numerical apertures of lenses used were: 10 X, 0.30 ; 20x,0.50 and 40X, 1.30 oil. Images were processed using Adobe Photoshop 7.0.1.

2.2.11 NMJ analysis

Bouton number, bouton diameter, active zone number and density were determined by visualising the images in the Volocity Software (v5.5, Perkin Elmer) program and manually counting, or using the distance measurement tool. Bouton volume, mitochondrial number and mitochondrial volume measurements were performed in Volocity using the Measurements tool. The intensity threshold levels were adjusted depending on the experiment and each experiment analysed separately.

2.2.12 Behavioural assays

Viability

Virgin motoneuron driver flies were crossed to UAS lines in grape-juice plate cages. 50 first instar larvae from these plates were placed in vials containing fly food. Larvae were incubated at 25^0C and the number of eclosed adult flies counted. Six vials were tested for each genotype. For *TFAM* overexpression the number of pupae were also counted.

Larval Locomotion

15cm petri dishes (Thermo Scientific, nunc) containing 1.5% agarose (Eurogentec) in PBS was prepared by adding 0.9g of agarose in 60ml of PBS per plate. This mixture was heated in the microwave until it became clear. The agarose solution was poured into each plate and allowed to cool to room temperature.

Solidified agar plates were transferred to the dark room for the test. Third instar larvae were picked up gently using a moist paintbrush, to avoid any injury to larva. Food residue was removed by transferring the larvae in a small volume of water. Larvae were accustomed and trained in a small petri dish containing agar prior to testing for 30 seconds. Larvae were then placed in the middle of a 15cm petri dish for 2 minutes under safe light conditions. The trail larvae left on agar surface was traced using a marker pen on the dish surface. The petri dish was then scanned and the distance travelled measured using ImageJ 1.45b software (Wayne Rosband, NIH, USA, http://imagej.nih.gov/ij).

Adult climbing (Negative geotaxis assay)

Climbing assays were carried out on 2 to 3 day old male flies unless otherwise mentioned. After the eclosion adult flies were anaesthetised using CO_2 and approximately 20 male flies separated into a fresh vial. These flies were kept at 25^0C for around 24 hours to minimise the effect of anaesthetic on climbing performance. To standardise the effects of circadium rhythm, flies were tested at 9 o'clock in the morning. The tip of a 5ml Falcon pipette was cut off and using a mouth aspirator, a single fly was aspirated into the pipette. The pipette was then inverted and tapped against bench so that the fly fell to the bottom of the pipette. The fly instinctively climbs the wall of the pipette and the distance travelled by each fly was measured after 10 seconds of continuous climbing (runs in which flies paused during the climb were ignored). Each fly was tested 3 times and the average value for each fly was used to determine the average distance climbed for each genotype.

Jumping ability

These experiments were performed by Dr. Chris Eliott as previously described in Vincent, 2012 (VINCENT *et al.* 2012).

2.2.13 Statistical tests and graphs

Data analysis and statistical analysis of data were performed using GraphPad Prism 5 (GraphPad Software Inc) using the Student's t-test. Significance was determined using p value and values of $p \leq 0.05$ were considered significant. P values >0.05 were considered non-significant. Graphs were generated using GraphPad Prism software.

Chapter 3. Development of a neuronal model for mtDNA loss in *Drosophila*

3.1 Introduction

The principal function of mitochondria is to generate energy for the cell. Mitochondria have their own genome, encoding 37 genes. The number of mitochondrial DNA (mtDNA) copies varies between different cells and tissues. Maintaining a healthy mtDNA copy number is crucial for mitochondria to perform their cellular function within a dynamic network. Furthermore, morphological changes in mitochondrial structure through fusion/fission events have also been shown to be important for mtDNA maintenance (CHEN *et al.* 2007).

Given that mitochondria are highly abundant in muscle, owing to their high ATP requirement, mitochondrial dynamics are of utmost importance in muscle cells. Another group of cells in which mitochondrial activity is vital are nerve cells. Neurons have a high energy demand and control the function of other cells and tissues via signal transmission. This signal transmission occurs via neurotransmitter release at contact sites known as synapses. Synapses need an abundant supply of ATP for signal transmission, thus synaptic mitochondria are critical to synaptic function (LI *et al.* 2004; SCHUMAN and CHAN 2004). One subset of neurons which are particularly dependent on mitochondrial activity are motoneurons. Their synapses terminate at neuromuscular junctions to regulate muscle activity. It has been reported that unhealthy mitochondria at the synapses can lead to neuronal dysfunction (DU *et*

al. 2010). However, the actual mechanism linking mtDNA abnormalities and neuronal dysfunction is not well studied. In this chapter I have developed a model utilising the powerful genetic tools available in the fruit fly *Drosophila melanogaster* in an attempt to understand the relationship between mtDNA loss and neuronal dysfunction.

3.2 The effect of ethidium bromide treatment on *Drosophila* development and longevity

It has been previously reported that the DNA intercalating agent ethidium bromide (EtBr) can bind to mtDNA and inhibit in vivo transcription of mtDNA (FUKUHARA and KUJAWA 1970). This binding can have adverse effects on mtDNA homeostasis and was previously demonstrated to induce mutations in the mtDNA of yeast (SLONIMSKI *et al.* 1968). Furthermore, EtBr treatment of *Drosophila* KC167 cells resulted in changes in mtDNA content between 2-184%, while most of the cases (90%) showed some level of reduction in mtDNA level (MOREL *et al.* 1999). Therefore, EtBr could be a useful tool for investigating the phenotypic consequences of mtDNA loss in *Drosophila.* Given the affect of EtBr on mtDNA and that it has previously been reported that EtBr treatment results in developmental defects (FLEMING *et al.* 1981), I hypothesized that EtBr consumption may be an effective method to deplete mtDNA in flies. Firstly, the effect of EtBr on larval development was tested. A reduced number of third instar larvae were observed with increasing concentrations of EtBr in the food (Figure 3.1A). The pupal stage and adult stages

were still reached by larvae that consumed up to 1mM of EtBr. However, higher concentrations of EtBr caused developmental arrest at the larval stage (Figure 3.1A).

To investigate whether this phenotype was related to mtDNA maintenance, mtDNA levels were analysed at the third instar larval stage. Larvae grown in food containing 1mM EtBr had slightly reduced levels of mtDNA, compared to control larvae grown on non-EtBr containing media (Figure 3.1B), which was close to reaching significance ($p=0.0578$). In order to investigate the effects of EtBr on adults, larvae were grown in normal (non EtBr containing) food and fully developed adult flies were then transferred to EtBr containing food. Therefore by introducing EtBr in the growth media after larval development, the effects of EtBr consumption on adult flies could be investigated independently of developmental abnormalities. The effect of EtBr on the lifespan of adult flies was investigated by ageing flies in 0.2mM EtBr or 2mM EtBr containing food and normal food. The maximum lifespan of both EtBr treated and untreated flies was the same, at around 50 days (Figure 3.1C). Median lifespan, which is the time when 50% of the population are alive, was also calculated and for all of the conditions this was around 34 days (Figure 3.1D). In conclusion, no lifespan effect was observed for either low or high concentrations of EtBr and median survival was the same for control flies and flies grown on 0.2mM and 2mM EtBr containing food (Figure 3.1C and 3.1D).

MtDNA levels in aged flies was analysed, achieved by extraction of DNA and qPCR from two day old control flies, 40 day old control and 40 day old flies grown on 0.2mM and 2mM EtBr containing food. It has been previously reported that age-related decline of mtDNA occurs in skeletal muscle and liver of rats (Barazzoni 2000). Similar results were also recently reported in fish (the shortlived fish *Nothobranchius furzeri*) (HARTMANN *et al.* 2011). In accordance with these studies

old flies (40 days) had a significantly lower level of mtDNA than young flies (2 days old). In addition, mtDNA levels were found to decrease as EtBr concentration increased. A slight but not significant reduction in mtDNA levels was observed in flies grown on food containing 0.2mM EtBr and a significant reduction was observed in those grown on food containing 2mM EtBr, when compared to age-matched flies grown on normal food (Figure 3.1E). To summarise, EtBr treatment results in developmental defects at larval stage and causes a slight but not significant decrease in mtDNA level. Interestingly, although EtBr treatment does not affect lifespan, it does reduce the mtDNA copy number significantly in aged adults. Although EtBr treatment may be useful to induce mtDNA loss, it may also induce non-specific toxicity and may not affect all tissues equally. Therefore I investigated ways of inducing mtDNA loss using genetic tools.

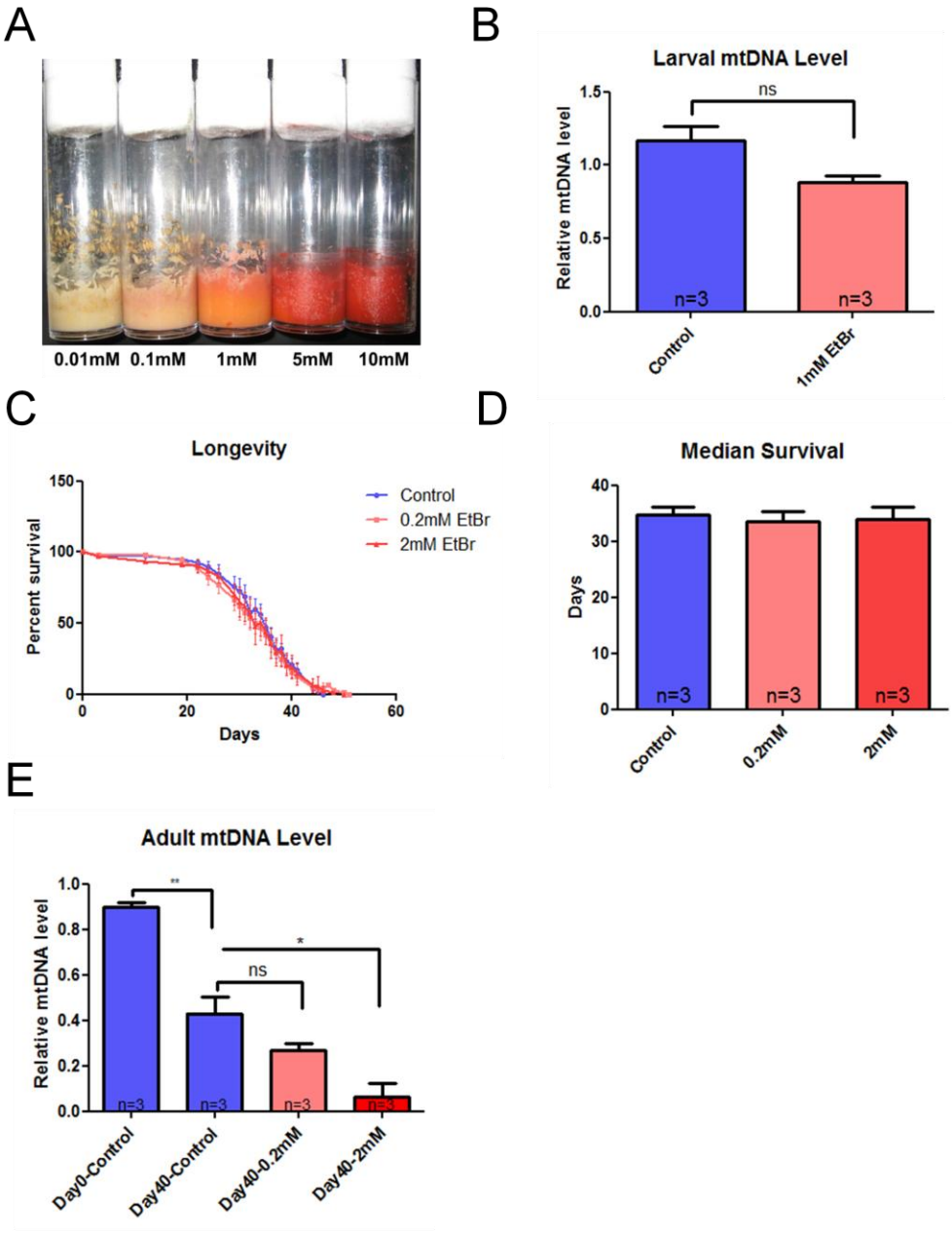
A
0.01mM 0.1mM 1mM 5mM 10mM
B
Larval mtDNA Level
Relative mtDNA level
ns
n=3
n=3
Control
1mM EtBr
C
Longevity
Percent survival
Days
Control
0.2mM EtBr
2mM EtBr
D
Median Survival
Days
n=3
n=3
n=3
Control
0.2mM
2mM
E
Adult mtDNA Level
Relative mtDNA level
**
*
ns
Day0-Control
Day40-Control
Day40-0.2mM
Day40-2mM

Figure 3.1 Effect of EtBr on *Drosophila* development and ageing

(A) High concentrations of EtBr has detrimental effects on larval development. 100 wild-type embryos grown on EtBr concentrations ranging between 0.01 to 10 mM. Larval development was severely affected with 5 and 10mM EtBr. **(B)** Feeding larvae with 1mM EtBr during development causes slight a reduction (not significant but the p value was 0.0578) in mtDNA level at third instar larval stage. qPCR was performed on DNA isolated from 5 larva per sample. **(C)** Both low and high doses of EtBr do not affect adult lifespan. 100 flies were aged on either control, 0.2mM or 2mM EtBr containing food at 25^0C. **(D)** Graph showing median lifespan of flies aged in control, 0.2mM and 2mM EtBr containing media. Lifespan repeated three times and average median lifespan plotted. **(E)** EtBr reduces mtDNA level in aged flies. Adult flies developed on control media aged for 40 days on either control, 0.2mM or 2mM EtBr containing media. QPCR was performed on DNA isolated from five male flies. Aged control flies had significantly less mtDNA content compared to young flies. 0.2mM EtBr treatment reduced the mtDNA level slightly ($p=0.1104$), however 2mM treatment resulted in a significant reduction ($p=0.0183$). Mean values +/- SEM plotted on graphs. *=$p<0.05$, **=$p<0.01$

3.3 Knockdown of mtDNA replication genes to deplete mtDNA in *Drosophila*

The maintenance of mtDNA is vital for a healthy and a functional mitochondrial network, which is itself crucial in cell functioning and survival. In order to investigate mtDNA maintenance, we decided to take a genetic approach. Proteins encoded by the nuclear genome have a major role in assembling the mtDNA replication machinery and stabilizing mtDNA and defects in these genes can result in mitochondrial disease (SUOMALAINEN and KAUKONEN 2001). We investigated the hypothesis that mtDNA associated proteins encoded by the nuclear genome are necessary for the viability of the organism. We used various RNAi lines from different sources (shown in the Table 3.1) to knockdown nuclear genes, which encode proteins that are known to be required for mtDNA replication. The candidate genes included *tamas* (the catalytic subunit of mtDNA polymerase), *Polγ-35* (the accessory subunit of mtDNA polymerase), *DNK* (deoxyribonucleoside kinase), *Twinkle* (the mtDNA helicase) and *TFAM* (mitochondrial transcription factor A). All of these genes have been shown to take part in regulating mtDNA copy number and are required in mtDNA replication (reviewed in (MORAES 2001)). Using these RNAi lines, we knocked-down the genes ubiquitously by crossing to the *Actin-Gal4* driver (Table 2.1) and adult viability was then analysed for each cross (Table 3.1). All of the *tamas*-RNAi lines were viable. However, three of the five different RNAi lines against *Polγ35* were lethal. Two of these lines target the same part of the gene, however the region targeted by the remaining line only partially overlaps with the others (Figure 3.2). One of the *Twinkle*-RNAi, all of the *DNK*-RNAi and *TFAM*-RNAi lines were lethal when ubiquitously expressed (Table 3.1). Only two of the

TFAM-RNAi lines targeted the same region of the gene, however two partially overlap with this region and one targets a completely different part of the gene (Figure 3.2). These results proved the requirement of these genes for the viability of *Drosophila* and helped us to narrow down our list for future experiments.

Ubiquitous knockdown of mtDNA related genes by *Actin-Gal4* highlighted the importance of these genes for survival of the organism. *DNK,* which is not directly associated with the mtDNA replication fork but takes part in maintaining the dNTP pool, has been identified to be a multisubstrate enzyme (JOHANSSON *et al.* 1999). In humans, the three essential enzymes which maintain the mitochondrial dNTP pool are dGK (deoxyguanosine kinase), TK2 (thymidine kinase) and dNT2 (5(3)-deoxyribonucleotidase) (MATHEWS and SONG 2007; SAADA-REISCH 2004). It has been shown that mutations in *dGK* and *TK2* are linked to mtDNA depletion in humans (MANDEL *et al.* 2001; SAADA *et al.* 2001). In *Drosophila*, DNK (deoxyribonucleoside kinase) is a global deoxynucleoside kinase and has a broader substrate specificity with roles in overall dNTP metabolism in the cell and higher catalytic activity compared to multiple enzymes in mammals (MUNCH-PETERSEN *et al.* 1998a; MUNCH-PETERSEN *et al.* 1998b). As DNK has a more general role compared to the mammalian dNTP maintenance enzymes, I did not use RNAi against *DNK* for the further experiments.

In conclusion, these experiments demonstrate that mtDNA replication genes are necessary for viability in *Drosophila*

Stock name	Source (Stock No)	Gene (CG No)	Inserted Chromosome	*Actin-Gal4* Phenotype
tamasIR-1	VDRC (3135)	*tamas* (CG8987)	2	Viable
tamasIR-2	VDRC (3133)	*tamas* (CG8987)	2	Viable
tamasIR-3	VDRC (106955)	*tamas* (CG8987)	2	Viable
PolG35IR-1	VDRC (30483)	*PolG35* (CG33650)	3	**Lethal**
PolG35IR-2	VDRC (30484)	*PolG35* (CG33650)	3	Viable
PolG35IR-3	VDRC (49769)	*PolG35* (CG33650)	3	Viable
PolG35IR-4	NIGFLY (8969R-2)	*PolG35* (CG33650)	3	**Lethal**
PolG35IR-5	NIGFLY (8969R-3)	*PolG35* (CG33650)	2	**Lethal**
DNKIR-1	VDRC (39137)	*DNK* (CG5452)	3	**Lethal**
DNKIR-2	VDRC (103385)	*DNK* (CG5452)	2	**Lethal**
TwinkleIR-1	NIGFLY (5924R-3)	*Twinkle* (CG5924)	3	Viable
TwinkleIR-2	NIGFLY (5924R-1)	*Twinkle* (CG5924)	2	**Lethal**
TFAMIR-1	NIGFLY (4217R-2)	*TFAM* (CG4217)	2	**Lethal**
TFAMIR-2	VDRC (107191)	*TFAM* (CG4217)	2	**Lethal**
TFAMIR-3	NIGFLY (4217R-1)	*TFAM* (CG4217)	3	**Lethal**
TFAMIR-4	Bloomington (26744)	*TFAM* (CG4217)	3	**Lethal**
TFAMIR-5	VDRC (37819)	*TFAM* (CG4217)	3	**Lethal**

Table 3.1 List of RNAi lines used to cross to the *Actin-Gal4* driver

First column shows the nomenclature used in this study. Second column showing the stock centre and stock number. Final column shows the results of the *Actin-Gal4* crosses.

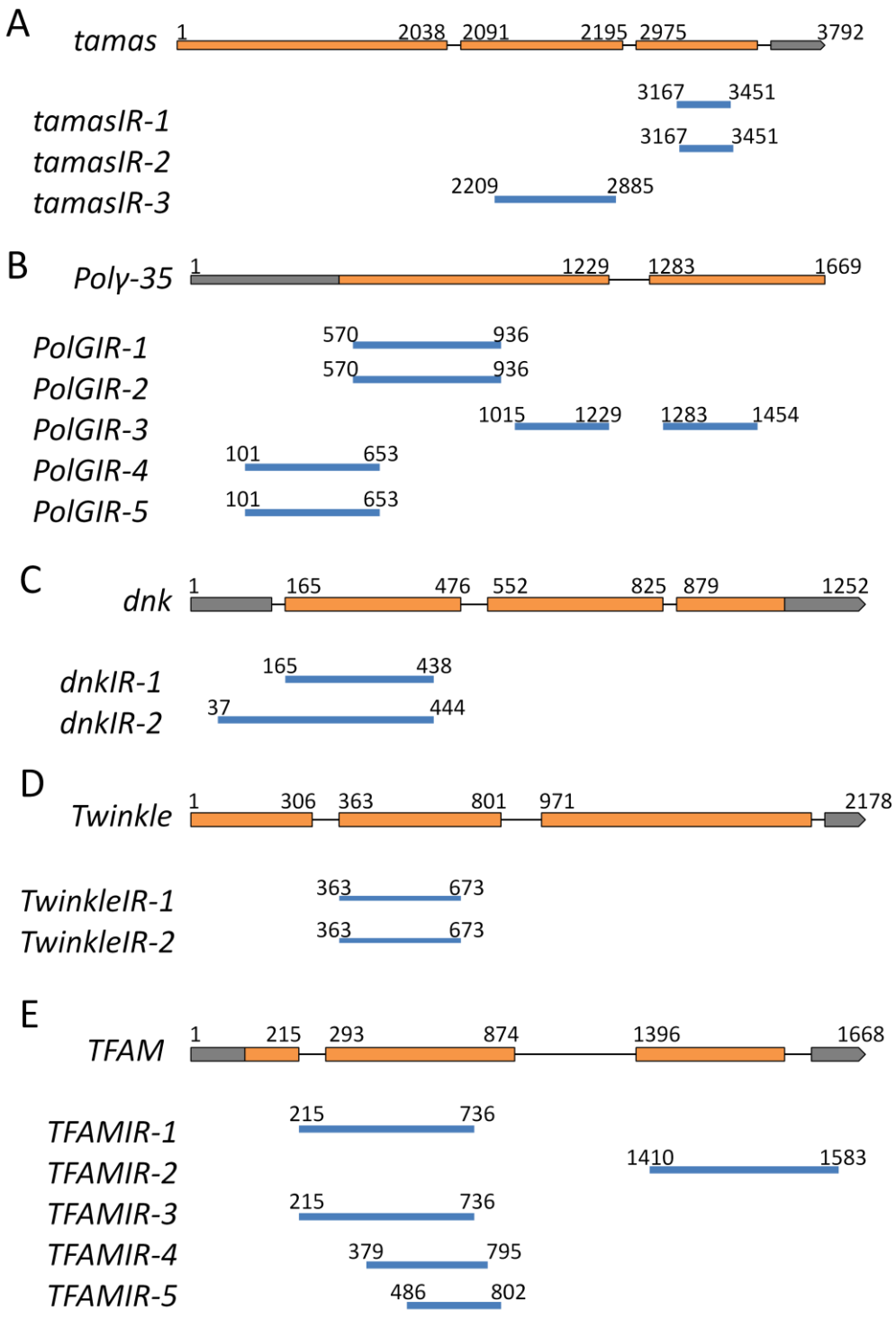
A
tamas
1
2038
2091
2195
2975
3792
tamasIR-1
3167
3451
tamasIR-2
3167
3451
tamasIR-3
2209
2885
B
Poly-35
1
1229
1283
1669
PolGIR-1
570
936
PolGIR-2
570
936
PolGIR-3
1015
1229
1283
1454
PolGIR-4
101
653
PolGIR-5
101
653
C
dnk
1
165
476
552
825
879
1252
dnkIR-1
165
438
dnkIR-2
37
444
D
Twinkle
1
306
363
801
971
2178
TwinkleIR-1
363
673
TwinkleIR-2
363
673
E
TFAM
1
215
293
874
1396
1668
TFAMIR-1
215
736
TFAMIR-2
1410
1583
TFAMIR-3
215
736
TFAMIR-4
379
795
TFAMIR-5
486
802

Figure 3.2 Schematic representation of RNAi lines used to knockdown mtDNA replication genes ubiquitously

(A) Two of the three *tamas* RNAi lines target the same region. **(B)** There are three different regions targeted by five *PolG35* RNAi lines. **(C)** Two partially overlapping *dnk* RNAi lines. **(D)** Both of the *Twinkle* RNAi lines target the same region. **(E)** Only two of five of the *TFAM* RNAi lines target exactly the same region.

3.4 Knockdown of mtDNA replication genes using a pan-neuronal driver

In order to study the requirements for the mtDNA replication genes *Polγ*, *Twinkle* and *TFAM* in neurons the pan-neuronal driver *Elav-Gal4* was used. *Polγ*, *Twinkle* and *TFAM* RNAi lines crossed to *Elav-Gal4* resulted in viable progeny. Adult CNS tissue was dissected from the male progeny to quantify the mtDNA levels by qPCR. DNA was isolated from 5 brains per genotype and 3 samples were tested by qPCR. Most of the lines tested showed a variable result and had no effect on mtDNA levels apart from two *Polγ* RNAi lines, which resulted in a variable but significant increase (Figure 3.3).

The main function of mitochondria is to produce energy in the form of ATP by oxidative phosphorylation. In order to analyse the ATP levels in neurons the *Elav-Gal4* driver was used to knockdown *Polγ*, *Twinkle* and *TFAM* by RNAi in the nervous system and luciferase assays were carried out on pools of twenty adult CNS preparations. *TFAM* and *Twinkle* RNAi lines showed a reduction in ATP levels in female flies. In contrast, *Polγ* RNAi resulted in increased levels (Figure 3.4A). The same assay was also carried out on male flies, with a reduced level of ATP observed in all of the RNAi lines tested (Figure 3.4B). These results suggested that, although I did not detect a reduction in mtDNA levels in the adult brain, ATP levels were reduced, at least in male flies. To confirm this, these assays need to be repeated with more samples.

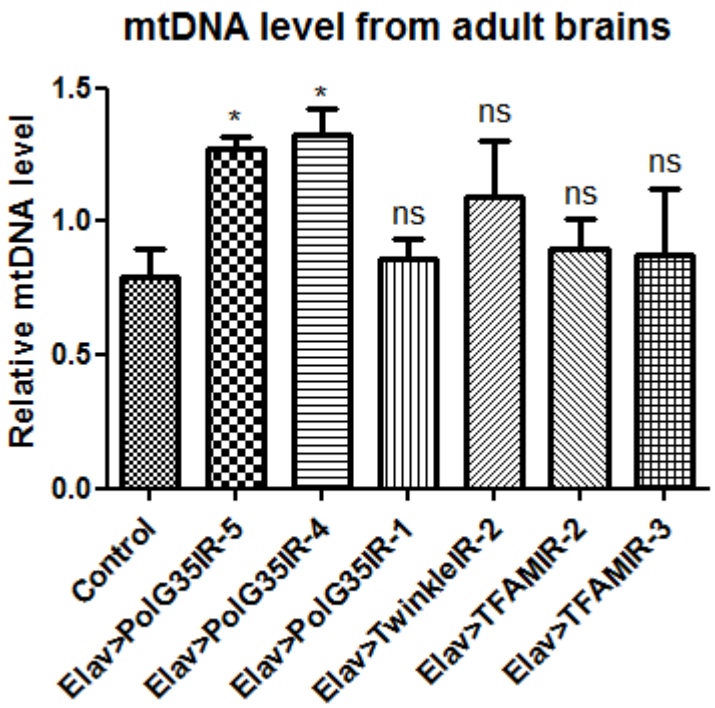

Figure 3.3 Pan-neuronal RNAi of *Polγ*, *Twinkle* and *TFAM* does not cause mtDNA depletion.

Three different *Polγ*, one *Twinkle* and two different *TFAM* RNAi lines were crossed to *Elav-Gal4* driver. All of the brain samples tested had approximately the same level of mtDNA compared to the control apart from two *Polγ* lines. Control samples were obtained from *OreR* flies crossed to the *Elav-Gal4* driver. QPCR was performed on DNA isolated from 5 brains dissected from adult flies. Results represent relative mtDNA levels. Mean values +/- SEM plotted on graph. *=$p<0.05$

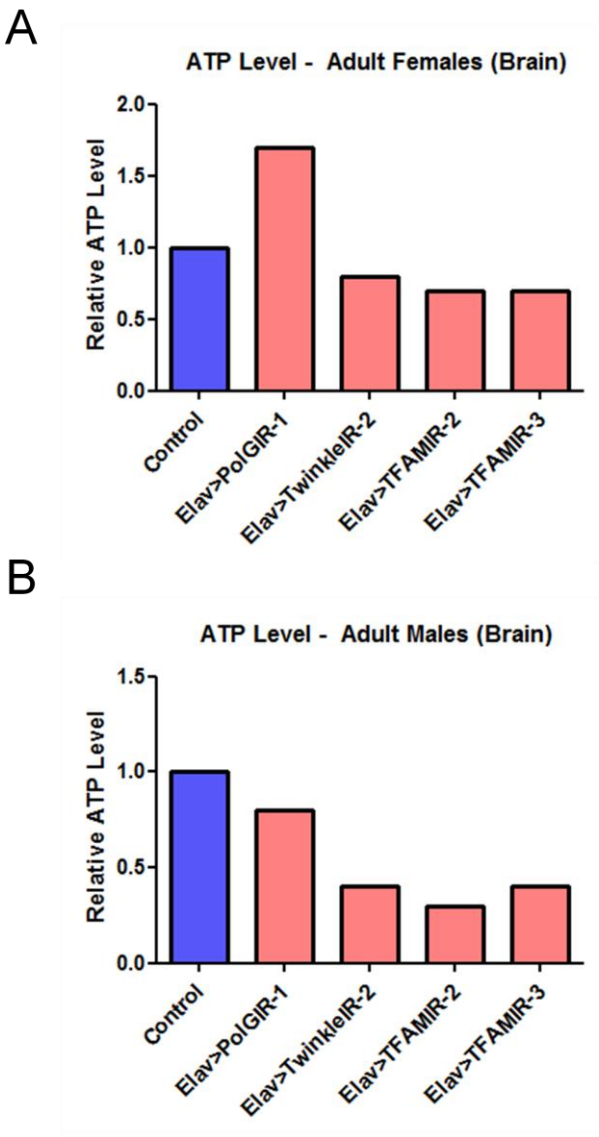

Figure 3.4 Pan-neuronal RNAi of *Polγ*, *Twinkle* and *TFAM* shows a reduction in ATP level in male flies.

Samples were prepared by dissecting 20 adult CNS from 2-3 day old flies. One sample was prepared for each genotype and normalised to total protein level by Bradford assay. Luciferase assays show a slight reduction in the level of ATP in CNS in males upon knockdown of *Polγ*, *Twinkle* and *TFAM* **(B)**, however there was no effect in female flies apart from an increase in ATP levels upon *Polγ* knockdown **(A)**. Control samples were obtained from progeny of *OreR* crossed to the *Elav-Gal4* driver.

3.5 Neuroblast-specific knockdown of *Polγ, Twinkle* and *TFAM* reduces mtDNA copy number and affects behaviour.

Mutants and RNAi of nuclear encoded factors required for mtDNA replication have been associated with mtDNA depletion in different model organisms (OLIVEIRA *et al.* 2010). As explained in detail in the introduction, *Polγ-α* and *Polγ-β*, *Twinkle*, *TFAM*, *mtSSB* and *RNase H1* knockdown have been previously used to induce mtDNA loss in cell culture (Section 1.4.4). Since RNAi of several of these genes in neurons using *Elav-Gal4* did not induce a detectable reduction in mtDNA levels the neuroblast driver *MZ1407-Gal4* was used to express the RNAi lines previously described. *MZ1407-Gal4* drives expression in neuroblasts (from embryonic stage 10/11) and subsequently in most neurons of the CNS and all neurons in PNS (LUO *et al.* 1994). Using the *MZ1407-Gal4* driver, dsRNAs against *Polγ*, *Twinkle* and *TFAM* were expressed in developing neuroblasts and subsequently in neurons in the CNS and in the PNS. These crosses gave viable progeny at 21^0C, so allowing us to carry out experiments at the adult stage. MtDNA levels were measured by qPCR using DNA isolated from fly heads. All of the RNAi lines tested showed a trend of slight reduction in the mtDNA levels but none of them reached a significant level (Figure 3.5). The expression pattern of the *MZ1407-Gal4* driver was checked by crossing the driver to *UAS-nlsGFP* and staining with an antibody against Miranda, used as a neuroblast marker. Confocal imaging showed broad GFP expression throughout the CNS in Miranda positive neuroblasts and in neurons in the optic lobes, central brain and thoracic ventral nerve cord (VNC) (Figure 3.6). These data confirmed the previously described expression pattern of *MZ1407-Gal4* in the CNS (LUO *et al.* 1994).

As RNAi of *TFAM* produced the strongest decrease in the mtDNA levels (Figure 3.5) when driven by *MZ1407-Gal4*, we analysed this gene in detail by using independent *TFAM* RNAi lines (Figure 3.2). *TFAMIR-2* was lethal when crossed to *MZ1407-Gal4* at 25^0C (Figure 3.7A). Therefore *TFAMIR-3* and *TFAMIR-2* were crossed *to MZ1407-Gal4* and developed at 21^0C. Both of the lines were viable, however *TFAMIR-3* flies had reduced viability compared to controls (Figure 3.7B). Furthermore, larval locomotion assays were carried out at the larval stage and both of the lines had significant defects in larval movement (Figure 3.7C), with a significant reduction observed in the total distance travelled by larvae in two minutes compared to the control (Figure 3.7C). All viable *TFAM RNAi* lines crossed to *MZ1407-Gal4* showed a wing expansion phenotype at 25^0C (Figure 3.8 A-E). Climbing assays on adult flies grown at 21^0C were also carried out and a significant reduction was observed both in males and females, for both *TFAMIR-2* and *TFAMIR-3* (Figure 3.8F and 3.8G).

In order to investigate the reasons underlying the behavioural phenotypes caused by *MZ1407-Gal4* induced knockdown of *TFAM*, CNS tissue was dissected and analysed by confocal microscopy. I hypothesised that loss of *TFAM* may cause reduced neuroblast proliferation. Therefore, Miranda staining was used to quantify neuroblast number in the larval VNC. No difference was observed in the number of neuroblasts in the larval VNC in *TFAM* RNAi animals compared to controls (Figure 3.9A,B). This shows that RNAi of *TFAM* using *MZ1407-Gal4* driver does not affect neuroblast number and so the locomotion phenotype, at least at the larval stage, is unlikely to be caused by loss of neuroblasts.

In conclusion, expression of several different dsRNAs against *TFAM* using *MZ1407-Gal4* all resulted in slight but not significant decrease in mtDNA levels and result in

developmental and behavioural defects. Therefore, RNAi of mtDNA replication genes using *MZ1407-Gal4* could be a useful system for investigating the consequences of mtDNA loss in neuroblasts and differentiated neurons throughout the majority of the CNS.

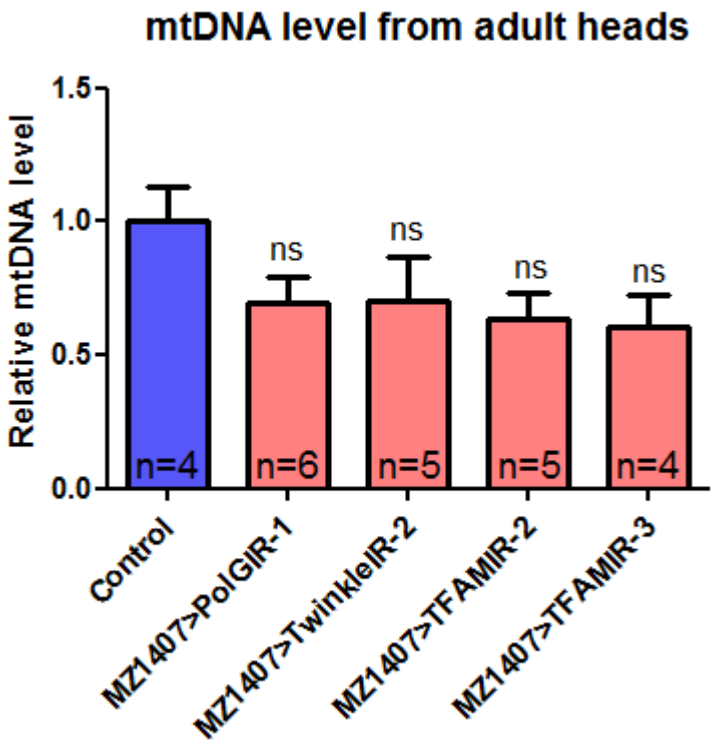

Figure 3.5 RNAi of mtDNA replication genes using *MZ1407-Gal4* causes mtDNA loss.

MtDNA content of DNA extracted from 5 fly heads was quantified using qPCR. A slight reduction was observed with all of the dsRNA lines expressed using *MZ1407-Gal4* at 21^0C compared to control samples. Control samples were obtained using the driver line crossed to CyO balancer flies. Mean values +/- SEM plotted on graph.. P values were 0.0942 for *PolGIR-1*, 0.2153 for *TwinkleIR-2*, 0.0529 for *TFAMIR-2* and 0.0650 for *TFAMIR-3*.

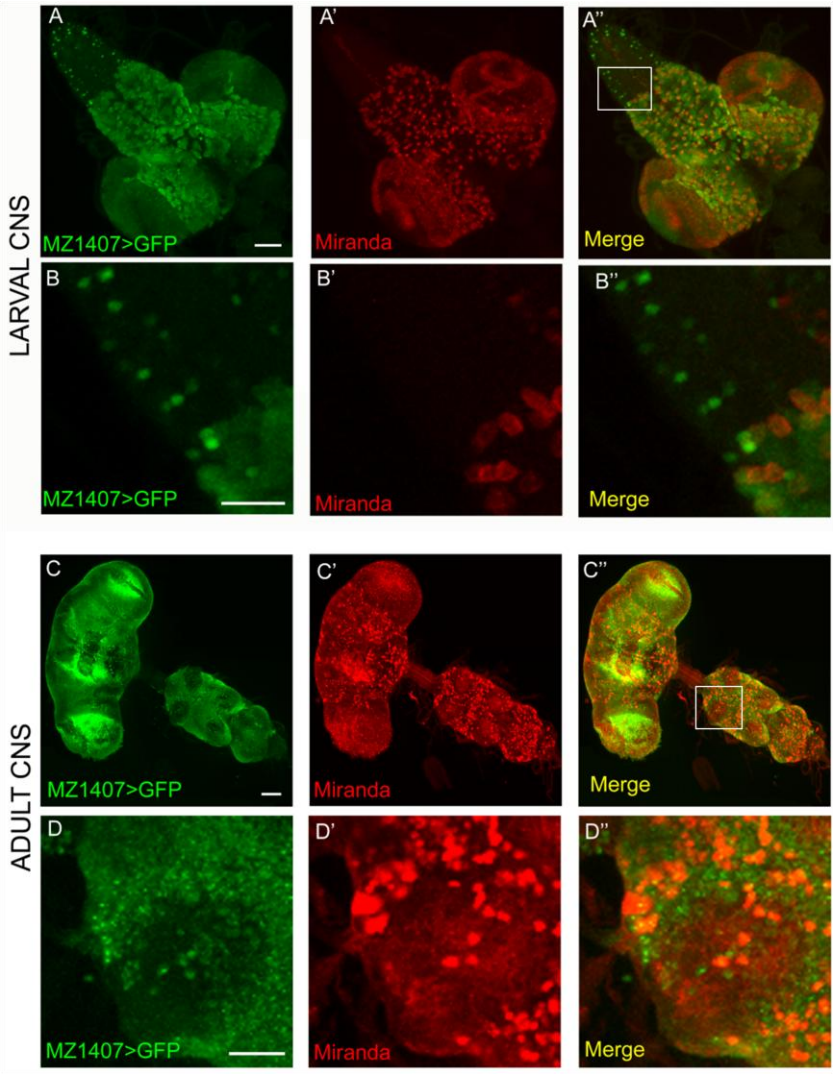

Figure 3.6 The *MZ1407-Gal4* driver has a broad expression in the CNS.

Confocal microscopy carried out to visualize the expression pattern of the *MZ1407-Gal4* driver. *MZ1407-Gal4* driver line flies crossed to *UAS-nlsGFP*. The expression pattern of the *MZ1407* driver (green) shows wider signal compared to the neuroblast specific antibody Miranda (red) in the larval CNS (A-B''), and adult CNS (C-D''). Scale bars show 100 μm in A and C and 20 μm in B and D.

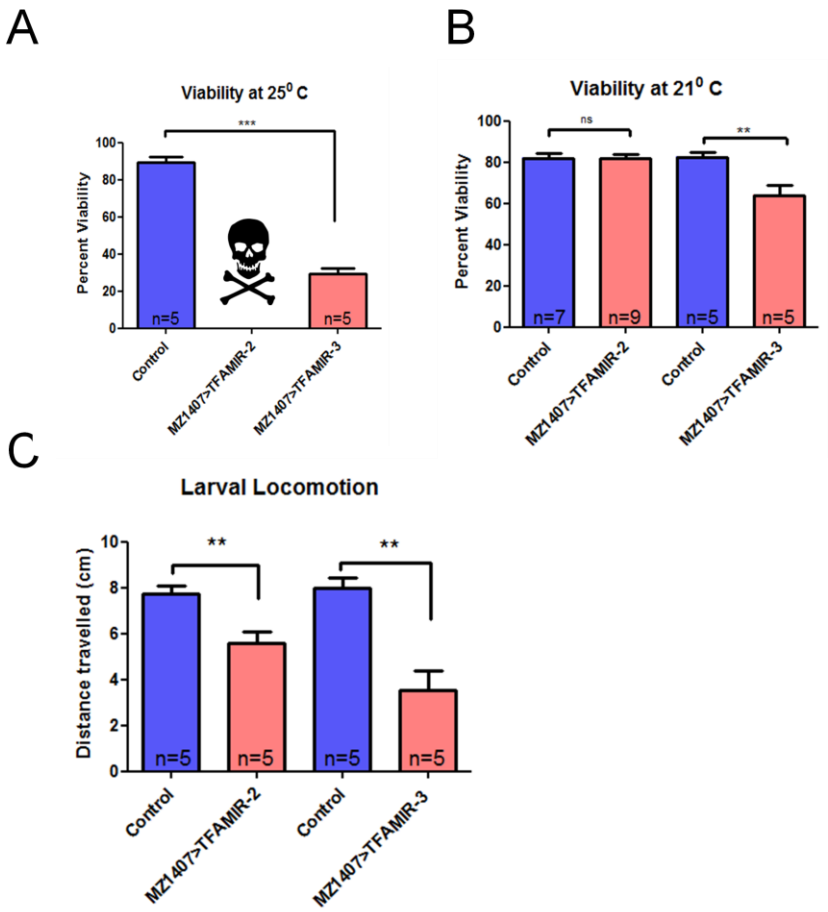

Figure 3.7 *TFAM* knockdown using *MZ1407-Gal4* driver causes reduced viability and reduced larval locomotion.

Fifty first instar larvae were transferred to vials containing normal food and developed until they reached the adult stage. The number of eclosed adults was then quantified. **(A)** *TFAMIR-3* affects viability and *TFAMIR-2* causes lethality when flies were developed at 25^{0}C. **(B)** *TFAMIR-3* has a negative effect on viability when developed at 21^{0}C. **(C)** Larval movement was reduced both in *TFAMIR-2* and *TFAMIR-3* crosses at 21^{0}C. Five larvae per genotype were tested on an agar surface under light controlled conditions. For all of the assays separate control flies were used for each *TFAM* RNAi line. RNAi lines were balanced over an RFP reporter prior crossing to the driver line. RFP expressing progeny were used as a control in subsequent experiments. Mean values +/- SEM plotted on graph. **=p<0.01, ***=p<0.001.

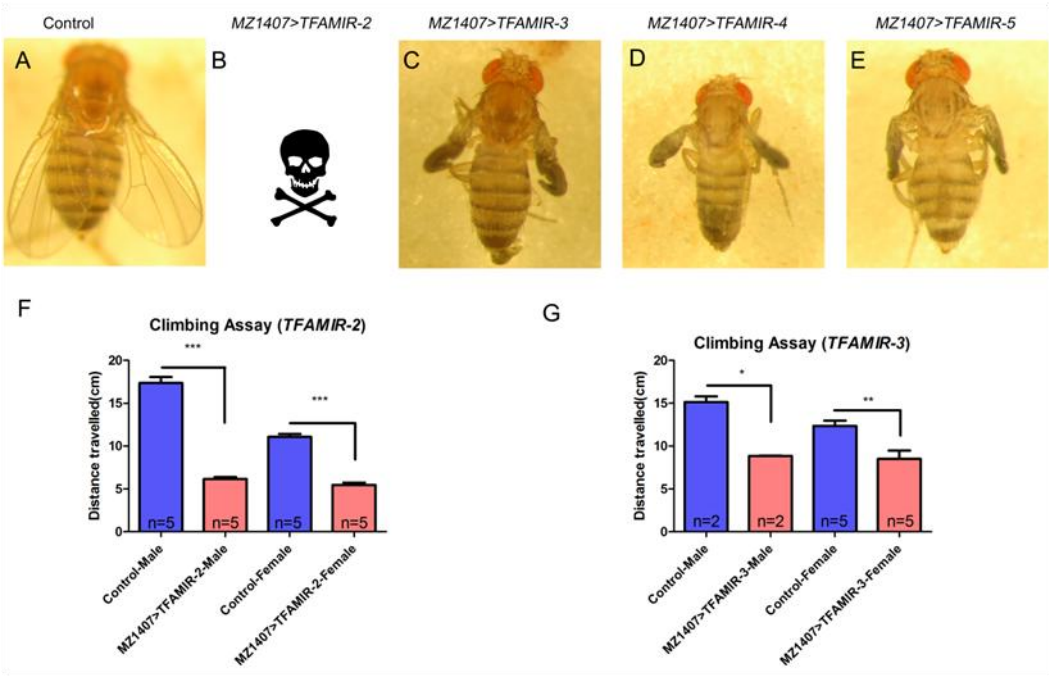

Figure 3.8 *TFAM* RNAi expressed using *MZ1407-Gal4* causes developmental and behavioural defects in adults.

Four different RNAi lines were crossed to the *MZ1407-Gal4* driver at 25^0C. *TFAMIR-2* was lethal, however the other lines developed to the adult stage. **(A-E)** All of the *TFAM* RNAi lines tested had defects in wing expansion. Two of the *TFAM* RNAi lines were also tested for climbing behaviour. Both *TFAMIR-2* **(F)** and *TFAMIR-3* **(G)** flies had climbing defects when developed at 21^0C. For both of the assays separate control flies used for each *TFAM* RNAi line. RNAi lines were balanced over an RFP reporter prior crossing to the driver line. RFP expressing progeny were used as a control in subsequent experiments. Mean values +/- SEM plotted on graph. *=p<0.05, **=p<0.01, ***=p<0.001

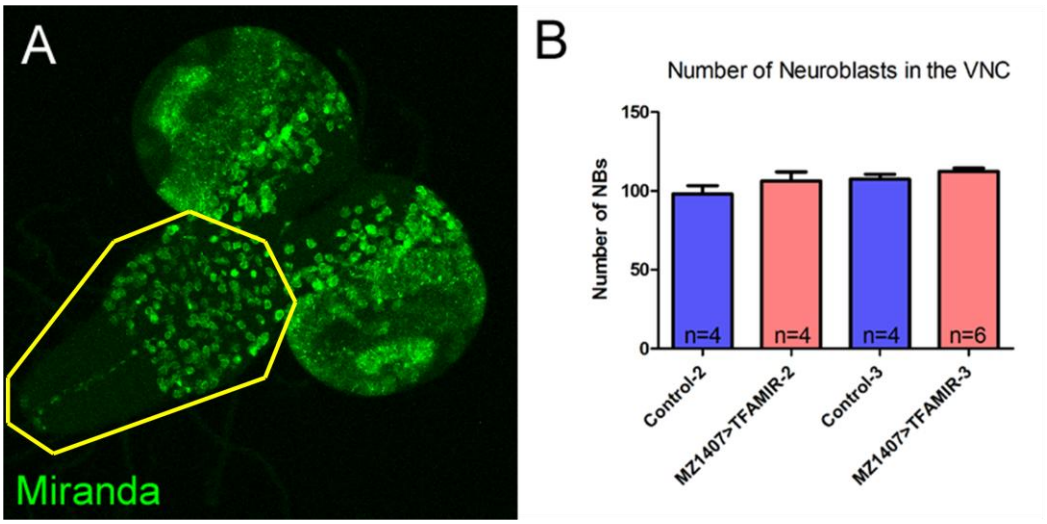

Figure 3.9 Effect of *TFAM* RNAi on neuroblasts

(A) Representative figure illustrating neuroblasts using Miranda staining. Highlighted region shows the area quantified. **(B)** Knockdown of *TFAM* using *MZ1407-Gal4* does not affect the number of neuroblasts in the VNC. Control flies were RFP expressing flies either on the second chromosome (Control-2) or third chromosome (Control-3). Mean values +/- SEM plotted on graph.

3.6 Knockdown of *Polγ*, *Twinkle* and *TFAM* in mushroom body neurons

The *Drosophila* CNS consists of many of different neuronal types. During development, axons extending from neuronal cell bodies follow a stereotypical path in order to reach to their targets. Mushroom body (MB) neurons have a very distinct axonal morphology (Figure 3.10A, (CRITTENDEN *et al.* 1998)) and are involved in olfactory learning and memory (MCGUIRE *et al.* 2001; ROMAN and DAVIS 2001; WOLF *et al.* 1998). These neurons have been previously used in many studies to assess the functions of genes needed for neuronal development and survival. Furthermore, MB neurons are very convenient to model axonal degeneration.

In order to investigate mtDNA loss in neurons at a cellular level, RNAi lines were crossed to the MB specific driver *OK107-Gal4* (CONNOLLY *et al.* 1996). *Polγ*, *Twinkle* and *TFAM* RNAi lines were crossed to the *OK107-Gal4,CD8-GFP* driver and the progeny aged for 30 days. A MB specific driver expressing a CD8-GFP reporter was used to analyse the morphology of these neurons in detail. Aged fly CNS' were dissected and investigated using confocal microscopy. The α/α' lobe, which is oriented dorsally, and the medially orientated β lobe were the two regions analysed (Figure 3.10A). Slightly thinner neuronal branches were observed in the α' lobe of the *Polγ* and *TFAM* knockdown flies (Figure 3.10C,E). *Polγ* RNAi flies displayed a slight axonal overextension phenotype at the β lobe, however β lobe morphology was normal in the other lines tested (Figure 3.10). Although MB neurons can be useful to analyse axonal degeneration, it is very difficult to assess functional phenotypes with this group of neurons.

Therefore, knockdown of mtDNA replication genes produce distinct phenotypes in MB neurons. This system could potentially be used to investigate the consequences of mtDNA loss on axonal pathfinding and degeneration and any resultant learning and memory phenotypes.

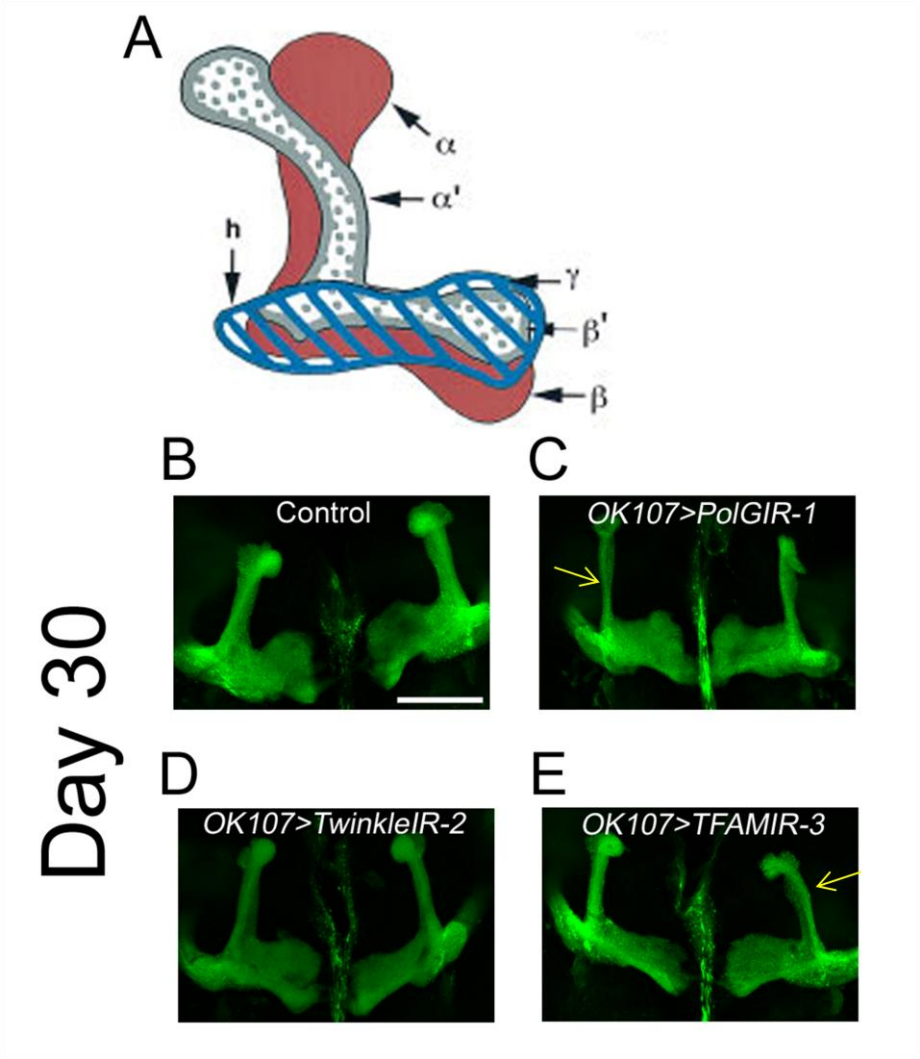

Figure 3.10 Mushroom body specific RNAi of *Polγ* and *TFAM* results in thinner axons.

(A) Representative cartoon of mushroom body lobes (Crittenden et al. 1998). α /α' lobes are dorsal (up) and β/β' lobes face medially. *Polγ* **(C)** and *TFAM* RNAi **(E)** in mushroom bodies caused thinner α' lobes in aged flies. **(B)** However, the other branches looked similar to the control (*OreR* crossed to the *OK107-Gal4,UAS-cd8GFP* driver). Arrows indicate thinner branches. All of the genotypes were imaged at the same magnification. Scale bar: 100μm

3.7 Motoneuron specific knockdown of *Polγ*, *Twinkle* and *TFAM* affects larval and adult behaviour

The *Drosophila* nervous system is a powerful model, with an extensive genetic toolbox available. *Drosophila* motoneurons have been used as a model by many laboratories and there are various drivers available that are specific to these neurons. Approximately 80 motoneurons per hemisegment are generated during embryogenesis from 30 neuroblasts (LANDGRAF and THOR 2006a; LANDGRAF and THOR 2006b). In order to fulfil their functions, motoneuron axons extend to their particular target muscles to form synapses. These neurons are needed for motor function as they control muscle activity through synapses at neuromuscular junctions (NMJs). The requirement of proteins involved in mtDNA replication machinery was investigated in this neuronal population using the *OK371-Gal4* driver. *OK371-Gal4* is an enhancer trap element inserted upstream of the vesicular glutamate transporter (*VGlut*), which is expressed specifically in motoneurons and some neuronal clusters in the brain (MAHR and ABERLE 2006). *OK371-Gal4* was used to knock-down *Polγ*, *Twinkle* and *TFAM* in motoneurons. Larval motility assays were carried out in (see Behavioural Assays section in Chapter 2) to assess the effect of motoneuron-specific knockdown of mtDNA related genes on locomotion. *Polγ* RNAi larvae displayed no reduction in larval movement, however both *Twinkle* and *TFAM* RNAi larvae showed a significant reduction (Figure 3.11A). *TFAMIR-3* was further tested with two controls. *OK371-Gal4* crossed to *OreR* flies were used as external controls, while larvae expressing RFP developed in the same tube as the *TFAMIR-3* larvae, were used as internal controls. In order to generate the internal control, *PRSP2* flies were crossed to *TFAMIR-3* and the progeny of this cross (*TFAMIR-3/PRSP*) was

subsequently crossed to the *OK371-Gal4* driver. *PRSP2* is a construct generated using an enhancer element from the gene *pointed* to drive RFP expression in oenocytes and other tissues (KAUL and BATEMAN 2009). Larval locomotion of internal and external controls were similar, while *TFAM* knockdown larvae had reduced larval locomotion compared to both controls (Figure 3.11B).

Flies with motoneuron specific knockdown of *Polγ*, *Twinkle* and *TFAM* were viable. Climbing assays were carried out in order to test adult behaviour. All three RNAi lines had reduced climbing performance compared to controls when male flies were tested (Figure 3.12A). In female flies there was a significantly lower climbing performance upon expression of dsRNAs against *Polγ* and *TFAM*, but not *Twinkle* (Figure 3.12B). Since RNAi of *TFAM* gave the most severe locomotion phenotype, I investigated the effects of *TFAM* knockdown in detail.

Motoneuron specific *TFAM* knockdown flies were aged for 30 days to test whether the climbing phenotype worsened with age. In order to reduce the variability, more flies were tested compared to the previous assay presented in Figure 3.12. 12-15 flies were tested on day 2 and 10 flies were tested on day 30. As shown in Figure 3.13A, a similar level of reduction was observed in male flies at both of the time points. Interestingly, when female flies were tested using 12 flies as opposed to 5 (in the previous assay shown in Figure 3.12), there was no difference in climbing performance on day 2 (Figure 3.13B). However, 10 female flies tested on day 30 had a significant reduction in the distance travelled compared to control flies (Figure 3.13B). Female control flies at 30 days had significantly reduced climbing activity compared female controls at 2 days, while male control flies performance did not change with age. *TFAMIR* male flies exhibited a climbing defect early on inlife and

this did not change after 30 days. In contrast, female flies had a normal climbing performance early in life, but reduced climbing activity after 30 days.

In summary, expressing dsRNA lines against mtDNA related genes in motoneurons did not cause lethality, but affected larval and adult behaviour. Furthermore, *TFAM* knockdown resulted in the strongest larval locomotion phenotype, compared to *Polγ* and *Twinkle* knockdown. Therefore, knockdown of *TFAM* using *OK371-Gal4* provides a potential platform for testing the consequences of mtDNA loss in motoneurons. The advantages of *Drosophila* larval motoneurons as an experimental model led us to focus on this system as a way to investigate neuronal mtDNA loss.

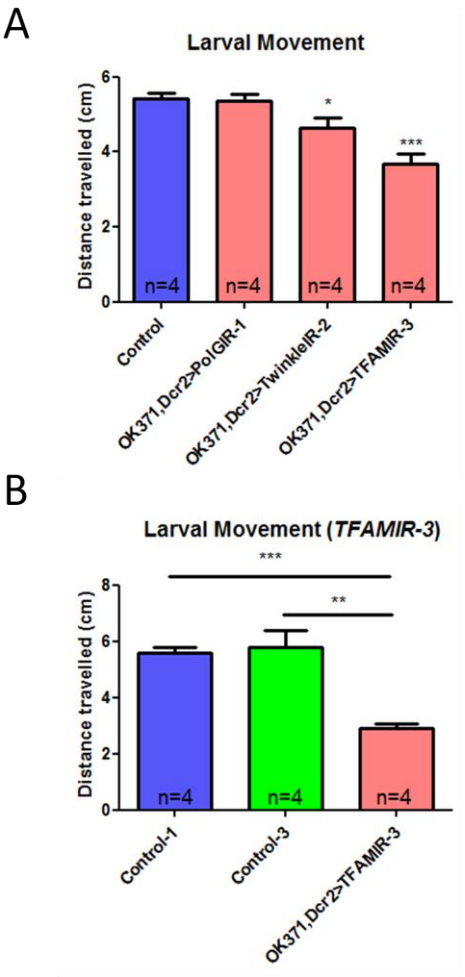

Figure 3.11 Motoneuron specific RNAi of *Twinkle* and *TFAM* causes larval locomotion defects.

(A) Four larvae were tested per genotype for larval locomotion under light controlled conditions. Motoneuron specific knockdown of *Twinkle* and *TFAM* using the *OK371,CD8GFP,Dcr2* driver line resulted in reduced larval movement compared to wild type (OreR) flies crossed to the driver. **(B)** Knockdown of *TFAM* using *TFAMIR-3* significantly reduced larval movement compared to an internal control (Control-3, green bar) and an external control (Control-1, blue bar). Mean values +/- SEM plotted on graph. *=p<0.05, **=p<0.01, ***=p<0.001

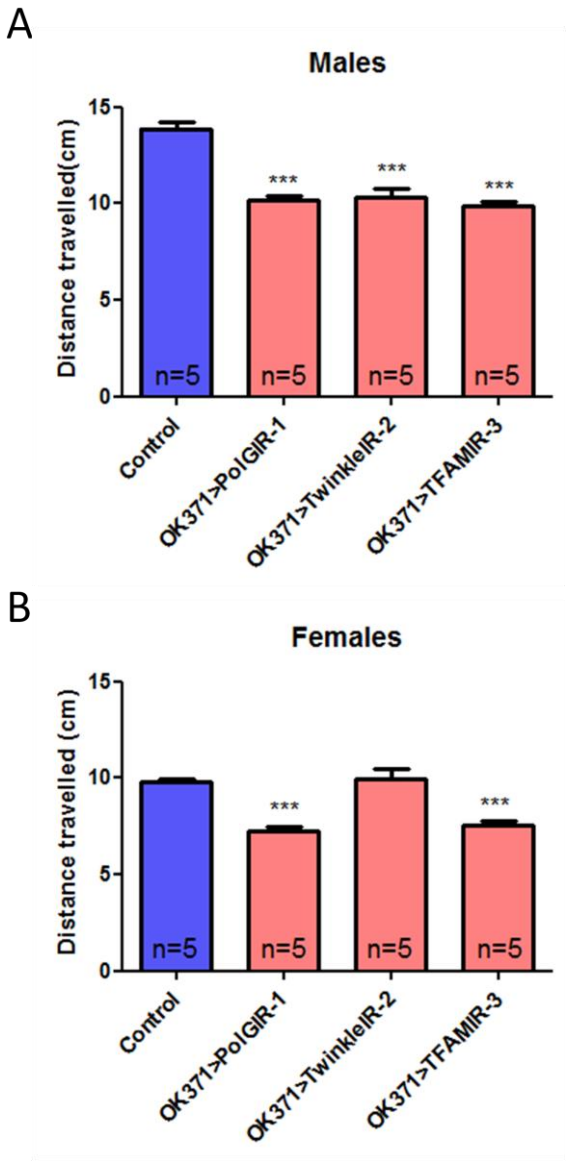

Figure 3.12 Motoneuron specific RNAi of *Polγ*, *Twinkle* and *TFAM* causes reduction in climbing ability.

(A) *Polγ*, *Twinkle* and *TFAM* RNAi male flies all show significantly reduced climbing performance compared to wild-type (*OreR*) flies crossed to the motoneuron driver *OK371-Gal4*. **(B)** Only *PolγIR-1* and *TFAMIR-3* were affected in female flies. Mean values +/- SEM plotted on graph ***=p<0.001

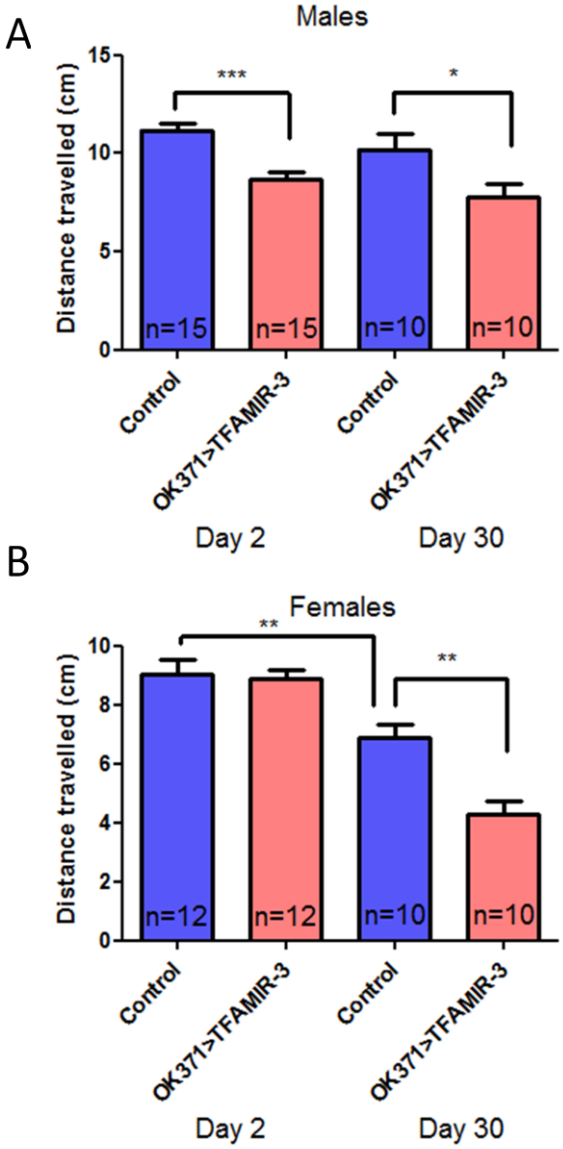

Figure 3.13 Motoneuron specific knockdown of *TFAM* causes age dependent defects in the climbing performance of female flies.

(A) Male *TFAM* motoneuron knockdown flies have similarly reduced climbing activity at both 2 and 30 days. (B) In female *TFAM* motoneuron knockdown flies climbing ability is reduced at 30 days but not at 2 days. Controls were also reduced after 30 days compared to 2 days. Distance climbed in 10 seconds was tested in male and female flies separately. Mean values +/- SEM plotted on graph *=$p<0.05$, **=$p<0.01$, ***=$p<0.001$

3.8 Summary

In this chapter, I have presented work which has resulted in the preliminary characterisation of a neuronal specific system to study mtDNA loss. Firstly, I demonstrated that EtBr can be used as a tool to deplete mtDNA levels in *Drosophila*. In order to study the consequences of mtDNA depletion at the cellular level, I adopted a gene-specific approach and studied the effects of various RNAi lines targeting mtDNA replication genes. I tested the requirement for several nuclear encoded proteins that are components of the mtDNA replication machinery for viability in *Drosophila,* by ubiquitous RNAi and scoring of lethality. Most of the RNAi lines tested caused lethality when ubiquitously expressed and so were further investigated to ascertain the necessity of these genes in neurons. This was undertaken by knockdown of these using driver lines in specific neuronal populations. Using *MZ1407-Gal4*, a neuroblast and neuronal specific driver resulted in marginally decreased mtDNA levels in fly heads. Further to this, using the *MZ1407-Gal4* driver to knockdown *TFAM* affected larval development and caused behavioural phenotypes at both the larval and adult stage, even though neuroblast number was not affected at the larval stage.

Gal4 drivers for two specific neuronal populations were also used to knockdown mtDNA replication genes. The mushroom body specific driver *OK107-Gal4* driver was used to determine whether any of the RNAi lines affected axonal development. Finally, I used motoneurons as a model system to investigate mtDNA depletion. I observed behavioural phenotypes both at larval and adult stages for all three RNAi lines tested and motoneuron specific *TFAM RNAi* resulted in age-dependent climbing

defects in female flies. Overall the data presented provide the foundation for the subsequent detailed analysis of the consequences of mtDNA loss in a specific neuronal cell type in *Drosophila*.

Chapter 4. Manipulation of *TFAM* levels to induce mtDNA loss in motoneurons

4.1 Introduction

Mitochondrial disorders have been linked to abnormalities in mtDNA, such as mutations and deletions. Furthermore, loss of mtDNA results in a group of diseases known as mtDNA depletion syndromes (MDS). Replication of mtDNA is necessary to maintain an adequate mtDNA copy number. Manipulating *TFAM* expression levels has been reported to affect the mtDNA replication machinery, however the exact mechanisms are not known (reviewed in (CAMPBELL *et al.* 2012a)). In the previous chapter, I showed that expressing a dsRNA against *TFAM* in motoneurons caused behavioural defects. Additionally, pan-neuronal *TFAM* knockdown using *MZ1407-Gal4* resulted in slight but not significant depletion of mtDNA in neurons, which is in accordance with previous studies. Overexpression of *TFAM* has also been shown to result in mtDNA depletion in tissue culture cells (POHJOISMAKI *et al.* 2006). Taken together, the results in the previous chapter and other published studies indicate that *TFAM* knockdown and *TFAM* overexpression can be used as methods to deplete mtDNA.

In order to investigate the consequences of mtDNA depletion in detail, a tissue specific approach was taken. Ubiquitous depletion of mtDNA levels results in lethality in different organisms (OLIVEIRA *et al.* 2010). It has been previously shown that generation of tissue specific *TFAM* knockout mice results in cell death in cardiac

tissues (WANG *et al.* 2001). Several groups have studied *Polγ* mutants, the mtDNA specific polymerase, as a model of mtDNA depletion. Recently, RNAi of *Polγ* was shown to cause dopaminergic cell loss in flies (HUMPHREY *et al.* 2012). Motoneurons have distinct morphological features, in that synapses are formed on muscles to generate the neuromuscular system. *SOD1* mutant rat motoneurons were recently used as an ALS (amyothropic lateral sclerosis) model to investigate synaptic alterations (MAGRANE *et al.* 2012). Synaptic dysfunction and loss of synapses has also been implicated in AD (SHENG and CAI 2012). In the previous chapter I showed that RNAi of *TFAM* in motoneurons results in defects in locomotion. I thus aimed to understand the mechanism which underlies these observed behavioural abnormalities.

4.2 Ubiquitous knockdown and overexpression of *TFAM* causes different levels of mtDNA depletion

Ubiquitous expression of two RNAi lines against *TFAM*, *TFAMIR-2* and *TFAMIR-3*, caused lethality during the pupal stage (Table 3.1). However, it was possible to analyse larvae to determine whether *TFAM* mRNA levels were affected. In order to quantify *TFAM* transcript levels at the larval stage, qPCR against *TFAM* and *RpL1* (a large ribosomal subunit gene) was carried out. Both of the *TFAM* RNAi lines were shown to have reduced *TFAM* transcript levels, although due to the variability only *TFAMIR-3* reached significance (Figure 4.1A). After demonstrating a reduction in *TFAM* expression at the level of mRNA, mtDNA levels were analysed at the third instar larval stage. qPCR analysis showed a reduction in mtDNA levels in both

TFAM RNAi lines when ubiquitously expressed, although only *TFAMIR-3* reached significance (Figure 4.1B).

It has been previously reported that *TFAM* overexpression can result in mtDNA depletion in cultured human cells (POHJOISMAKI *et al.* 2006). To test whether *TFAM* overexpression causes mtDNA loss in *Drosophila,* the *Drosophila TFAM* cDNA was cloned into pUAST and pTWG (generating a C-terminal GFP fusion) and used to generate transgenic flies (Materials and Methods). When ubiquitously overexpressed using *Actin-Gal4*, *TFAMGFP* and *TFAM* overexpression caused developmental arrest in the first and second instar respectively. The effects of ubiquitous *TFAM* overexpression on mtDNA levels was analysed by qPCR of genomic DNA isolated from first instar larvae (Materials and Methods). Ubiquitous expression of *TFAM* using *Actin-Gal4* resulted in a significant decrease in mtDNA copy number (Figure 4.1 C), while *TFAMGFP* overexpression also caused a moderate decrease, but this did not reach significance (Figure 4.1 C). Similar to third instar larvae (Figure 4.1 B), first instar *TFAM* RNAi larvae had significantly reduced mtDNA levels (Figure 4.1 C). Taken together these data reveal *TFAM* RNAi can cause a slight reduction in mtDNA levels and show that *TFAM* overexpression also causes mtDNA loss in *Drosophila*.

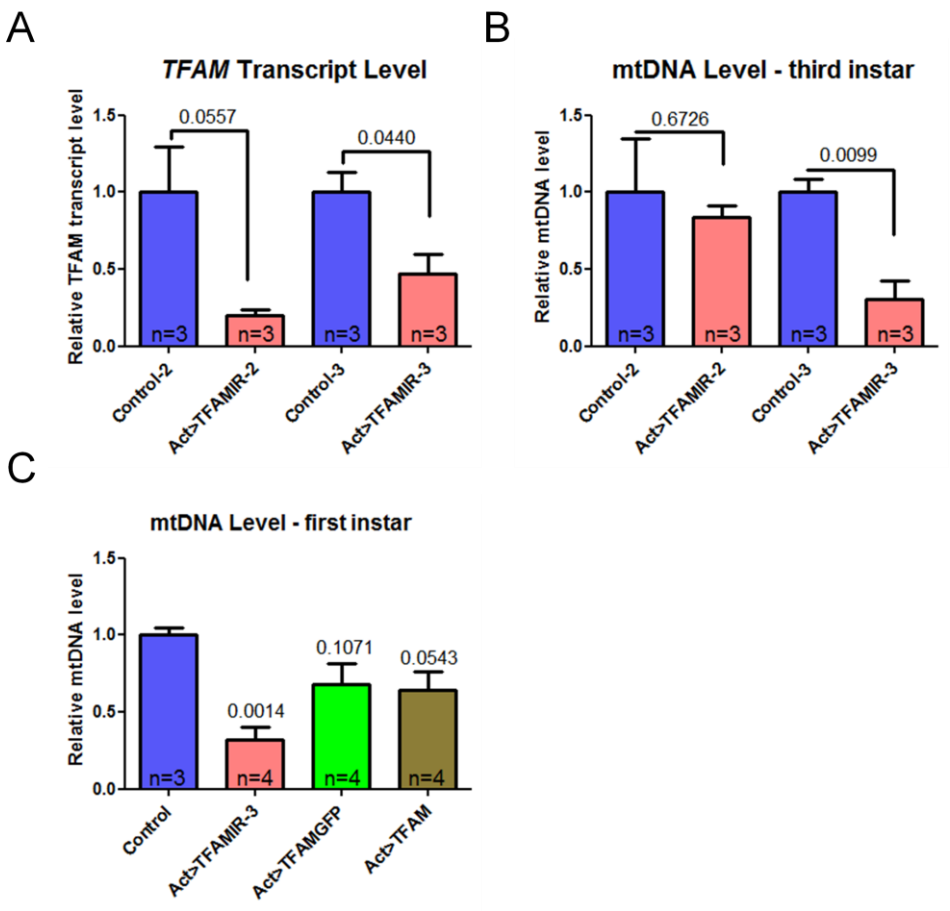

Figure 4.1 Ubiquitous *TFAM* knockdown and overexpression causes variable levels of mtDNA depletion.

(A) *TFAM* transcript levels were reduced at the third instar larval stage in two of the *TFAM-RNAi* lines tested by qPCR. Control-2 and Control-3 were the RFP expressing larvae on the second and third chromosome respectively. *TFAMIR-2* line was nearly significant, with a p value of 0.0557. **(B)** *TFAMIR-3* larvae had a significantly lower level of mtDNA compared to RFP expressing control larvae at the third instar larval stage. **(C)** MtDNA levels were reduced both in *TFAM* knockdown and overexpression lines at the first instar larval stage. Control samples were obtained by crossing w^{1118} flies to *Actin-Gal4* driver flies. P values for each of the experiments are shown above the bars. Mean values +/- SEM plotted on graphs A, B and C.

4.3 *TFAM* RNAi and overexpression disrupts wing development

In order to assess the effect of *TFAM* RNAi and overexpression at the protein level I used a commercially available antibody that recognises *Drosophila TFAM*. Initial characterisation of this antibody showed that it gave strong punctate cytoplasmic staining that co-localised with mitochondrially-targeted GFP expression by immunofluorescence (not shown), similar to the expression pattern of TFAM seen in vertebrate cells (LEGROS *et al.* 2004). I decided to use the wing imaginal disc as a system to initially analyse the effect of *TFAM* RNAi and overexpression at the protein level by using *MS1096-Gal4*. *MS1096-Gal4* is an X-linked *Gal4* enhancer trap inserted in *Beadex* and is expressed in the dorsal compartment of the wing (CAPDEVILA and GUERRERO 1994). Given that the ventral compartment of the wing is unaffected, it can therefore be used as an internal control. Wingless (Wg) staining can be used to differentiate between the dorsal and ventral compartments (Figure 4.2 A-A'). Staining of wing discs with the TFAM antibody from larvae in which *TFAM* RNAi was driven with *MS1096-Gal4* showed that in the dorsal compartment there was a reduction in the level of diffuse TFAM staining and small TFAM puncta, while larger puncta were more apparent (Figure 4.2B-B'). The effect of *TFAM* and *TFAMGFP* overexpression was also analysed in the wing using *MS1096-Gal4*. Expression of both *TFAM* and *TFAMGFP* caused a dramatic increase in TFAM protein levels (Figure 4.2 C-C',D). These data confirm that RNAi and overexpression of *TFAM* causes either decreased or increased TFAM expression respectively, at the protein level.

Adult flies generated by RNAi or overexpression of *TFAM* with *MS1096-Gal4* had distinct wing phenotypes. Wings from *TFAM* RNAi flies were curved upwards and were reduced in size compared to controls (Figure 4.3A,B). Both *TFAM* and *TFAMGFP* overexpression resulted in more severe phenotypes compared to the *TFAM* knockdown. *TFAM* overexpression wings were extremely small and abnormal compared both to controls and *TFAM* RNAi wings (Figure 4.3C,D). The basis for these phenotypes was not investigated further, but could result from decreased proliferation, increased apoptosis, or inhibition of specific developmental processes.

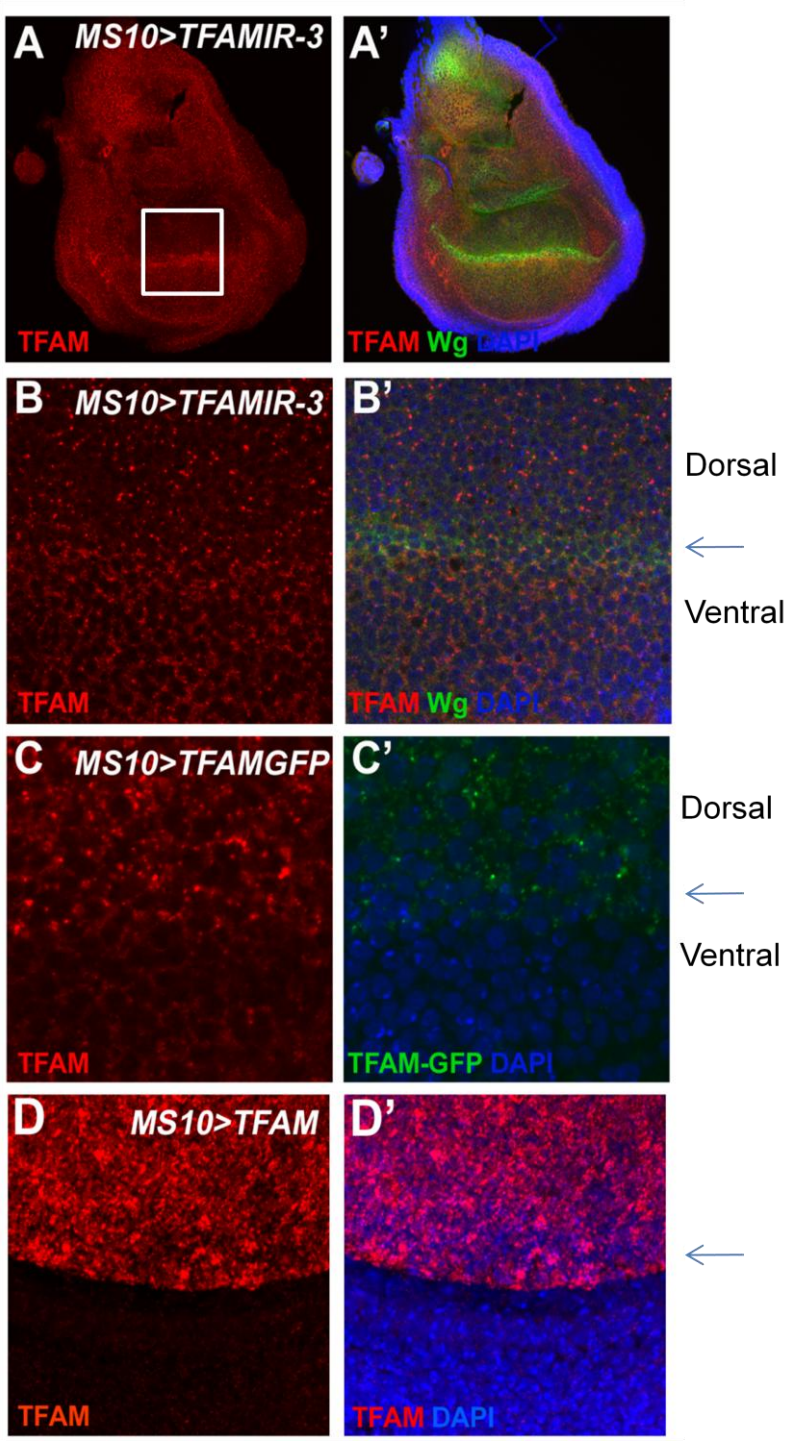
A
MS10>TFAMIR-3
TFAM
A'
TFAM Wg DAPI
B
MS10>TFAMIR-3
TFAM
B'
TFAM Wg DAPI
Dorsal
Ventral
C
MS10>TFAMGFP
TFAM
C'
TFAM-GFP DAPI
Dorsal
Ventral
D
MS10>TFAM
TFAM
D'
TFAM DAPI

Figure 4.2 TFAM staining in the larval wing disc.

(A-A') Whole wing disc from a third instar larvae. Reduced TFAM staining can be observed in the dorsal compartment (upper half of the box) wing imaginal disc where the dsRNA against *TFAM* is driven by the *MS1096-Gal4* driver. Wingless (green) staining shows the boundary between dorsal and ventral compartments. Antibody staining against TFAM is shown in red and DAPI (blue) stained cell nuclei**. (B-B')** Close up scan of the boxed area in the A-A'. Expressing a dsRNA against *TFAM* in the dorsal compartment of the wing disc results in a decrease in TFAM staining. Increased TFAM staining was observed in the upper half of the panels when *TFAMGFP* and *TFAM* was expressed using *MS1096-Gal4* **(C-C')** and **(D-D')**. Overexpression of *TFAM* was seen in a wider area than *TFAM* RNAi and *TFAMGFP*, but the close-up images were scanned at the expression boundaries (arrows).

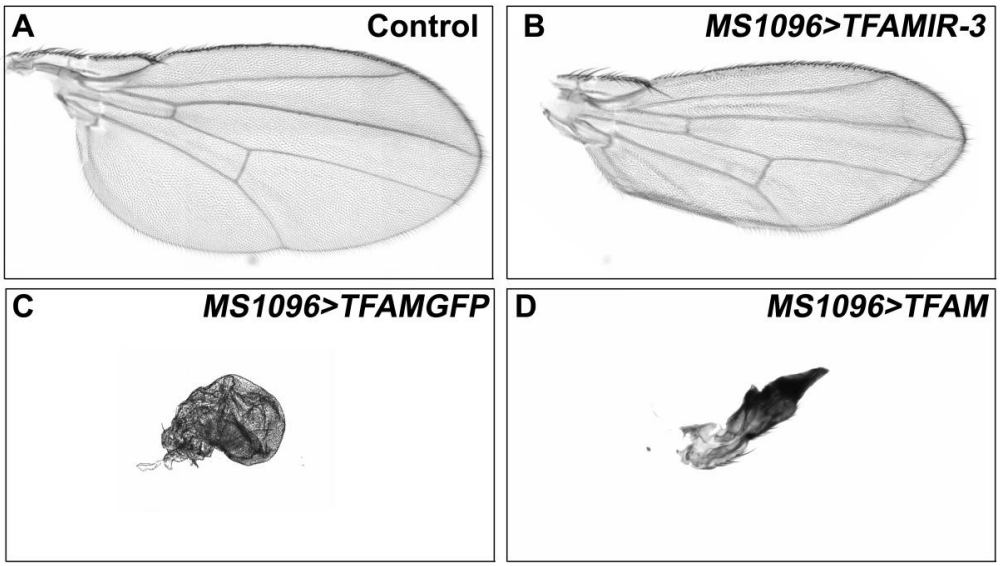

Figure 4.3 RNAi or overexpression of *TFAM* disrupts wing development.

Control (w^{1118}), *TFAMIR-3*, *UAS-TFAMGFP* and *UAS-TFAM* flies were crossed to the *MS1096-Gal4* driver and developed at 25^0C. Expressing a dsRNA against *TFAM* using *MS1096-Gal4* resulted in slightly curved and smaller wings **(B)** compared to control **(A)**. **(C-D)** Expressing *TFAMGFP* and *TFAM* in the dorsal part of the wing resulted in complete disruption of wing morphology.

4.4 Effect of *TFAM* RNAi and overexpression on TFAM protein in motoneuron cell bodies

In the previous section I demonstrated that I was able to visualize both knockdown and overexpression of *TFAM* in the wing disc using an antibody against TFAM. These experiments not only confirmed that *TFAM* RNAi and overexpression had the expected effects at the protein level, but also validated the specificity of the TFAM antibody. However, the main aim of this study was to generate a neuronal model of mtDNA depletion. In order to investigate the consequences of mtDNA depletion in a neuronal specific system, TFAM levels were manipulated in the motoneuron population by using the *OK371-Gal4* driver. The *OK371-Gal4* stock included a UAS-CD8-GFP reporter transgene, so that cells expressing *Gal4* could be visualized by fluorescence microscopy.

When control (w^{1118}) flies were crossed to the *OK371-Gal4,UAS-CD8-GFP* driver uniform TFAM staining was observed in the GFP expressing motoneuron cell bodies in the VNC (Figure 4.4A-A''). However, when *TFAM-RNAi* flies were crossed to the driver line, there was a reduction in the TFAM protein levels (Figure 4.4B-B''). Furthermore, most of the small TFAM puncta disappeared, with only large punctate structures being observed (Figure 4.4B-B''). Expression of *TFAM* or *TFAMGFP* resulted in an increase in TFAM staining throughout the motoneuron cell body (Figure 4.4.C-D''). In conclusion, similar to the results in the wing imaginal disc, manipulation of *TFAM* levels in motoneurons can be visualized using an antibody against TFAM. These data also confirm that RNAi and overexpression of *TFAM* using *OK371-Gal4* has the expected effects at the protein level in motoneurons.

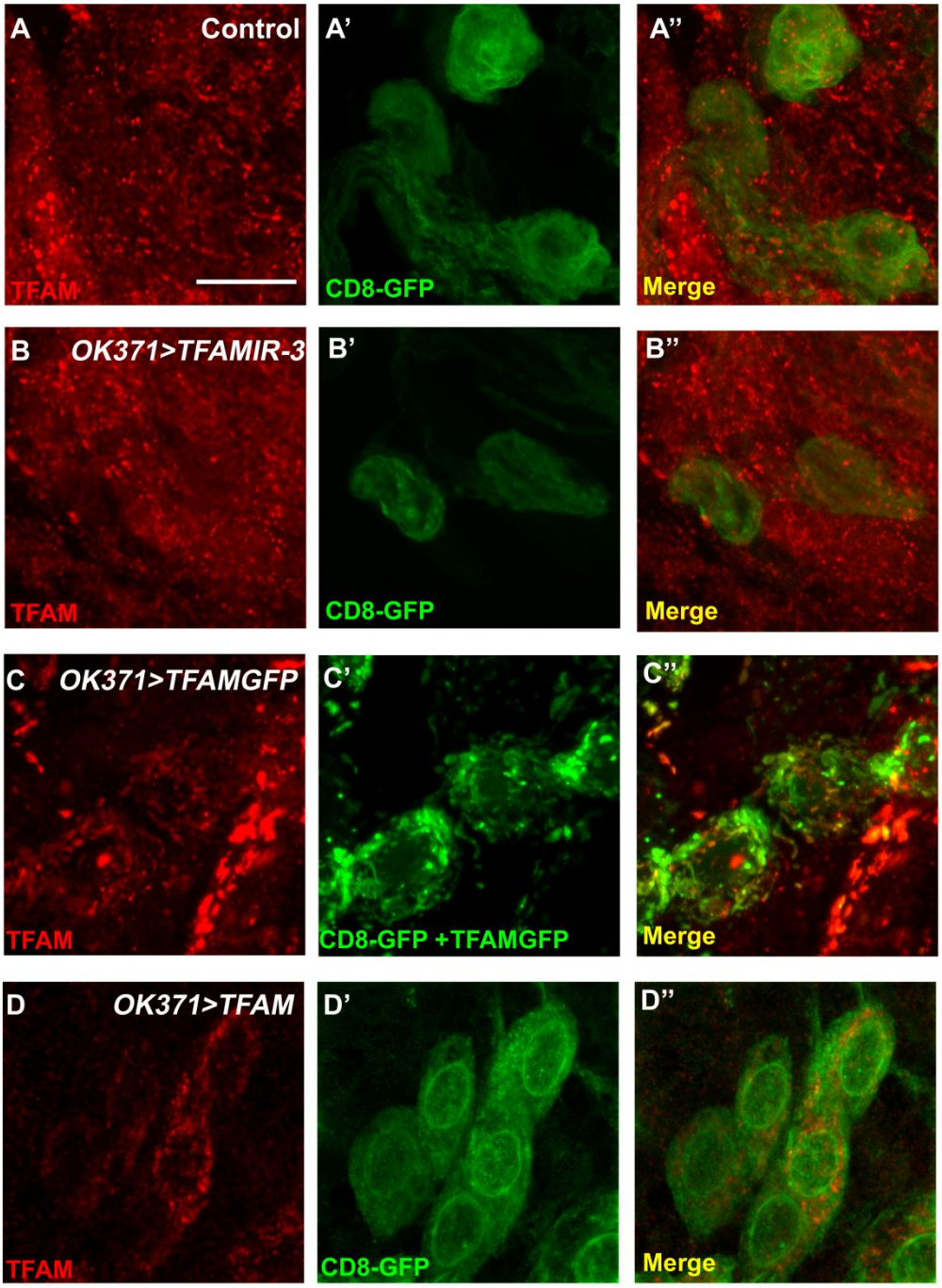
A
Control
TFAM
A'
CD8-GFP
A''
Merge
B
OK371>TFAMIR-3
TFAM
B'
CD8-GFP
B''
Merge
C
OK371>TFAMGFP
TFAM
C'
CD8-GFP +TFAMGFP
C''
Merge
D
OK371>TFAM
TFAM
D'
CD8-GFP
D''
Merge

Figure 4.4 Manipulating *TFAM* levels in motoneuron cell bodies.

(A-A'') TFAM staining is distributed homogenously throughout the VNC in control brains. *OK371-Gal4,UASCD8-GFP* was used to knockdown or overexpress *TFAM* in larval motoneurons. TFAM antibody staining is shown in red and motoneuron cell bodies in green. Decreased TFAM staining was observed in the cell bodies expressing a dsRNA against *TFAM* **(B-B''),** compared to control cell bodies **(A-A'').** Control samples were dissected from the progeny of w^{1118} flies crossed to the *OK371-Gal4,UASCD8-GFP* line. Increased TFAM expression was observed in both *TFAMGFP* **(C-C'')** and *TFAM* expressing cell bodies **(D-D'')**. Scale bar shows 10 μm.

4.5 *TFAM* RNAi and overexpression in motoneurons causes behavioural defects

In the previous chapter, it was shown that knockdown of *TFAM* in motoneurons resulted in larval locomotion and adult climbing defects. Developmental and behavioural effects upon motoneuron manipulation of *TFAM* levels were investigated in more detail. Both RNAi and overexpression of *TFAM* in motoneurons appeared to result in viable progeny. To determine quantitatively whether there was any effect on viability egg laying cages were used and 300 first instar larvae were transferred to vials (50 larvae per vial) and the percentage of the adults that eclosed from each vial was documented. RNAi or overexpression of *TFAMGFP* resulted in similar numbers of viable adults to the control. However, overexpression of *TFAM* caused a significant decrease in the number of eclosed adults, although the number of pupae was unaffected (Figure 4.5A,B). Therefore motoneuron-specific knockdown of *TFAM* does not affect viability, while *TFAM* overexpression can reduce the ability of pupae to eclose from the pupal case (Figure 4.5.A).

I also repeated the larval locomotion assay, which previously showed that motoneuron-specific RNAi of *TFAM* caused reduced locomotion (Figure 3.11), this time including *TFAM* and *TFAMGFP* overexpression. Both knockdown and overexpression of *TFAM* and *TFAMGFP* resulted in a significant decrease in larval motility (Figure 4.5C).

Climbing assays were also carried out at the adult stage. In accordance with the climbing data in the previous chapter, RNAi of *TFAM* resulted in a decrease in climbing compared to controls in male flies (Figure 4.6A). Superficial examination

of motoneuron-specific *TFAM* or *TFAMGFP* overexpression revealed that, although viable, these flies had severe locomotion defects and had difficulty climbing. Quantification of climbing ability showed that motoneuron-specific expression of both *TFAM* and *TFAMGFP* caused a strong reduction, with *TFAM* expression causing a 90% decrease in climbing ablility compared to control flies (Figure 4.6A).

I also asked whether overexpression of *TFAMGFP* could rescue the climbing phenotype caused by *TFAM* RNAi in motoneurons. This experiment is complicated by the fact that *TFAMGFP* overexpression also causes a climbing phenotype and that *TFAM* dsRNA expression will target both the endogenous *TFAM* expression and *TFAMGFP* transgenic expression. *OK371-Gal4* driven expression of *TFAM* RNAi and *TFAMGFP* in the same flies resulted in a climbing phenotype similar to *TFAM* RNAi alone (Figure 4.6B). This result can be interpreted as a failure to 'rescue' *TFAM* RNAi by *TFAM-GFP* expression, but this seems unlikely given that *TFAMGFP* has a stronger climbing phenotype than *TFAM* RNAi. It seems more likely that expression of the *TFAM* RNAi weakens the *TFAMGFP* phenotype by reducing the level of *TFAMGFP* expression. Further analysis will be required to determine which of these interpretations is correct, but this result highlights the difficulting in performing rescue experiments when overexpression of a particular gene causes a similar, or enhanced, phenotype to loss-of-function.

In collaboration with Dr. Chris Elliot from the University of York, adult flies were tested in a jump response assay (see Section 2.2.12). A small, but significant reduction in the jump response was observed in motoneuron-specific *TFAM* RNAi flies, while overexpression of *TFAMGFP* resulted in a stronger defect (Figure 4.6C).

The effect of motoneuron-specific *TFAM* manipulation on lifespan was also tested. Male and female flies were tested separately, given that the sex of the flies can affect lifespan (BALLARD *et al.* 2007). *TFAM* knockdown and control flies had similar lifespan curves. However, expression of *TFAMGFP* resulted in a very strong reduction in lifespan (Figure 4.6 D-E). The median lifespan of control female and *TFAM* knockdown females was 40 days, while the median lifespan with *TFAMGFP* overexpression was 18 days. Male flies with the *TFAM* knockdown had slightly longer median lifespan compared to control, at 53 days versus 42 respectively and approached significance (p=0.0597). In contrast, the median lifespan of *TFAMGFP* overexpression males was significantly reduced (6 days). In order to be confident about the results, the longevity assays were repeated and similar results were observed with *TFAMGFP* overexpression (medium lifespan was 5 days for males and 17 days for females, compared to 49 days in males controls and 40 days in female controls). However, the lifespan increase in males upon *TFAM* knockdown did not repeat (they had a similar median lifespan (49 days) to controls (49 days). Motoneuron-specific *TFAM* overexpression flies were not tested since they died within a few days of eclosion.

In conclusion, these data show that manipulating *TFAM* levels results in behavioural defects both at the larval and adult stages. Furthermore, overexpressing *TFAM* severely reduces median and maximum lifespan.

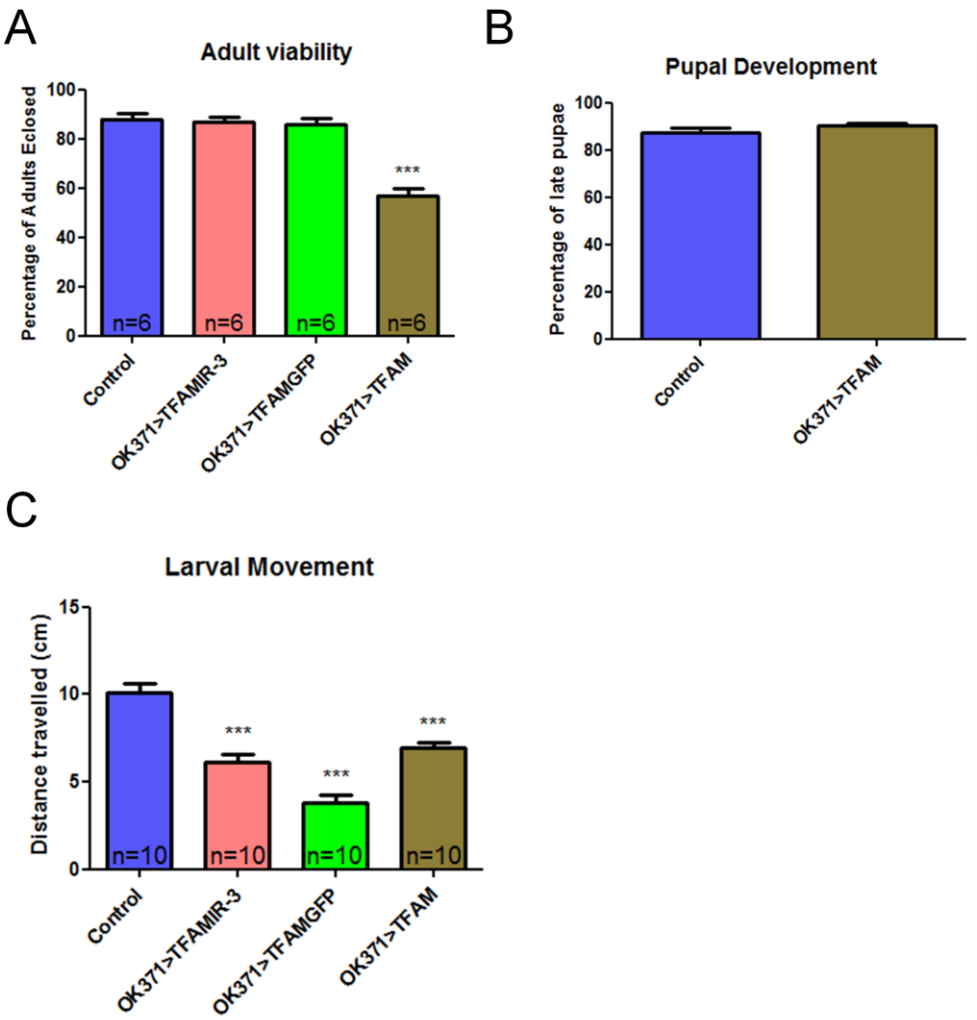

Figure 4.5 Motoneuron specific *TFAM* knockdown or overexpression causes behavioural defects at larval stage.

Manipulation of *TFAM* levels does not affect larval development. (A) The number of larvae developed into adult flies was similar to controls in *TFAM* RNAi and *TFAMGFP* over-expression. (A- B) Expression of *TFAM* results in fewer eclosed adult flies, however the number of late pupae was similar to controls. (C) Larval locomotion assay shows a reduction in larval movement when *TFAM* was knocked-down or overexpressed. Mean values +/- SEM plotted on graph. ***=p<0.001

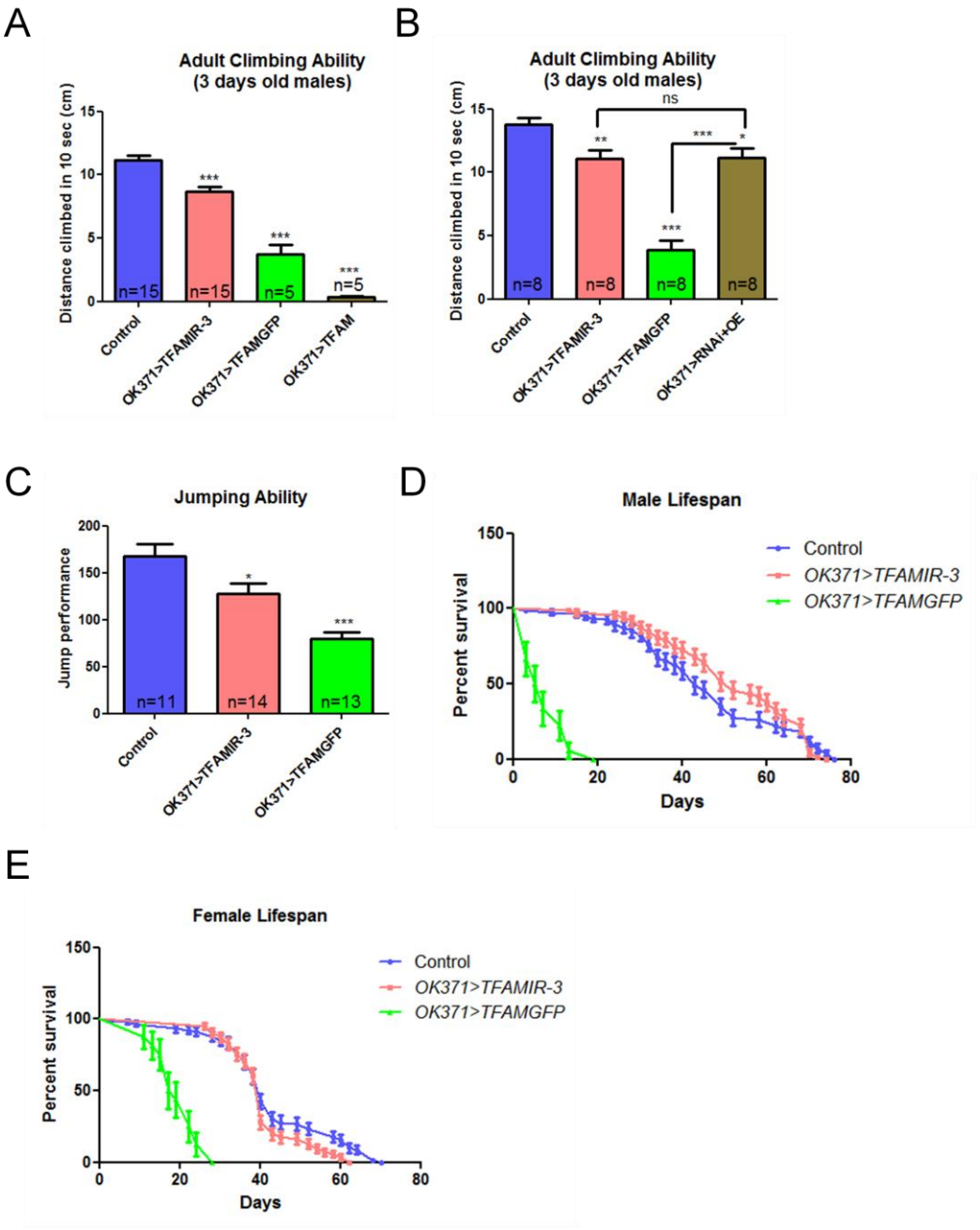
A
Adult Climbing Ability
(3 days old males)
Distance climbed in 10 sec (cm)
15
10
5
0
***
***
***
n=15
n=15
n=5
n=5
Control
OK371>TFAMIR-3
OK371>TFAMGFP
OK371>TFAM
B
Adult Climbing Ability
(3 days old males)
Distance climbed in 10 sec (cm)
ns
**
***
*
***
n=8
n=8
n=8
n=8
Control
OK371>TFAMIR-3
OK371>TFAMGFP
OK371>RNAi+OE
C
Jumping Ability
Jump performance
200
150
100
50
0
*
***
n=11
n=14
n=13
Control
OK371>TFAMIR-3
OK371>TFAMGFP
D
Male Lifespan
Percent survival
150
100
50
0
0
20
40
60
80
Days
Control
OK371>TFAMIR-3
OK371>TFAMGFP
E
Female Lifespan
Percent survival
150
100
50
0
0
20
40
60
80
Days
Control
OK371>TFAMIR-3
OK371>TFAMGFP

Figure 4.6 Manipulating *TFAM* levels results in behavioural defects in adult flies.

(A) Climbing assays were carried out on flies developed at 29^0C. Both *TFAM* knockdown and overexpression causes climbing defects. **(B)** *TFAMGFP* overexpression does not rescue the climbing defect caused by *TFAM* knockdown. **(C)** Jump ability is reduced both in *TFAMIR-3* and *TFAMGFP* flies. **(D-E)** Lifespan of *TFAMIR-3* flies was not significantly different from control flies (w^{1118} flies crossed to the driver line). 100 control and *TFAM* RNAi flies and 20 *TFAMGFP* flies were tested for lifespan. However, motoneuron specific expression of *TFAMGFP* significantly reduced lifespan both in male and females. Mean values +/- SEM plotted on graphs A, B and C. *=$p<0.05$, **=$p<0.01$, ***=$p<0.001$

4.6 *TFAM* overexpression disrupts synapse development

Potential mechanisms causing behavioural phenotypes were investigated in the motoneuron system at a cellular level. The morphological properties of larval motoneurons are well characterized, which make them a valuable neuronal model (reviewed in (LANDGRAF and THOR 2006b; TISSOT and STOCKER 2000)). Motoneuron cell bodies are located in the larval VNC and axons extend to muscles to form synapses. It has been previously shown that murine *TFAM-/-* mutant embryos have a dramatic increase in apoptosis and tissue-specific *TFAM* knockouts cause apoptosis in the mouse heart (WANG *et al.* 2001). I knocked-down *TFAM* and overexpressed *TFAM* and *TFAMGFP* in motoneurons by crossing to *OK371-Gal4,UAS-CD8-GFP* flies. In order to investigate if mtDNA depletion resulted in cell death, the number of motoneuron cell bodies in the VNC were quantified. Motoneurons were visualized by confocal microscopy using the CD8-GFP reporter. MtDNA depletion using either *TFAM* RNAi or overexpresson did not have any effect on the number of motoneuron cell bodies (Figure 4.7B). These data show that depletion of mtDNA levels in motoneurons does not effect cell survival at the larval stage.

A more detailed analysis of motoneurons was carried out after eliminating the possibility of cell death. The morphological properties of different regions of motoneurons can be investigated since they have a well characterised morphology. It has been hypothesized that neurodegeneration is more severe in the distal compartments such as the synapses and mitochondrial transport to synapses is vital for neuronal function (MACASKILL and KITTLER 2010; STOWERS *et al.* 2002).

Drosophila motoneuron synapses are formed at different muscle groups known as neuromuscular junctions (NMJs). Altogether there are 30 muscle groups in each larval hemi-segment (numbered from 1 to 30), which are innervated by motoneurons through six nerve branches (HOANG and CHIBA 2001). Two of the most widely used synaptic models are NMJ 4 and NMJ 6/7, named since they form synapses on muscle groups 4 and 6/7 respectively. The morphology of these NMJs was visualized using a Cy3 conjugated HRP antibody (Figure 4.8). HRP antibodies are widely used to visualise neuronal membranes (JAN and JAN 1982). The circular structures observed at NMJs are termed boutons, and are the contact points between the neuron and muscle where neurotransmitter release occurs. There are two main types of boutons at NMJ 4 and 6/7, type Ib and type Is, both of which are glutamatergic. Type Ib boutons are large (about 3-6μm), while type Is are slightly smaller (2-4μm) and originate from different cell bodies (HOANG and CHIBA 2001). Additionally, NMJ 4 has type II boutons, which are smaller still at about 1-2 μm and their neurostransmitter type is not known (HOANG and CHIBA 2001).

To characterise the pattern of *OK371-Gal4* expression at NMJ 4 and 6/7, driver expression was visualized by imaging GFP expression. Comparing GFP expression and HRP staining showed that the *OK371-Gal4* drove strong GFP expression in type Ib boutons, but expression was weak or completely absent in type Is boutons of NMJ 6/7 (Figure 4.8). When the same analysis was carried out on NMJ 4, it revealed that the driver was also strongly expressed strongly in type Ib boutons, but expression was very weak in the type Is boutons (Figure 4.8). Type Ib and Is boutons localize very close to each other at NMJ 6/7 and most of the time they overlap, making them difficult to distinguish. However, at NMJ 4, type Ib and Is localize to different parts of the muscle, which makes them much easier to distinguish compared to NMJ 6/7.

For this reason I used NMJ 4 to analyse the effects of *TFAM* RNAi and overexpression on motoneuron morphology.

Firstly I quantified the number of type Ib boutons at NMJ4 in abdominal segment 3 (A3) for *TFAM* RNAi and *TFAMGFP* overexpression. Analysis of untagged *TFAM* overexpression was performed separately and is shown in Figure 4.10, but the results were similar to the overexpression of *TFAMGFP* described below. Both RNAi and overexpression of *TFAM* did not result in changes in bouton number compared to the control (Figure 4.9D). However, there did appear to be a difference in the morphology of *TFAM* overexpressing NMJs. Therefore, bouton size was determined by measuring bouton diameter (see Materials and Methods). The average diameter of the *TFAMGFP* expressing boutons was approximately 30% smaller than the control (Figure 4.9E). By contrast *TFAM* RNAi did not cause any reduction in bouton size (Figure 4.9E). Therefore, neither RNAi or overexpression of *TFAM* affect bouton number, but *TFAM* overexpression causes a reduction in bouton size.

Boutons have both pre-synaptic and post synaptic contact sites. An antibody against the synaptic protein bruchpilot (brp), known as Nc82, was used to locate active zones (WAGH *et al.* 2006). Active zones are presynaptic neurotransmitter release sites, which are visualized as small punctuate structures in boutons. The number of active zone puncta was quantified in each of the boutons that were previously analysed for diameter. In accordance with the bouton diameter phenotype, *TFAM* knockdown did not affect the number of active zones per bouton. However, expression of *TFAMGFP* in motoneurons resulted in a significant decrease in the number of active zones (Figure 4.9F). In order to analyse whether the reduction in the number of active zones was proportional to the size of the bouton, active zone density was calculated. There was no difference in the active zone density between the control and *TFAM*

knockdown (Figure 4.9G). However, active zone density in *TFAMGFP* expressing boutons was significantly less than the control (Figure 4.9G). These data suggest that the reduction in active zone number caused by *TFAM* overexpression is not simply a result of the reduction in bouton size, but that additional mechanisms may directly affect active zone development. A similar active zone reduction phenotype was observed upon overexpression of *TFAM* (Figure 4.10E,F).

In summary these results show that mtDNA depletion does not affect motoneuron cell number. However, *TFAM* overexpression caused defects in synapse size at NMJ 4. Furthermore, overexpressing *TFAM* resulted in fewer active zones. These phenotypes may contribute to the severe locomotion defects caused by motoneuron-specific overexpression of *TFAM*.

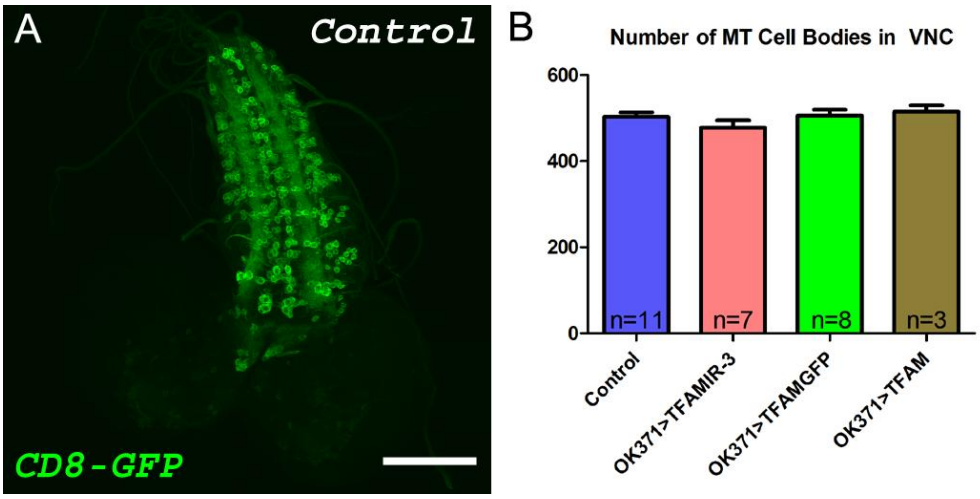

Figure 4.7 *TFAM* RNAi or overexpression does not affect the number of motoneurons in the VNC.

(A) The *OK371-Gal4* driver was used with CD8-GFP to visualize motoneurons. Representative figure showing motoneuron cell bodies in the VNC of control (w^{1118} crossed to the motoneuron driver) larval CNS. GFP expressing cells were counted in the VNC. **(B)** Number of motoneurons was not significantly changed upon *TFAM* knockdown and *TFAM* overexpression**.** Mean values +/- SEM plotted on graph. Scale bar shows 100 μm.

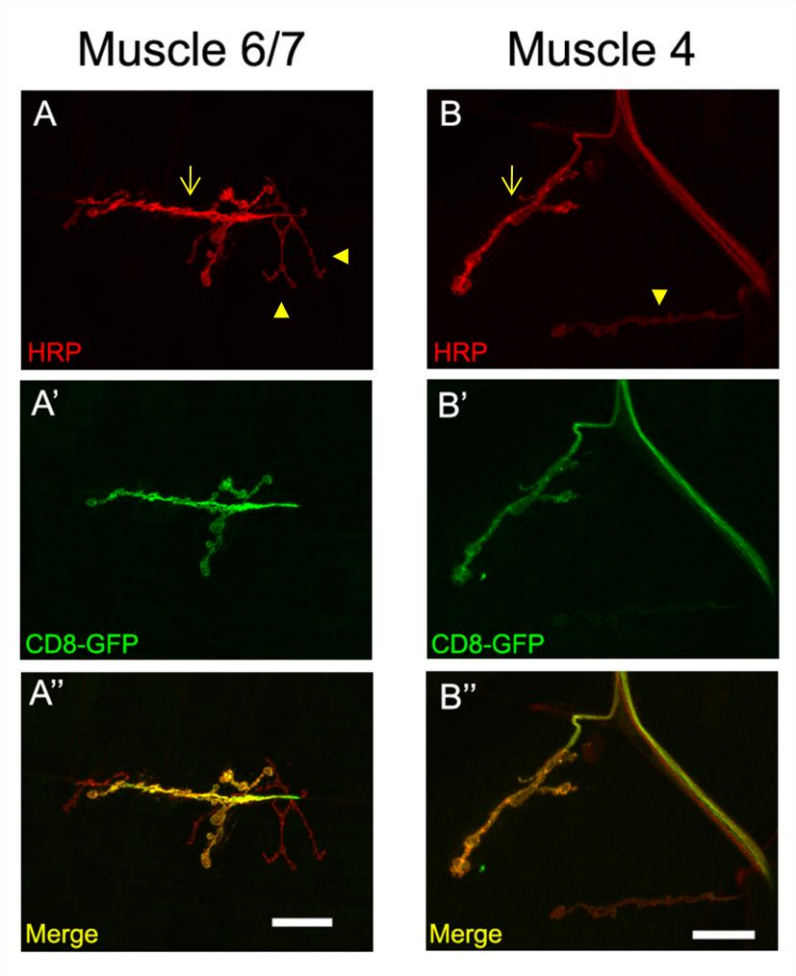

Figure 4.8 *OK371-Gal4* drives strongly in type Ib, but weakly in type Is motoneurons.

(A-A'') An HRP antibody was used to visualize neuronal membranes at NMJ 6/7 and NMJ 4. GFP expression was under control of the *OK371-Gal4* driver to visualize the expression pattern of the driver. Left panel shows that HRP and *OK371* specific GFP expression overlaps in type Ib boutons (arrows), but not in type Is (arrowheads) in NMJ 6/7. **(B-B'')** Right panel shows that all of the type Ib boutons in NMJ 4 express *OK371* (arrow). Type Is boutons are not overlapping with type Ib boutons (arrowheads) and have a lower level of GFP expression. Scale bars show 20 µm.

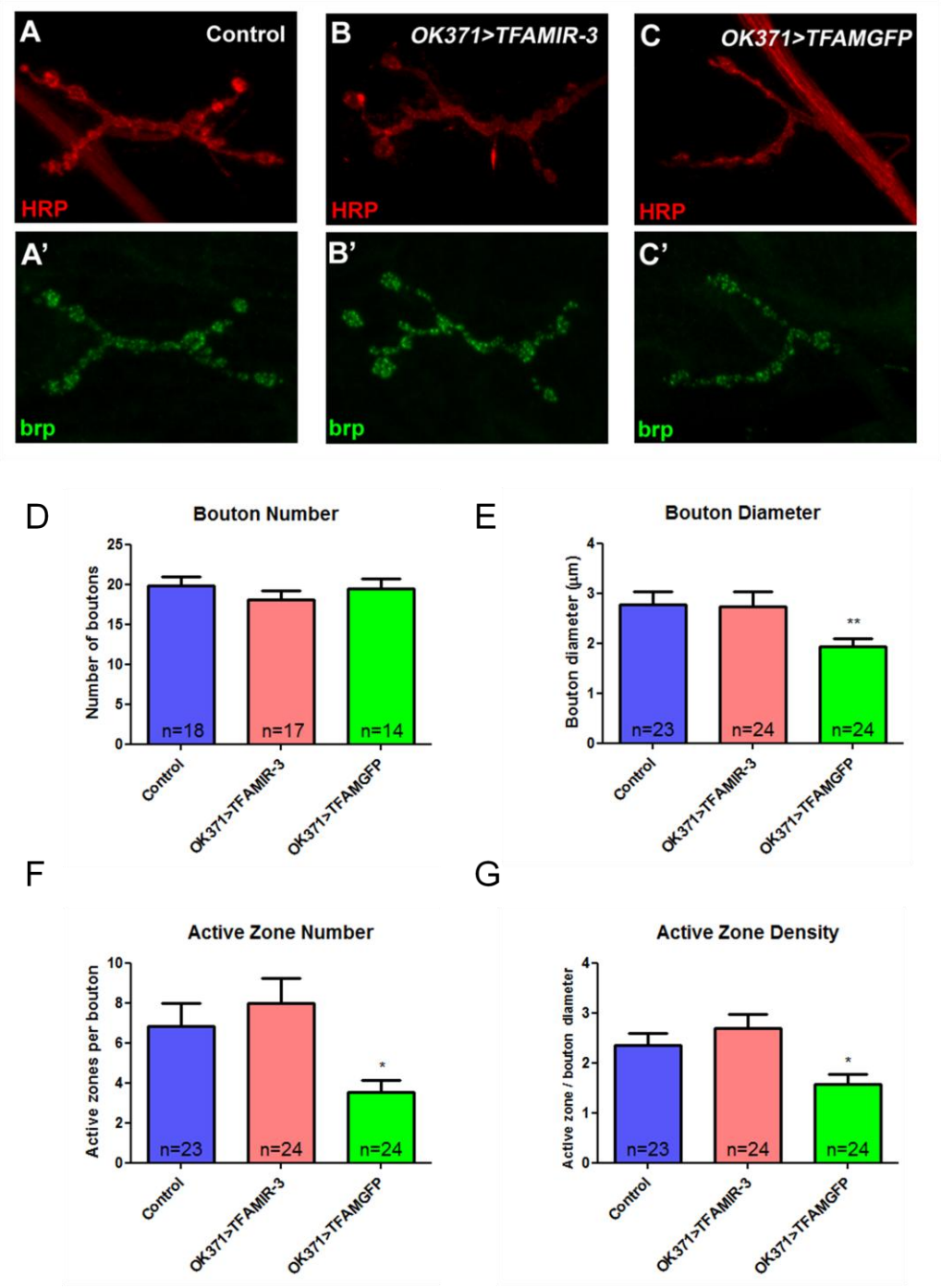
A
Control
HRP
B
OK371>TFAMIR-3
HRP
C
OK371>TFAMGFP
HRP
A'
brp
B'
brp
C'
brp
D
Bouton Number
Number of boutons
n=18
n=17
n=14
Control
OK371>TFAMIR-3
OK371>TFAMGFP
E
Bouton Diameter
Bouton diameter (µm)
**
n=23
n=24
n=24
Control
OK371>TFAMIR-3
OK371>TFAMGFP
F
Active Zone Number
Active zones per bouton
*
n=23
n=24
n=24
Control
OK371>TFAMIR-3
OK371>TFAMGFP
G
Active Zone Density
Active zone / bouton diameter
*
n=23
n=24
n=24
Control
OK371>TFAMIR-3
OK371>TFAMGFP

Figure 4.9 Motoneuron specific *TFAM* over expression results in smaller boutons and fewer active zones at NMJ 4.

Representative scans of NMJ 4 of control **(A-A')**, *TFAM-RNAi* **(B-B')** and *TFAMGFP* **(C-C')**. **(A-C')** HRP (red) was used to stain NMJ boutons and brp (green) is a marker for active zones. **(D)** The number of boutons at NMJ 4 is similar for all three genotypes. Bouton diameter **(E)**, number of active zones **(F)** and density of active zones **(G)** was similar between control and *TFAM* knockdown, however all were significantly decreased in *TFAMGFP* expressing boutons. Mean values +/- SEM plotted on graphs D, E, F and G. *=$p<0.05$, **=$p<0.01$.

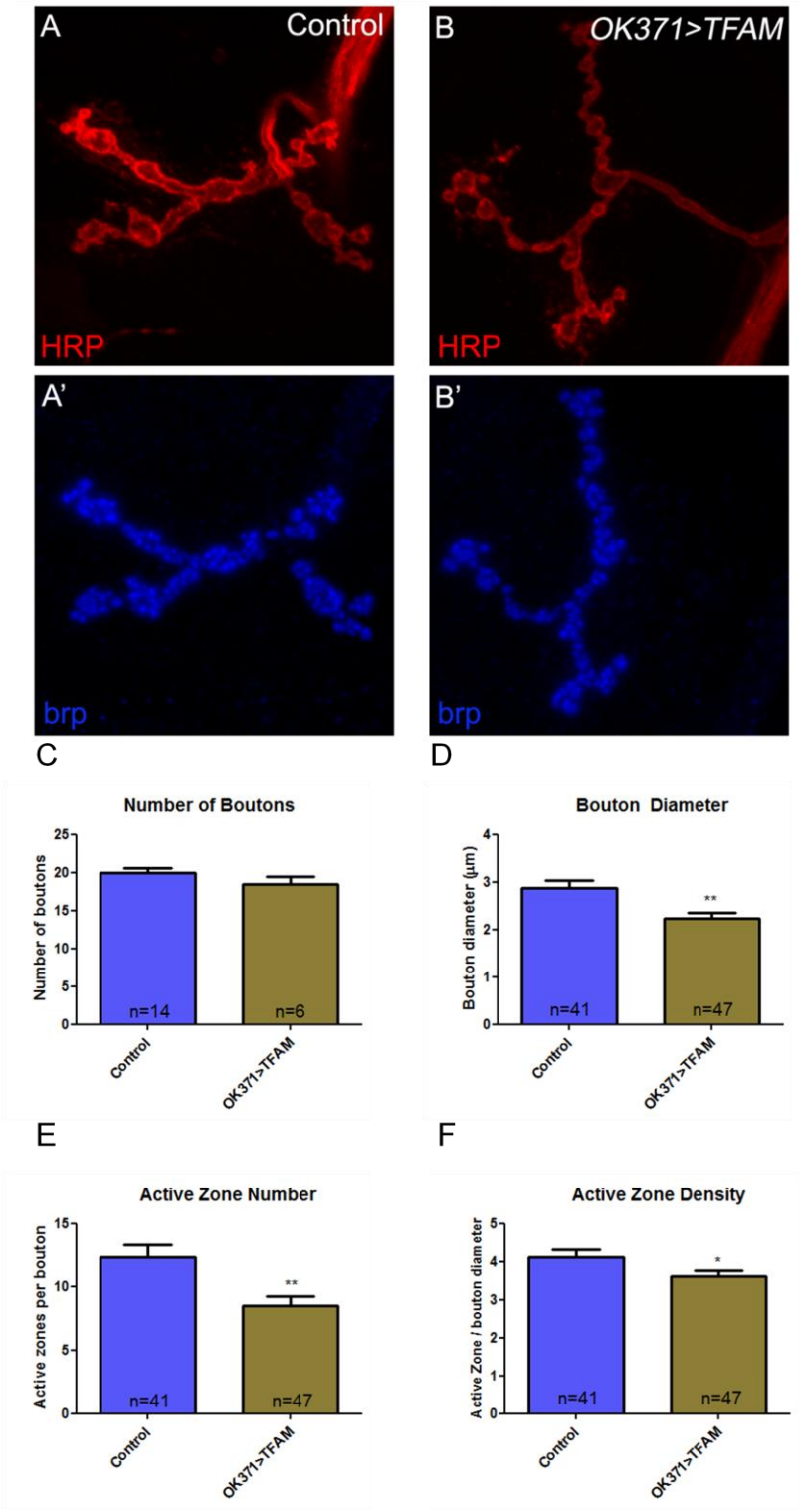
A
Control
HRP
B
OK371>TFAM
HRP
A'
brp
B'
brp
C
D
Number of Boutons
Number of boutons
25
20
15
10
5
0
n=14
n=6
Control
OK371>TFAM
Bouton Diameter
Bouton diameter (µm)
4
3
2
1
0
**
n=41
n=47
Control
OK371>TFAM
E
F
Active Zone Number
Active zones per bouton
15
10
5
0
**
n=41
n=47
Control
OK371>TFAM
Active Zone Density
Active Zone / bouton diameter
5
4
3
2
1
0
*
n=41
n=47
Control
OK371>TFAM

Figure 4.10 Overexpression of *TFAM* results in similar synaptic phenotypes to overexpression of *TFAMGFP* in motoneurons

Representative scans of control (A-A') and *TFAM* overexpressing (B-B') NMJ 4. HRP (red) stains neuronal membranes and brp (blue) stains active zones. Overexpressing *TFAM* did not change the number of boutons (C), however it resulted in smaller boutons (D). (E-F) Both active zone number and active zone density was reduced compared to control. Mean values +/- SEM plotted on graphs C, D, E and F. *=$p<0.05$, **=$p<0.01$.

4.7 *TFAM* RNAi and overexpression causes depletion of synaptic mitochondria

Transport of mitochondria to the synapse is of particular importance and is necessary for synaptic function (SHENG and CAI 2012). It has been previously shown that NMJs are the first regions to degenerate in mitochondrial-related motoneuron disease (FREY *et al.* 2000; MAGRANE *et al.* 2012). Under normal conditions, all of the boutons in the *Drosophila* NMJ contain mitochondria (VERSTREKEN *et al.* 2005). To determine whether RNAi or overexpression of *TFAM* affected synaptic mitochondria type Ib boutons at NMJ 4 were analysed for their mitochondrial content. To achieve this a P-element containing a mitochondrially-targeted *GFP* (*mito-GFP*) (HORIUCHI *et al.* 2005), under *UAS* control, was recombined onto the same chromosome as *OK371-Gal4*. This stock was then used to knockdown or overexpress *TFAM* in motoneurons that simultaneously expressed *mito-GFP*, enabling visualisation of mitochondria. *TFAMGFP* expression was not used for analysis of mitochondria since there was no way to distinguish between the GFP signal from mito-GFP and TFAMGFP.

In control boutons at NMJ 4 (segment A3) a range of numbers and sizes of mitochondria were observed in nearly all of the boutons in control NMJs (Figure 4.11). This finding is in agreement with a previously published study which showed 100% of the boutons have mitoGFP in NMJs (VERSTREKEN *et al.* 2005). Occasional small terminal boutons lacking mitochondria were observed in the control NMJs (not shown). Furthermore, I also observed that satellite boutons lacked mitochondria (arrows figure 4.11 A-A'), but these are not included in the quantifications. Satellite

boutons are usually attacted to big boutons, and are continuously formed and degraded depending on synaptic activity. The number of boutons containing mitochondria were counted following *TFAM* knockdown and *TFAM* overexpression. This analysis showed that the percentage of boutons with mitochondria was the same both in the control and *TFAM* RNAi, at around 98% (Figure 4.11D). However, significantly more boutons lacked mitochondria when *TFAM* was overexpressed compared to the control, with this leading to mitochondrial absence in approximately 14% of boutons at NMJ 4 (Figure 4.11D).

It can be seen from the representative scans that there was a generalised reduction in mitoGFP signal at the NMJ of motoneurons expressing the dsRNA against *TFAM* and also in those overexpressing *TFAM* (Figure 4.11A-C). Therefore I quantified these mitochondria in more detail. The number of mitochondria was slightly (but not significantly) reduced in *TFAM* knockdown NMJs (Figure 4.11E). Although the percentage of boutons with mitochondria was same in control and *TFAM* knockdown NMJs (Figure 4.11E), the mitochondrial volume was significantly reduced in these boutons (Figure 4.11F). Overexpressing *TFAM* resulted in more severe phenotypes, with only 86% of the boutons displaying mitoGFP expression, (Figure 4.11D). Boutons with mitochondria were then analysed in more in detail. There was usually only a single, small mitoGFP signal in these boutons (Figure 4.11C). Mitochondrial abundance was consequently analysed and compared to control boutons. Significantly fewer mitochondria were found in boutons overexpressing *TFAM* and the mitochondrial volume was also significantly reduced (Figure 4.11E,F).

In summary, the synaptic localization of mitochondria was investigated in detail. *TFAM* overexpression, but not knockdown, resulted in a significant increase in boutons completely devoid of mitochondria. In addition, mtDNA depletion via

TFAM knockdown resulted in smaller mitochondria in NMJ 4, while *TFAM* overexpression resulted in a dramatic reduction in the number and size of mitochondria at this NMJ. These mitochondrial phenotypes may potentially contribute to the defects in bouton size and active zone number described in section 4.5.

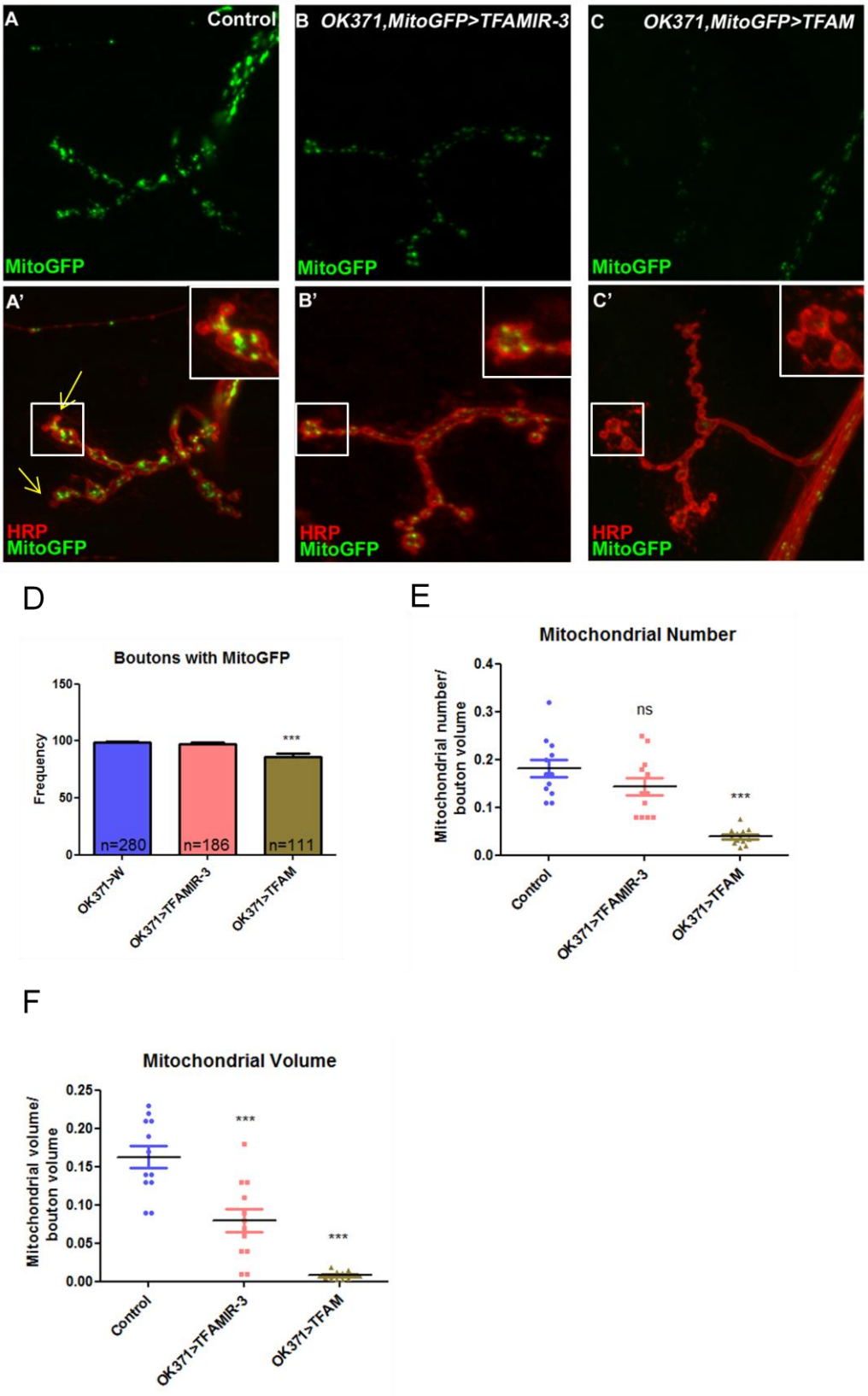
A
Control
MitoGFP
B OK371,MitoGFP>TFAMIR-3
MitoGFP
C OK371,MitoGFP>TFAM
MitoGFP
A'
HRP
MitoGFP
B'
HRP
MitoGFP
C'
HRP
MitoGFP
D
Boutons with MitoGFP
Frequency
150
100
50
0
n=280
n=186
n=111
***
OK371>W
OK371>TFAMIR-3
OK371>TFAM
E
Mitochondrial Number
Mitochondrial number/ bouton volume
0.4
0.3
0.2
0.1
0.0
ns
***
Control
OK371>TFAMIR-3
OK371>TFAM
F
Mitochondrial Volume
Mitochondrial volume/ bouton volume
0.25
0.20
0.15
0.10
0.05
0.00
***
***
Control
OK371>TFAMIR-3
OK371>TFAM

Figure 4.11 *TFAM* overexpression results in boutons that lack mitochondria.

(A-C'') Representative scans showing mitochondrial localization at NMJ 4. HRP stains neuronal membranes and was used to visualize boutons. Mitochondrial targetted GFP (mitoGFP) used to visualize mitochondria. Arrows indicate satellite boutons devoid of mitochondria that were not included in the analysis. **(D)** There were fewer boutons with mitochondria in *TFAM* overexpressing NMJs. Control boutons have a range of number and sized mitochondria, however both *TFAM* knockdown and and overexpression resulted in a weaker mitoGFP signal. **(E)** There were slightly fewer mitochondria in boutons expressing the dsRNA against *TFAM* and even fewer in *TFAM* overexpressing motoneurons. **(F)** The mitochondrial volume was reduced in boutons upon *TFAM* knockdown and overexpression. Mean values +/- SEM plotted on graph D. ***=$p<0.001$.

4.8 Effects of *TFAM* RNAi and overexpression on motoneuron cell body and axonal mitochondria

In order to analyse whether mtDNA depletion caused mitochondrial defects only at synapses, or whether it had a more global effect, other regions of motoneurons were investigated. Firstly, the mitochondrial network in cell bodies was visualized by confocal microscopy. Groups of dorsal motoneuron cell bodies at the terminal segment of the VNC were imaged (Figure 4.12A). In control cells, a reticular mitochondrial network was observed. *TFAM* overexpression caused disruption of this reticular mitochondrial network (Figure 4.12D). Mitochondria were more fragmented and punctate in the cell bodies of motoneurons overexpressing *TFAM* (Figure 4.12D). *TFAM* RNAi did not result in a dramatic change in mitochondrial morphology in motoneuron cell bodies, compared to controls (Figure 4.12C). This suggests that *TFAM* overexpression results in a stronger phenotype when compared to *TFAM* knockdown, which correlates with the previous findings at the NMJ.

Mitochondrial morphology, mitochondrial distribution along the axon, mitochondrial activity and axonal transport of mitochondria are all factors that can affect neuronal function (reviewed in (CHO *et al.* 2010; SCHON and PRZEDBORSKI 2011)). Proximal and distal segments of axons of motoneurons in which *TFAM* was knocked-down or overexpressed were imaged and the mitochondrial properties analysed. In order to analyse proximal segments, the initial segments of the axons exiting the VNC were scanned. In the proximal segments, RNAi of *TFAM* did not affect mitochondrial number (Figure 4.13 B,D,E). However, overexpression of *TFAM* resulted in a significantly reduced number of mitochondria (Figure 4.13 C,D). The average

volume of mitochondria in the proximal part of the axons was similar in control and both *TFAM* knockdown and overexpression motoneurons (Figure 4.13 B,C,E).The distal part of the axons close to NMJ 4 showed more dramatic phenotypes. RNAi and overexpression of *TFAM* resulted in smaller and fewer mitochondria in the distal part of the axon (Figure 4.13 F-J).

In conclusion, *TFAM* RNAi resulted in a progressive mitochondrial phenotypes moving distally from the cell body. Overexpression of *TFAM* resulted in mitochondrial abnormalities in all regions analysed, that is, cell bodies, distal and proximal axons (this section) and synapses (section 4.6).

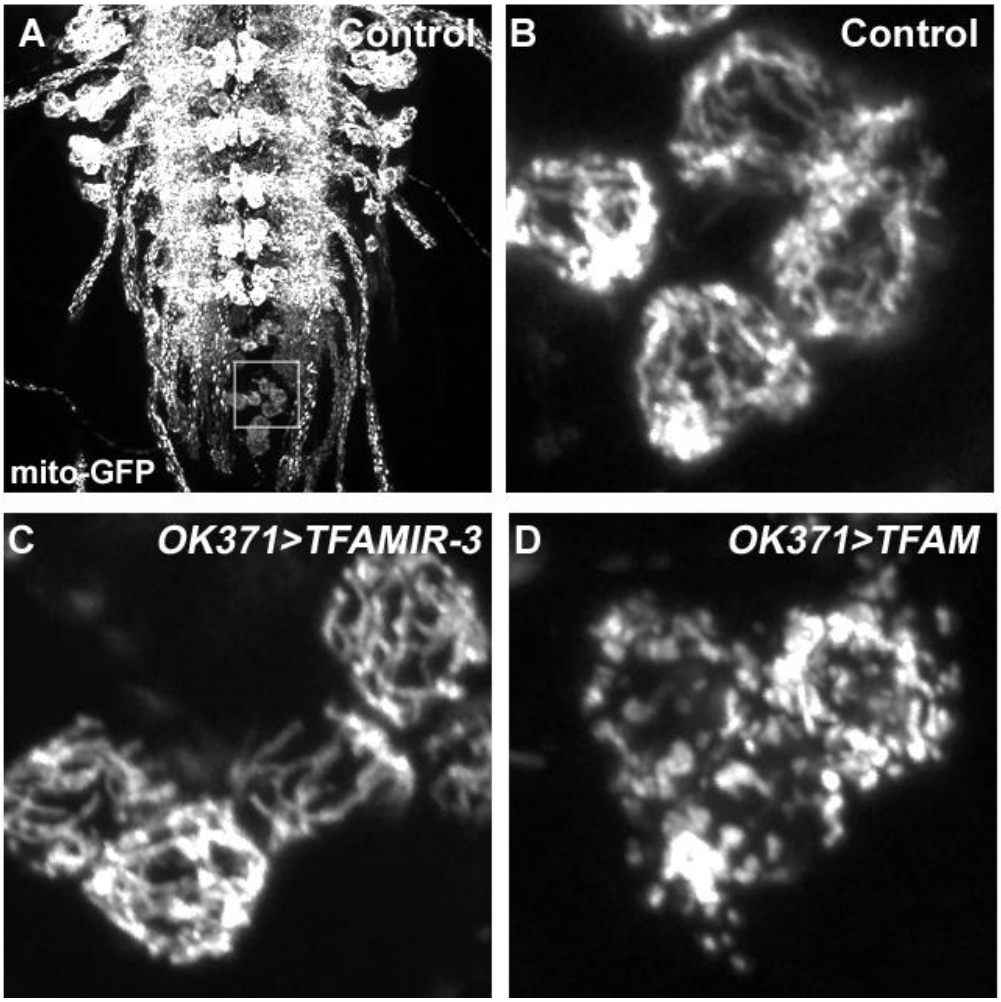

Figure 4.12 *TFAM* overexpression disrupts the mitochondrial network in motoneuron cell bodies.

Mitochondrial specific GFP expression was used to visualize the mitochondrial network in motoneuron cell bodies. **(A)** Specific groups of dorsal motoneuron cell bodies were scanned. **(B-C)** A tubular mitochondrial network can be seen in control cell bodies (driver line crossed to w^{1118} flies) and *TFAM* knockdown (*TFAMIR-3*). **(D)** Overexpression of *TFAM* results in smaller and more punctate mitochondria in the cell bodies. Images taken by Dr. Joseph Bateman.

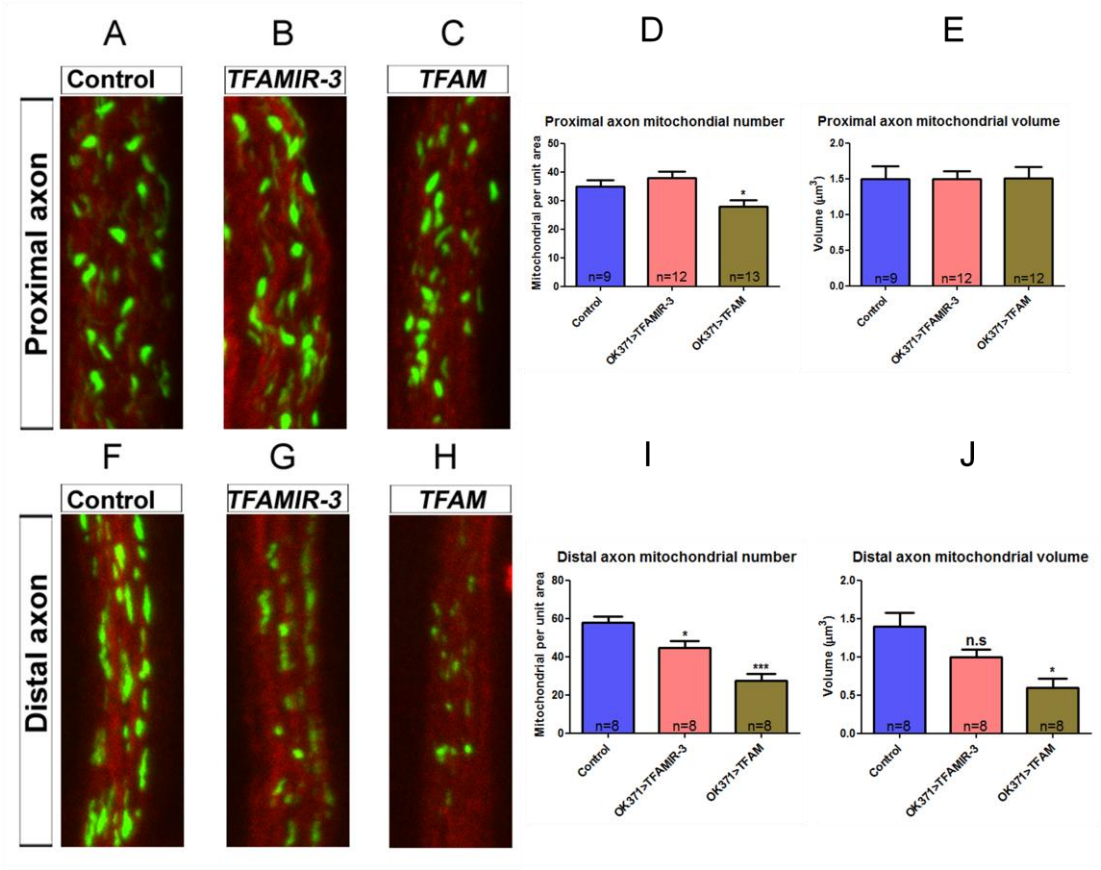

Figure 4.13 *TFAM* knockdown and overexpression results in a decrease in axonal mitochondria.

Representative scans of two axonal compartments: proximal axons **(A-C)** and distal axons **(F-H)**. **(D-E)** There were slightly fewer mitochondria in the proximal parts of the axons upon *TFAM* overexpression, but no effect was observed at proximal axons when *TFAM* was knocked-down. **(I-J)** There were significantly fewer mitochondria in the motoneuron axons both in *TFAM* knockdown (TFAMIR-3) and *TFAM* overexpression, compared to control (w^{1118} crossed to driver) at the distal part of axons. However, mitochondrial volume was significantly reduced only upon *TFAM* overexpression, while *TFAM* knockdown slightly, but not significantly, (p=0.0789), reduced the mitochondrial volume. Quantification was performed in 150 X 50 µm areas. Mean values +/- SEM plotted on graphs C,D,E and F. *=p<0.05.

4.9 Summary

In order to understand the consequences of mtDNA depletion in neurons, *Drosophila* motoneurons were used as a model system. Motoneuron cell bodies in the VNC were visualized upon *TFAM* manipulation. MtDNA depletion in motoneurons was shown to cause behavioural defects in both the larval and adult stages. However, only overexpression of *TFAM* resulted in a decrease in lifespan. The synaptic properties of motoneurons were investigated in detail and smaller boutons were observed in *TFAM* overexpressing motoneurons, suggesting synaptic developmental defects (Table 4.1). I was able to visualize the mitochondrial network throughout the motoneurons by using mitochondrial targeted GFP, which revealed that loss of mtDNA caused depletion of synaptic mitochondria. Other parts of the motoneurons were also visualized in an attempt to analyse mitochondrial phenotypes. Overexpression of *TFAM* resulted in smaller mitochondria, compared to the filamentous mitochondrial network observed in control cell bodies. Furthermore, the proximal and distal parts of the motoneuron axons were analysed. Only overexpression of *TFAM* resulted in a reduced number of mitochondria in the proximal axon. The more distal regions of the axons were affected more severely by mtDNA depletion, as both *TFAM* knockdown and overexpression resulted in smaller and fewer mitochondria. To conclude, mtDNA depletion results in abnormalities in the mitochondrial network, which worsens progressively from the cell bodies through to the synapses (Table 4.2).

NMJ 4 Phenotypes	*TFAM* RNAi	*TFAM* Overexpression
Bouton Number	No effect	No effect
Bouton Size	No effect	Smaller
No of Active Zones	No effect	Reduced
Active Zone Density	No effect	Reduced

Table 4.1 Summary of the developmental phenotypes observed at NMJ 4 upon *TFAM* knockdown and overexpression

Mitochondrial Phenotypes	*TFAM* RNAi	*TFAM* O/E
Cell Body	No effect	Smaller mitochondria
Proximal Axon	No effect	Smaller and fewer mitochondria
Distal Axon	Slightly smaller (but not significant) and fewer mitochondria	Smaller and fewer mitochondria
NMJ 4	Smaller and fewer (not significant) mitochondria	Smaller and fewer mitochondria Complete lossin some boutons.

Table 4.2 Summary of the mitochondrial localization phenotypes observed in the motoneurons upon *TFAM* knockdown and overexpression.

Chapter 5. Use of a mitochondrially targeted restriction enzyme to induce mtDNA loss in motoneurons

5.1 Introduction

TFAM knockdown and overexpression are two very useful models for depleting mtDNA, but the mechanism underlying the observed phenotypes is yet to be established. Additionally, TFAM is a transcription factor, meaning that mtDNA related transcriptional inhibition may contribute to the phenotypes observed in the previous chapters. Therefore, modelling mtDNA depletion in motoneurons using multiple methods could prove useful in attempts to understand the mechanisms causing the phenotypes observed. Specifically, using *TFAM*-independent methods of mtDNA depletion may be of value. In this chapter I aimed to use an alternative method of depleting mtDNA. *TFAM* manipulation caused aberrant synaptic development and a dramatic depletion of synaptic mitochondria. I hypothesised that these phenotypes were a general feature of neuronal mtDNA loss, rather than a specific feature of *TFAM* knockdown or overexpression. To test this hypothesis I investigated whether an alternative means of inducing mtDNA loss, expression of a mitochondrially targeted restriction enzyme, produced similar phenotypes.

5.2 Expression of a mitochondrially-targeted restriction enzyme affects mtDNA nucleoid morphology

Restriction enzymes cut DNA in a sequence specific manner. Moraes and colleagues targeted various restriction enzymes to mitochondria as a way of introducing double-strand breaks and depleting mtDNA (SRIVASTAVA and MORAES 2001; SRIVASTAVA and MORAES 2005). Cutting mtDNA once with a single cutter restriction enzyme linearizes mtDNA and results in the stalling of mtDNA replication (Figure 5.1A). One of these single cutting restriction enzymes is XhoI, which cuts within the *Drosophila mtCoI* gene, specifically at the –actcgagct- sequence (Figure 5.1 B-C). Xu et al. (2008) generated a construct using *XhoI* with an N-terminal mitochondrial targeting sequence and a C-terminal myc tag (XU *et al.* 2008). They showed that this construct can successfully target XhoI to mitochondria (Figure 5.1D).

Firstly, the effect of mitochondrially targeted *XhoI* (*mitoXhoI*) expression on development was analysed (Table 5.1). Crossing *UASp-mitoXhoI* flies to the ubiquitous *Actin-Gal4* driver resulted in embryonic lethality. Next, the pan-neuronal driver *Elav-Gal4* was used to express *mitoXhoI* and also resulted in embryonic lethality. Motoneuron specific expression of *mitoXhoI* was carried out by crossing these flies to *OK371-Gal4,UAS-CD8GFP* flies. The progeny of this cross were able and developed to the larval stage, however pupal development was affected (Table 5.1). Larval motoneuron activity was analysed using a locomotion assay under light controlled conditions. These larvae showed a significant reduction in locomotion (Figure 5.1E).

Motoneuron cell bodies were investigated in detail following *mitoXhoI* expression. *UASp-mitoXhoI* flies were crossed to *OK371-Gal4,CD8GFP* flies. CD8-GFP expression is specific to motoneuron cells and motoneuron cell bodies and can be visualized by confocal imaging. TFAM staining was carried out to visualize mtDNA nucleoids. Control cell bodies had evenly distributed punctuate TFAM staining (Figure 5.2A-A'). However expression of *mitoXhoI* resulted in changes in TFAM localisation. In some cases a slight reduction in the TFAM levels was observed (Figure 5.2B-B'), whereas in other cell bodies diffuse TFAM staining was observed (Figure 5.2C-D'), compared to the TFAM localisation seen in the control cell bodies (Figure 5.2A).

These results shows that mitochondrially targeted XhoI expression can lead to motoneuron dysfunction and dysmorphic mtDNA nucleoids. Thus, mitoXhoI is a useful tool for studying the affect of mtDNA loss in motoneurons.

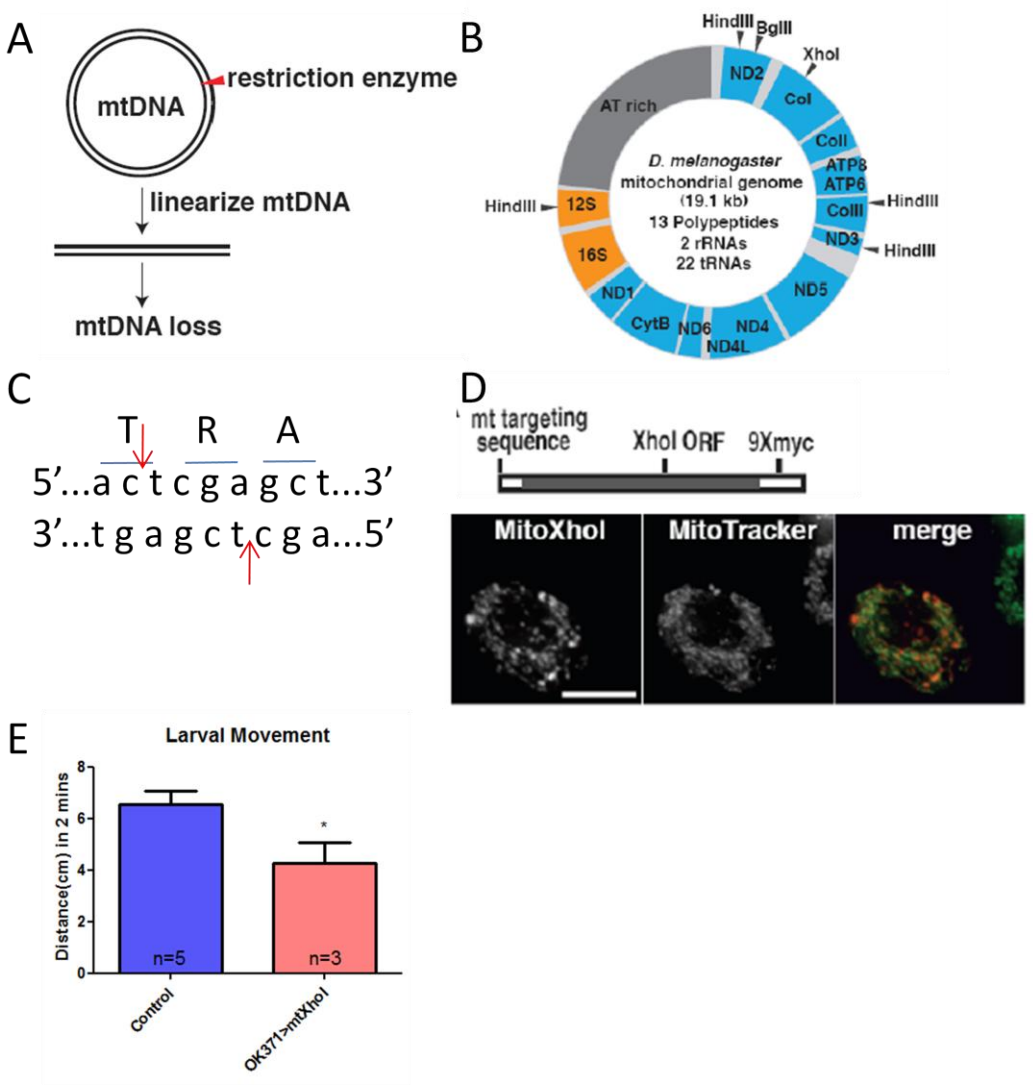

Figure 5.1 Introduction to restriction enzyme mediated mtDNA loss in flies.

(A) Cutting mtDNA via a restriction enzyme linearizes mtDNA and results in replication inhibition which depletes mtDNA. **(B)** XhoI cuts mtDNA once in the *mtCoI* gene (position 2369). **(C)** Amino acid and DNA sequence of XhoI cutting site in *mtCOI* gene. **(D)** XhoI is targetted to mitochondria with a mitochondrial targeting sequence and myc staining was used to determine XhoI localization. Adapted from Xu and O'Farell (2008). **(E)** Motoneuron specific expression of *mitoXhoI* causes behavioural defects at the larval stage compared to control (w^{1118} crossed to *OK371-Gal4*) flies. Mean values +/- SEM plotted on graph. *=p<0.05

	UASp-mitoXhoI
Actin-Gal4	Embryonic Lethal
Elav-Gal4	Embryonic Lethal
OK371-Gal4	Pupal Lethal

Table 5.1 Motoneuron specific expression of *mitoXhoI* results in developmental behavioural defects.

Crossing *UASp-mitoXhoI* to *Actin-Gal4* and *Elav-Gal4* at 25^0C resulted in embryonic lethality. Motoneuron specific expression of *mitoXhoI* results in pupal lethality.

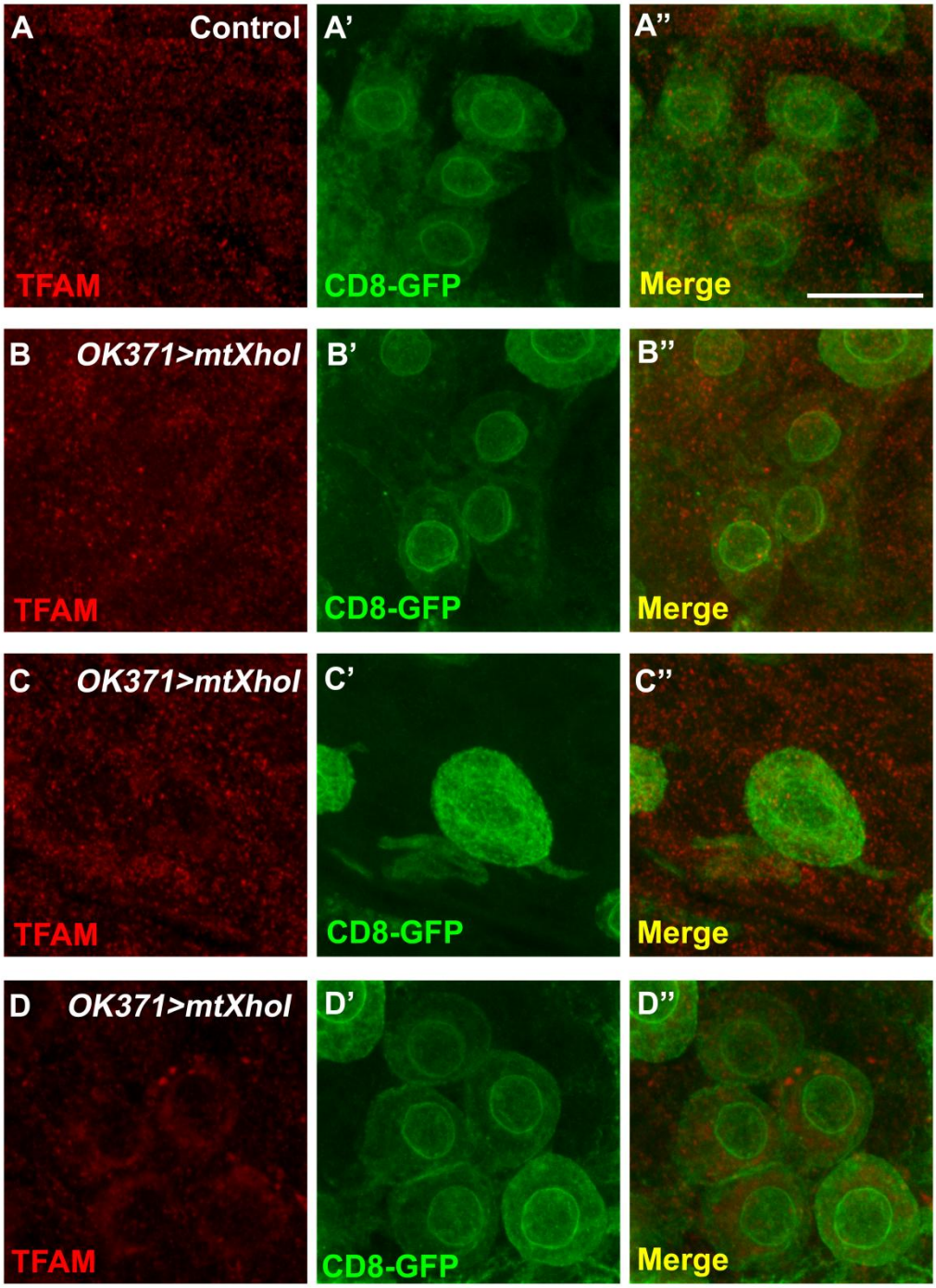
A
Control
TFAM
A'
CD8-GFP
A''
Merge
B
OK371>mtXhol
TFAM
B'
CD8-GFP
B''
Merge
C
OK371>mtXhol
TFAM
C'
CD8-GFP
C''
Merge
D
OK371>mtXhol
TFAM
D'
CD8-GFP
D''
Merge

Figure 5.2 Motoneuron specific expression of *UASp-mitoXhoI* disrupts nucleoid structure.

The *OK371,CD8-GFP* driver line crossed to control (w^{1118}) and *UASp-mitoXhoI* flies. GFP expression shows motoneuron cell bodies and TFAM antibody is shown in red. **(A-A')** Control cell bodies have evenly distributed TFAM nucleoids. **(B-D')** Expressing *mitoXhoI* results in variable phenotypes which ranged from a slight decrease in TFAM staining (B-B''), to more severe disruptions in TFAM localization (C-D''). All images were scanned at the same magnification and the scale bar shows 10μm.

5.3 Motoneuron specific expression of *mitoXhoI* results in synaptic defects

Motoneuron synapses were investigated in detail in the previous chapter. It was shown that motoneuron specific knockdown and overexpression of *TFAM* resulted in smaller synaptic boutons and fewer active zones (Chapter 4.5).

The developmental properties of NMJ 4 were investigated upon motoneuron specific *mitoXhoI* expression and compared to control crosses. The number of boutons was similar to controls, at around 20 (Figure 5.3C). However, motoneuron specific expression of *mitoXhoI* resulted in significantly smaller boutons (Figure 5.3 D). Bruchpilot (Nc82) staining was also carried out to visualize active zones. *mitoXhoI* expressing motoneurons had significantly fewer active zones and also resulted in significantly less dense active zones compared to control boutons (Figure 5.3F). Altogether these results show that *mitoXhoI* expression results in similar defects to those observed in motoneurons with *TFAM* overexpression-mediated mtDNA depletion.

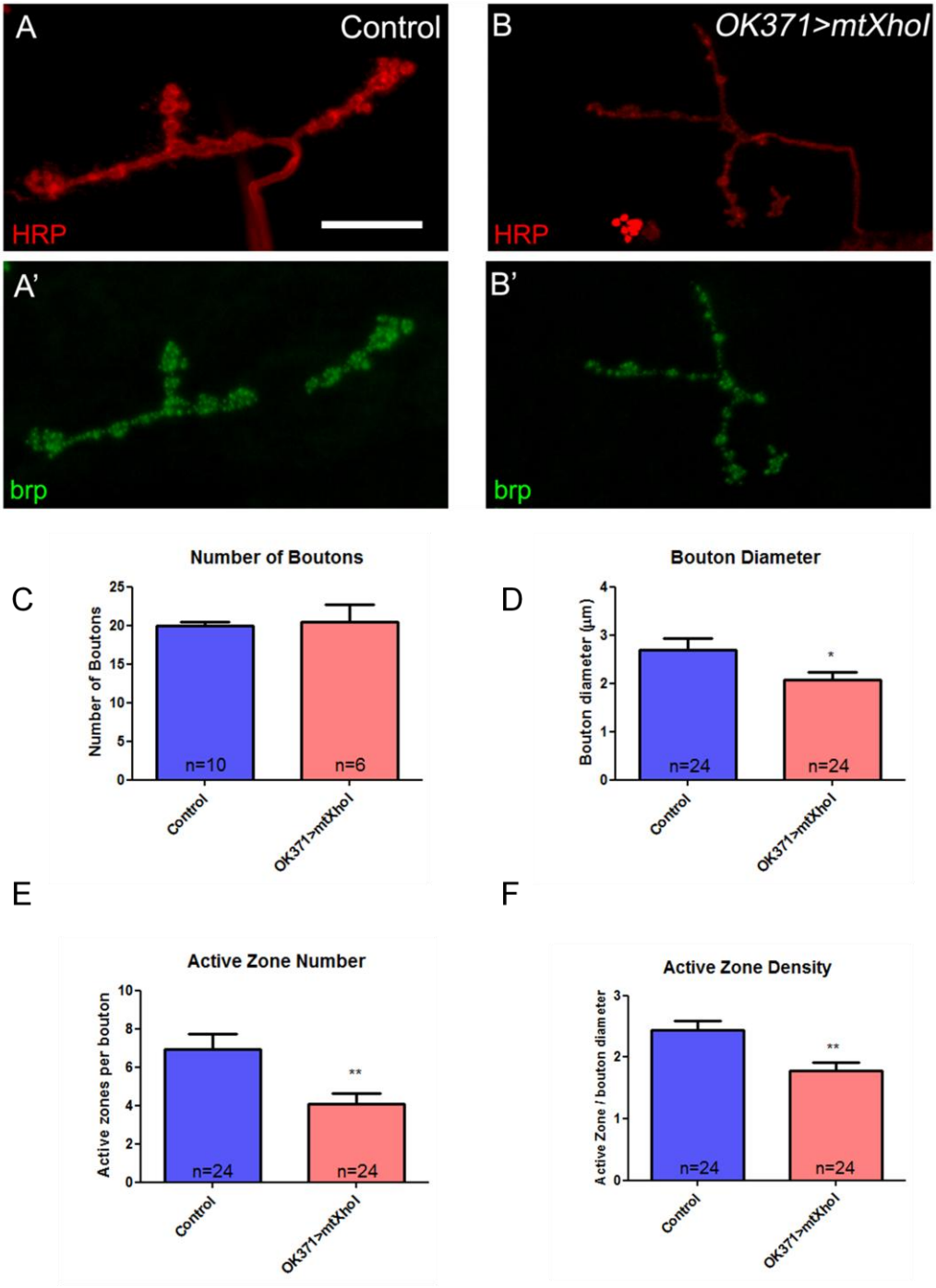
A
Control
HRP
B
OK371>mtXhoI
HRP
A'
brp
B'
brp
C
Number of Boutons
Number of Boutons
25
20
15
10
5
0
n=10
n=6
Control
OK371>mtXhoI
D
Bouton Diameter
Bouton diameter (µm)
4
3
2
1
0
*
n=24
n=24
Control
OK371>mtXhoI
E
Active Zone Number
Active zones per bouton
10
8
6
4
2
0
**
n=24
n=24
Control
OK371>mtXhoI
F
Active Zone Density
Active Zone / bouton diameter
3
2
1
0
**
n=24
n=24
Control
OK371>mtXhoI

Figure 5.3 Motoneuron specific expression of *mitoXhoI* results in smaller boutons and fewer active zones.

Representative scans of control (A-A') and *mitoXhoI* (B-B') expressing boutons. HRP (red) stains for neuronal membranes and brp (green) was used to visualize active zones. **(C-D)** The number of boutons was similar, however boutons were significantly smaller upon expression of *mitoXhoI*. **(E-F)** Average number of active zones and density of active zones in boutons were significantly reduced in *mitoXhoI* expressing motoneurons. Mean values +/- SEM plotted on graph C,D,E and F. *=$p<0.05$, **=$p<0.01$, scale bar=20μm.

5.4 Motoneuron specific *mitoXhoI* expression depletes synaptic mitochondria

In order to analyse mitochondrial localization in motoneuron synapses, mitochondrial targeted GFP was used with the *OK371-Gal4* driver. Control and *UASp-mitoXhoI* flies were crossed to this driver and NMJ 4 synapses were imaged. Control synapses had evenly distributed mitochondria in boutons, while *mitoXhoI* expressing synapses had less mitochondrial GFP (Figure 5.4 A-B'). Nearly all of the boutons had at least one mitochondrion in control synapses, while 12% of boutons completely lacked mitochondria upon *mitoXhoI* expression (Figure 5.4C). This was very similar to what was observed with motoneuron specific *TFAM* overexpression (Chapter 4).

The mitochondrial content of those boutons containing mitochondria was investigated in detail. There were fewer mitochondria in the *mitoXhoI* expressing boutons (Figure 5.4D). Furthermore, the mitochondrial volume to bouton volume ratio was significantly reduced upon *mitoXhoI* expression (Figure 5.4E). In conclusion, *mitoXhoI* expression resulted in the complete loss of mitochondria in some boutons, while those boutons retaining mitochondria had smaller and fewer mitochondria.

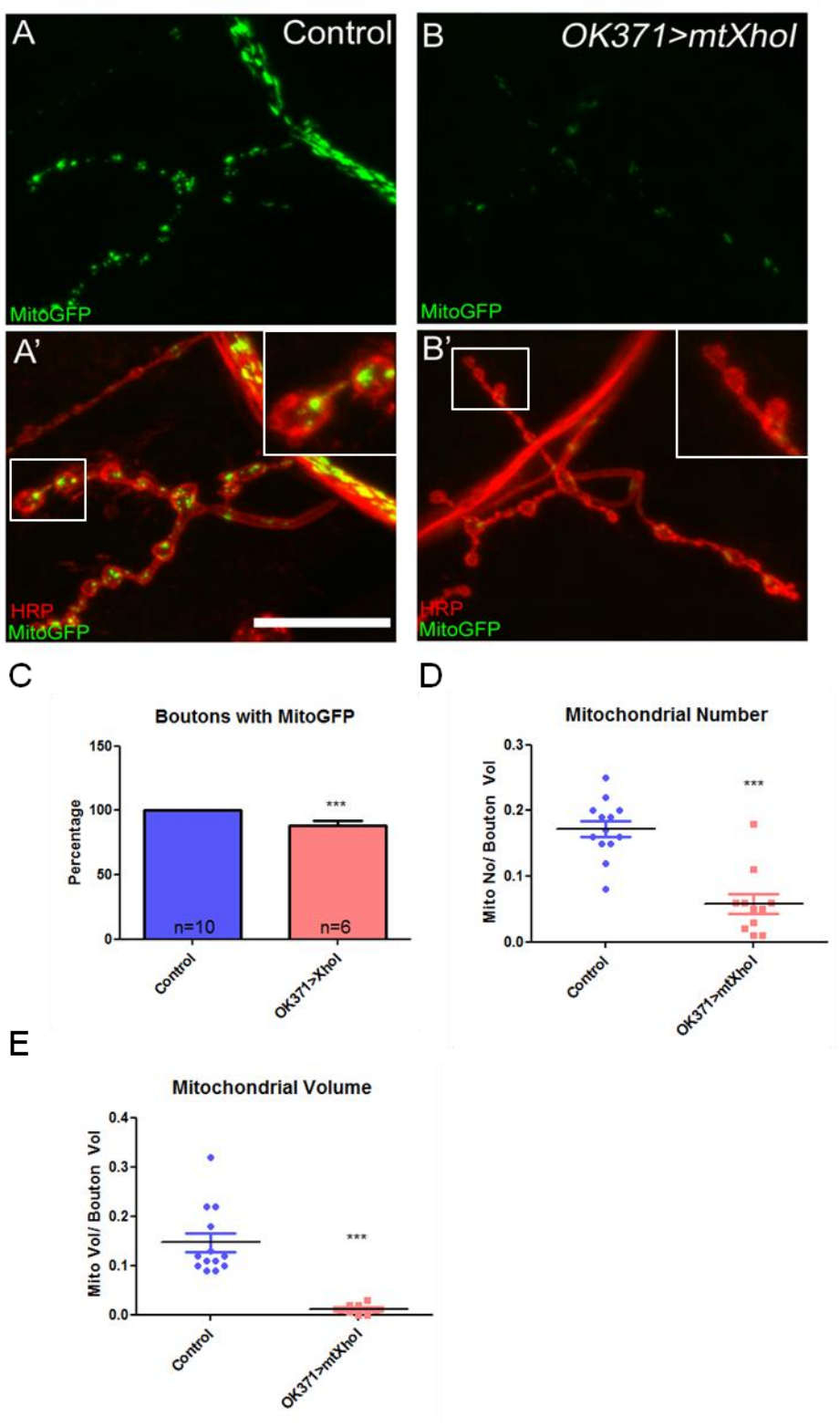
A
Control
MitoGFP
B
OK371>mtXhoI
MitoGFP
A'
HRP
MitoGFP
B'
HRP
MitoGFP
C
Boutons with MitoGFP
Percentage
150
100
50
0
***
n=10
n=6
Control
OK371>XhoI
D
Mitochondrial Number
Mito No/ Bouton Vol
0.3
0.2
0.1
0.0
***
Control
OK371>mtXhoI
E
Mitochondrial Volume
Mito Vol/ Bouton Vol
0.4
0.3
0.2
0.1
0.0
***
Control
OK371>mtXhoI

Figure 5.4 Motoneuron specific expression of *mitoXhoI* depletes synaptic mitochondria.

(A-B') Representative scans showing mitochondrial localization at the NMJ 4. GFP shows the mitochondrial targeted GFP and HRP (red) stains boutons. Boxes highlight the areas in A' and B'. Control NMJ 4 has more mitoGFP compared to *mitoXhoI* expressing motoneurons. **(C)** In control NMJs, all of the boutons have mitoGFP, however upon expression of *mitoXhoI* 12% of the boutons completely lack mitoGFP. **(D)** Expression of *mitoXhoI* in the motoneurons resulted in a reduction in mitochondrial number. **(E)** Approximately 15 % of the bouton volume consists of mitochondria in control NMJs, however this percentage is greatly reduced upon *mitoXhoI* expression. Mean values +/- SEM plotted on graphs. ***=$p<0.001$. Scale bar=20μm

5.5 Motoneuron specific *mitoXhoI* expression affects axonal and cell body mitochondria

In order to analyse the effect of *mitoXhoI* expression on mitochondrial properties in other parts of the motoneurons, axonal branches were analysed. I showed that mitochondrial number and volume was reduced very strongly in distal axons (close to the NMJ) upon *TFAM* manipulation (Figure 5.5). Therefore I analysed both proximal and distal compartments of motoneuron axons expressing *mitoXhoI*. *OK371-Gal4, UAS-mitoGFP* flies were crossed to *UASp-mitoXhoI* flies and third instar larval motoneuron axons were imaged. Significantly fewer mitochondria were observed in proximal axons in motoneurons expressing *mitoXhoI* (Figure 5.5B). Average mitochondrial volume was slightly higher compared to mitochondria in control axons, but this was not significant (Figure 5.5B,C). In distal axons significantly fewer and smaller mitochondria were observed in *mitoXhoI* expressing motoneurons compared to controls (Figure 5.5 E,F).

Mitochondrial morphology in motoneuron cells bodies expressing *mitoXhoI* was also investigated. Similar to overexpression of *TFAM*, mitochondria in cell bodies of motoneurons expressing *mitoXhoI* were fragmented and more punctate than mitochondria in control cell bodies (Figure 5.5G,H).

Next, the physiological state of axonal mitochondria was investigated. MtDNA loss beyond a critical threshold results in reduced ETC function and decreased mitochondrial membrane potential. It has been shown that mitochondria with depleted mtDNA were less functional than the mitochondria having normal levels of mtDNA. In order to analyse mitochondrial activity, Rhodamine-1,2,3 (Rh-123)

fluorescence was used as an indirect measurement of mitochondrial membrane potential. Mitochondrial membrane potential is generated by pumping of protons out of the mitochondrial matrix across the inner mitochondrial membrane by complex I, III and IV. This proton gradient results in an electrochemical potential and pH difference and across the inner mitochondrial membrane and is referred to as the mitochondrial membrane potential ($\Delta\Psi$) (SUGRUE and TATTON 2001). In control axons nearly all mitochondria stained strongly with Rh-123 (Figure 5.6A-A'). In order to check the sensitivity of the Rh-123 staining, control axons were treated with sodium azide (which inhibits cytochrome c oxidase) to deplete the mitochondrial membrane potential (BENNETT *et al.* 1996). In these axons Rh-123 fluorescence was much weaker than in controls (Figure 5.6 B-B'), confirming that Rh-123 fluorescence decreases when the mitochondrial membrane potential is depleted. Expression of *mitoXhoI* resulted decreased Rh-123 fluorescence, similar to that observed in sodium azide treated axons (Figure 5.6 C-C'). In order to quantify the level of staining, Rh-123 levels were normalized to mitoGFP levels. Both sodium azide treated and *mitoXhoI* expressing motoneurons had significantly lower Rh-1,2,3 levels than controls (Figure 5.6 D).

Overall, these data show that *mitoXhoI* expression in motoneurons results in aberrant cell body mitochondrial morphology, fewer mitochondria in axons and the remaining mitochondria have reduced membrane potential.

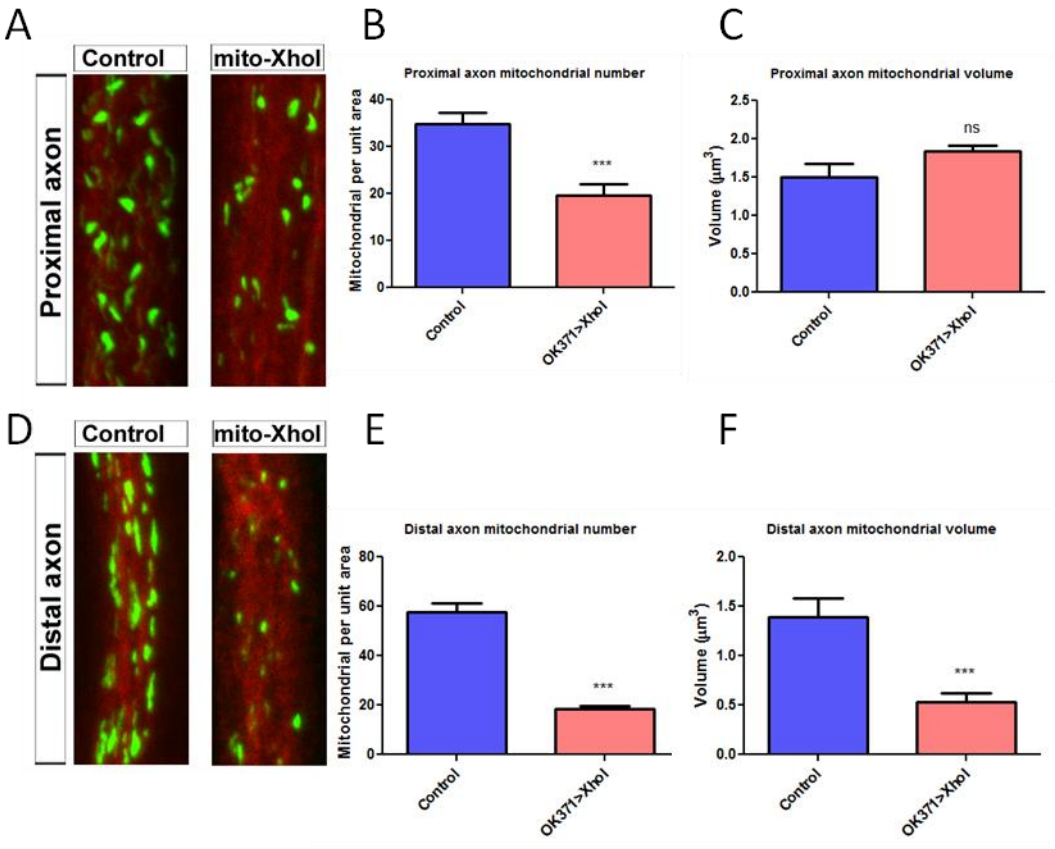
A
Control
mito-Xhol
Proximal axon
B
Proximal axon mitochondrial number
Mitochondrial per unit area
***
Control
OK371>Xhol
C
Proximal axon mitochondrial volume
Volume (µm3)
ns
Control
OK371>Xhol
D
Control
mito-Xhol
Distal axon
E
Distal axon mitochondrial number
Mitochondrial per unit area
***
Control
OK371>Xhol
F
Distal axon mitochondrial volume
Volume (µm3)
***
Control
OK371>Xhol

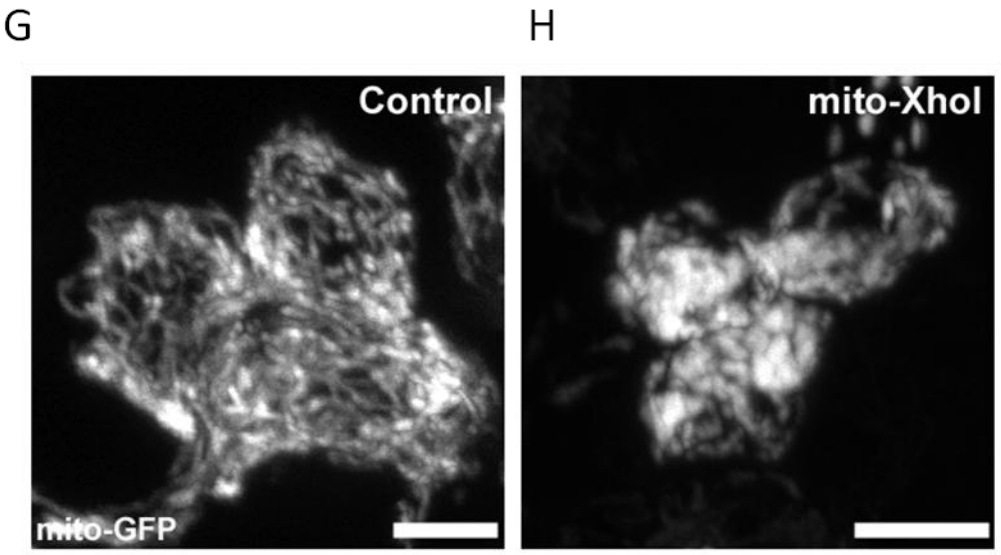
G
Control
mito-GFP
H
mito-Xhol

Figure 5.5 Axonal mitochondrial distribution is affected upon mito*XhoI* expression.

(A ,D) Representative scans showing proximal and distal axons. **(B,E)** *mitoXhoI* expression resulted in fewer mitochondria both at proximal and distal axons with a greater effect at distal sites. **(C,F)** Average mitochondrial volume was slightly (but not significantly) increased, however mitochondrial at distal parts of axons were smaller upon expression of mito*XhoI.* The area quantified was 50 X 150 μm. Mean values +/- SEM plotted on graphs. **(G,H)** Mitochondria in the cell bodies were fragmented upon *mitoXhoI* expression compared to the control. Scale bars represent 5μm. ***=p<0.001. Images acquired by Dr. Joseph Bateman.

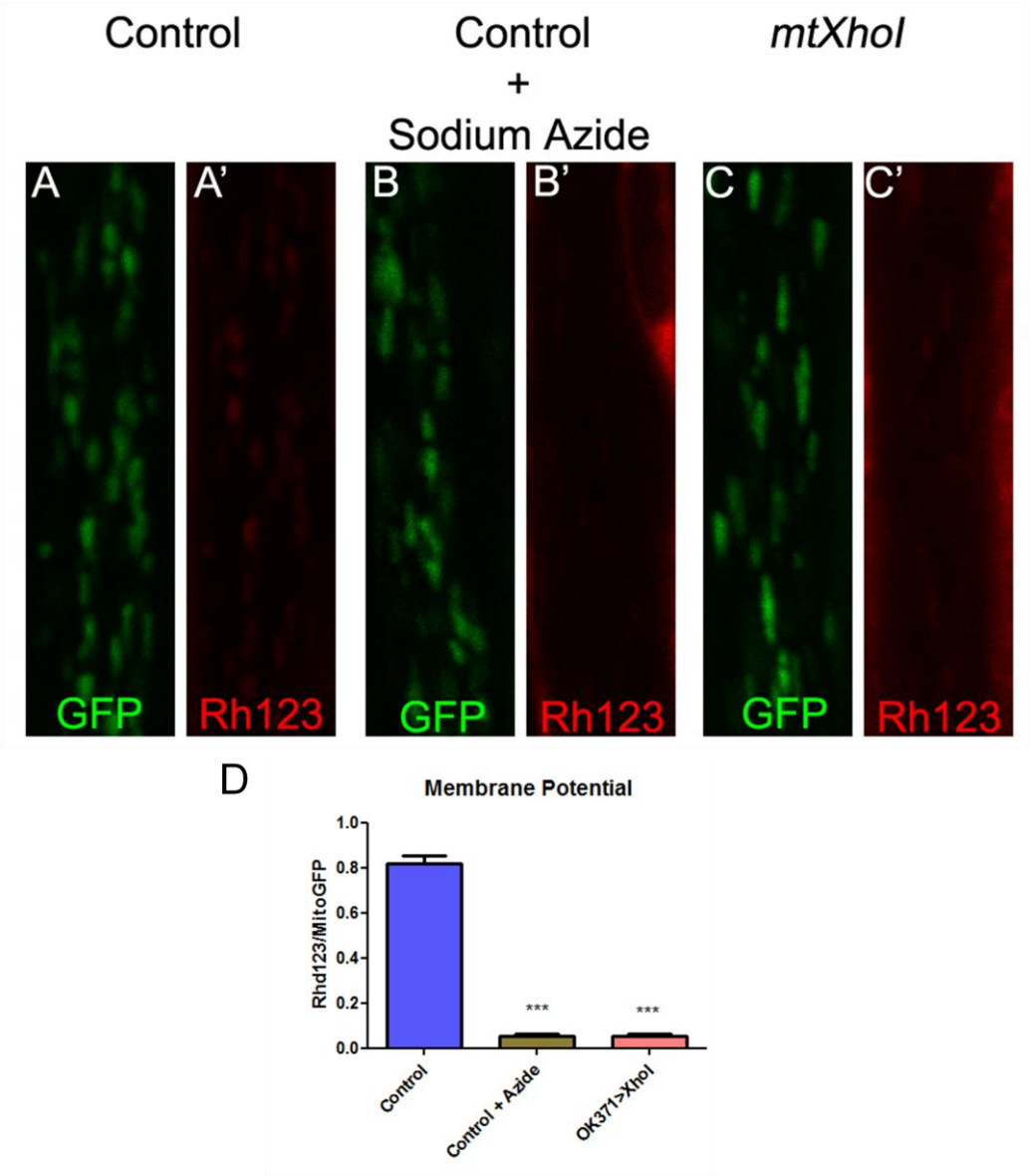

Figure 5.6 Expression of *mitoXhoI* in motoneurons reduces the membrane potential of axonal mitochondria.

Mitochondria visualized by mitochondrially targetted GFP and Rh-1,2,3 (red) staining used to estimate changes in mitochondrial membrane potential. Control axons **(A-A')** had a higher level of Rh-1,2,3 fluorescence compared to *mitoXhoI* expressing motoneurons **(C-C')** . **(B-B')** Sodium azide was used to deplete the membrane potential of mitochondria. **(D)** Rh-1,2,3 levels normalized to mitoGFP levels and a significant reduction was observed in sodium azide treated controls and *mitoXhoI* expressing motoneurons. ***=p<0.001 ; error bars= SEM.

5.6 Summary

In this chapter I firstly analysed different regions of motoneurons upon mtDNA depletion via expression of the mitochondrially targeted restriction enzyme *XhoI*. Expression of this enzyme in motoneurons resulted in reduced larval motility. Motoneuron cell bodies showed abnormal mtDNA nucleoid morphology upon staining with an antibody against TFAM. Synaptic properties were investigated in detail as a potential cause of the observed behavioural phenotypes. I observed smaller boutons with fewer active zones and a reduction in synaptic mitochondria in the boutons. The synaptic phenotypes observed with *mitoXhoI* expression phenocopied those observed upon *TFAM* overexpression. The mitochondrial network was also investigated in the motoneuron axons. Fewer mitochondria were observed in the axons and the membrane potential of the axonal mitochondria was reduced. In conclusion, mitochondrially targeted *XhoI* expression in motoneurons phenocopies *TFAM* overexpression.

Chapter 6. Investigating the affects of manipulation of the TOR pathway on motoneuron development and synaptic mitochondria

6.1 Introduction

The *TFAM* overexpression and *mitoXhoI* motoneuron phenotypes have several common features. In both of the cases, smaller boutons, fewer active zones and a dramatic depletion of synaptic mitochondria were observed, ultimately resulting in motoneuron dysfunction. The reduced bouton size could be explained by defects in translation, while depletion of synaptic mitochondria could be the result of increased mitophagy (mitochondrial specific autophagy) (Figure 6.1) (TWIG *et al.* 2008a). Autophagy is a survival mechanism that is a response to stress and starvation. Autophagy is vital for the recycling of unwanted and damaged organelles, such as dysfunctional mitochondria. It has been reported that dysfunctional mitochondria can be degraded by the autophagy machinery (NARENDRA *et al.* 2008). The TOR (target of rapamycin) signalling pathway has been shown to regulate autophagy and translation in both lower and higher eukaryotes (Figure 6.1). Upstream regulators of this pathway include growth factors, nutrients, ATP levels and hypoxia (reviewed in (WULLSCHLEGER *et al.* 2006)). One of the proximal upstream components of this pathway is PI3K (phosphatidylinositol 3-kinase), which is recruited upon binding of insulin/insulin like growth factors (IGFs) to their receptors. The TOR pathway has been shown to regulate synaptic size in vertebrates and activation of PI3K, or the TOR target S6 kinase results in increased bouton size in *Drosophila* motoneurons

(CHENG *et al.* 2011; KNOX *et al.* 2007). The TOR pathway also senses energy levels, since the cellular energy sensor AMP kinase inhibits TOR activity through regulation of TSC2 (HARDIE *et al.* 2012). Given the roles of the TOR pathway in mitophagy and translational control I investigated the effects of TOR pathway activation and inhibition on motoneuron function and development.

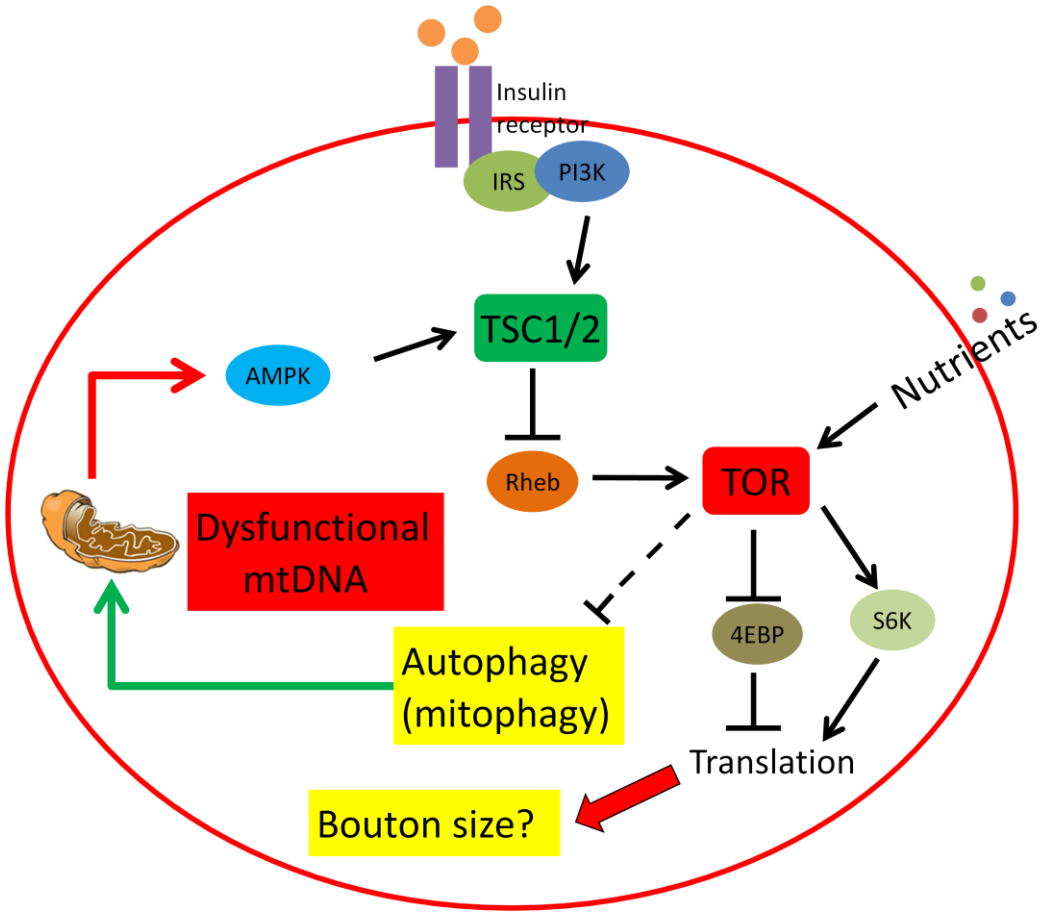

Figure 6.1 Schematic representation of TOR signalling pathway and its possible interaction with mitochondrial homeostasis.

TOR is at the central point linking the TSC1/2 complex with processes such as translation and autophagy. The possible relationships with mitochondrial dysfunction are also highlighted.

6.2 Effects of motoneuron specific TOR pathway manipulation on behaviour

The TOR pathway has been implicated in regulation of mitochondrial oxygen consumption and oxidative capacity (SCHIEKE *et al.* 2006). The effect of inhibition of the TOR pathway on *Drosophila* NMJ development was studied recently (PENNEY *et al.* 2012). However, there are no detailed studies on the relationship of the TOR pathway with mitochondrial localization at *Drosophila* motoneuron synapses. Investigating the mitochondrial phenotypes in motoneuron synapses upon regulation of TOR pathway components may provide an explanation for the previous phenotypes observed. Therefore, both activation and inhibition of the TOR pathway was investigated in motoneurons. A dominant negative form of TOR (TOR^{DN}) and an activated form of Dp110 ($Dp110^{active}$), which is a membrane targeted (activated) form of catalytic subunit of PI3K, were used to investigate the effects of TOR pathway manipulation in motoneurons.

Climbing assays carried out on flies expressing TOR^{DN} and $Dp110^{active}$ in motoneurons using *OK371-Gal4*. Both resulted in a slight reduction in the climbing performance and $Dp110^{active}$ expression resulted in significant reduction, however TOR^{DN} expression was not significant with the number of flies (n=10) tested (Figure 6.2). In summary, manipulation of TOR pathway resulted in defects in adult climbing performance.

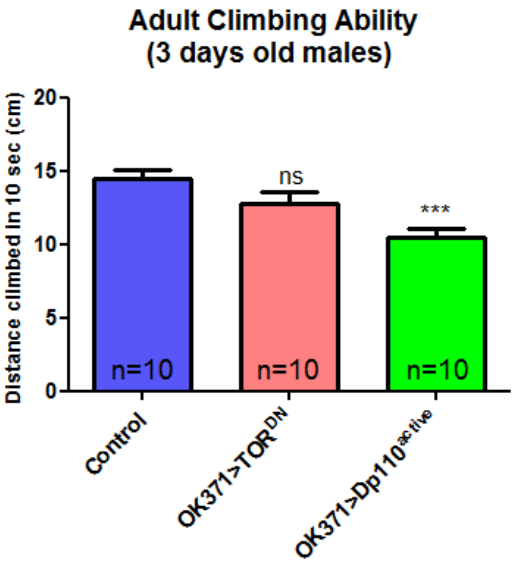

Figure 6.2 Manipulation of the TOR pathway causes climbing defects.

Expressing *TOR*^{DN} in motoneurons results in slightly decreased (not statistically significant with p=0.0618) climbing performance. However, *Dp110*^{active} expression results in significantly reduced climbing performance compared to control flies (*w*^{1118} flies crossed to the *OK371-Gal4* driver). Mean values +/- SEM plotted on graph . ***=p<0.001 . Experiments were performed by Naomi Lomeli.

6.3 Motoneuron specific manipulation of the TOR pathway affects synapse development

TFAM and *mitoXhoI* overexpression experiments were carried out by expressing these genes in motoneurons using *OK371-Gal4* driver and investigating behavioral and synaptic phenotypes. The same analyses were carried out upon expression of TOR^{DN} and $Dp110^{active}$ in motoneurons. Firstly, the number of boutons at NMJ 4 was quantified and compared to controls. There was a significant increase in bouton number upon expression of $Dp110^{active}$. Furthermore, these synapses had more satellite boutons (Figure 6.3C). Satellite boutons were not included in the quantification of the bouton number and subsequent analyses. TOR^{DN} expression did not affect bouton number (Figure 6.3D). Bouton diameter was quantified in control, $TOR^{DN}$and $Dp110^{active}$ expressing motoneurons. Motoneurons expressing $Dp110^{active}$ had similar sized boutons to controls, however TOR^{DN} expressing boutons were significantly smaller (Figure 6.3E). Next, Bruchpilot (Nc82) staining was carried out to quantify the number of active zones in boutons (Figure 6.3 A', B', C'). The number of active zones per bouton in motoneurons expressing $Dp110^{active}$ was reduced, but this was not significant (Figure 6.3F). Expression of TOR^{DN} resulted in significantly fewer active zones in per bouton (Figure 6.3F). The density of active zones in these boutons was calculated as a ratio of the number of active zones to bouton diameter. This quantification showed that both expression of TOR^{DN} and $Dp110^{active}$ resulted in a significant reduction in active zone density. Moreover, the reduction in active zone density was significantly greater with TOR^{DN} expression than $Dp110^{active}$ expression (Figure 6.3G). Therefore, both inhibition and activation of the TOR pathway affect motoneuron synaptic development.

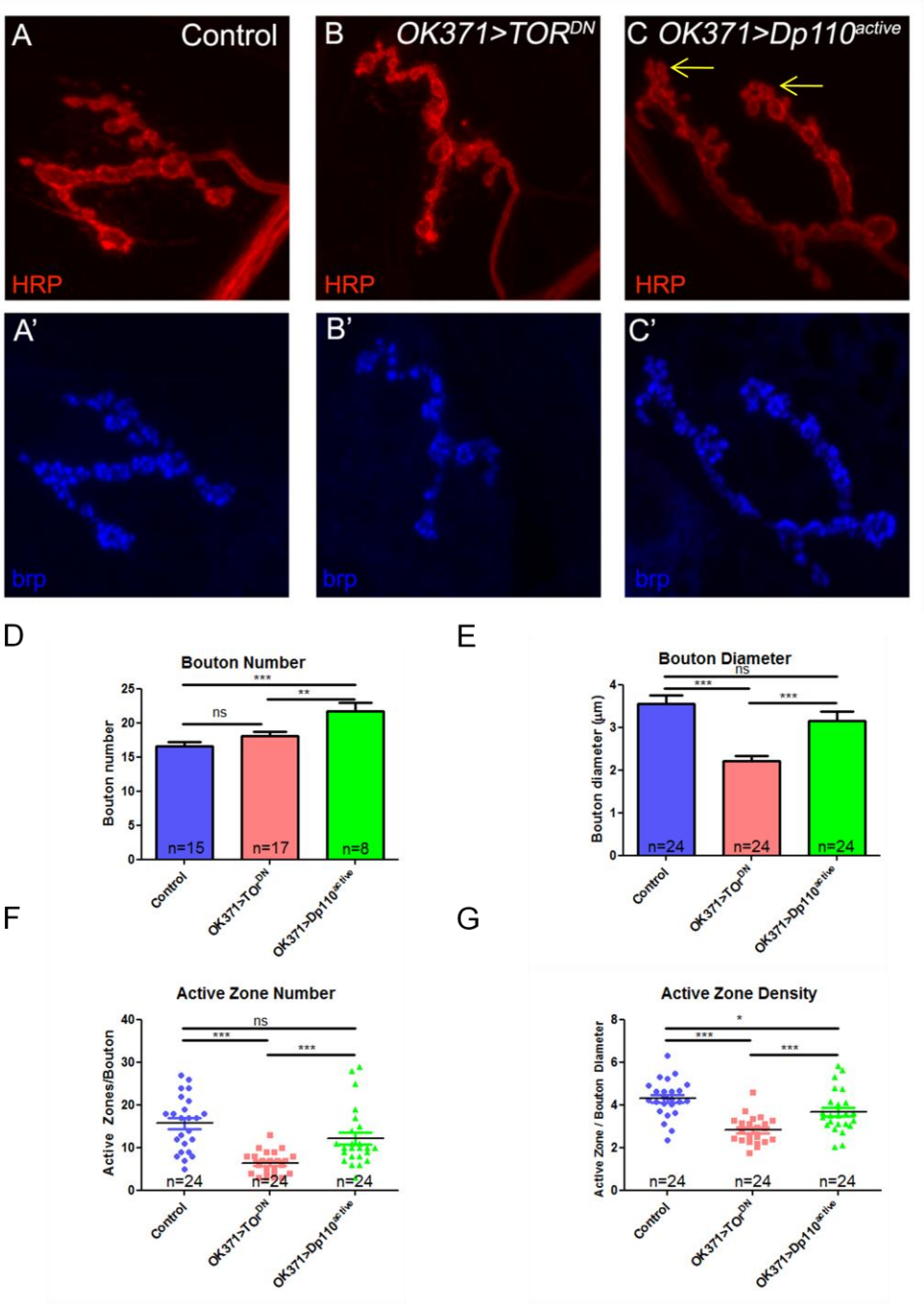
A Control
B OK371>TOR^DN
C OK371>Dp110^active
HRP
HRP
HRP
A'
B'
C'
brp
brp
brp
D
Bouton Number
Bouton number
n=15
n=17
n=8
Control
OK371>TOR^DN
OK371>Dp110^active
E
Bouton Diameter
Bouton diameter (µm)
n=24
n=24
n=24
F
Active Zone Number
Active Zones/Bouton
G
Active Zone Density
Active Zone / Bouton Diameter

Figure 6.3 The effect of TOR activity on motoneuron synapse development.

Representative NMJ 4 images of control **(A-A')**, motoneuron specific expression of TOR^{DN} **(B-B')** and $Dp110^{active}$ **(C-C')**. HRP (red) stains neuronal membranes and brp (blue) is a marker of active zones. **(C)** Yellow arrows show satellite boutons. **(D-E)** Expression of $Dp110^{active}$ resulted in an increase in bouton number, however expressing TOR^{DN} resulted in smaller boutons. **(F-G)** Active zone number and density was reduced upon TOR^{DN} expression. Expressing activated $Dp110^{active}$ had a slight affect on active zone number and density. Mean values +/- SEM plotted on graph D and E. Individual data plotted as circle (control), squares (TOR^{DN}) and triangles ($Dp110^{active}$) and means are shown as black lines on graph F and G.. *=p<0.05, **=p<0.01, ***=p<0.001.

6.4 Motoneuron specific manipulation of the TOR pathway alters synaptic mitochondrial localization

The TOR pathway regulates macroautophagy via inhibition of the protein kinase Atg1, which is a core component of the the autophagic machinary (KAMADA *et al.* 2000). Mitophagy is a form of autophagy specific to mitochondria and loss of the mitochondrial membrane potential induces mitophagy in mammalian and *Drosophila* cultured cells (NARENDRA *et al.* 2008; YOULE and NARENDRA 2011; ZIVIANI and WHITWORTH 2010). Therefore, the effect of TOR pathway manipulation upon mitochondrial localization was investigated at motoneuron synapses. Expressing TOR^{DN} resulted in a strong reduction in the appearance of mitochondria at NMJ 4, compared to controls (Figure 6.4B-B'). However, none of the boutons were entirely devoid of mitoGFP expression. This shows that the reduction of mitochondria with TOR^{DN} expression was not as strong as with overexpression of *TFAM* or mito*XhoI*. The same analysis was carried out for motoneurons expressing $Dp110^{active}$ (Figure 6.4C-C'). Strong levels of mitoGFP expression were observed in NMJ 4 boutons and the number of boutons containing mitochondria was similar to controls (Figure 6.4D).

Mitochondrial volume and number were also quantified in motoneurons expressing TOR^{DN} and $Dp110^{active}$. Both the number of mitochondria and mitochondrial volume were significantly reduced upon expression of TOR^{DN} (Figure 6.4 E-F). Expression of $Dp110^{active}$ resulted in a more variable phenotype. The ratio of mitochondrial volume to bouton volume was similar to control boutons, however there were significantly fewer mitochondria in these boutons (Figure 6.4 E-F). These data

suggested that mitochondrial volume may be increased. Therefore absolute mitochondrial volume was determined for the same boutons and was found to be nearly 85% increased, compared to control mitochondria, although this did not reach significance (Figure 6.4G). However, upon $Dp110^{active}$ expression I observed more mitochondria with a larger volume.These data suggest that activation of the TOR pathway causes synaptic mitochondrial volume to increase, but numbers of individual mitochondria to decrease. Conversely, inhibition of TOR signalling causes a strong reduction in both synaptic mitochondrial volume and mitochondrial number. Therefore TOR signalling has profound effects on synaptic mitochondria in *Drosophila* motoneurons.

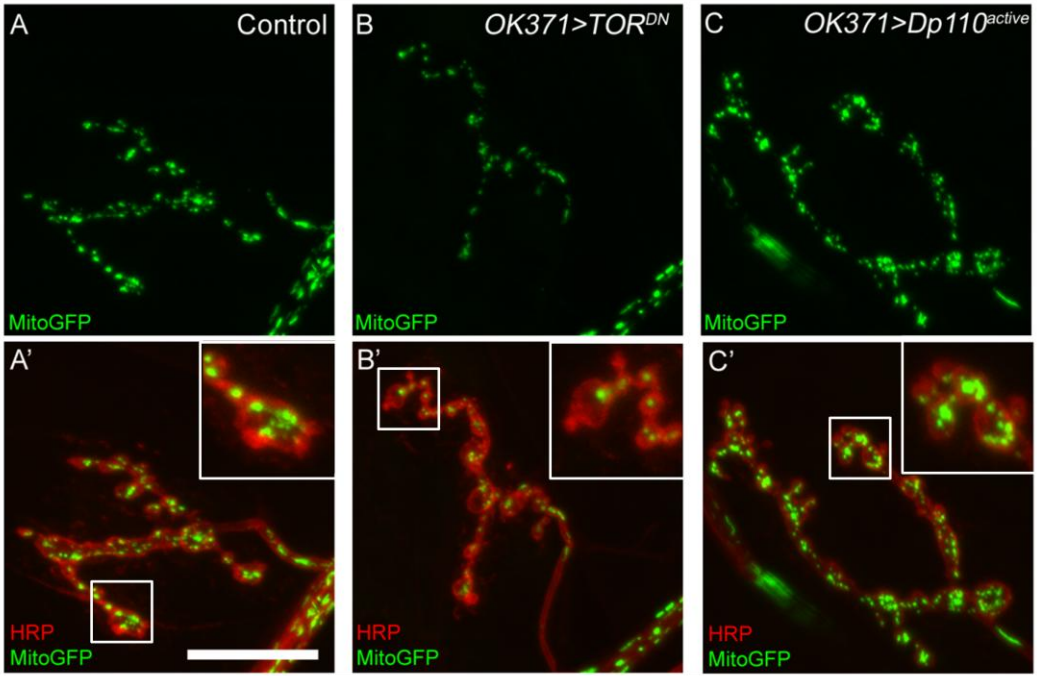
A
Control
MitoGFP
B
OK371>TOR^DN
MitoGFP
C
OK371>Dp110^active
MitoGFP
A'
HRP
MitoGFP
B'
HRP
MitoGFP
C'
HRP
MitoGFP

D

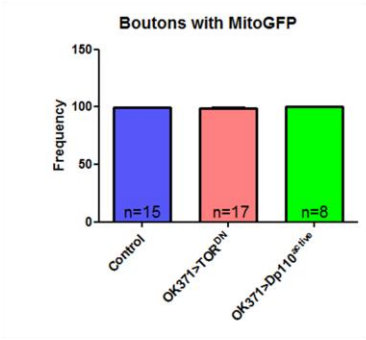
Boutons with MitoGFP
Frequency
150
100
50
0
n=15
n=17
n=8
Control
OK371>TOR^DN
OK371>Dp110^active

E

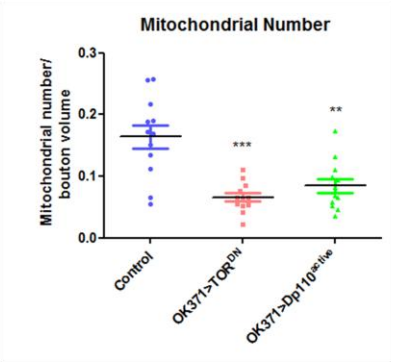
Mitochondrial Number
Mitochondrial number/ bouton volume
0.3
0.2
0.1
0.0
***
**
Control
OK371>TOR^DN
OK371>Dp110^active

F

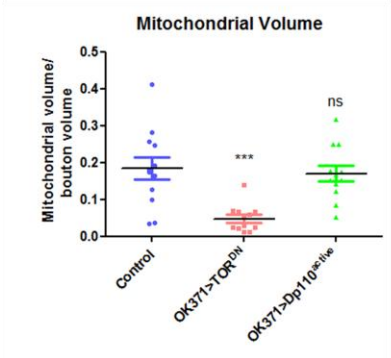
Mitochondrial Volume
Mitochondrial volume/ bouton volume
0.5
0.4
0.3
0.2
0.1
0.0
***
ns
Control
OK371>TOR^DN
OK371>Dp110^active

G

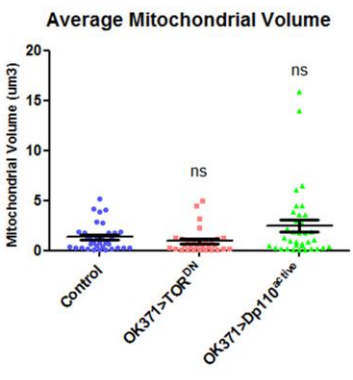
Average Mitochondrial Volume
Mitochondrial Volume (um3)
20
15
10
5
0
ns
ns
Control
OK371>TOR^DN
OK371>Dp110^active

Figure 6.4 Expressing *TOR^{DN}* and *Dp110^{activated}* affects synaptic mitochondria in motoneurons.

(A-C') Representative scans of NMJ 4. MitoGFP was used to visualize mitochondria and HRP (red) stains neuronal membranes. Scale bar is 20μm. **(D)** There was a slight reduction in the overall mitoGFP expression in the motoneurons expressing *TOR^{DN}*, however the number of boutons with mitoGFP was similar for all of the genotypes tested. **(E-F)** Both number and volume of mitochondria in boutons was reduced upon expression of *TOR^{DN}*. In contrast, *Dp110^{active}* expression resulted in boutons with slightly fewer mitochondria compared to control boutons (*w^{1118}* crossed to the driver line). **(G)** Average volume of each mitochondria was slightly larger upon expression of *Dp110^{active}* (p=0.08). Mean values +/- SEM plotted on graphs D and G. Individual data plotted on graphs E and F with mean values shown as black lines.

6.5 Directly increasing autophagy depletes synaptic mitochondria

Inhibition of TOR signalling increases autophagy, but TOR regulates many other processes in addition to autophagy. In order to test whether direct activation of autophagy affects synaptic mitochondria, I overexpressed the *Atg1* in motoneurons using using the *OK371-Gal4* driver. Overexpression of *Atg1* in motoneurons caused pupal lethality, suggesting motoneuron function was severly perturbed. Autophagy genes have been shown to be required for motoneuron development in *Drosophila*. Mutants in *Atg1*, *Atg2*, *Atg6* and *Atg18* were shown to have reduced bouton numbers at NMJ 4 (SHEN and GANETZKY 2009). Overexpression of *Atg1* in motoneurons was also shown to increase bouton numbers (SHEN and GANETZKY 2009). In agreement with this I found that motoneuron specific *Atg1* overexpression resulted in a 25% increase in bouton number (Figure 6.5C). In addition, *Atg1* overexpression resulted in smaller boutons (Figure 6.5D). Active zone number and density were also analysed. Both the number of active zones in each bouton and the density of active zones were significantly reduced compared to control boutons (Figure 6.5 E-F). These results show that, in addition to the previously documented increase in bouton number, direct activation of autophagy causes decreased bouton size, active zone number and active zone density and inhibits motoneuron function.

Mitochondrial localization was analysed in motoneurons overexpressing *Atg1*. *Atg1* overexpression resulted in a dramatic depletion of synaptic mitochondria. Nearly 45% of the boutons at NMJ4 were devoid of mitochondria upon *Atg1* overexpression (Figure 6.6C). Those boutons containing mitochondria were then further analysed. They were found to mostly contain one single small mitochondrion (Figure 6.6B).

Quantification showed that the total volume and number of mitochondria in these boutons was much less than in control boutons (Figure 6.6 D,E). In conclusion, direct activation of autophagy in motoneurons by *Atg1* overexpression resulted in a severe loss of synaptic mitochondria.

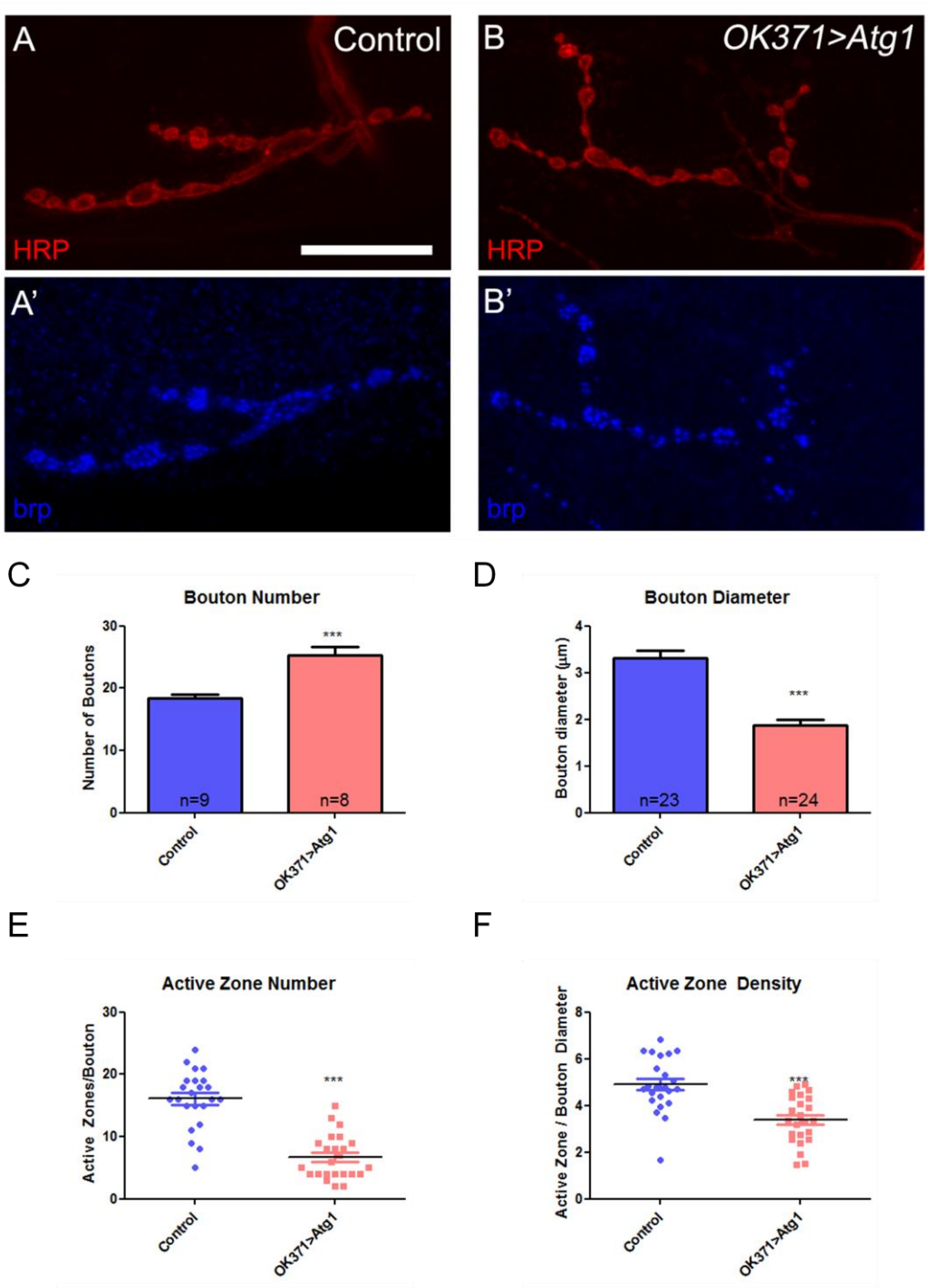
A
Control
HRP
B
OK371>Atg1
HRP
A'
brp
B'
brp
C
Bouton Number
Number of Boutons
***
n=9
n=8
Control
OK371>Atg1
D
Bouton Diameter
Bouton diameter (µm)
***
n=23
n=24
Control
OK371>Atg1
E
Active Zone Number
Active Zones/Bouton
***
Control
OK371>Atg1
F
Active Zone Density
Active Zone / Bouton Diameter
***
Control
OK371>Atg1

Figure 6.5 Activation of autophagy affects synaptic development.

(A-B') Representative scans of NMJ 4 showing boutons (red) and active zones (brp, blue) upon *Atg1* overexpression. Scale bar is 20μm. **(C-D)** *Atg1* overexpression results in increased bouton number and smaller boutons. **(E-F)** *Atg1* overexpression results in fewer active zones and decreased active zone density**.** Mean values +/- SEM plotted on graph C and D. Individual data plotted as circles (control), squares (*Atg1*) and means shown as black lines on graphs E and F. ***=$p<0.001$

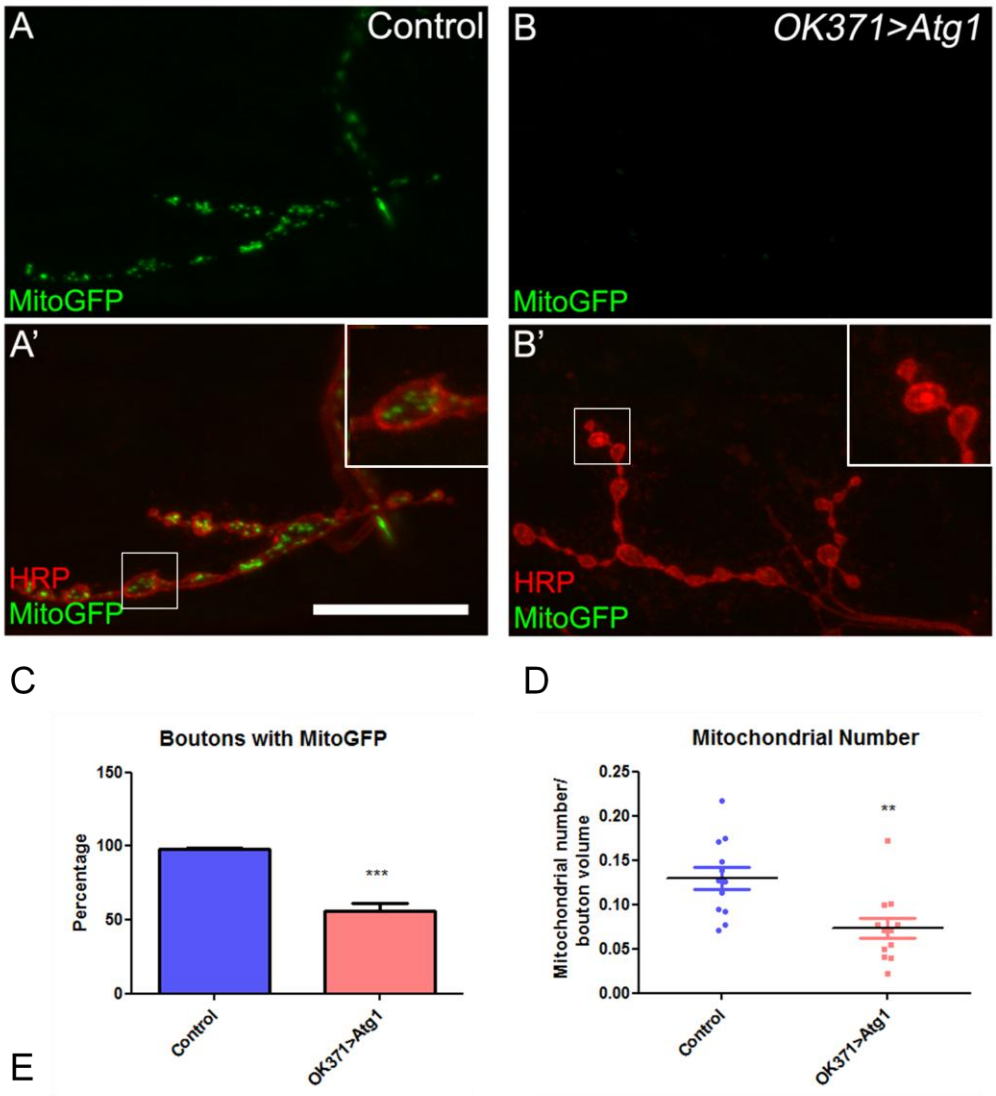
A
Control
MitoGFP
B
OK371>Atg1
MitoGFP
A'
HRP
MitoGFP
B'
HRP
MitoGFP
C
Boutons with MitoGFP
Percentage
150
100
50
0
***
Control
OK371>Atg1
D
Mitochondrial Number
Mitochondrial number/ bouton volume
0.25
0.20
0.15
0.10
0.05
0.00
**
Control
OK371>Atg1
E
Mitochondrial Volume
Mitochondrial volume/ bouton volume
0.5
0.4
0.3
0.2
0.1
0.0
***
Control
OK371>Atg1

Figure 6.6 Activation of autophagy depletes synaptic mitochondria.

(A-B') Representative scans of NMJ 4 showing mitoGFP (green) and boutons (HRP, red) in control and boutons overexpressing *Atg1*. Scale bar is 20 μm. **(C)** Mitochondria are absent in approximately 45 % of the boutons upon motoneuron specific *Atg1* expression. **(D-E)** Mitochondrial number and mitochondrial volume per bouton were significantly reduced upon *Atg1* overexpression. Mean values +/- SEM plotted on graph C. Individual values plotted with mean values shown as black lines in graphs. **=p<0.01, ***=p<0.001.

6.6 Summary

In order to investigate the possible mechanisms contributing to the motoneuron dysfunction caused by mtDNA loss, the TOR signalling pathway was investigated. Activating the TOR pathway by expressing an activated form of PI3K resulted in an increase in bouton number, while the mitochondrial network was similar to the control cells. However, inhibiting the pathway by expressing a dominant negative form of TOR resulted in adverse phenotypes in motoneurons. Synaptic boutons were smaller and they had fewer active zones. Although I did not observe complete depletion of mitochondria in these boutons, there were fewer mitochondria in the synapses. Reduction in the amount of mitochondria in the synapses suggested mitochondrial specific autophagy (mitophagy) may be the mechanism responsible for this phenotype. I expressed *Atg1* in order to activate autophagy in motoneurons and observed an increased number of smaller boutons that had fewer active zones. Strikingly, the number and volume of mitochondria was dramatically reduced in these boutons, suggesting that activation of autophagy directly depletes synaptic mitochondria.

In summary, the motoneuron synaptic phenotypes observed with mtDNA loss can also be produced by inhibition of the TOR pathway and promotion of autophagy.

Chapter 7. Discussion, Conclusion and Future Directions

7.1 Characterization of a *Drosophila* model of neuronal mtDNA loss

The primary function of mitochondria is to produce energy in the form of ATP, via oxidative phosphorylation. Mitochondria are unique organelles in most animal cells in that they have their own genome, mtDNA, which is approximately 19.5 kb in flies. The genome encodes 13 polypeptides, all of which are components of the OXPHOS machinery. Mutations and deletions in mtDNA have been reported in various disease states (PARK and LARSSON 2011). Furthermore, depletion of mtDNA copy number constitutes a risk factor for neurodegenerative diseases (SUOMALAINEN and ISOHANNI 2010). The cellular mtDNA copy number varies between 1000 to 10000, dependent on cell type (COPELAND 2008). My main aim in this study was to develop a model of mtDNA depletion in flies and to investigate its link to neuronal function and potentially neurodegeneration.

The first method trialled in my attempts to deplete mtDNA levels was to feed flies with EtBr. This was in light of the fact that it has been previously shown that EtBr, which is a DNA intercalating dye, can disrupt mtDNA replication, inhibit mtDNA transcription and break-down existing mtDNA (FUKUHARA and KUJAWA 1970; SLONIMSKI *et al.* 1968). It has also been shown that EtBr treatment can result in abnormal mitochondrial structures and cause aberrant larval development. In the same study also observed a slight increase in the lifespan of flies (FLEMING *et al.* 1981). I demonstrated that EtBr treatment in larvae resulted in defective larval

development, similar to that observed in previous studies (Figure 3.1A). I hypothesized that low levels of EtBr consumption could cause mtDNA depletion. I found that 1 mM EtBr treatment slightly decreased mtDNA copy number at the third instar larval stage, while very high concentrations of EtBr (5mM) caused arrested development. This may be due to a greater reduction in mtDNA copy number, or alternatively owing to EtBr exerting toxic effects when consumed at this high concentration. Furthermore, I tested the consequences of EtBr treatment on adult flies developed on normal food and then transferred to EtBr containing media. No difference was observed in the lifespan of the flies aged on either 0.2mM or 2mM EtBr containing media, compared to media without EtBr. Interestingly however, EtBr consumption at the adult stage did result in mtDNA depletion. The observed phenotypes are difficult to explain as it is hard to determine the actual target of EtBr once it enters the body. It is plausible that ingested EtBr does not reach some tissues, such as neuronal structures, while other tissues such as the gut could be strongly affected, meaning that the lifespan of the organism is not significantly impacted. This could therefore explain my observations that reduced mtDNA levels had no effect on adult lifespan. Future studies could investigate the degree to which EtBr is taken up by different tissues and how tissue-specific mtDNA levels are affected during development and in adult flies.

Owing to the limitations presented by using a DNA intercalating agent, namely the potential toxic effects and that it is not tissue specific, I decided to take a genetic approach to study mtDNA depletion. The extensive genetic toolkit afforded by *Drosophila* meant I was able to exploit the advantages of the yeast-derived *UAS*/*Gal4* system. This system has been adapted for use in flies in order to facilitate the tissue-specific expression of genes via the *Gal4* transcription factor (BRAND and

PERRIMON 1993). Firstly, I used various RNAi lines targeting genes involved in mtDNA replication (Table 3.1). RNAi lines against *Polγ*, *Twinkle*, *TFAM* and *DNK* were crossed to the *Act-Gal4* driver in order to cause ubiquitous knockdown of these genes. Most of the dsRNA lines were found to be lethal when expressed ubiquitously, as I had anticipated given that mtDNA replication is necessary for viability. *Polγ* has been studied in flies previously and mutations in the *tamas* gene were found to cause lethality just before pupariation (IYENGAR *et al.* 1999). Similar to this and my observations, null mutations in the accessory subunit of *Polγ* cause lethality at the early pupal stage (IYENGAR *et al.* 2002). This could be because maternal mtDNA is sufficient for the organism to develop until the late larval stage, however efficient mtDNA replication is needed for further developmental processes. Alternatively, the maternal contribution of the mtDNA polymerase could be sufficient to maintain mtDNA levels until the late larval stage.

In order to determine whether these RNAi lines deplete mtDNA in the nervous system, I crossed them to the pan-neuronal driver *Elav-Gal4*. I subsequently performed qPCR on genomic DNA extracted from the dissected adult CNS from the progeny of these crosses. However, I did not observe any difference in mtDNA levels using dsRNAs against *Polγ*, *Twinkle* or *TFAM*. It is important to bear in mind that there are other cells in the CNS, such as glia and fat body cells, which were not targeted in these crosses, given that *Elav-Gal4* expression is neuron specific. These cells constitute a significant proportion of the CNS and so could therefore be the reason why I did not observe a reduction in mtDNA copy number. This could potentially be circumvented by using fluorescent activated cells sorting (FACS) to purify neurons from the CNS, followed by qPCR to determine mtDNA levels in this enriched population. This experiment was also carried out with three samples per

genotype and five brains were dissected per sample. It is possible that these numbers may not be sufficient to generate a significant difference (Figure 3.2).

The next assay I carried out in the neuronal specific knockdown was to measure ATP levels. In the brain samples from male flies, I observed a reduction in the ATP levels (Figure 3.3B). Furthermore, there was a reduction in the ATP levels in the CNS of female flies, apart from in the *Polγ RNAi* (Figure 3.3A). However, this experiment was only performed once and so would need to be repeated to determine if the decrease was genuine. Given that I observed mild phenotypes in the previous neuronal experiments, I subsequently decided to use a stronger neuronal driver line. It has been previously published that overexpression of catalytic subunit of *Polγ* using *MZ1407-Gal4* caused mtDNA depletion, increased apoptosis and reduced lifespan in flies (MARTINEZ-AZORIN *et al.* 2008). *MZ1407-Gal4* is an enhancer trap line, which has been used as an early neuroblast specific driver, and is also expressed in most of the neurons in CNS and in all neurons of the PNS (LUO *et al.* 1994). Firstly, I analysed mtDNA levels by isolating DNA from whole fly heads. From this I observed a mild consistent reduction in the mtDNA levels in all of the RNAi lines tested although this reduction did not reach significance compared to the control (Figure 3.5). This was an interesting result compared to the previous mtDNA measurements using *Elav-Gal4*, in which I found no effect on mtDNA levels. These data suggest either that *MZ1407-Gal4* is a stronger driver than *Elav-Gal4*, or that strong expression in neuroblasts caused by *MZ1407-Gal4* is sufficient to cause a detectable reduction in mtDNA levels in the CNS.

I also checked the *MZ1407-Gal4* driver expression pattern by crossing to *UAS-nGFP* and then staining neuroblasts with an antibody against Miranda. From this, I observed that GFP positive cells colocalised with the Miranda staining. Also, GFP

positive neurons were observed throughout the optic lobes, central brain and thoracic VNC. These data confirmed that *MZ1407-Gal4* is expressed in neuroblasts and also in neurons throughout the majority of the CNS.

Since I had shown that RNAi of mtDNA replication genes using *MZ1407-GAL4* causes a slight reduction in mtDNA levels, which although it was not statistically significant, was a consistent down regulation and more experiments were carried out with this driver to analyse if this results in other defects. I decided to investigate larval and adult behaviour using two *TFAM* RNAi lines (*TFAMIR-2* and *TFAMIR-3*). I crossed both of these lines to the *MZ1407-Gal4* driver at 25^0C and found that *TFAMIR-2* was lethal and *TFAMIR-3* has reduced viability compared to the control (Figure 3.7A). The same crosses performed at 21^0C rather than $25\ ^0$C rescued the viability of *TFAMIR-2* completely and *TFAMIR-3* partially (Figure 3.7B). Furthermore, both dsRNAs against *TFAM* resulted in a reduction in larval movement (Figure 3.7C). In order to verify the specificity of *TFAM-RNAi*, I used other *TFAM RNA*i lines in addition to *TFAMIR-2* and *TFAMIR-3*. Apart from the *TFAMIR-2* line, all the other *TFAM* RNAi lines were viable at 25^0C. However, all of the viable *TFAM RNAi* lines expressed with *MZ1407-Gal4* had defects in the wing expansion (Figure 3.8A-E). Testing both overlapping and non-overlapping *TFAM* RNAi lines and observing similar phenotypes reduces the likelihood that the phenotypes are the result of off-target effects. Furthermore, both *TFAMIR-2* and *TFAMIR-3* resulted in climbing defects both in male and female flies (Figure 3.8B and C). It is possible that these observed defects may be the result of neuroblast cell death or reduced proliferation. In order to test this hypothesis, I counted the number of neuroblasts in the VNC, but observed no differences in either of the *TFAM RNAi* lines tested compared to the control (Figure 3.9B).

Taken together these experiments demonstrate that *MZ1407-Gal4* is a useful driver, when combined with RNAi of mtDNA replication genes, to reduce mtDNA levels throughout the CNS. In contrast *Elav-Gal4* may not be strong enough, or have the correct spatio-temporal expression pattern to significantly deplete mtDNA using these RNAi lines. However, my aim was to deplete mtDNA levels specifically in differentiated neurons, rather than proliferating neuronal progenitors. In light of this, I decided to test neuronal-specific *Gal4* drivers to deplete mtDNA levels in specific neuronal populations using RNAi of *Polγ*, *Twinkle*, *TFAM.*

MB neurons have been widely used to model neurodegeneration in flies, specifically for axonal degeneration using the MB γ axons (LUO and O'LEARY 2005). *OK107-Gal4* is the MB-specific driver and I used this driver together with a *CD8-GFP* reporter to enable visualisation of neuronal morphology. dsRNAs against *Polγ*, *Twinkle* and *TFAM* were expressed in the MBs and I found that flies aged for one month had the strongest phenotype. MB morphology was normal in young adult flies (data not shown), but I observed thinner α/α' lobe branches in *Polγ* and *TFAM* RNAi flies (Figure 3.10). This shows that depleting mtDNA levels in MB neurons can induce axonal degeneration and that knockdown of *Polγ* and *TFAM* are useful tools for this.

In addition to the MB neurons I also used a second specific neuronal population, the motoneurons, to study the effects of mtDNA loss. Motoneurons have been previously used as a model to study neurodegenerative diseases (reviewed in (KESHISHIAN *et al.* 1996)). The *OK371-Gal4* driver has been shown to be expressed in motoneurons and inter neurons (MAHR and ABERLE 2006). I used *OK371-Gal4* to knockdown *Polγ*, *Twinkle* and *TFAM* in motoneurons. This resulted in reduced larval motility with *Twinkle* and *TFAM* RNAi lines, although no difference was observed with *Polγ*

RNAi (Figure 3.11A). Behavioural assays can be affected by environmental conditions and nutrition and so variation in larval density between vials can potentially affect locomotion phenotypes. To circumvent this, I used larvae carrying an RFP reporter grown in the same vials as an internal control. External control (*OreR*) and internal control RFP expressing larvae travelled approximately the same distances, while *TFAMIR-3* larvae displayed a reduction in locomotion (Figure 3.11B). This test thus verified the larval locomotion defect observed previously and highlighted the requirement for *TFAM* expression in motoneurons for normal larval locomotor activity.

Motoneuron specific knockdown of *Polγ*, *Twinkle* and *TFAM* resulted in viable adult flies that were used to test climbing ability. *Polγ* and *TFAM* RNAi resulted in reduced climbing ability both in mean male and female flies, while only female *Twinkle* RNAi flies displayed a reduction (Figure 3.12). The climbing phenotype observed with motoneuron specific *TFAM* knockdown concurs with the results of previous behavioural assays. Thus, expression of mtDNA replication genes are likely required in motoneurons throughout development. To confirm the climbing phenotypes with *TFAM* RNAi, I repeated the climbing assay using more flies. Repeating the experiment with 15 male flies still resulted in a climbing defect and ageing them for 1 month had no effect on the level of reduction (Figure 3.12A). Interestingly, when the climbing assay of *TFAM* RNAi flies was repeated using 12 female flies, no difference was observed compared to controls. However, when I aged these flies for 1 month, they displayed significantly reduced climbing activity (Figure 3.12B). This sexual dimorphism could be due to a difference in *OK371-Gal4* driver strength between males and females, although this is unlikely as the *Gal4* insertion is autosomal. Alternatively, I observed that male flies climb significantly

faster than female flies and so male flies may be more sensitive to deficits in motoneuron function. A study in *Drosophila simulans*, showed that female flies have a higher mtDNA levels and higher levels of hydrogen peroxide production (BALLARD *et al.* 2007). Therefore, the reason that I observed a stronger affect on locomotion in males than females upon motoneuron-specific *TFAM* knockdown could be because female flies have a higher mtDNA copy number and so are more resistant to reductions in *TFAM* expression than to male flies. It would be interesting in future to compare mtDNA copy number in wild-type and *TFAM* knockdown male and female flies.

Most of the dsRNA lines used against genes involved in mtDNA replication showed these genes to be necessary for viability, although tissue specific knockdown of these genes mostly resulted in viable adult flies. Expression of dsRNAs against *TFAM* generally resulted in the strongest phenotypes. In addition, motoneuron function can be analysed using behavioural tests, by imaging and electrophysiologically and so motoneuron-specific knockdown of *TFAM* was further characterised as a means of studying the effects of neuronal mtDNA loss.

7.2 Manipulation of *TFAM* expression to deplete mtDNA in motoneurons

Adequate mtDNA levels are vital for the survival of the cells and organisms. The main mechanism regulating the mtDNA content of the cell is the rate of mtDNA replication, with various nuclear encoded proteins having roles in this process (see

Chapter 3.1). TFAM has multiple functions in mtDNA metabolism and is essential for mtDNA maintenance and replication. It has been shown previously that *TFAM* knockdown results in mtDNA depletion (reviewed in (OLIVEIRA *et al.* 2010)). Ubiquitous expression of dsRNAs against *TFAM* caused lethality at the early pupal stage. This is similar to mutants in the catalytic and regulatory subunits of *Pol-γ*, which are also pupal lethal (IYENGAR *et al.* 2002; IYENGAR *et al.* 1999). I used two non-overlapping RNAi lines against *TFAM (TFAMIR-2* and *TFAMIR-3)*. The *TFAMIR-3* line resulted in a much stronger reduction in *TFAM* transcript level. I also observed a significant depletion in mtDNA level when *TFAMIR-3* was crossed to the ubiquitous driver *Actin-Gal4*. Furthermore, qPCR analysis using first instar larvae showed a significant reduction in mtDNA copy number. These data show that *TFAM* knockdown causes a reduction in the level of mtDNA from an early developmental stage. *ActGal4>TFAMIR* larvae develop up to the third instar larval stage and pupate with an approximately 50% reduction in the mtDNA level. Reduced *TFAM* levels results in reduced mtDNA replication, which in turn affects the development of the organism. MtDNA related disorders vary in phenotype depending on the severity of the mtDNA depletion or amount of mutated mtDNA. Several studies have shown that mutant mtDNA, or the level of depleted mtDNA, must reach a 'critical threshold' in order to severely affect the organism (LARSSON and CLAYTON 1995; WALLACE and FAN 2009). Maternal contribution of mtDNA may be sufficient for the organism to pass through the early developmental stages. However, in order to complete development the organism may require efficient mtDNA replication to maintain mtDNA levels above the critical threshold. Defects in the mtDNA replication machinery resulted in arrest of development at the early pupal stage. It is thus clear that passage from the early pupal stage to the adult requires mtDNA levels

above a threshold of around 50%. I did not establish the mechanism causing the failure of *TFAM* RNAi pupae to develop to adulthood. It could be that the lack of an external food supply makes pupae particularly sensitive to mitochondrial dysfunction. Alternatively, the morphogenesis of adult structures, that occurs during the pupal stage, may arrest if mtDNA levels are below a specific threshold.

Increased *TFAM* levels have been linked to various phenotypes in previous studies, depending on the genetic background, with overexpression of human *TFAM* shown to improve some mitochondrial disease phenotypes in mouse models (IKEUCHI *et al.* 2005; MORIMOTO *et al.* 2012; NISHIYAMA *et al.* 2010). Overexpression of human *TFAM* in HeLa cells resulted in an increase in mtDNA copy number after 14 days, since it takes 10 days to express TFAM stably (KANKI *et al.* 2004). Furthermore expression of human *TFAM* at physiological levels in mice can result in an increase in mtDNA copy number (YLIKALLIO *et al.* 2010). However, the Jacobs group investigated the effects of human *TFAM* overexpression in HEK cells and observed a decrease in mtDNA level upon *TFAM* overexpression after 10 days, although a slight increase was observed after 16 hours (POHJOISMAKI *et al.* 2006). Ubiquitous overexpression of *TFAM* in *Drosophila* resulted in lethality at the first or second larval instar. Both *TFAM* and *TFAMGFP* expression resulted in reduction in mtDNA levels. The level of reduction was not as strong as that caused by *TFAM* knockdown, although developmental arrest occurred earlier in *TFAM* overexpressing flies. I hypothesized that although mtDNA depletion was not as strong as *TFAM* knock down flies, *TFAM* overexpression can cause more detrimental effects through additional mechanisms. TFAM is a transcription factor and so increased TFAM levels could affect mitochondrial gene transcription. Mouse and human TFAM differ in their C-terminal region, which is required for transcriptional activity. Expression

of human *TFAM* in a mouse *TFAM-/-* mutant does not rescue the embryonic lethality and this has been suggested to be due to differences in transcriptional activity between the two proteins (EKSTRAND *et al.* 2004).

The role of TFAM in binding and packaging mtDNA has been widely studied. Overexpressing *TFAM* could result in excessive binding to mtDNA, making it inaccessible to the replication and transcription machineries. The contradictory results of *TFAM* overexpression observed in different systems could be due to the different binding efficiency of different forms of TFAM (human versus mouse or *Drosophila*) over-expressed in different cell types. Furthermore, the level of expression could be different in different systems. I suggest that overcrowding the mtDNA with very high amounts of TFAM may be detrimental and cause mtDNA loss, while a slight increase in TFAM levels could stabilize mtDNA and increase mtDNA replication and transcription.

Ubiquitous knockdown of *TFAM* resulted in pupal lethality, which limits investigations into the consequences of mtDNA loss at later stages in development and in adults. Furthermore, using a ubiquitous driver is not suitable to investigate the cell type specific requirements for mtDNA. In light of these reasons I decided to use a tissue specific driver. One of the tissues that is widely used for developmental studies in *Drosophila* is the wing. RNAi of *TFAM* using *MS1096-Gal4* resulted in smaller adult wings, while overexpression of *TFAM* affected wing development more severely (Figure 4.2). I observed a reduction in the level of diffuse TFAM staining and small TFAM puncta, while larger puncta were more apparent upon RNAi of *TFAM* (Figure 4.2). This observation is similar to what has been reported in human tissue culture cells (KASASHIMA *et al.* 2011). In this study, PicoGreen staining (a DNA specific dye) was used to visualize mtDNA and it was shown that knockdown

of *TFAM* resulted in nucleoid enlargement (KASASHIMA *et al.* 2011). Despite attempts to stain mtDNA nucleoids in the wing disc using several DNA-specific dyes I was not able to consistently visualise these structures. Therefore I was not able to confirm that the alteration in TFAM localisation in *TFAM* RNAi cells caused nucleoid enlargement in my experiments. Expression of both GFP tagged and untagged forms of *TFAM* in the wing disc caused an increase in TFAM levels and both knockdown and overexpression of *TFAM* caused abnormal adult wing morphology (Figure 4.3). In accordance with the earlier lethality caused by ubiquitous overexpression of *TFAM* compared to *TFAM* knockdown, I observed stronger morphological defects in the *TFAM* overexpressing wings, compared to *TFAM* knockdown. Altogether this data shows that maintenance of mtDNA is required for proper development of the *Drosophila* wing. The underlying mechanism causing these phenotypes is not known, however this is potentially a useful phenotype to screen for novel genes that interact with *TFAM* and that are involved in mtDNA maintenance.

In the previous chapter I identified the motoneuron system as a model to investigate the consequences of mtDNA depletion in neurons. *TFAM* knockdown in motoneurons caused behavioural phenotypes both at larval and adult stages. In *TFAM* RNAi motoneuron cell bodies I observed a reduced level of TFAM expression with several enlarged TFAM puncta (Figure 4.4). This finding correlated with TFAM staining in the wing (Figure 4.3) and with previous studies in tissue culture cells (KASASHIMA *et al.* 2011). I observed increased TFAM antibody staining in *TFAM* and *TFAMGFP* overexpressing motoneuron cell bodies (Figure 4.4). In some motoneuron cell bodies expressing TFAMGFP very large green fluorescent puncta were observed that did not colocalise with TFAM antibody staining. These

very large puncta were never observed in motoneurons overexpressing un-tagged TFAM and so are presumably aggregates that result from the GFP fusion. Whether these puncta contain mtDNA could not be determined as I was not able to stain motoneuron cell bodies with a DNA-specific dye. Until it is known whether these aggregates are benign, or cause defects that are specific to the tagged protein, results obtained with TFAMGFP overexpression should be treated with caution and reproduced with un-tagged TFAM.

Next, I tested if mtDNA depletion in motoneurons impaired development. Viablity tests were performed, showing that approximately the same percentage of adult flies eclosed with motoneuron-specific *TFAM* RNAi or *TFAMGFP* expression as with controls. However, motoneuron specific expression of *TFAMGFP*, but not *TFAM* RNAi, resulted in reduced adult lifespan. Overexpression of un-tagged *TFAM* in motoneurons resulted reduced viability, caused by a defect in late pupal development, as the numbers of pupae were similar to the controls. Although the majority of *TFAM* overexpressing flies did eclose they died within a few days. Therefore, as with the viability upon ubiquitous expression and wing expression phenotypes, *TFAM* overexpression in motoneurons caused a stronger phenotype than *TFAM* RNAi.

I observed reduced larval movement with motoneuron-specific RNAi and overexpression of *TFAM*, suggesting that maintenance of mtDNA is required for normal larval motoneuron activity. I also wanted to test whether the behavioural defects occurred in adult flies. I found that RNAi and overexpression of *TFAM* resulted in defects in adult climbing. Both GFP tagged and untagged overexpression of *TFAM* resulted in stronger climbing defects compared to *TFAM* knockdown (Figure 4.6). Jump assays also demonstrated that *TFAM* overexpression caused a

more severe phenotype than *TFAM* RNAi. These data strongly suggested that mtDNA loss affects motoneuron function throughout development and led me to investigate the effects of manipulation of *TFAM* levels on motoneuron development.

In a recent study the catalytic subunit of *Polγ* was silenced in specific neurons (cholinergic, dopaminergic and serotonergic) in adult flies and only dopaminergic neuron specific RNAi of *Polγ-α* was found to cause climbing defects. In the same study, open field motion was analysed and similar results were obtained (HUMPHREY *et al.* 2012). It would be interesting to manipulate *TFAM* levels in these neuronal types and to assess behavioural performance to determine whether *TFAM*-induced mtDNA loss gives similar phenotypes to knockdown of *Polγ-α*. It has been previously reported that mtDNA depletion via over-expression of *Polγ-α* can reduce the median lifespan of *Drosophila* (MARTINEZ-AZORIN *et al.* 2008). I analysed the lifespan of male and female flies separately and found no difference in the flies expressing dsRNA against *TFAM*. In correlation with the strong behavioural defects observed, overexpressing *TFAMGFP* resulted in a significantly shorter lifespan. This further suggests that overexpressing *TFAM* results in more detrimental defects than *TFAM* knockdown, which might not only be caused by mtDNA depletion but also through other mechanisms as discussed above.

I then investigated motoneuron dysfunction at a cellular level using confocal microscopy. Firstly I hypothesized that cell death may be responsible for the motoneuron dysfunction caused by *TFAM* RNAi and overexpression since it has been shown that *TFAM* knockout mice have increased apoptosis (WANG *et al.* 2001). In order to test this hypothesis, motoneurons in the ventral nerve cord were counted, but no difference was found between the control and *TFAM* RNAi or overexpression. Therefore, the observed behavioural phenotypes were not caused by motoneuron cell

death. I next hypothesized that either development of the motoneurons or disruption of the mitochondrial network might contribute to the behavioural abnormalities.

Larval motoneuron axons exit from the VNC and span up to several hundred microns to reach target muscles and form synapses. Two of the most widely analysed synapses are at muscle groups 4 and 6/7. In checking the expression of the *OK371-Gal4* driver in boutons at these NMJs, I observed that it was strongly expressed in type Ib, but only weakly in type Is. This difference in expression of *OK371-Gal4* has not been described previously and could have important experimental consequences for quantification of bouton phenotypes using this driver. I therefore decided to analyse only type Ib boutons. NMJ 6/7 is not ideal for this purpose, as type Ib and Is boutons are found very close to each other and are not easy to differentiate one from the other. However, at NMJ 4 I was able to easily differentiate type Ib and Is boutons.

One of the most common ways to study synapse development is to count the number of boutons in the NMJ. I observed around 20 boutons in controls at NMJ 4, which is similar to other studies (CHEN and GANETZKY 2012; SHEN and GANETZKY 2009). I found that bouton number was not changed by *TFAM* knockdown or overexpression. Therefore I decided to analyse the size of the boutons by quantifying bouton diameter. The average diameter of the boutons was significantly reduced when *TFAM* was overexpressed. However, there was no difference to controls in the *TFAM* knockdown boutons at NMJ 4. Most of the previous studies on *Drosophila* NMJs have analysed bouton number rather than bouton size. For example, studies of *Neuroligin 1* (*dnlg1*) mutants and *spinster* mutants (a lysosomal storage disease model) found that bouton number was increased, but did not analyse bouton size (BANOVIC *et al.* 2010) and recently a *Drosophila* model of ALS (overexpression of

Fus/Caz) found a decrease in bouton number (XIA *et al.* 2012). *Atg* mutants have been shown to have reduced bouton number and appear to also have smaller boutons, but bouton size was not analysed (SHEN and GANETZKY 2009). The fact that bouton size is reduced without affecting bouton number suggests that these properties are separable. However, reduction of either bouton size or number both result in reduced NMJ area and so may have similar phenotypic consequences.

To better understand why *TFAM* overexpression caused bouton size defects I investigated other properties of motoneurons. There are several synaptic markers for *Drosophila* NMJs, one of which is an antibody against bruchpilot (Nc82), an antibody used to visualize active zones, which highlight the regions of presynaptic release sites. *TFAM* overexpression caused a decrease in the number of active zones per bouton and the density of active zones. These data suggest that mtDNA loss directly affects active zone development, over and above the expected reduction in active zone number as a consequence of reduced bouton size. Loss of mtDNA could affect synaptic mitochondria causing local synaptic energy defects, which affect active zone development. The mechanism by which active zones are affected requires further investigation and could result from a requirement for ATP directly during active zone development, or indirectly through aberrant motor neuron development affecting active zone number.

I then investigated the relationship between synapse development and synaptic mitochondria. The mitochondrial network is highly dynamic in neurons and mitochondria are transported both in anteriograde and retrograde directions along axons. The mitochondrial supply to synapses is maintained via this axonal transport of mitochondria. I hypothesized that the mitochondrial network may be more disrupted in distal regions of the motoneuron.

In control and *TFAM* knockdown boutons, almost all boutons had mitochondria. However, overexpression of *TFAM* resulted in loss of mitochondria in around 14% of the boutons. Although I observed a same percentage of boutons to contain mitochondria and the similar number of mitochondria per bouton as controls when *TFAM* was knocked-down, there was a reduction in mitochondrial volume in these boutons. By contrast, in boutons overexpressing *TFAM* I found there was typically only one mitochondrion present and mitochondrial volume was dramatically reduced. It is not known whether the absence of mitochondria caused the reduced bouton size, or whether smaller boutons caused by developmental defects resulted in the depletion of mitochondria. However, it is interesting that *TFAM* RNAi did not result in smaller boutons, nor complete depletion of mitochondria in boutons, but did result in reduced mitochondrial volume, suggesting that mtDNA loss primarily affects mitochondrial abundance. The fact the *TFAM* RNAi causes a mild mitochondrial phenotype and did not affect bouton size, while *TFAM* overexpression caused a strong mitochondrial phenotype and reduced bouton size suggests that there is a threshold of mitochondrial depletion below which bouton size is affected.

Mitochondrial depletion has been recently reported in DA (dopamine) neurons of MitoPark mice, which is a DA neuron-specific *TFAM* knockout (STERKY *et al.* 2011).These neurons were found to contain more fragmented mitochondria in the cell bodies, similar to my observation upon *TFAM* overexpression. MitoPark mice exhibit a progressive parkinsonian phenotype, with the initial defects in motorfunction (reduced locomotion and rearing) observed around 14-15 weeks of age (EKSTRAND *et al.* 2007). Neurochemical and electrophysiological defects were also observed at earlier timepoints in the asymptomatic mice. DA release was impaired and HCN (hyperpolarization-activated cyclic nucleotide-gated) ion channel

function was reduced in the MitoPark mice (GOOD *et al.* 2011). This may suggest that motoneuron dysfunction observed in my experiments was due to defects in neurotransmitter release and ion channel properties. Furthermore, loss of DA neurons was first observed at 12 weeks of age, several weeks after the neurochemical and electrophysiological phenotypes were first observed (EKSTRAND *et al.* 2007). I did not observe any motoneuron cell loss in adult *TFAM* RNAi or overexpression flies (preliminary data, not shown here), but it would be interesting to repeat this experiment in aged flies. Alternatively, motoneurons might be less sensitive to mtDNA loss than DA neurons, similar to the difference between cholinergic and DA neurons (HUMPHREY *et al.* 2012).

I also analysed mitochondrial morphology in other regions of the motoneuron. In control motoneurons cell body mitochondria formed in a filamentous network. mtDNA depletion using *TFAM* knockdown did not cause morphological defects in the cell body. However, overexpression of *TFAM* resulted in smaller mitochondria and overall disruption of the mitochondrial network. In order to understand the overall effect of mtDNA depletion, I analysed proximal and distal axons. RNAi or overexpression of *TFAM* did not affect the mitochondrial number at proximal axons, however mitochondrial volume was reduced when *TFAM* was overexpressed (Figure 4.13). Thus, similar to the cell body, only *TFAM* overexpression caused a mitochondrial phenotype in the proximal axon. In distal axons both *TFAM* knockdown and overexpression caused mitochondrial phenotypes. These data suggest that fewer mitochondria are transported along axons to the synapses when *TFAM* is knocked-down or overexpressed. Another possible mechanism is dysregulation of fusion/fission events, as it has been previously shown that increased fission can cause smaller mitochondria in neurons (SESAKI and JENSEN 1999).

Mitochondrial distribution in neurons is of particular importance and transport of mitochondria to regions with a high energy demand is vital for neuronal function. It was previously reported that synapses may consume up to 10% of the energy required for neuronal signalling (LAUGHLIN 2001). *Drosophila* photoreceptor terminals have been used as a model to investigate the importance of synaptic mitochondria and depletion of mitochondria found to cause blindness and failure in synaptic transmission (STOWERS *et al.* 2002). Furthermore *Miro* (mitochondrial Rho-GTPase) mutants have depleted synaptic mitochondria at NMJ 6/7 (GUO *et al.* 2005). *Miro* mutants have impaired larval locomotion such that larval crawling behaviour is affected. These studies highlight the importance of axonal transport of mitochondria to synapses and the behavioural phenotypes I observed with motoneuron specific *TFAM* manipulation could thus be a consequence of reduced mitochondrial transport to synapses. Future experiments will analyse mitochondrial transport in axons upon manipulation of TFAM levels.

Another possible explanation for the mitochondrial phenotypes observed could be linked to mitochondrial quality control mechanisms. Observing smaller sized mitochondria at synapses upon *TFAM* RNAi and overexpression could be related to inbalanced mitochondrial fusion/fission or increased mitophagy. Mitophagy is the selective autophagy of mitochondria and requires mitochondrial fragmentation (TWIG *et al.* 2008a). Opa1 (dynamin-related GTPase optic atrophy 1) and MFN (mitofusins) 1 and 2 are fusion related proteins, while mitochondrial fission is controlled by DRP1 (CIPOLAT *et al.* 2004; SANTEL and FULLER 2001; SMIRNOVA *et al.* 2001). It has been recently shown that upon induction on autophagy, mitochondria elongate and are spared from autophagic degradation in a DRP1 dependent manner (GOMES *et al.* 2011). This further demonstrates the dynamic nature of the mitochondrial network

and how fusion/fission and the autophagy machinery work together to shape a healthy mitochondrial network. In the same study silencing target of rapamycin (TOR) expression caused mitochondrial elongation (GOMES *et al.* 2011).

In conclusion, axonal transport of mitochondria, mitochondrial quality control and autophagy could all potentially contribute to the phenotypes observed. Investigating the bioenergetic properties of mitochondria in motoneurons with reduced or increased *TFAM* expression could provide insight into the role of mitochondrial quality control. In order to test which these potential mechanisms contribute to the observed phenotypes, genetic interaction experiments could be carried out. Manipulating levels of DRP1 or autophagy related proteins (such as Atg1, or TOR pathway proteins) in combination with *TFAM* RNAi or overexpression could be insightful.

7.3 mitoXhoI as a tool to induce mtDNA loss in motoneurons

In Chapter 3 and 4 I showed that mtDNA loss can be studied in motoneuron synapses using *TFAM* mediated methods. However, regulating mtDNA homeostasis and causing mtDNA loss in motoneurons via alternative mechanisms may prove useful for number of reasons. Firstly, depleting mtDNA in motoneurons and observing similar phenotypes would make us more confident about the previous results. Secondly, these other methods could be used as new models to study mtDNA depletion. Finally, any similarities and differences observed using the new models could provide mechanistic insight into the underlying cause of synaptic dysfunction.

Moraes and colleagues introduced a new method for studying mtDNA, by expressing mitochondrially targeted restriction enzymes (SRIVASTAVA and MORAES 2001; SRIVASTAVA and MORAES 2005). Xu and O'Farell adapted this method for flies and by isolating suppressors from crosses in which *mitoXhoI* was expressed in the germline, used it to generate mutations in the mitochondrial genome (XU *et al.* 2008). XhoI cuts the *Drosophila* mtDNA once and thus linearizes the mtDNA, resulting in reduced mtDNA replication. Expressing *mitoXhoI* using drivers such as the ubiquitous driver *Actin-Gal4* and the panneuronal driver *Elav-Gal4* caused lethality (at third instar larval stage). Motoneuron specific expression resulted in pupal lethality, meaning third instar larvae could be used to investigate mtDNA related defects.

In order to investigate the effect of *mitoXhoI* expression on mtDNA nucleoids, motoneuron cell bodies were stained with an antibody against TFAM. In control cell bodies homogeneous, punctate nucleoids were observed, which contrasted with various phenotypes upon *mitoXhoI* expression. The most striking phenotype was diffuse TFAM staining, as opposed to the punctate structures seen in control cell bodies (Figure 5.2), suggesting that nucleoid morphology was severely disrupted. Studies from the Moraes lab have shown that mitochondrially targeted restriction enzyme expression in cardiac tissues in mice causes both mtDNA deletions and depletion (XU *et al.* 2008). The precise affect of mitoXhoI on mtDNA in *Drosophila* motoneurons can only be inferred from my observations and future studies will be required to determine the precise affect of mitoXhoI on mtDNA in these cells.

NMJ 4 in *mitoXhoI* expressing motoneurons was subsequently investigated. I found that the number of boutons remained the same as controls, but *mitoXhoI* expression resulted in smaller boutons. This was similar to what was observed upon *TFAM*

overexpression. Furthermore active zone number and active zone density were reduced, again similar to what was observed upon *TFAM* overexpression. The next analysis was of mitochondrial localization at NMJ 4. Approximately 12% of the boutons completely lacked mitochondria and boutons with mitochondria had smaller and fewer mitochondria compared to control boutons (Figure 5.4). Overall these results show that mtDNA depletion via different methods results in similar phenotypes, including smaller boutons, fewer active zones, depletion of synaptic mitochondria and motoneuron dysfunction.

The bioenergetic properties of axonal mitochondria were analysed in *mitoXhoI* expressing motoneurons using Rh-1,2,3. Expression of *mitoXhoI* resulted in mitochondria with decreased membrane potential, suggesting that mtDNA loss, caused by *mitoXhoI* expression, leads to inhibition of the proton motive force used to generate the mitochondrial membrane potential. It will be interesting in future to determine the mitochondrial membrane potential in motoneurons with knocked-down or overexpressed *TFAM*. I would predict that *TFAM* overexpression would cause a strong reduction in membrane potential, similar to *mitoXhoI* expression, while *TFAM* RNAi would have a much weaker effect.

Mitochondrial targeted restriction enzyme expression in dopaminergic neurons has been reported as a PD model in mice (PICKRELL *et al.* 2011). These mice had defects in motor-related behaviour, tested using the pole test and rotarod. Progressive DA neuron loss was observed after 9 months in these mice. Dopamine levels were significantly reduced both in 4 months and >12 month oldmice. ι-DOPA treatment was shown to improve these symptoms. Overall these results correlate with the phenotypes seen in the “MitoPark” mice and confirm that loss of mtDNA in DA neurons results in defects in neurotransmission and neurodegeneration.

7.4 Potential mechanisms contributing to the defects in motoneuron development caused by mtDNA loss

7.4.1 Motoneuron specific TOR inhibition or *Atg1* overexpression phenocopy *TFAM* overexpression

The most striking phenotypes caused by *TFAM* overexpression and *mitoXhoI* expression were smaller boutons completely lacking, or with fewer mitochondria. Furthermore both resulted in fewer active zones in these boutons. The mechanisms causing these phenotypes are not known. However, these phenotypes suggest the possible involvement of a signalling pathway since both developmental and activity related phenotypes were observed. The central regulator of cell growth and metabolism is the serine/threonine kinase TOR. Given its pivotal role in cell growth and metabolism, the TOR pathway has been implicated in metabolic diseases, neurodegeneration, cancer and ageing (LAPLANTE and SABATINI 2012; ZONCU *et al.* 2011). In mammalian cells there are two TOR complexes, mTORC1 and mTORC2, which regulate other kinases such as S6 kinase (S6K) and Akt (ZONCU *et al.* 2011). An increasing number of cellular processes have been show to be controlled by the TOR pathway including protein synthesis, lipid synthesis, autophagy, lysosome biogenesis, energy metabolism, cell survival and cytoskeleton organization (reviewed in (LAPLANTE and SABATINI 2012)). Several of these processes can be linked with mitochondrial biology and could potentially contribute to the phenotypes I observed upon mtDNA depletion (Figure 6.1). Furthermore there is growing evidence linking the TOR pathway to synaptic plasticity and the modulation of

behaviour (COSTA-MATTIOLI *et al.* 2009; HOEFFER and KLANN 2010; SWIECH *et al.* 2008; TANG *et al.* 2002). I hypothesized that inhibition of the TOR pathway may affect mitochondrial localization in motoneuron synapses, similar to what was observed with *TFAM* overexpression and *mito-XhoI* expression.

In order to analyse the functional role of TOR at synapses I used genetic tools causing both inhibition and activation of the pathway. PI3K an upstream component of the TOR pathay that is recruited to insulin or IGF receptor upon binding of insulin or growth factors. It has been previously reported that neuronal specific activation of the TOR pathway via Rheb and PI3K expression results in larger boutons and enhanced synaptic function in *Drosophila* NMJ 6/7 (KNOX *et al.* 2007; MARTIN-PENA *et al.* 2006). Furthermore, several studies have found that mutations in S6K do not to affect bouton number, but result in smaller boutons (CHENG *et al.* 2011; KNOX *et al.* 2007; SHEN and GANETZKY 2009). I found that inhibition of the TOR pathway, by expressing a dominant negative form of TOR resulted in same number, but smaller boutons. A recent study of transheterozygous TOR mutant larvae showed that these larvae had similar bouton size and number presynaptic active zones to controls (PENNEY *et al.* 2012). However in the same study, it has been shown that expression of TOR postsynaptically triggered a retrograde increase in neurotransmitter release. Although the smaller boutons I observed are contradictory to this study, there are experimental differences in that I expressed TOR^{DN} presynaptically rather than using mutant larvae and also the mutant combination used in the previous study resulted in hypomorphic phenotypes.

Activation of the TOR pathway by expressing an activated form of Dp110 significantly increased the number of boutons and resulted in an increased appearance of satellite boutons (Figure 6.3). As a measure of synaptic function, I

quantified the number of active zones in each bouton. Expressing a dominant negative form of TOR resulted in a strong reduction in the number and density of active zones in each bouton. In contrast, expression of the activated form of Dp110 caused a significant decrease in the density of active zones in each bouton, while the number of active zones was approximately same. Therefore activation of the TOR pathway may not perturb synaptic function, as the increased bouton number could compensate for the marginal decrease in active zone density. Having more boutons may result in there being similar numbers of active zones throughout the synapse. In contrast, inhibition of the TOR pathway by expressing a dominant negative form of TOR resulted smaller boutons with fewer and less dense active zones. Taken together, the PI3K and TOR data confirm the importance of the TOR pathway in motoneuron synapse development and activity. Interestingly both inhibition and activation of the TOR pathway resulted in decreased climbing performance. Expression of TOR^{DN} caused only a slight defect, while expression of $Dp110^{active}$ resulted in stronger climbing defect (Figure 6.3). This is in contrast to a previous study that found that overexpression of wild-type *Dp110* in *Drosophila* motoneurons caused an increase in locomotion activity in larvae (MARTIN-PENA *et al.* 2006). Future experiments will investigate further the effects of TOR pathway activation on motoneuron function.

As a first step to testing the hypothesis that the mitochondrial phenotypes caused by mtDNA loss in motoneurons were due to misregulation of the TOR pathway I analysed mitochondrial morphology. Expression of TOR^{DN} and $Dp110^{active}$ did not result in the total loss of mitochondria from boutons. However, there was an overall reduction of mitochondria upon expression of TOR^{DN} (Figure 6.4). There was not a dramatic effect on mitochondrial localization upon activation of $Dp110^{active}$.

Therefore I investigated the boutons in detail. Expressing TOR^{DN} resulted in smaller and fewer mitochondria in each bouton (Figure 6.4). Conversely, activation of PI3K resulted in significantly fewer but larger mitochondria (Figure 6.4E-G). Surprisingly therefore, both inhibition and activation of the TOR pathway affected synaptic mitochondria. It has been reported that siRNA of TOR in tissue culture cells results in elongated mitochondria, which is different to what I observed (GOMES *et al.* 2011). It will be useful to visualize other compartments of the motoneurons to understand the global effect of TOR pathway inhibition on mitochondrial morphology.

The effect of $PI3K^{active}$ expression on synaptic mitochondria is interesting in that, similar to *TFAM* RNAi, there was a mitochondrial phenotype, but no effect on bouton size or active zone number. This again suggests that synaptic mitochondrial phenotypes may occur before effects on overall synapse development. The reason that I did not observe an increase in the mitochondrial volume to bouton volume ratio with expression of $PI3K^{active}$ could be that mitochondrial volume may be at the physiological limit. The reduction in the motor behaviour in $PI3K^{active}$ expressing flies could be the result of larger synaptic mitochondria, or of increased bouton number.

Motoneuron specific expression of *Atg1* resulted in late third instar developmental arrest.I observed increased bouton number upon Atg1 overexpression, however these boutons were significantly smaller compared to control boutons. Furthermore fewer active zones were observed in these boutons, confirming previous observations that autophagy affects motoneuron synaptic development (SHEN and GANETZKY 2009). The specific type of autophagy that is implicated in the clearance of damaged mitochondria is termed “mitophagy”. Several studies have shown that mitophagy is

responsible for degrading dysfunctional mitochondria in a *Drosophila* PD model (LIU *et al.* 2012). Furthermore, the PINK1/Parkin pathway is currently being studied in detail as a mitochondrial quality control mechanism (WHITWORTH and PALLANCK 2009). I observed a dramatic depletion of mitochondria from synapses upon *Atg1* overexpression in motoneurons. Approximately 45 % of boutons were completely devoid of mitochondria upon autophagy activation (Figure 6.6). These data are consistent with the hypothesis that mtDNA loss causes increased mitophagy leading to loss of synaptic mitochondria and potentially motoneuron dysfunction.

In order to evaluate the consequences of mtDNA loss in motoneurons, it is important to try to understand the relationships of the phenotypes observed. I will discuss the potential mechanisms contributing to the following phenotypes: (i) the decrease in bouton size and active zones at NMJs, (ii) the mitochondrial alterations resulting from mtDNA loss in motoneurons.

7.4.2 Potential mechanisms responsible for bouton size and active zone number reduction in motoneurons with depleted mtDNA

Mitochondrial dysfunction causing reduced ATP levels is the most likely result of mtDNA loss. This could directly retard bouton growth due to inhibition of one or multiple ATP dependent processes. The identity of these processes are not known but restoring ATP levels would be a potential way of suppressing the developmental phenotypes observed. Before considering attempting such experiments it would be

important analyse the ATP levels in mtDNA depleted motoneurons. One possible method of doing would be using luciferase activity in motor neurons to detect ATP levels. Luciferase expression in the fly brain has been used as a readout of circadian rhythm (CHEN *et al.* 2011), but has not been adapted for in vivo ATP detection in *Drosophila* and requires highly sensitive imaging techniques and a method to add the substrate, luciferin, to the target tissue.

Mitochondrial ATP generation has been suggested to be critical for motoneuron activity in a mouse model of motoneuron disease that expresses the G93A mutant SOD1 enzyme. In this model inhibition of glycolysis, which restricts ATP production to mitochondria, caused a reduction in evoked synaptic transmission; while synaptic activity was similar to controls in glucose containing media (which allows ATP generation via glycolysis) (CARRASCO *et al.* 2012). However, a *Drosophila* study modelling the mitochondrial encephalopathy Leigh Syndrome, using a mutant in mitochondrial complex II, showed that progressive synapse degeneration at photoreceptors was independent of ATP levels (MAST *et al.* 2008). The synaptic degeneration observed was related to increased ROS levels. ROS levels were also shown to be important for NMJ development in *Drosophila,* where induction of oxidative stress resulted in NMJ overgrowth (increased bouton number) of NMJ 6/7 (MILTON *et al.* 2011). It seems unlikely therefore that the NMJ phenotypes I observed upon *TFAM* or *mitoXhoI* overexpression are due primarily to increased ROS as bouton number was not increased. In summary, ATP and ROS levels can result in various phenotypes depending on the neuronal cell type or disease model.

A second possible mechanism that could contribute to reduced bouton size upon mtDNA loss could be reduced translation. The decreased bouton size observed upon expression of TOR^{DN} supports this hypothesis as TOR is a major regulator of growth

through translational regulation. Furthermore *S6k* mutant larvae were found to have a similar phenotype in that bouton number was not affected but the bouton size was reduced by 40% (CHENG *et al.* 2011). I propose a model in which mitochondrial dysfunction, resulting from mtDNA loss, inhibits TOR signalling (via activation of AMPK due to decreased ATP levels), which leads to reduced translation and so decreased bouton size (Figure 6.1). In order to test if mtDNA depletion results in TOR inhibition, staining of motoneurons overexpressing *TFAM* or *mitoXhoI* with a phospho-S6k (P-S6k) specific antibody, or western blot analysis of P-S6k in larvae overexpressing *TFAM* or *mitoXhoI*, could be performed to determine whether TOR activity is affected by mtDNA loss. Subsequently, rescue experiments could be performed to determine whether activation of the TOR pathway restores activity in motoneurons overexpressing *TFAM* or *mitoXhoI*.

Motoneuron specific mtDNA loss resulted in a reduction in the number of active zones. The data presented in chapters 4, 5 and 6 show that the active zone reduction is probably not simply due to the bouton size reduction as active zone density is reduced upon overexpression of *TFAM*, *mitoXhoI* and TOR^{DN}. This is an interesting and important point, highlighting the specific effect of mtDNA depletion on active zone development. One possible reason for this could be inhibition of ATP dependent processes regulating active zone development. Neurotransmitter release is an ATP-dependent process in part because synaptic vesicle priming (exocytosis of docked vesicles) is regulated by the NSF (N-ethyl-maleimide-sensitive factor) protein, which has two ATPase domains (ZHENG and BOBICH 1998). The molecular composition of the active zone in *Drosophila* is only beginning to be understood, with the identification of key components such as Rab3-interacting molecule (RIM)-

binding protein (DRBP) (LIU *et al.* 2011). The potential regulation of active zone development by ATP levels will be an important future direction.

7.4.3 Potential mechanisms that contribute to the mitochondrial phenotypes caused by motoneuron mtDNA loss

I observed a progressive defect in mitochondrial localization from motoneuron cell bodies to the synapses with some synaptic boutons completely devoid of mitochondria upon overexpression of *TFAM* and *mitoXhoI*. This could result from defective axonal transport of mitochondria to the cell bodies. It has been shown in *Drosophila* that mutations in *Miro,* which is required for anteriograde transport, result in depletion of synaptic mitochondria (GORSKA-ANDRZEJAK *et al.* 2003; GUO *et al.* 2005; STOWERS *et al.* 2002). It will be important to analyse mitochondrial transport in motoneuron axons by live imaging to determine if transport defects contribute to the depletion of synaptic mitochondria in motoneurons with decreased mtDNA. If so, increasing mitochondrial transport could be a means of rescuing the phenotypes observed upon mtDNA depletion.

Alterations in the fission/fusion machinery could also result in defects in the mitochondrial network and it has been shown that down-regulation of *Drp1* expression in mammalian cells results in mtDNA loss (PARONE *et al.* 2008). Overexpression of *TFAM* and *mitoXhoI* result in smaller mitochondria at synapses and in axons. Additionally, overexpression of *TFAM* and *mitoXhoI* caused morphological changes in motoneuron cell body mitochondria. These morphological

changes may be due to an increase in fission events and would suggest that mtDNA depletion may result in activation of mitochondrial fission. Enhancing mitochondrial fusion or inhibiting mitochondrial fission may therefore compensate for the mitochondrial phenotypes observed upon mtDNA depletion. In a recent study, loss of membrane potential and mitochondrial fragmentation were linked. ARL4D, a member of the ADP-ribosylation factor/ARF-like protein (ARF/ARL) family of GTPases, which are involved in membrane transport, organelle integrity, membrane lipid modification and cytoskeletal dynamics, was shown to be targeted to mitochondria with altered mitochondrial membrane potential where it affected mitochondrial morphology (LI *et al.* 2012). This represents a potential mechanism linking loss of mtDNA and the resulting decreased membrane potential with alterations in mitcochondrial morphology.

The TOR pathway is a regulator of autophagy. Autophagy is a response mechanism which is activated in stress conditions, such as starvation, to recover cellular nutrients. TOR complex 1 (mTORC1) inhibits autophagy by interacting with Atg13 (KAMADA *et al.* 2000). Furthermore activation of PI3K can suppress autophagy in *C. elegans*, mammalian cells and human tissue culture cells (MELENDEZ *et al.* 2003; PETIOT *et al.* 2000; SEGLEN and BOHLEY 1992). It has also been shown that the PI3K pathway is linked with programmed autophagy (which is followed by cell death for tissue remodelling) in the *Drosophila* fat body, such that downregulation of PI3K by ecdysone signalling results in induction of programmed autophagy (RUSTEN *et al.* 2004). Approximately 20 ATG genes (autophagy related genes) have been identified in yeast (KLIONSKY *et al.* 2003). It has been also been reported that overexpression of *Atg1* is sufficient to induce autophagy in flies and this inhibits cell growth (SCOTT *et al.* 2007). In the same study, *Atg1* expression was also shown to result in negative

regulation of TOR activity. Interestingly, it has been shown that increased autophagy promotes synapse development in flies (SHEN and GANETZKY 2009). In my experiments overexpression of *Atg1* in motoneurons resulted in more, but smaller boutons. It would be interesting to see what effect inhibition of autophagy has on the mitochondrial and motoneuron developmental defects caused by overexpression of *TFAM* or *mitoXhoI*.

Strong mitochondrial depletion at synapses could also result from a reduction in mitochondrial biogenesis. PGC-1α is the main regulator of mitochondrial biogenesis in vertebrates and *PGC-1α* -overexpression in mouse skeletal muscle and heart increases mitochondrial biogenesis and mitochondrial function (LEHMAN *et al.* 2000; WENZ *et al.* 2008). It has been shown that overexpression of *PGC-1α* in mtDNA mutator mice (which express a proofreading deficient version of Polγ), results in increased mitochondrial biogenesis, which can ameliorate the skeletal and heart phenotypes without decreasing (even slightly increases) the accumulation of mtDNA mutations (DILLON *et al.* 2012). The PGC-1α homologue in *Drosophila* is Spargel and it has been shown that Spargel regulates mitochondrial activity, cell growth and transcription in response to insulin signalling in the *Drosophila* fat body (TIEFENBOCK *et al.* 2010). Loss of mtDNA in motoneurons may activate a retrograde signal to the nucleus to down regulate Spargel expression and reduce mitochondrial biogenesis. Mitochondrial-to-nuclear retrograde signalling has not been widely studied in *Drosophila*. However in *C. elegans* the unfolded protein response (UPR) is a well characterised mechanism in which abnormalities in protein folding in mitochondrial matrix cause signalling to the nucleus that regulates the expression of nuclear encoded mitochondrial genes (HAYNES and RON 2010). It would thus be

interesting to analyse the expression of *Spargel* and other genes involved in mitochondrial biogenesis in motoneurons overexpressing *TFAM* or *mitoXhoI*.

Although I have discussed them separately the bouton size, active zone and mitochondrial phenotypes caused by loss of mtDNA in motoneurons are likely to be linked by common mechanisms. In the model I have proposed mitochondrial dysfunction is linked to bouton size regulation through the TOR pathway (Figure 6.1). However, as discussed above, TOR signalling regulates autophagy and so inhibition of TOR signalling by mtDNA loss could then activate autophagy, resulting in the degradation of synaptic mitochondria. Increased mitophagy may then further decrease ATP levels in a feed-forward loop that further inhibits TOR signalling. It may therefore be difficult to separate the phenotypes observed by inhibition or overexpression of regulators of these processes. However, as discussed above, analysis of the phenotype of motoneuron specific RNAi of *TFAM* suggests that synaptic mitochondrial depletion may be the primary driver of the motoneuron dysfunction resulting from mtDNA loss.

7.5 Conclusion and Future Directions

I have developed a *Drosophila* model for studying mtDNA depletion in motoneurons via manipulation of *TFAM* levels. In summary, the phenotypes observed upon mtDNA depletion were reduced motor function, mitochondrial depletion at synapses and axons and synaptic developmental defects. Similar phenotypes were observed by depletion of mtDNA levels using a mitochondrially targeted restriction enzyme.

These phenotypes may represent the initial pathological consequences of mtDNA loss in neurodegenerative disease. Application of other techniques such as electron microscopy and electrophysiology, (both of which are ongoing in the lab or through collaborations), will further our understanding of the consequences of mtDNA loss in neurons. Investigation of the TOR pathway and autophagy machinery are suggested as a potential mechanistic route by which mtDNA loss causes the motoneuron development phenotypes I observed. My results have suggested a number of experiments which will help to further our understanding of the consequences of neuronal mtDNA loss. In future this understanding may lead to therapeutic approaches to treat mitochondrial dysfunction in neurodegenerative disease.

Chapter 8. REFERENCES

AGOSTINO, A., L. VALLETTA, P. F. CHINNERY, G. FERRARI, F. CARRARA *et al.*, 2003 Mutations of ANT1, Twinkle, and POLG1 in sporadic progressive external ophthalmoplegia (PEO). Neurology **60:** 1354-1356.

ALAM, T. I., T. KANKI, T. MUTA, K. UKAJI, Y. ABE *et al.*, 2003 Human mitochondrial DNA is packaged with TFAM. Nucleic Acids Res **31:** 1640-1645.

ALAVI, M. V., S. BETTE, S. SCHIMPF, F. SCHUETTAUF, U. SCHRAERMEYER *et al.*, 2007 A splice site mutation in the murine Opa1 gene features pathology of autosomal dominant optic atrophy. Brain **130:** 1029-1042.

ALEXANDER, C., M. VOTRUBA, U. E. PESCH, D. L. THISELTON, S. MAYER *et al.*, 2000 OPA1, encoding a dynamin-related GTPase, is mutated in autosomal dominant optic atrophy linked to chromosome 3q28. Nat Genet **26:** 211-215.

ANDERSON, S., A. T. BANKIER, B. G. BARRELL, M. H. DE BRUIJN, A. R. COULSON *et al.*, 1981 Sequence and organization of the human mitochondrial genome. Nature **290:** 457-465.

ANDREWS, R. M., I. KUBACKA, P. F. CHINNERY, R. N. LIGHTOWLERS, D. M. TURNBULL *et al.*, 1999 Reanalysis and revision of the Cambridge reference sequence for human mitochondrial DNA. Nat Genet **23:** 147.

ANDREYEV, A. Y., Y. E. KUSHNAREVA and A. A. STARKOV, 2005 Mitochondrial metabolism of reactive oxygen species. Biochemistry (Mosc) **70:** 200-214.

ARNOULT, D., N. RISMANCHI, A. GRODET, R. G. ROBERTS, D. P. SEEBURG *et al.*, 2005 Bax/Bak-dependent release of DDP/TIMM8a promotes Drp1-mediated mitochondrial fission and mitoptosis during programmed cell death. Curr Biol **15:** 2112-2118.

BALLARD, J. W., R. G. MELVIN, J. T. MILLER and S. D. KATEWA, 2007 Sex differences in survival and mitochondrial bioenergetics during aging in Drosophila. Aging Cell **6:** 699-708.

BANOVIC, D., O. KHORRAMSHAHI, D. OWALD, C. WICHMANN, T. RIEDT *et al.*, 2010 Drosophila neuroligin 1 promotes growth and postsynaptic differentiation at glutamatergic neuromuscular junctions. Neuron **66:** 724-738.

BAQRI, R. M., B. A. TURNER, M. B. RHEUBEN, B. D. HAMMOND, L. S. KAGUNI *et al.*, 2009 Disruption of Mitochondrial DNA Replication in Drosophila Increases Mitochondrial Fast Axonal Transport In Vivo. PLoS One **4:** e7874.

BATEMAN, J. M., M. IACOVINO, P. S. PERLMAN and R. A. BUTOW, 2002a Mitochondrial DNA instability mutants of the bifunctional protein Ilv5p have altered organization in mitochondria and are targeted for degradation by Hsp78 and the Pim1p protease. J Biol Chem **277:** 47946-47953.

BATEMAN, J. M., P. S. PERLMAN and R. A. BUTOW, 2002b Mutational bisection of the mitochondrial DNA stability and amino acid biosynthetic functions of ilv5p of budding yeast. Genetics **161:** 1043-1052.

BENDER, A., K. J. KRISHNAN, C. M. MORRIS, G. A. TAYLOR, A. K. REEVE *et al.*, 2006 High levels of mitochondrial DNA deletions in substantia nigra neurons in aging and Parkinson disease. Nat Genet **38:** 515-517.

BENDER, A., R. M. SCHWARZKOPF, A. MCMILLAN, K. J. KRISHNAN, G. RIEDER *et al.*, 2008 Dopaminergic midbrain neurons are the prime target for mitochondrial DNA deletions. J Neurol **255:** 1231-1235.

BENNETT, M. C., G. W. MLADY, Y. H. KWON and G. M. ROSE, 1996 Chronic in vivo sodium azide infusion induces selective and stable inhibition of cytochrome c oxidase. J Neurochem **66:** 2606-2611.

BENSCH, K. G., J. L. MOTT, S. W. CHANG, P. A. HANSEN, M. A. MOXLEY *et al.*, 2009 Selective mtDNA mutation accumulation results in beta-cell apoptosis and diabetes development. Am J Physiol Endocrinol Metab **296:** E672-680.

BEREITER-HAHN, J., 1990 Behavior of mitochondria in the living cell. Int Rev Cytol **122:** 1-63.

BETTS, J., R. N. LIGHTOWLERS and D. M. TURNBULL, 2004 Neuropathological aspects of mitochondrial DNA disease. Neurochem Res **29:** 505-511.

BOEKEMA, E. J., and H. P. BRAUN, 2007 Supramolecular structure of the mitochondrial oxidative phosphorylation system. J Biol Chem **282:** 1-4.

BOGENHAGEN, D. F., and D. A. CLAYTON, 2003a Concluding remarks: The mitochondrial DNA replication bubble has not burst. Trends Biochem Sci **28:** 404-405.

BOGENHAGEN, D. F., and D. A. CLAYTON, 2003b The mitochondrial DNA replication bubble has not burst. Trends Biochem Sci **28:** 357-360.

BOGENHAGEN, D. F., Y. WANG, E. L. SHEN and R. KOBAYASHI, 2003 Protein components of mitochondrial DNA nucleoids in higher eukaryotes. Mol Cell Proteomics **2:** 1205-1216.

BOORE, J. L., 1999 Animal mitochondrial genomes. Nucleic Acids Res **27:** 1767-1780.

BORNSTEIN, B., E. AREA, K. M. FLANIGAN, J. GANESH, P. JAYAKAR *et al.*, 2008 Mitochondrial DNA depletion syndrome due to mutations in the RRM2B gene. Neuromuscul Disord **18:** 453-459.

BOSSY-WETZEL, E., A. PETRILLI and A. B. KNOTT, 2008 Mutant huntingtin and mitochondrial dysfunction. Trends Neurosci **31:** 609-616.

BOURDON, A., L. MINAI, V. SERRE, J. P. JAIS, E. SARZI *et al.*, 2007 Mutation of RRM2B, encoding p53-controlled ribonucleotide reductase (p53R2), causes severe mitochondrial DNA depletion. Nat Genet **39:** 776-780.

BRAND, A. H., and N. PERRIMON, 1993 Targeted gene expression as a means of altering cell fates and generating dominant phenotypes. Development **118:** 401-415.

BREUER, M. E., W. J. KOOPMAN, S. KOENE, M. NOOTEBOOM, R. J. RODENBURG *et al.*, 2012 The role of mitochondrial OXPHOS dysfunction in the development of neurologic diseases. Neurobiol Dis.

BREWER, B. J., and W. L. FANGMAN, 1987 The localization of replication origins on ARS plasmids in S. cerevisiae. Cell **51:** 463-471.

BROWN, T. A., A. N. TKACHUK, G. SHTENGEL, B. G. KOPEK, D. F. BOGENHAGEN *et al.*, 2011 Superresolution fluorescence imaging of mitochondrial nucleoids reveals their spatial range, limits, and membrane interaction. Mol Cell Biol **31:** 4994-5010.

BUNN, C. L., D. C. WALLACE and J. M. EISENSTADT, 1974 Cytoplasmic inheritance of chloramphenicol resistance in mouse tissue culture cells. Proc Natl Acad Sci U S A **71:** 1681-1685.

CAI, Q., C. GERWIN and Z. H. SHENG, 2005 Syntabulin-mediated anterograde transport of mitochondria along neuronal processes. J Cell Biol **170:** 959-969.

CALVO, S. E., and V. K. MOOTHA, 2010 The mitochondrial proteome and human disease. Annu Rev Genomics Hum Genet **11:** 25-44.

CAMPBELL, C. T., J. E. KOLESAR and B. A. KAUFMAN, 2012a Mitochondrial transcription factor A regulates mitochondrial transcription initiation, DNA packaging, and genome copy number. Biochim Biophys Acta.

CAMPBELL, G. R., Y. KRAYTSBERG, K. J. KRISHNAN, N. OHNO, I. ZIABREVA *et al.*, 2012b Clonally expanded mitochondrial DNA deletions within the choroid plexus in multiple sclerosis. Acta Neuropathol **124:** 209-220.

CAPDEVILA, J., and I. GUERRERO, 1994 Targeted expression of the signaling molecule decapentaplegic induces pattern duplications and growth alterations in Drosophila wings. EMBO J **13:** 4459-4468.

CARRASCO, D. I., E. K. BICHLER, M. M. RICH, X. WANG, K. L. SEBURN *et al.*, 2012 Motor terminal degeneration unaffected by activity changes in SOD1(G93A) mice; a possible role for glycolysis. Neurobiol Dis **48:** 132-140.

CARTONI, R., B. LEGER, M. B. HOCK, M. PRAZ, A. CRETTENAND *et al.*, 2005 Mitofusins 1/2 and ERRalpha expression are increased in human skeletal muscle after physical exercise. J Physiol **567:** 349-358.

CHANG, D. T., G. L. RINTOUL, S. PANDIPATI and I. J. REYNOLDS, 2006 Mutant huntingtin aggregates impair mitochondrial movement and trafficking in cortical neurons. Neurobiol Dis **22:** 388-400.

CHEN, H., and D. C. CHAN, 2005 Emerging functions of mammalian mitochondrial fusion and fission. Hum Mol Genet **14 Spec No. 2:** R283-289.

CHEN, H., and D. C. CHAN, 2009 Mitochondrial dynamics--fusion, fission, movement, and mitophagy--in neurodegenerative diseases. Hum Mol Genet **18:** R169-176.

CHEN, H., S. A. DETMER, A. J. EWALD, E. E. GRIFFIN, S. E. FRASER *et al.*, 2003 Mitofusins Mfn1 and Mfn2 coordinately regulate mitochondrial fusion and are essential for embryonic development. J Cell Biol **160:** 189-200.

CHEN, H., J. M. MCCAFFERY and D. C. CHAN, 2007 Mitochondrial fusion protects against neurodegeneration in the cerebellum. Cell **130:** 548-562.

CHEN, H., M. VERMULST, Y. E. WANG, A. CHOMYN, T. A. PROLLA *et al.*, 2010 Mitochondrial fusion is required for mtDNA stability in skeletal muscle and tolerance of mtDNA mutations. Cell **141:** 280-289.

CHEN, K. F., N. PESCHEL, R. ZAVODSKA, H. SEHADOVA and R. STANEWSKY, 2011 QUASIMODO, a Novel GPI-anchored zona pellucida protein involved in light input to the Drosophila circadian clock. Curr Biol **21:** 719-729.

CHEN, X., and B. GANETZKY, 2012 A neuropeptide signaling pathway regulates synaptic growth in Drosophila. J Cell Biol **196:** 529-543.

CHEN, X. J., and R. A. BUTOW, 2005 The organization and inheritance of the mitochondrial genome. Nat Rev Genet **6:** 815-825.

CHEN, Y. C., E. B. TAYLOR, N. DEPHOURE, J. M. HEO, A. TONHATO *et al.*, 2012 Identification of a protein mediating respiratory supercomplex stability. Cell Metab **15:** 348-360.

CHENG, L., C. LOCKE and G. W. DAVIS, 2011 S6 kinase localizes to the presynaptic active zone and functions with PDK1 to control synapse development. J Cell Biol **194:** 921-935.

CHINNERY, P. F., S. DIMAURO, S. SHANSKE, E. A. SCHON, M. ZEVIANI *et al.*, 2004 Risk of developing a mitochondrial DNA deletion disorder. Lancet **364:** 592-596.

CHINNERY, P. F., and M. ZEVIANI, 2008 155th ENMC workshop: polymerase gamma and disorders of mitochondrial DNA synthesis, 21-23 September 2007, Naarden, The Netherlands. Neuromuscul Disord **18:** 259-267.

CHO, D. H., T. NAKAMURA and S. A. LIPTON, 2010 Mitochondrial dynamics in cell death and neurodegeneration. Cell Mol Life Sci **67:** 3435-3447.
CIPOLAT, S., O. MARTINS DE BRITO, B. DAL ZILIO and L. SCORRANO, 2004 OPA1 requires mitofusin 1 to promote mitochondrial fusion. Proc Natl Acad Sci U S A **101:** 15927-15932.
CLARK, I. E., M. W. DODSON, C. JIANG, J. H. CAO, J. R. HUH *et al.*, 2006 Drosophila pink1 is required for mitochondrial function and interacts genetically with parkin. Nature **441:** 1162-1166.
CLAYTON, D. A., 1982 Replication of animal mitochondrial DNA. Cell **28:** 693-705.
CLAYTON, D. A., and J. VINOGRAD, 1967 Circular dimer and catenate forms of mitochondrial DNA in human leukaemic leucocytes. Nature **216:** 652-657.
COLIN, E., D. ZALA, G. LIOT, H. RANGONE, M. BORRELL-PAGES *et al.*, 2008 Huntingtin phosphorylation acts as a molecular switch for anterograde/retrograde transport in neurons. EMBO J **27:** 2124-2134.
CONNOLLY, J. B., I. J. ROBERTS, J. D. ARMSTRONG, K. KAISER, M. FORTE *et al.*, 1996 Associative learning disrupted by impaired Gs signaling in Drosophila mushroom bodies. Science **274:** 2104-2107.
COPELAND, W. C., 2008 Inherited mitochondrial diseases of DNA replication. Annu Rev Med **59:** 131-146.
CORRAL-DEBRINSKI, M., T. HORTON, M. T. LOTT, J. M. SHOFFNER, M. F. BEAL *et al.*, 1992a Mitochondrial DNA deletions in human brain: regional variability and increase with advanced age. Nat Genet **2:** 324-329.
CORRAL-DEBRINSKI, M., J. M. SHOFFNER, M. T. LOTT and D. C. WALLACE, 1992b Association of mitochondrial DNA damage with aging and coronary atherosclerotic heart disease. Mutat Res **275:** 169-180.
COSKUN, P., J. WYREMBAK, S. E. SCHRINER, H. W. CHEN, C. MARCINIACK *et al.*, 2012 A mitochondrial etiology of Alzheimer and Parkinson disease. Biochim Biophys Acta **1820:** 553-564.
COSTA-MATTIOLI, M., W. S. SOSSIN, E. KLANN and N. SONENBERG, 2009 Translational control of long-lasting synaptic plasticity and memory. Neuron **61:** 10-26.
COTTRELL, D. A., E. L. BLAKELY, M. A. JOHNSON, P. G. INCE, G. M. BORTHWICK *et al.*, 2001a Cytochrome c oxidase deficient cells accumulate in the hippocampus and choroid plexus with age. Neurobiol Aging **22:** 265-272.
COTTRELL, D. A., E. L. BLAKELY, M. A. JOHNSON, P. G. INCE and D. M. TURNBULL, 2001b Mitochondrial enzyme-deficient hippocampal neurons and choroidal cells in AD. Neurology **57:** 260-264.
CRITTENDEN, J. R., E. M. SKOULAKIS, K. A. HAN, D. KALDERON and R. L. DAVIS, 1998 Tripartite mushroom body architecture revealed by antigenic markers. Learn Mem **5:** 38-51.
CUMMINGS, D. J., 1992 Mitochondrial genomes of the ciliates. Int Rev Cytol **141:** 1-64.
DAGDA, R. K., and C. T. CHU, 2009 Mitochondrial quality control: insights on how Parkinson's disease related genes PINK1, parkin, and Omi/HtrA2 interact to maintain mitochondrial homeostasis. J Bioenerg Biomembr **41:** 473-479.
DAIRAGHI, D. J., G. S. SHADEL and D. A. CLAYTON, 1995 Addition of a 29 residue carboxyl-terminal tail converts a simple HMG box-containing protein into a transcriptional activator. J Mol Biol **249:** 11-28.
DALLABONA, C., R. M. MARSANO, P. ARZUFFI, D. GHEZZI, P. MANCINI *et al.*, 2010 Sym1, the yeast ortholog of the MPV17 human disease protein, is a stress-

induced bioenergetic and morphogenetic mitochondrial modulator. Hum Mol Genet **19:** 1098-1107.

DAVIES, V. J., A. J. HOLLINS, M. J. PIECHOTA, W. YIP, J. R. DAVIES *et al.*, 2007 Opa1 deficiency in a mouse model of autosomal dominant optic atrophy impairs mitochondrial morphology, optic nerve structure and visual function. Hum Mol Genet **16:** 1307-1318.

DELETTRE, C., G. LENAERS, J. M. GRIFFOIN, N. GIGAREL, C. LORENZO *et al.*, 2000 Nuclear gene OPA1, encoding a mitochondrial dynamin-related protein, is mutated in dominant optic atrophy. Nat Genet **26:** 207-210.

DENG, H., M. W. DODSON, H. HUANG and M. GUO, 2008 The Parkinson's disease genes pink1 and parkin promote mitochondrial fission and/or inhibit fusion in Drosophila. Proc Natl Acad Sci U S A **105:** 14503-14508.

DETMER, S. A., and D. C. CHAN, 2007 Functions and dysfunctions of mitochondrial dynamics. Nat Rev Mol Cell Biol **8:** 870-879.

DI RE, M., H. SEMBONGI, J. HE, A. REYES, T. YASUKAWA *et al.*, 2009 The accessory subunit of mitochondrial DNA polymerase gamma determines the DNA content of mitochondrial nucleoids in human cultured cells. Nucleic Acids Res **37:** 5701-5713.

DIAZ, F., M. P. BAYONA-BAFALUY, M. RANA, M. MORA, H. HAO *et al.*, 2002 Human mitochondrial DNA with large deletions repopulates organelles faster than full-length genomes under relaxed copy number control. Nucleic Acids Res **30:** 4626-4633.

DILLON, L. M., S. L. WILLIAMS, A. HIDA, J. D. PEACOCK, T. A. PROLLA *et al.*, 2012 Increased mitochondrial biogenesis in muscle improves aging phenotypes in the mtDNA mutator mouse. Hum Mol Genet **21:** 2288-2297.

DIMAURO, S., and E. A. SCHON, 2003 Mitochondrial respiratory-chain diseases. N Engl J Med **348:** 2656-2668.

DODSON, M. W., and M. GUO, 2007 Pink1, Parkin, DJ-1 and mitochondrial dysfunction in Parkinson's disease. Curr Opin Neurobiol **17:** 331-337.

DU, H., L. GUO, S. YAN, A. A. SOSUNOV, G. M. MCKHANN *et al.*, 2010 Early deficits in synaptic mitochondria in an Alzheimer's disease mouse model. Proc Natl Acad Sci U S A **107:** 18670-18675.

DUBEC, S. J., R. AURORA and H. P. ZASSENHAUS, 2008 Mitochondrial DNA mutations may contribute to aging via cell death caused by peptides that induce cytochrome c release. Rejuvenation Res **11:** 611-619.

EKSTRAND, M. I., M. FALKENBERG, A. RANTANEN, C. B. PARK, M. GASPARI *et al.*, 2004 Mitochondrial transcription factor A regulates mtDNA copy number in mammals. Hum Mol Genet **13:** 935-944.

EKSTRAND, M. I., M. TERZIOGLU, D. GALTER, S. ZHU, C. HOFSTETTER *et al.*, 2007 Progressive parkinsonism in mice with respiratory-chain-deficient dopamine neurons. Proc Natl Acad Sci U S A **104:** 1325-1330.

ELPELEG, O., C. MILLER, E. HERSHKOVITZ, M. BITNER-GLINDZICZ, G. BONDI-RUBINSTEIN *et al.*, 2005 Deficiency of the ADP-forming succinyl-CoA synthase activity is associated with encephalomyopathy and mitochondrial DNA depletion. Am J Hum Genet **76:** 1081-1086.

ELSON, J. L., D. C. SAMUELS, D. M. TURNBULL and P. F. CHINNERY, 2001 Random intracellular drift explains the clonal expansion of mitochondrial DNA mutations with age. Am J Hum Genet **68:** 802-806.

ERNSTER, L., and G. SCHATZ, 1981 Mitochondria: a historical review. J Cell Biol **91:** 227s-255s.

EXNER, N., B. TRESKE, D. PAQUET, K. HOLMSTROM, C. SCHIESLING *et al.*, 2007 Loss-of-function of human PINK1 results in mitochondrial pathology and can be rescued by parkin. J Neurosci **27:** 12413-12418.

FALKENBERG, M., M. GASPARI, A. RANTANEN, A. TRIFUNOVIC, N. G. LARSSON *et al.*, 2002 Mitochondrial transcription factors B1 and B2 activate transcription of human mtDNA. Nat Genet **31:** 289-294.

FALKENBERG, M., N. G. LARSSON and C. M. GUSTAFSSON, 2007 DNA replication and transcription in mammalian mitochondria. Annu Rev Biochem **76:** 679-699.

FANNIN, S. W., E. J. LESNEFSKY, T. J. SLABE, M. O. HASSAN and C. L. HOPPEL, 1999 Aging selectively decreases oxidative capacity in rat heart interfibrillar mitochondria. Arch Biochem Biophys **372:** 399-407.

FARR, C. L., Y. MATSUSHIMA, A. T. LAGINA, 3RD, N. LUO and L. S. KAGUNI, 2004 Physiological and biochemical defects in functional interactions of mitochondrial DNA polymerase and DNA-binding mutants of single-stranded DNA-binding protein. J Biol Chem **279:** 17047-17053.

FAYET, G., M. JANSSON, D. STERNBERG, A. R. MOSLEMI, P. BLONDY *et al.*, 2002 Ageing muscle: clonal expansions of mitochondrial DNA point mutations and deletions cause focal impairment of mitochondrial function. Neuromuscul Disord **12:** 484-493.

FERNANDEZ-VIZARRA, E., V. TIRANTI and M. ZEVIANI, 2009 Assembly of the oxidative phosphorylation system in humans: what we have learned by studying its defects. Biochim Biophys Acta **1793:** 200-211.

FISHER, R. P., T. LISOWSKY, M. A. PARISI and D. A. CLAYTON, 1992 DNA wrapping and bending by a mitochondrial high mobility group-like transcriptional activator protein. J Biol Chem **267:** 3358-3367.

FISHER, R. P., M. A. PARISI and D. A. CLAYTON, 1989 Flexible recognition of rapidly evolving promoter sequences by mitochondrial transcription factor 1. Genes Dev **3:** 2202-2217.

FLEMING, J. E., H. A. LEON and J. MIQUEL, 1981 Effects of ethidium bromide on development and aging of Drosophila: implications for the free radical theory of aging. Exp Gerontol **16:** 287-293.

FREISINGER, P., N. FUTTERER, E. LANKES, K. GEMPEL, T. M. BERGER *et al.*, 2006 Hepatocerebral mitochondrial DNA depletion syndrome caused by deoxyguanosine kinase (DGUOK) mutations. Arch Neurol **63:** 1129-1134.

FREY, D., C. SCHNEIDER, L. XU, J. BORG, W. SPOOREN *et al.*, 2000 Early and selective loss of neuromuscular synapse subtypes with low sprouting competence in motoneuron diseases. J Neurosci **20:** 2534-2542.

FUKUHARA, H., and C. KUJAWA, 1970 Selective inhibition of the in vivo transcription of mitochondrial DNA by ethidium bromide and by acriflavin. Biochem Biophys Res Commun **41:** 1002-1008.

FUKUI, H., and C. T. MORAES, 2009 Mechanisms of formation and accumulation of mitochondrial DNA deletions in aging neurons. Hum Mol Genet **18:** 1028-1036.

GARRIDO, N., L. GRIPARIC, E. JOKITALO, J. WARTIOVAARA, A. M. VAN DER BLIEK *et al.*, 2003 Composition and dynamics of human mitochondrial nucleoids. Mol Biol Cell **14:** 1583-1596.

GASPARI, M., M. FALKENBERG, N. G. LARSSON and C. M. GUSTAFSSON, 2004 The mitochondrial RNA polymerase contributes critically to promoter specificity in mammalian cells. EMBO J **23:** 4606-4614.

GILKERSON, R. W., E. A. SCHON, E. HERNANDEZ and M. M. DAVIDSON, 2008 Mitochondrial nucleoids maintain genetic autonomy but allow for functional complementation. J Cell Biol **181:** 1117-1128.

GOFFART, S., H. M. COOPER, H. TYYNISMAA, S. WANROOIJ, A. SUOMALAINEN *et al.*, 2009 Twinkle mutations associated with autosomal dominant progressive external ophthalmoplegia lead to impaired helicase function and in vivo mtDNA replication stalling. Hum Mol Genet **18:** 328-340.

GOMES, L. C., G. DI BENEDETTO and L. SCORRANO, 2011 During autophagy mitochondria elongate, are spared from degradation and sustain cell viability. Nat Cell Biol **13:** 589-598.

GOOD, C. H., A. F. HOFFMAN, B. J. HOFFER, V. I. CHEFER, T. S. SHIPPENBERG *et al.*, 2011 Impaired nigrostriatal function precedes behavioral deficits in a genetic mitochondrial model of Parkinson's disease. FASEB J **25:** 1333-1344.

GORSKA-ANDRZEJAK, J., R. S. STOWERS, J. BORYCZ, R. KOSTYLEVA, T. L. SCHWARZ *et al.*, 2003 Mitochondria are redistributed in Drosophila photoreceptors lacking milton, a kinesin-associated protein. J Comp Neurol **463:** 372-388.

GOTO, A., Y. MATSUSHIMA, T. KADOWAKI and Y. KITAGAWA, 2001 Drosophila mitochondrial transcription factor A (d-TFAM) is dispensable for the transcription of mitochondrial DNA in Kc167 cells. Biochem J **354:** 243-248.

GOTO, Y., I. NONAKA and S. HORAI, 1990 A mutation in the tRNA(Leu)(UUR) gene associated with the MELAS subgroup of mitochondrial encephalomyopathies. Nature **348:** 651-653.

GRAY, M. W., G. BURGER and B. F. LANG, 1999 Mitochondrial evolution. Science **283:** 1476-1481.

GRAZIEWICZ, M. A., M. J. LONGLEY and W. C. COPELAND, 2006 DNA polymerase gamma in mitochondrial DNA replication and repair. Chem Rev **106:** 383-405.

GREAVES, L. C., A. K. REEVE, R. W. TAYLOR and D. M. TURNBULL, 2012 Mitochondrial DNA and disease. J Pathol **226:** 274-286.

GREENE, J. C., A. J. WHITWORTH, I. KUO, L. A. ANDREWS, M. B. FEANY *et al.*, 2003 Mitochondrial pathology and apoptotic muscle degeneration in Drosophila parkin mutants. Proc Natl Acad Sci U S A **100:** 4078-4083.

GUO, X., G. T. MACLEOD, A. WELLINGTON, F. HU, S. PANCHUMARTHI *et al.*, 2005 The GTPase dMiro is required for axonal transport of mitochondria to Drosophila synapses. Neuron **47:** 379-393.

HAKONEN, A. H., S. HEISKANEN, V. JUVONEN, I. LAPPALAINEN, P. T. LUOMA *et al.*, 2005 Mitochondrial DNA polymerase W748S mutation: a common cause of autosomal recessive ataxia with ancient European origin. Am J Hum Genet **77:** 430-441.

HAKONEN, A. H., P. ISOHANNI, A. PAETAU, R. HERVA, A. SUOMALAINEN *et al.*, 2007 Recessive Twinkle mutations in early onset encephalopathy with mtDNA depletion. Brain **130:** 3032-3040.

HALLBERG, B. M., and N. G. LARSSON, 2011 TFAM forces mtDNA to make a U-turn. Nat Struct Mol Biol **18:** 1179-1181.

HANCE, N., M. I. EKSTRAND and A. TRIFUNOVIC, 2005 Mitochondrial DNA polymerase gamma is essential for mammalian embryogenesis. Hum Mol Genet **14:** 1775-1783.

HARDIE, D. G., F. A. ROSS and S. A. HAWLEY, 2012 AMPK: a nutrient and energy sensor that maintains energy homeostasis. Nat Rev Mol Cell Biol **13:** 251-262.

HARMAN, D., 1972 The biologic clock: the mitochondria? J Am Geriatr Soc **20:** 145-147.

HARTMANN, N., K. REICHWALD, I. WITTIG, S. DROSE, S. SCHMEISSER *et al.*, 2011 Mitochondrial DNA copy number and function decrease with age in the short-lived fish Nothobranchius furzeri. Aging Cell **10:** 824-831.

HATEFI, Y., 1985 The mitochondrial electron transport and oxidative phosphorylation system. Annu Rev Biochem **54:** 1015-1069.

HAYNES, C. M., and D. RON, 2010 The mitochondrial UPR - protecting organelle protein homeostasis. J Cell Sci **123:** 3849-3855.

HE, C., and D. J. KLIONSKY, 2009 Regulation mechanisms and signaling pathways of autophagy. Annu Rev Genet **43:** 67-93.

HERMANN, G. J., J. W. THATCHER, J. P. MILLS, K. G. HALES, M. T. FULLER *et al.*, 1998 Mitochondrial fusion in yeast requires the transmembrane GTPase Fzo1p. J Cell Biol **143:** 359-373.

HOANG, B., and A. CHIBA, 2001 Single-cell analysis of Drosophila larval neuromuscular synapses. Dev Biol **229:** 55-70.

HOEFFER, C. A., and E. KLANN, 2010 mTOR signaling: at the crossroads of plasticity, memory and disease. Trends Neurosci **33:** 67-75.

HOLLENBECK, P. J., and W. M. SAXTON, 2005 The axonal transport of mitochondria. J Cell Sci **118:** 5411-5419.

HOLT, I. J., A. E. HARDING and J. A. MORGAN-HUGHES, 1988 Deletions of muscle mitochondrial DNA in patients with mitochondrial myopathies. Nature **331:** 717-719.

HOLT, I. J., H. E. LORIMER and H. T. JACOBS, 2000 Coupled leading- and lagging-strand synthesis of mammalian mitochondrial DNA. Cell **100:** 515-524.

HORIUCHI, D., R. V. BARKUS, A. D. PILLING, A. GASSMAN and W. M. SAXTON, 2005 APLIP1, a kinesin binding JIP-1/JNK scaffold protein, influences the axonal transport of both vesicles and mitochondria in Drosophila. Curr Biol **15:** 2137-2141.

HOWELL, N., L. A. BINDOFF, D. A. MCCULLOUGH, I. KUBACKA, J. POULTON *et al.*, 1991 Leber hereditary optic neuropathy: identification of the same mitochondrial ND1 mutation in six pedigrees. Am J Hum Genet **49:** 939-950.

HUDSON, G., and P. F. CHINNERY, 2006 Mitochondrial DNA polymerase-gamma and human disease. Hum Mol Genet **15 Spec No 2:** R244-252.

HUMPHREY, D. M., R. B. PARSONS, Z. N. LUDLOW, T. RIEMENSPERGER, G. ESPOSITO *et al.*, 2012 Alternative oxidase rescues mitochondria-mediated dopaminergic cell loss in Drosophila. Hum Mol Genet.

IACOVINO, M., C. GRANYCOME, H. SEMBONGI, M. BOKORI-BROWN, R. A. BUTOW *et al.*, 2009 The conserved translocase Tim17 prevents mitochondrial DNA loss. Hum Mol Genet **18:** 65-74.

IBORRA, F. J., H. KIMURA and P. R. COOK, 2004 The functional organization of mitochondrial genomes in human cells. BMC Biol **2:** 9.

IKEUCHI, M., H. MATSUSAKA, D. KANG, S. MATSUSHIMA, T. IDE *et al.*, 2005 Overexpression of mitochondrial transcription factor a ameliorates mitochondrial deficiencies and cardiac failure after myocardial infarction. Circulation **112:** 683-690.

INOUE, K., K. NAKADA, A. OGURA, K. ISOBE, Y. GOTO *et al.*, 2000 Generation of mice with mitochondrial dysfunction by introducing mouse mtDNA carrying a deletion into zygotes. Nat Genet **26:** 176-181.

ITOH, K., S. WEIS, P. MEHRAEIN and J. MULLER-HOCKER, 1996 Cytochrome c oxidase defects of the human substantia nigra in normal aging. Neurobiol Aging **17:** 843-848.

IYENGAR, B., N. LUO, C. L. FARR, L. S. KAGUNI and A. R. CAMPOS, 2002 The accessory subunit of DNA polymerase gamma is essential for mitochondrial DNA maintenance and development in Drosophila melanogaster. Proc Natl Acad Sci U S A **99:** 4483-4488.

IYENGAR, B., J. ROOTE and A. R. CAMPOS, 1999 The tamas gene, identified as a mutation that disrupts larval behavior in Drosophila melanogaster, codes for the mitochondrial DNA polymerase catalytic subunit (DNApol-gamma125). Genetics **153:** 1809-1824.

JAN, L. Y., and Y. N. JAN, 1982 Antibodies to horseradish peroxidase as specific neuronal markers in Drosophila and in grasshopper embryos. Proc Natl Acad Sci U S A **79:** 2700-2704.

JOHANSSON, M., A. R. VAN ROMPAY, B. DEGREVE, J. BALZARINI and A. KARLSSON, 1999 Cloning and characterization of the multisubstrate deoxyribonucleoside kinase of Drosophila melanogaster. J Biol Chem **274:** 23814-23819.

JOHNS, D. R., M. J. NEUFELD and R. D. PARK, 1992 An ND-6 mitochondrial DNA mutation associated with Leber hereditary optic neuropathy. Biochem Biophys Res Commun **187:** 1551-1557.

JOHNSON, M. A., D. M. TURNBULL, D. J. DICK and H. S. SHERRATT, 1983 A partial deficiency of cytochrome c oxidase in chronic progressive external ophthalmoplegia. J Neurol Sci **60:** 31-53.

KAGUNI, L. S., 2004 DNA polymerase gamma, the mitochondrial replicase. Annu Rev Biochem **73:** 293-320.

KAMADA, Y., T. FUNAKOSHI, T. SHINTANI, K. NAGANO, M. OHSUMI *et al.*, 2000 Tor-mediated induction of autophagy via an Apg1 protein kinase complex. J Cell Biol **150:** 1507-1513.

KANE, L. A., and R. J. YOULE, 2011 PINK1 and Parkin Flag Miro to Direct Mitochondrial Traffic. Cell **147:** 721-723.

KANKI, T., and D. J. KLIONSKY, 2008 Mitophagy in yeast occurs through a selective mechanism. J Biol Chem **283:** 32386-32393.

KANKI, T., K. OHGAKI, M. GASPARI, C. M. GUSTAFSSON, A. FUKUOH *et al.*, 2004 Architectural role of mitochondrial transcription factor A in maintenance of human mitochondrial DNA. Mol Cell Biol **24:** 9823-9834.

KASASHIMA, K., M. SUMITANI and H. ENDO, 2011 Human mitochondrial transcription factor A is required for the segregation of mitochondrial DNA in cultured cells. Exp Cell Res **317:** 210-220.

KAUFMAN, B. A., N. DURISIC, J. M. MATIVETSKY, S. COSTANTINO, M. A. HANCOCK *et al.*, 2007 The mitochondrial transcription factor TFAM coordinates the assembly of multiple DNA molecules into nucleoid-like structures. Mol Biol Cell **18:** 3225-3236.

KAUFMAN, B. A., S. M. NEWMAN, R. L. HALLBERG, C. A. SLAUGHTER, P. S. PERLMAN *et al.*, 2000 In organello formaldehyde crosslinking of proteins to mtDNA: identification of bifunctional proteins. Proc Natl Acad Sci U S A **97:** 7772-7777.

KAUL, A. K., and J. M. BATEMAN, 2009 A novel RFP reporter to aid in the visualization of the eye imaginal disc in Drosophila. J Vis Exp.

KENNEDY, E. P., and A. L. LEHNINGER, 1949 Oxidation of fatty acids and tricarboxylic acid cycle intermediates by isolated rat liver mitochondria. J Biol Chem **179:** 957-972.

KESHISHIAN, H., K. BROADIE, A. CHIBA and M. BATE, 1996 The drosophila neuromuscular junction: a model system for studying synaptic development and function. Annu Rev Neurosci **19:** 545-575.

KIRBY, D. M., R. MCFARLAND, A. OHTAKE, C. DUNNING, M. T. RYAN *et al.*, 2004 Mutations of the mitochondrial ND1 gene as a cause of MELAS. J Med Genet **41:** 784-789.

KITADA, T., S. ASAKAWA, N. HATTORI, H. MATSUMINE, Y. YAMAMURA *et al.*, 1998 Mutations in the parkin gene cause autosomal recessive juvenile parkinsonism. Nature **392:** 605-608.

KLIONSKY, D. J., J. M. CREGG, W. A. DUNN, JR., S. D. EMR, Y. SAKAI *et al.*, 2003 A unified nomenclature for yeast autophagy-related genes. Dev Cell **5:** 539-545.

KNOX, S., H. GE, B. D. DIMITROFF, Y. REN, K. A. HOWE *et al.*, 2007 Mechanisms of TSC-mediated control of synapse assembly and axon guidance. PLoS One **2:** e375.

KOLLBERG, G., N. DARIN, K. BENAN, A. R. MOSLEMI, S. LINDAL *et al.*, 2009 A novel homozygous RRM2B missense mutation in association with severe mtDNA depletion. Neuromuscul Disord **19:** 147-150.

KOPEK, B. G., G. SHTENGEL, C. S. XU, D. A. CLAYTON and H. F. HESS, 2012 Correlative 3D superresolution fluorescence and electron microscopy reveal the relationship of mitochondrial nucleoids to membranes. Proc Natl Acad Sci U S A **109:** 6136-6141.

KORHONEN, J. A., M. GASPARI and M. FALKENBERG, 2003 TWINKLE Has 5' -> 3' DNA helicase activity and is specifically stimulated by mitochondrial single-stranded DNA-binding protein. J Biol Chem **278:** 48627-48632.

KORHONEN, J. A., X. H. PHAM, M. PELLEGRINI and M. FALKENBERG, 2004 Reconstitution of a minimal mtDNA replisome in vitro. EMBO J **23:** 2423-2429.

KRAYTSBERG, Y., E. KUDRYAVTSEVA, A. C. MCKEE, C. GEULA, N. W. KOWALL *et al.*, 2006 Mitochondrial DNA deletions are abundant and cause functional impairment in aged human substantia nigra neurons. Nat Genet **38:** 518-520.

KRISHNAN, K. J., L. C. GREAVES, A. K. REEVE and D. M. TURNBULL, 2007 Mitochondrial DNA mutations and aging. Ann N Y Acad Sci **1100:** 227-240.

KRISHNAN, K. J., T. E. RATNAIKE, H. L. DE GRUYTER, E. JAROS and D. M. TURNBULL, 2012 Mitochondrial DNA deletions cause the biochemical defect observed in Alzheimer's disease. Neurobiol Aging **33:** 2210-2214.

KRISHNAN, K. J., A. K. REEVE, D. C. SAMUELS, P. F. CHINNERY, J. K. BLACKWOOD *et al.*, 2008 What causes mitochondrial DNA deletions in human cells? Nat Genet **40:** 275-279.

KUJOTH, G. C., P. C. BRADSHAW, S. HAROON and T. A. PROLLA, 2007 The role of mitochondrial DNA mutations in mammalian aging. PLoS Genet **3:** e24.

KUJOTH, G. C., A. HIONA, T. D. PUGH, S. SOMEYA, K. PANZER *et al.*, 2005 Mitochondrial DNA mutations, oxidative stress, and apoptosis in mammalian aging. Science **309:** 481-484.

KUKAT, C., C. A. WURM, H. SPAHR, M. FALKENBERG, N. G. LARSSON *et al.*, 2011 Super-resolution microscopy reveals that mammalian mitochondrial nucleoids have a uniform size and frequently contain a single copy of mtDNA. Proc Natl Acad Sci U S A **108:** 13534-13539.

LANDGRAF, M., and S. THOR, 2006a Development and structure of motoneurons. Int Rev Neurobiol **75:** 33-53.
LANDGRAF, M., and S. THOR, 2006b Development of Drosophila motoneurons: specification and morphology. Semin Cell Dev Biol **17:** 3-11.
LANE, N., 2005 *Power, sex, suicide : mitochondria and the meaning of life*. Oxford University Press, Oxford ; New York.
LANG, B. F., G. BURGER, C. J. O'KELLY, R. CEDERGREN, G. B. GOLDING *et al.*, 1997 An ancestral mitochondrial DNA resembling a eubacterial genome in miniature. Nature **387:** 493-497.
LAPLANTE, M., and D. M. SABATINI, 2012 mTOR signaling in growth control and disease. Cell **149:** 274-293.
LARSSON, N. G., 2010 Somatic mitochondrial DNA mutations in mammalian aging. Annu Rev Biochem **79:** 683-706.
LARSSON, N. G., and D. A. CLAYTON, 1995 Molecular genetic aspects of human mitochondrial disorders. Annu Rev Genet **29:** 151-178.
LARSSON, N. G., J. WANG, H. WILHELMSSON, A. OLDFORS, P. RUSTIN *et al.*, 1998 Mitochondrial transcription factor A is necessary for mtDNA maintenance and embryogenesis in mice. Nat Genet **18:** 231-236.
LAUGHLIN, S. B., 2001 Energy as a constraint on the coding and processing of sensory information. Curr Opin Neurobiol **11:** 475-480.
LECRENIER, N., P. VAN DER BRUGGEN and F. FOURY, 1997 Mitochondrial DNA polymerases from yeast to man: a new family of polymerases. Gene **185:** 147-152.
LEFAI, E., M. CALLEJA, I. RUIZ DE MENA, A. T. LAGINA, 3RD, L. S. KAGUNI *et al.*, 2000 Overexpression of the catalytic subunit of DNA polymerase gamma results in depletion of mitochondrial DNA in Drosophila melanogaster. Mol Gen Genet **264:** 37-46.
LEGROS, F., F. MALKA, P. FRACHON, A. LOMBES and M. ROJO, 2004 Organization and dynamics of human mitochondrial DNA. J Cell Sci **117:** 2653-2662.
LEHMAN, J. J., P. M. BARGER, A. KOVACS, J. E. SAFFITZ, D. M. MEDEIROS *et al.*, 2000 Peroxisome proliferator-activated receptor gamma coactivator-1 promotes cardiac mitochondrial biogenesis. J Clin Invest **106:** 847-856.
LEWIS, W., B. J. DAY, J. J. KOHLER, S. H. HOSSEINI, S. S. CHAN *et al.*, 2007 Decreased mtDNA, oxidative stress, cardiomyopathy, and death from transgenic cardiac targeted human mutant polymerase gamma. Lab Invest **87:** 326-335.
LI, C. C., T. S. WU, C. F. HUANG, L. T. JANG, Y. T. LIU *et al.*, 2012 GTP-Binding-Defective ARL4D Alters Mitochondrial Morphology and Membrane Potential. PLoS One **7:** e43552.
LI, Z., K. OKAMOTO, Y. HAYASHI and M. SHENG, 2004 The importance of dendritic mitochondria in the morphogenesis and plasticity of spines and synapses. Cell **119:** 873-887.
LIEMBURG-APERS, D. C., H. IMAMURA, M. FORKINK, M. NOOTEBOOM, H. G. SWARTS *et al.*, 2011 Quantitative glucose and ATP sensing in mammalian cells. Pharm Res **28:** 2745-2757.
LIESA, M., M. PALACIN and A. ZORZANO, 2009 Mitochondrial dynamics in mammalian health and disease. Physiol Rev **89:** 799-845.
LIM, S. E., M. J. LONGLEY and W. C. COPELAND, 1999 The mitochondrial p55 accessory subunit of human DNA polymerase gamma enhances DNA binding,

promotes processive DNA synthesis, and confers N-ethylmaleimide resistance. J Biol Chem **274:** 38197-38203.

LINDER, T., C. B. PARK, J. ASIN-CAYUELA, M. PELLEGRINI, N. G. LARSSON *et al.*, 2005 A family of putative transcription termination factors shared amongst metazoans and plants. Curr Genet **48:** 265-269.

LINNANE, A. W., S. MARZUKI, T. OZAWA and M. TANAKA, 1989 Mitochondrial DNA mutations as an important contributor to ageing and degenerative diseases. Lancet **1:** 642-645.

LIU, K. S., M. SIEBERT, S. MERTEL, E. KNOCHE, S. WEGENER *et al.*, 2011 RIM-binding protein, a central part of the active zone, is essential for neurotransmitter release. Science **334:** 1565-1569.

LIU, S., T. SAWADA, S. LEE, W. YU, G. SILVERIO *et al.*, 2012 Parkinson's disease-associated kinase PINK1 regulates Miro protein level and axonal transport of mitochondria. PLoS Genet **8:** e1002537.

LONGLEY, M. J., D. NGUYEN, T. A. KUNKEL and W. C. COPELAND, 2001 The fidelity of human DNA polymerase gamma with and without exonucleolytic proofreading and the p55 accessory subunit. J Biol Chem **276:** 38555-38562.

LONGLEY, M. J., R. PRASAD, D. K. SRIVASTAVA, S. H. WILSON and W. C. COPELAND, 1998 Identification of 5'-deoxyribose phosphate lyase activity in human DNA polymerase gamma and its role in mitochondrial base excision repair in vitro. Proc Natl Acad Sci U S A **95:** 12244-12248.

LUFT, R., D. IKKOS, G. PALMIERI, L. ERNSTER and B. AFZELIUS, 1962 A case of severe hypermetabolism of nonthyroid origin with a defect in the maintenance of mitochondrial respiratory control: a correlated clinical, biochemical, and morphological study. J Clin Invest **41:** 1776-1804.

LUO, L., Y. J. LIAO, L. Y. JAN and Y. N. JAN, 1994 Distinct morphogenetic functions of similar small GTPases: Drosophila Drac1 is involved in axonal outgrowth and myoblast fusion. Genes Dev **8:** 1787-1802.

LUO, L., and D. D. O'LEARY, 2005 Axon retraction and degeneration in development and disease. Annu Rev Neurosci **28:** 127-156.

LUOMA, P., A. MELBERG, J. O. RINNE, J. A. KAUKONEN, N. N. NUPPONEN *et al.*, 2004 Parkinsonism, premature menopause, and mitochondrial DNA polymerase gamma mutations: clinical and molecular genetic study. Lancet **364:** 875-882.

MACASKILL, A. F., and J. T. KITTLER, 2010 Control of mitochondrial transport and localization in neurons. Trends Cell Biol **20:** 102-112.

MAGRANE, J., M. A. SAHAWNEH, S. PRZEDBORSKI, A. G. ESTEVEZ and G. MANFREDI, 2012 Mitochondrial Dynamics and Bioenergetic Dysfunction Is Associated with Synaptic Alterations in Mutant SOD1 Motor Neurons. J Neurosci **32:** 229-242.

MAHR, A., and H. ABERLE, 2006 The expression pattern of the Drosophila vesicular glutamate transporter: a marker protein for motoneurons and glutamatergic centers in the brain. Gene Expr Patterns **6:** 299-309.

MAIER, D., C. L. FARR, B. POECK, A. ALAHARI, M. VOGEL *et al.*, 2001 Mitochondrial single-stranded DNA-binding protein is required for mitochondrial DNA replication and development in Drosophila melanogaster. Mol Biol Cell **12:** 821-830.

MANDEL, H., R. SZARGEL, V. LABAY, O. ELPELEG, A. SAADA *et al.*, 2001 The deoxyguanosine kinase gene is mutated in individuals with depleted hepatocerebral mitochondrial DNA. Nat Genet **29:** 337-341.

MARGULIS, L., 1970 Recombination of non-chromosomal genes in Chlamydomonas: assortment of mitochondria and chloroplasts? J Theor Biol **26:** 337-342.

MARIOTTI, C., V. TIRANTI, F. CARRARA, B. DALLAPICCOLA, S. DIDONATO *et al.*, 1994 Defective respiratory capacity and mitochondrial protein synthesis in transformant cybrids harboring the tRNA(Leu(UUR)) mutation associated with maternally inherited myopathy and cardiomyopathy. J Clin Invest **93:** 1102-1107.

MARTIN-PENA, A., A. ACEBES, J. R. RODRIGUEZ, A. SORRIBES, G. G. DE POLAVIEJA *et al.*, 2006 Age-independent synaptogenesis by phosphoinositide 3 kinase. J Neurosci **26:** 10199-10208.

MARTINEZ-AZORIN, F., M. CALLEJA, R. HERNANDEZ-SIERRA, C. L. FARR, L. S. KAGUNI *et al.*, 2008 Over-expression of the catalytic core of mitochondrial DNA (mtDNA) polymerase in the nervous system of Drosophila melanogaster reduces median life span by inducing mtDNA depletion. J Neurochem **105:** 165-176.

MAST, J. D., K. M. TOMALTY, H. VOGEL and T. R. CLANDININ, 2008 Reactive oxygen species act remotely to cause synapse loss in a Drosophila model of developmental mitochondrial encephalopathy. Development **135:** 2669-2679.

MATHEWS, C. K., and S. SONG, 2007 Maintaining precursor pools for mitochondrial DNA replication. FASEB J **21:** 2294-2303.

MATSUSHIMA, Y., C. L. FARR, L. FAN and L. S. KAGUNI, 2008 Physiological and biochemical defects in carboxyl-terminal mutants of mitochondrial DNA helicase. J Biol Chem **283:** 23964-23971.

MATSUSHIMA, Y., and L. S. KAGUNI, 2007 Differential phenotypes of active site and human autosomal dominant progressive external ophthalmoplegia mutations in Drosophila mitochondrial DNA helicase expressed in Schneider cells. J Biol Chem **282:** 9436-9444.

MATSUSHIMA, Y., and L. S. KAGUNI, 2009 Functional importance of the conserved N-terminal domain of the mitochondrial replicative DNA helicase. Biochim Biophys Acta **1787:** 290-295.

MCFARLAND, R., R. W. TAYLOR and D. M. TURNBULL, 2010 A neurological perspective on mitochondrial disease. Lancet Neurol **9:** 829-840.

MCGUIRE, S. E., P. T. LE and R. L. DAVIS, 2001 The role of Drosophila mushroom body signaling in olfactory memory. Science **293:** 1330-1333.

MELENDEZ, A., Z. TALLOCZY, M. SEAMAN, E. L. ESKELINEN, D. H. HALL *et al.*, 2003 Autophagy genes are essential for dauer development and life-span extension in C. elegans. Science **301:** 1387-1391.

MILTON, V. J., H. E. JARRETT, K. GOWERS, S. CHALAK, L. BRIGGS *et al.*, 2011 Oxidative stress induces overgrowth of the Drosophila neuromuscular junction. Proc Natl Acad Sci U S A **108:** 17521-17526.

MIQUEL, J., A. C. ECONOMOS, J. FLEMING and J. E. JOHNSON, JR., 1980 Mitochondrial role in cell aging. Exp Gerontol **15:** 575-591.

MORAES, C. T., 2001 What regulates mitochondrial DNA copy number in animal cells? Trends Genet **17:** 199-205.

MORAES, C. T., S. DIMAURO, M. ZEVIANI, A. LOMBES, S. SHANSKE *et al.*, 1989 Mitochondrial DNA deletions in progressive external ophthalmoplegia and Kearns-Sayre syndrome. N Engl J Med **320:** 1293-1299.

MORAES, C. T., S. SHANSKE, H. J. TRITSCHLER, J. R. APRILLE, F. ANDREETTA *et al.*, 1991 mtDNA depletion with variable tissue expression: a novel genetic abnormality in mitochondrial diseases. Am J Hum Genet **48:** 492-501.

MOREL, F., R. DEBISE, M. RENOUX, S. TOURAILLE, M. RAGNO *et al.*, 1999 Biochemical and molecular consequences of ethidium bromide treatment on Drosophila cells. Insect Biochem Mol Biol **29:** 835-843.

MOREL, F., M. RENOUX, P. LACHAUME and S. ALZIARI, 2008 Bleomycin-induced double-strand breaks in mitochondrial DNA of Drosophila cells are repaired. Mutat Res **637:** 111-117.

MORIMOTO, N., K. MIYAZAKI, T. KURATA, Y. IKEDA, T. MATSUURA *et al.*, 2012 Effect of mitochondrial transcription factor a overexpression on motor neurons in amyotrophic lateral sclerosis model mice. J Neurosci Res.

MOTT, J. L., D. ZHANG, J. C. FREEMAN, P. MIKOLAJCZAK, S. W. CHANG *et al.*, 2004 Cardiac disease due to random mitochondrial DNA mutations is prevented by cyclosporin A. Biochem Biophys Res Commun **319:** 1210-1215.

MOTT, J. L., D. ZHANG, M. STEVENS, S. CHANG, G. DENNIGER *et al.*, 2001 Oxidative stress is not an obligate mediator of disease provoked by mitochondrial DNA mutations. Mutat Res **474:** 35-45.

MULLER-HOCKER, J., 1989 Cytochrome-c-oxidase deficient cardiomyocytes in the human heart--an age-related phenomenon. A histochemical ultracytochemical study. Am J Pathol **134:** 1167-1173.

MUNCH-PETERSEN, B., J. PISKUR and L. SONDERGAARD, 1998a Four deoxynucleoside kinase activities from Drosophila melanogaster are contained within a single monomeric enzyme, a new multifunctional deoxynucleoside kinase. J Biol Chem **273:** 3926-3931.

MUNCH-PETERSEN, B., J. PISKUR and L. SONDERGAARD, 1998b The single deoxynucleoside kinase in Drosophila melanogaster, Dm-dNK, is multifunctional and differs from the mammalian deoxynucleoside kinases. Adv Exp Med Biol **431:** 465-469.

MURPHY, M. P., 2009 How mitochondria produce reactive oxygen species. Biochem J **417:** 1-13.

NAKADA, K., A. SATO, H. SONE, A. KASAHARA, K. IKEDA *et al.*, 2004 Accumulation of pathogenic DeltamtDNA induced deafness but not diabetic phenotypes in mito-mice. Biochem Biophys Res Commun **323:** 175-184.

NARENDRA, D., A. TANAKA, D. F. SUEN and R. J. YOULE, 2008 Parkin is recruited selectively to impaired mitochondria and promotes their autophagy. J Cell Biol **183:** 795-803.

NASS, M. M., and S. NASS, 1963a Intramitochondrial Fibers with DNA Characteristics. I. Fixation and Electron Staining Reactions. J Cell Biol **19:** 593-611.

NASS, S., and M. M. NASS, 1963b Intramitochondrial Fibers with DNA Characteristics. Ii. Enzymatic and Other Hydrolytic Treatments. J Cell Biol **19:** 613-629.

NAVIAUX, R. K., and K. V. NGUYEN, 2004 POLG mutations associated with Alpers' syndrome and mitochondrial DNA depletion. Ann Neurol **55:** 706-712.

NAVIAUX, R. K., W. L. NYHAN, B. A. BARSHOP, J. POULTON, D. MARKUSIC *et al.*, 1999 Mitochondrial DNA polymerase gamma deficiency and mtDNA depletion in a child with Alpers' syndrome. Ann Neurol **45:** 54-58.

NGO, H. B., J. T. KAISER and D. C. CHAN, 2011 The mitochondrial transcription and packaging factor Tfam imposes a U-turn on mitochondrial DNA. Nat Struct Mol Biol **18:** 1290-1296.

NIKALI, K., A. SUOMALAINEN, J. SAHARINEN, M. KUOKKANEN, J. N. SPELBRINK *et al.*, 2005 Infantile onset spinocerebellar ataxia is caused by recessive mutations

in mitochondrial proteins Twinkle and Twinky. Hum Mol Genet **14:** 2981-2990.

NISHINO, I., A. SPINAZZOLA and M. HIRANO, 1999 Thymidine phosphorylase gene mutations in MNGIE, a human mitochondrial disorder. Science **283:** 689-692.

NISHINO, I., A. SPINAZZOLA and M. HIRANO, 2001 MNGIE: from nuclear DNA to mitochondrial DNA. Neuromuscul Disord **11:** 7-10.

NISHIYAMA, S., H. SHITARA, K. NAKADA, T. ONO, A. SATO *et al.*, 2010 Over-expression of Tfam improves the mitochondrial disease phenotypes in a mouse model system. Biochem Biophys Res Commun **401:** 26-31.

NUNNARI, J., and A. SUOMALAINEN, 2012 Mitochondria: in sickness and in health. Cell **148:** 1145-1159.

OLIVEIRA, M. T., R. GARESSE and L. S. KAGUNI, 2010 Animal models of mitochondrial DNA transactions in disease and ageing. Exp Gerontol **45:** 489-502.

ONYANGO, I., S. KHAN, B. MILLER, R. SWERDLOW, P. TRIMMER *et al.*, 2006 Mitochondrial genomic contribution to mitochondrial dysfunction in Alzheimer's disease. J Alzheimers Dis **9:** 183-193.

ORR, A. L., S. LI, C. E. WANG, H. LI, J. WANG *et al.*, 2008 N-terminal mutant huntingtin associates with mitochondria and impairs mitochondrial trafficking. J Neurosci **28:** 2783-2792.

OSTERGAARD, E., E. CHRISTENSEN, E. KRISTENSEN, B. MOGENSEN, M. DUNO *et al.*, 2007 Deficiency of the alpha subunit of succinate-coenzyme A ligase causes fatal infantile lactic acidosis with mitochondrial DNA depletion. Am J Hum Genet **81:** 383-387.

PALADE, G. E., 1953 An electron microscope study of the mitochondrial structure. J Histochem Cytochem **1:** 188-211.

PARISI, M. A., and D. A. CLAYTON, 1991 Similarity of human mitochondrial transcription factor 1 to high mobility group proteins. Science **252:** 965-969.

PARK, C. B., and N. G. LARSSON, 2011 Mitochondrial DNA mutations in disease and aging. J Cell Biol **193:** 809-818.

PARONE, P. A., S. DA CRUZ, D. TONDERA, Y. MATTENBERGER, D. I. JAMES *et al.*, 2008 Preventing mitochondrial fission impairs mitochondrial function and leads to loss of mitochondrial DNA. PLoS One **3:** e3257.

PELLEGRINI, M., J. ASIN-CAYUELA, H. ERDJUMENT-BROMAGE, P. TEMPST, N. G. LARSSON *et al.*, 2009 MTERF2 is a nucleoid component in mammalian mitochondria. Biochim Biophys Acta **1787:** 296-302.

PENNEY, J., K. TSURUDOME, E. H. LIAO, F. ELAZZOUZI, M. LIVINGSTONE *et al.*, 2012 TOR is required for the retrograde regulation of synaptic homeostasis at the Drosophila neuromuscular junction. Neuron **74:** 166-178.

PERIER, C., and M. VILA, 2012 Mitochondrial biology and Parkinson's disease. Cold Spring Harb Perspect Med **2:** a009332.

PETIOT, A., E. OGIER-DENIS, E. F. BLOMMAART, A. J. MEIJER and P. CODOGNO, 2000 Distinct classes of phosphatidylinositol 3'-kinases are involved in signaling pathways that control macroautophagy in HT-29 cells. J Biol Chem **275:** 992-998.

PICKRELL, A. M., M. PINTO, A. HIDA and C. T. MORAES, 2011 Striatal dysfunctions associated with mitochondrial DNA damage in dopaminergic neurons in a mouse model of Parkinson's disease. J Neurosci **31:** 17649-17658.

PIKO, L., A. J. HOUGHAM and K. J. BULPITT, 1988 Studies of sequence heterogeneity of mitochondrial DNA from rat and mouse tissues: evidence for an increased frequency of deletions/additions with aging. Mech Ageing Dev **43:** 279-293.

POGSON, J. H., R. M. IVATT and A. J. WHITWORTH, 2011 Molecular mechanisms of PINK1-related neurodegeneration. Curr Neurol Neurosci Rep **11:** 283-290.

POHJOISMAKI, J. L., S. WANROOIJ, A. K. HYVARINEN, S. GOFFART, I. J. HOLT *et al.*, 2006 Alterations to the expression level of mitochondrial transcription factor A, TFAM, modify the mode of mitochondrial DNA replication in cultured human cells. Nucleic Acids Res **34:** 5815-5828.

PONAMAREV, M. V., M. J. LONGLEY, D. NGUYEN, T. A. KUNKEL and W. C. COPELAND, 2002 Active site mutation in DNA polymerase gamma associated with progressive external ophthalmoplegia causes error-prone DNA synthesis. J Biol Chem **277:** 15225-15228.

POOLE, A. C., R. E. THOMAS, L. A. ANDREWS, H. M. MCBRIDE, A. J. WHITWORTH *et al.*, 2008 The PINK1/Parkin pathway regulates mitochondrial morphology. Proc Natl Acad Sci U S A **105:** 1638-1643.

RAPAPORT, D., M. BRUNNER, W. NEUPERT and B. WESTERMANN, 1998 Fzo1p is a mitochondrial outer membrane protein essential for the biogenesis of functional mitochondria in Saccharomyces cerevisiae. J Biol Chem **273:** 20150-20155.

REYES, A., M. Y. YANG, M. BOWMAKER and I. J. HOLT, 2005 Bidirectional replication initiates at sites throughout the mitochondrial genome of birds. J Biol Chem **280:** 3242-3250.

ROMAN, G., and R. L. DAVIS, 2001 Molecular biology and anatomy of Drosophila olfactory associative learning. Bioessays **23:** 571-581.

RORBACH, J., R. SOLEIMANPOUR-LICHAEI, R. N. LIGHTOWLERS and Z. M. CHRZANOWSKA-LIGHTOWLERS, 2007 How do mammalian mitochondria synthesize proteins? Biochem Soc Trans **35:** 1290-1291.

ROTIG, A., V. CORMIER, S. BLANCHE, J. P. BONNEFONT, F. LEDEIST *et al.*, 1990 Pearson's marrow-pancreas syndrome. A multisystem mitochondrial disorder in infancy. J Clin Invest **86:** 1601-1608.

ROVIO, A. T., D. R. MARCHINGTON, S. DONAT, H. C. SCHUPPE, J. ABEL *et al.*, 2001 Mutations at the mitochondrial DNA polymerase (POLG) locus associated with male infertility. Nat Genet **29:** 261-262.

RUAN, H., X. D. TANG, M. L. CHEN, M. L. JOINER, G. SUN *et al.*, 2002 High-quality life extension by the enzyme peptide methionine sulfoxide reductase. Proc Natl Acad Sci U S A **99:** 2748-2753.

RUBIO-COSIALS, A., J. F. SIDOW, N. JIMENEZ-MENENDEZ, P. FERNANDEZ-MILLAN, J. MONTOYA *et al.*, 2011 Human mitochondrial transcription factor A induces a U-turn structure in the light strand promoter. Nat Struct Mol Biol **18:** 1281-1289.

RUSTEN, T. E., K. LINDMO, G. JUHASZ, M. SASS, P. O. SEGLEN *et al.*, 2004 Programmed autophagy in the Drosophila fat body is induced by ecdysone through regulation of the PI3K pathway. Dev Cell **7:** 179-192.

RUTHEL, G., and P. J. HOLLENBECK, 2003 Response of mitochondrial traffic to axon determination and differential branch growth. J Neurosci **23:** 8618-8624.

SAADA-REISCH, A., 2004 Deoxyribonucleoside kinases in mitochondrial DNA depletion. Nucleosides Nucleotides Nucleic Acids **23:** 1205-1215.

SAADA, A., A. SHAAG, H. MANDEL, Y. NEVO, S. ERIKSSON *et al.*, 2001 Mutant mitochondrial thymidine kinase in mitochondrial DNA depletion myopathy. Nat Genet **29:** 342-344.

SANTEL, A., and M. T. FULLER, 2001 Control of mitochondrial morphology by a human mitofusin. J Cell Sci **114:** 867-874.

SANTORELLI, F. M., K. TANJI, R. KULIKOVA, S. SHANSKE, L. VILARINHO *et al.*, 1997 Identification of a novel mutation in the mtDNA ND5 gene associated with MELAS. Biochem Biophys Res Commun **238:** 326-328.

SARASTE, M., 1999 Oxidative phosphorylation at the fin de siecle. Science **283:** 1488-1493.

SARZI, E., S. GOFFART, V. SERRE, D. CHRETIEN, A. SLAMA *et al.*, 2007 Twinkle helicase (PEO1) gene mutation causes mitochondrial DNA depletion. Ann Neurol **62:** 579-587.

SCARPULLA, R. C., 2008 Nuclear control of respiratory chain expression by nuclear respiratory factors and PGC-1-related coactivator. Ann N Y Acad Sci **1147:** 321-334.

SCHAEFER, A. M., R. MCFARLAND, E. L. BLAKELY, L. HE, R. G. WHITTAKER *et al.*, 2008 Prevalence of mitochondrial DNA disease in adults. Ann Neurol **63:** 35-39.

SCHAPIRA, A. H., J. M. COOPER, D. DEXTER, J. B. CLARK, P. JENNER *et al.*, 1990 Mitochondrial complex I deficiency in Parkinson's disease. J Neurochem **54:** 823-827.

SCHAPIRA, A. H., J. M. COOPER, D. DEXTER, P. JENNER, J. B. CLARK *et al.*, 1989 Mitochondrial complex I deficiency in Parkinson's disease. Lancet **1:** 1269.

SCHIEKE, S. M., D. PHILLIPS, J. P. MCCOY, JR., A. M. APONTE, R. F. SHEN *et al.*, 2006 The mammalian target of rapamycin (mTOR) pathway regulates mitochondrial oxygen consumption and oxidative capacity. J Biol Chem **281:** 27643-27652.

SCHON, E. A., and S. PRZEDBORSKI, 2011 Mitochondria: the next (neurode)generation. Neuron **70:** 1033-1053.

SCHON, E. A., R. RIZZUTO, C. T. MORAES, H. NAKASE, M. ZEVIANI *et al.*, 1989 A direct repeat is a hotspot for large-scale deletion of human mitochondrial DNA. Science **244:** 346-349.

SCHRINER, S. E., N. J. LINFORD, G. M. MARTIN, P. TREUTING, C. E. OGBURN *et al.*, 2005 Extension of murine life span by overexpression of catalase targeted to mitochondria. Science **308:** 1909-1911.

SCHUMAN, E., and D. CHAN, 2004 Fueling synapses. Cell **119:** 738-740.

SCOTT, R. C., G. JUHASZ and T. P. NEUFELD, 2007 Direct induction of autophagy by Atg1 inhibits cell growth and induces apoptotic cell death. Curr Biol **17:** 1-11.

SEGLEN, P. O., and P. BOHLEY, 1992 Autophagy and other vacuolar protein degradation mechanisms. Experientia **48:** 158-172.

SEO, A. Y., A. M. JOSEPH, D. DUTTA, J. C. HWANG, J. P. ARIS *et al.*, 2010 New insights into the role of mitochondria in aging: mitochondrial dynamics and more. J Cell Sci **123:** 2533-2542.

SESAKI, H., and R. E. JENSEN, 1999 Division versus fusion: Dnm1p and Fzo1p antagonistically regulate mitochondrial shape. J Cell Biol **147:** 699-706.

SHADEL, G. S., and D. A. CLAYTON, 1997 Mitochondrial DNA maintenance in vertebrates. Annu Rev Biochem **66:** 409-435.

SHEN, W., and B. GANETZKY, 2009 Autophagy promotes synapse development in Drosophila. J Cell Biol **187:** 71-79.

SHENG, Z. H., and Q. CAI, 2012 Mitochondrial transport in neurons: impact on synaptic homeostasis and neurodegeneration. Nat Rev Neurosci **13:** 77-93.
SHOFFNER, J. M., P. M. FERNHOFF, N. S. KRAWIECKI, D. B. CAPLAN, P. J. HOLT *et al.*, 1992 Subacute necrotizing encephalopathy: oxidative phosphorylation defects and the ATPase 6 point mutation. Neurology **42:** 2168-2174.
SHOUBRIDGE, E. A., 2012 Supersizing the mitochondrial respiratory chain. Cell Metab **15:** 271-272.
SILVA, J. P., M. KOHLER, C. GRAFF, A. OLDFORS, M. A. MAGNUSON *et al.*, 2000 Impaired insulin secretion and beta-cell loss in tissue-specific knockout mice with mitochondrial diabetes. Nat Genet **26:** 336-340.
SLONIMSKI, P. P., G. PERRODIN and J. H. CROFT, 1968 Ethidium bromide induced mutation of yeast mitochondria: complete transformation of cells into respiratory deficient non-chromosomal "petites". Biochem Biophys Res Commun **30:** 232-239.
SMEITINK, J., L. VAN DEN HEUVEL and S. DIMAURO, 2001 The genetics and pathology of oxidative phosphorylation. Nat Rev Genet **2:** 342-352.
SMIRNOVA, E., L. GRIPARIC, D. L. SHURLAND and A. M. VAN DER BLIEK, 2001 Dynamin-related protein Drp1 is required for mitochondrial division in mammalian cells. Mol Biol Cell **12:** 2245-2256.
SOLOGUB, M., D. LITONIN, M. ANIKIN, A. MUSTAEV and D. TEMIAKOV, 2009 TFB2 is a transient component of the catalytic site of the human mitochondrial RNA polymerase. Cell **139:** 934-944.
SOMEYA, S., T. YAMASOBA, G. C. KUJOTH, T. D. PUGH, R. WEINDRUCH *et al.*, 2008 The role of mtDNA mutations in the pathogenesis of age-related hearing loss in mice carrying a mutator DNA polymerase gamma. Neurobiol Aging **29:** 1080-1092.
SONG, W., J. CHEN, A. PETRILLI, G. LIOT, E. KLINGLMAYR *et al.*, 2011 Mutant huntingtin binds the mitochondrial fission GTPase dynamin-related protein-1 and increases its enzymatic activity. Nat Med **17:** 377-382.
SORIANO, F. X., M. LIESA, D. BACH, D. C. CHAN, M. PALACIN *et al.*, 2006 Evidence for a mitochondrial regulatory pathway defined by peroxisome proliferator-activated receptor-gamma coactivator-1 alpha, estrogen-related receptor-alpha, and mitofusin 2. Diabetes **55:** 1783-1791.
SPELBRINK, J. N., F. Y. LI, V. TIRANTI, K. NIKALI, Q. P. YUAN *et al.*, 2001 Human mitochondrial DNA deletions associated with mutations in the gene encoding Twinkle, a phage T7 gene 4-like protein localized in mitochondria. Nat Genet **28:** 223-231.
SPINAZZOLA, A., C. VISCOMI, E. FERNANDEZ-VIZARRA, F. CARRARA, P. D'ADAMO *et al.*, 2006 MPV17 encodes an inner mitochondrial membrane protein and is mutated in infantile hepatic mitochondrial DNA depletion. Nat Genet **38:** 570-575.
SRIVASTAVA, S., and C. T. MORAES, 2001 Manipulating mitochondrial DNA heteroplasmy by a mitochondrially targeted restriction endonuclease. Hum Mol Genet **10:** 3093-3099.
SRIVASTAVA, S., and C. T. MORAES, 2005 Double-strand breaks of mouse muscle mtDNA promote large deletions similar to multiple mtDNA deletions in humans. Hum Mol Genet **14:** 893-902.
STERKY, F. H., S. LEE, R. WIBOM, L. OLSON and N. G. LARSSON, 2011 Impaired mitochondrial transport and Parkin-independent degeneration of respiratory

chain-deficient dopamine neurons in vivo. Proc Natl Acad Sci U S A **108:** 12937-12942.

STOKIN, G. B., and L. S. GOLDSTEIN, 2006 Axonal transport and Alzheimer's disease. Annu Rev Biochem **75:** 607-627.

STOWERS, R. S., L. J. MEGEATH, J. GORSKA-ANDRZEJAK, I. A. MEINERTZHAGEN and T. L. SCHWARZ, 2002 Axonal transport of mitochondria to synapses depends on milton, a novel Drosophila protein. Neuron **36:** 1063-1077.

STROGOLOVA, V., A. FURNESS, M. ROBB-MCGRATH, J. GARLICH and R. A. STUART, 2012 Rcf1 and Rcf2, members of the hypoxia-induced gene 1 protein family, are critical components of the mitochondrial cytochrome bc1-cytochrome c oxidase supercomplex. Mol Cell Biol **32:** 1363-1373.

STUMPF, J. D., and W. C. COPELAND, 2011 Mitochondrial DNA replication and disease: insights from DNA polymerase gamma mutations. Cell Mol Life Sci **68:** 219-233.

SUGIYAMA, S., M. TAKASAWA, M. HAYAKAWA and T. OZAWA, 1993 Changes in skeletal muscle, heart and liver mitochondrial electron transport activities in rats and dogs of various ages. Biochem Mol Biol Int **30:** 937-944.

SUGRUE, M. M., and W. G. TATTON, 2001 Mitochondrial membrane potential in aging cells. Biol Signals Recept **10:** 176-188.

SUN, J., D. FOLK, T. J. BRADLEY and J. TOWER, 2002 Induced overexpression of mitochondrial Mn-superoxide dismutase extends the life span of adult Drosophila melanogaster. Genetics **161:** 661-672.

SUOMALAINEN, A., and P. ISOHANNI, 2010 Mitochondrial DNA depletion syndromes--many genes, common mechanisms. Neuromuscul Disord **20:** 429-437.

SUOMALAINEN, A., and J. KAUKONEN, 2001 Diseases caused by nuclear genes affecting mtDNA stability. Am J Med Genet **106:** 53-61.

SUOMALAINEN, A., A. MAJANDER, M. HALTIA, H. SOMER, J. LONNQVIST *et al.*, 1992 Multiple deletions of mitochondrial DNA in several tissues of a patient with severe retarded depression and familial progressive external ophthalmoplegia. J Clin Invest **90:** 61-66.

SWERDLOW, R. H., 2007 Mitochondria in cybrids containing mtDNA from persons with mitochondriopathies. J Neurosci Res **85:** 3416-3428.

SWERDLOW, R. H., J. M. BURNS and S. M. KHAN, 2010 The Alzheimer's disease mitochondrial cascade hypothesis. J Alzheimers Dis **20 Suppl 2:** S265-279.

SWERDLOW, R. H., and S. M. KHAN, 2004 A "mitochondrial cascade hypothesis" for sporadic Alzheimer's disease. Med Hypotheses **63:** 8-20.

SWERDLOW, R. H., J. K. PARKS, D. S. CASSARINO, D. J. MAGUIRE, R. S. MAGUIRE *et al.*, 1997 Cybrids in Alzheimer's disease: a cellular model of the disease? Neurology **49:** 918-925.

SWIECH, L., M. PERYCZ, A. MALIK and J. JAWORSKI, 2008 Role of mTOR in physiology and pathology of the nervous system. Biochim Biophys Acta **1784:** 116-132.

TANG, S. J., G. REIS, H. KANG, A. C. GINGRAS, N. SONENBERG *et al.*, 2002 A rapamycin-sensitive signaling pathway contributes to long-term synaptic plasticity in the hippocampus. Proc Natl Acad Sci U S A **99:** 467-472.

TANJI, K., and E. BONILLA, 2001 Optical imaging techniques (histochemical, immunohistochemical, and in situ hybridization staining methods) to visualize mitochondria. Methods Cell Biol **65:** 311-332.

TAYLOR, R. W., and D. M. TURNBULL, 2005 Mitochondrial DNA mutations in human disease. Nat Rev Genet **6:** 389-402.

TIEFENBOCK, S. K., C. BALTZER, N. A. EGLI and C. FREI, 2010 The Drosophila PGC-1 homologue Spargel coordinates mitochondrial activity to insulin signalling. EMBO J **29:** 171-183.

TISSOT, M., and R. F. STOCKER, 2000 Metamorphosis in drosophila and other insects: the fate of neurons throughout the stages. Prog Neurobiol **62:** 89-111.

TRIFUNOVIC, A., A. HANSSON, A. WREDENBERG, A. T. ROVIO, E. DUFOUR *et al.*, 2005 Somatic mtDNA mutations cause aging phenotypes without affecting reactive oxygen species production. Proc Natl Acad Sci U S A **102:** 17993-17998.

TRIFUNOVIC, A., and N. G. LARSSON, 2008 Mitochondrial dysfunction as a cause of ageing. J Intern Med **263:** 167-178.

TRIFUNOVIC, A., A. WREDENBERG, M. FALKENBERG, J. N. SPELBRINK, A. T. ROVIO *et al.*, 2004 Premature ageing in mice expressing defective mitochondrial DNA polymerase. Nature **429:** 417-423.

TROUNCE, I., E. BYRNE and S. MARZUKI, 1989 Decline in skeletal muscle mitochondrial respiratory chain function: possible factor in ageing. Lancet **1:** 637-639.

TRUSHINA, E., R. B. DYER, J. D. BADGER, 2ND, D. URE, L. EIDE *et al.*, 2004 Mutant huntingtin impairs axonal trafficking in mammalian neurons in vivo and in vitro. Mol Cell Biol **24:** 8195-8209.

TURNER, C. J., C. GRANYCOME, R. HURST, E. POHLER, M. K. JUHOLA *et al.*, 2005 Systematic segregation to mutant mitochondrial DNA and accompanying loss of mitochondrial DNA in human NT2 teratocarcinoma Cybrids. Genetics **170:** 1879-1885.

TWIG, G., A. ELORZA, A. J. MOLINA, H. MOHAMED, J. D. WIKSTROM *et al.*, 2008a Fission and selective fusion govern mitochondrial segregation and elimination by autophagy. EMBO J **27:** 433-446.

TWIG, G., B. HYDE and O. S. SHIRIHAI, 2008b Mitochondrial fusion, fission and autophagy as a quality control axis: the bioenergetic view. Biochim Biophys Acta **1777:** 1092-1097.

TWIG, G., and O. S. SHIRIHAI, 2011 The interplay between mitochondrial dynamics and mitophagy. Antioxid Redox Signal **14:** 1939-1951.

TYYNISMAA, H., K. P. MJOSUND, S. WANROOIJ, I. LAPPALAINEN, E. YLIKALLIO *et al.*, 2005 Mutant mitochondrial helicase Twinkle causes multiple mtDNA deletions and a late-onset mitochondrial disease in mice. Proc Natl Acad Sci U S A **102:** 17687-17692.

TYYNISMAA, H., H. SEMBONGI, M. BOKORI-BROWN, C. GRANYCOME, N. ASHLEY *et al.*, 2004 Twinkle helicase is essential for mtDNA maintenance and regulates mtDNA copy number. Hum Mol Genet **13:** 3219-3227.

TYYNISMAA, H., and A. SUOMALAINEN, 2009 Mouse models of mitochondrial DNA defects and their relevance for human disease. EMBO Rep **10:** 137-143.

TYYNISMAA, H., and A. SUOMALAINEN, 2010 Mouse models of mtDNA replication diseases. Methods **51:** 405-410.

TZAGOLOFF, A., and A. M. MYERS, 1986 Genetics of mitochondrial biogenesis. Annu Rev Biochem **55:** 249-285.

VAN GOETHEM, G., B. DERMAUT, A. LOFGREN, J. J. MARTIN and C. VAN BROECKHOVEN, 2001 Mutation of POLG is associated with progressive external ophthalmoplegia characterized by mtDNA deletions. Nat Genet **28:** 211-212.

VAN GOETHEM, G., P. LUOMA, M. RANTAMAKI, A. AL MEMAR, S. KAAKKOLA *et al.*, 2004 POLG mutations in neurodegenerative disorders with ataxia but no muscle involvement. Neurology **63:** 1251-1257.

VAN TUYLE, G. C., and P. A. PAVCO, 1985 The rat liver mitochondrial DNA-protein complex: displaced single strands of replicative intermediates are protein coated. J Cell Biol **100:** 251-257.

VERMULST, M., J. H. BIELAS, G. C. KUJOTH, W. C. LADIGES, P. S. RABINOVITCH *et al.*, 2007 Mitochondrial point mutations do not limit the natural lifespan of mice. Nat Genet **39:** 540-543.

VERSTREKEN, P., C. V. LY, K. J. VENKEN, T. W. KOH, Y. ZHOU *et al.*, 2005 Synaptic mitochondria are critical for mobilization of reserve pool vesicles at Drosophila neuromuscular junctions. Neuron **47:** 365-378.

VINCENT, A., L. BRIGGS, G. F. CHATWIN, E. EMERY, R. TOMLINS *et al.*, 2012 parkin-induced defects in neurophysiology and locomotion are generated by metabolic dysfunction and not oxidative stress. Hum Mol Genet **21:** 1760-1769.

VUKOTIC, M., S. OELJEKLAUS, S. WIESE, F. N. VOGTLE, C. MEISINGER *et al.*, 2012 Rcf1 mediates cytochrome oxidase assembly and respirasome formation, revealing heterogeneity of the enzyme complex. Cell Metab **15:** 336-347.

WAGH, D. A., T. M. RASSE, E. ASAN, A. HOFBAUER, I. SCHWENKERT *et al.*, 2006 Bruchpilot, a protein with homology to ELKS/CAST, is required for structural integrity and function of synaptic active zones in Drosophila. Neuron **49:** 833-844.

WALLACE, D. C., and W. FAN, 2009 The pathophysiology of mitochondrial disease as modeled in the mouse. Genes Dev **23:** 1714-1736.

WALLACE, D. C., G. SINGH, M. T. LOTT, J. A. HODGE, T. G. SCHURR *et al.*, 1988 Mitochondrial DNA mutation associated with Leber's hereditary optic neuropathy. Science **242:** 1427-1430.

WANG, J., J. P. SILVA, C. M. GUSTAFSSON, P. RUSTIN and N. G. LARSSON, 2001 Increased in vivo apoptosis in cells lacking mitochondrial DNA gene expression. Proc Natl Acad Sci U S A **98:** 4038-4043.

WANG, J., H. WILHELMSSON, C. GRAFF, H. LI, A. OLDFORS *et al.*, 1999 Dilated cardiomyopathy and atrioventricular conduction blocks induced by heart-specific inactivation of mitochondrial DNA gene expression. Nat Genet **21:** 133-137.

WANG, X., B. SU, S. L. SIEDLAK, P. I. MOREIRA, H. FUJIOKA *et al.*, 2008 Amyloid-beta overproduction causes abnormal mitochondrial dynamics via differential modulation of mitochondrial fission/fusion proteins. Proc Natl Acad Sci U S A **105:** 19318-19323.

WANG, X., B. SU, L. ZHENG, G. PERRY, M. A. SMITH *et al.*, 2009 The role of abnormal mitochondrial dynamics in the pathogenesis of Alzheimer's disease. J Neurochem **109 Suppl 1:** 153-159.

WANG, X., D. WINTER, G. ASHRAFI, J. SCHLEHE, Y. L. WONG *et al.*, 2011 PINK1 and Parkin Target Miro for Phosphorylation and Degradation to Arrest Mitochondrial Motility. Cell **147:** 893-906.

WANG, Y., and D. F. BOGENHAGEN, 2006 Human mitochondrial DNA nucleoids are linked to protein folding machinery and metabolic enzymes at the mitochondrial inner membrane. J Biol Chem **281:** 25791-25802.

WEIHOFEN, A., K. J. THOMAS, B. L. OSTASZEWSKI, M. R. COOKSON and D. J. SELKOE, 2009 Pink1 forms a multiprotein complex with Miro and Milton, linking Pink1 function to mitochondrial trafficking. Biochemistry **48:** 2045-2052.

WENZ, T., F. DIAZ, B. M. SPIEGELMAN and C. T. MORAES, 2008 Activation of the PPAR/PGC-1alpha pathway prevents a bioenergetic deficit and effectively improves a mitochondrial myopathy phenotype. Cell Metab **8:** 249-256.

WESTERMANN, B., 2010 Mitochondrial fusion and fission in cell life and death. Nat Rev Mol Cell Biol **11:** 872-884.

WHITWORTH, A. J., and L. J. PALLANCK, 2009 The PINK1/Parkin pathway: a mitochondrial quality control system? J Bioenerg Biomembr **41:** 499-503.

WHITWORTH, A. J., D. A. THEODORE, J. C. GREENE, H. BENES, P. D. WES *et al.*, 2005 Increased glutathione S-transferase activity rescues dopaminergic neuron loss in a Drosophila model of Parkinson's disease. Proc Natl Acad Sci U S A **102:** 8024-8029.

WOLF, R., T. WITTIG, L. LIU, G. WUSTMANN, D. EYDING *et al.*, 1998 Drosophila mushroom bodies are dispensable for visual, tactile, and motor learning. Learn Mem **5:** 166-178.

WOOD-KACZMAR, A., S. GANDHI, Z. YAO, A. Y. ABRAMOV, E. A. MILJAN *et al.*, 2008 PINK1 is necessary for long term survival and mitochondrial function in human dopaminergic neurons. PLoS One **3:** e2455.

WREDENBERG, A., R. WIBOM, H. WILHELMSSON, C. GRAFF, H. H. WIENER *et al.*, 2002 Increased mitochondrial mass in mitochondrial myopathy mice. Proc Natl Acad Sci U S A **99:** 15066-15071.

WU, Z., P. PUIGSERVER, U. ANDERSSON, C. ZHANG, G. ADELMANT *et al.*, 1999 Mechanisms controlling mitochondrial biogenesis and respiration through the thermogenic coactivator PGC-1. Cell **98:** 115-124.

WULLSCHLEGER, S., R. LOEWITH and M. N. HALL, 2006 TOR signaling in growth and metabolism. Cell **124:** 471-484.

XIA, R., Y. LIU, L. YANG, J. GAL, H. ZHU *et al.*, 2012 Motor neuron apoptosis and neuromuscular junction perturbation are prominent features in a Drosophila model of Fus-mediated ALS. Mol Neurodegener **7:** 10.

XU, H., S. Z. DELUCA and P. H. O'FARRELL, 2008 Manipulating the metazoan mitochondrial genome with targeted restriction enzymes. Science **321:** 575-577.

YANG, M. Y., M. BOWMAKER, A. REYES, L. VERGANI, P. ANGELI *et al.*, 2002 Biased incorporation of ribonucleotides on the mitochondrial L-strand accounts for apparent strand-asymmetric DNA replication. Cell **111:** 495-505.

YLIKALLIO, E., and A. SUOMALAINEN, 2011 Mechanisms of mitochondrial diseases. Ann Med.

YLIKALLIO, E., H. TYYNISMAA, H. TSUTSUI, T. IDE and A. SUOMALAINEN, 2010 High mitochondrial DNA copy number has detrimental effects in mice. Hum Mol Genet **19:** 2695-2705.

YOULE, R. J., and D. P. NARENDRA, 2011 Mechanisms of mitophagy. Nat Rev Mol Cell Biol **12:** 9-14.

ZEVIANI, M., C. T. MORAES, S. DIMAURO, H. NAKASE, E. BONILLA *et al.*, 1988 Deletions of mitochondrial DNA in Kearns-Sayre syndrome. Neurology **38:** 1339-1346.

ZEVIANI, M., S. SERVIDEI, C. GELLERA, E. BERTINI, S. DIMAURO *et al.*, 1989 An autosomal dominant disorder with multiple deletions of mitochondrial DNA starting at the D-loop region. Nature **339:** 309-311.

ZHANG, D., J. L. MOTT, S. W. CHANG, G. DENNIGER, Z. FENG *et al.*, 2000 Construction of transgenic mice with tissue-specific acceleration of mitochondrial DNA mutagenesis. Genomics **69:** 151-161.

ZHENG, X., and J. A. BOBICH, 1998 A sequential view of neurotransmitter release. Brain Res Bull **47:** 117-128.

ZHOU, C., Y. HUANG, Y. SHAO, J. MAY, D. PROU *et al.*, 2008 The kinase domain of mitochondrial PINK1 faces the cytoplasm. Proc Natl Acad Sci U S A **105:** 12022-12027.

ZIVIANI, E., and A. J. WHITWORTH, 2010 How could Parkin-mediated ubiquitination of mitofusin promote mitophagy? Autophagy **6:** 660-662.

ZONCU, R., A. EFEYAN and D. M. SABATINI, 2011 mTOR: from growth signal integration to cancer, diabetes and ageing. Nat Rev Mol Cell Biol **12:** 21-35.

ZUCHNER, S., I. V. MERSIYANOVA, M. MUGLIA, N. BISSAR-TADMOURI, J. ROCHELLE *et al.*, 2004 Mutations in the mitochondrial GTPase mitofusin 2 cause Charcot-Marie-Tooth neuropathy type 2A. Nat Genet **36:** 449-451.